SPECTROSCOPIC AND FUNCTIONAL MODELS FOR HMD HYDROGENASE

BY

AARON MATHEW ROYER

DISSERTATION

Submitted in partial fulfillment of the requirements
for the degree of Doctor of Philosophy in Chemistry
in the Graduate College of the
University of Illinois at Urbana-Champaign, 2010

Urbana, Illinois

Doctoral Committee:

Professor Thomas B. Rauchfuss, Chair
Professor Gregory S. Girolami
Professor John F. Hartwig
Professor Steven C. Zimmerman

Abstract

The hydrogenases are metalloenzymes that catalyze transformations of dihydrogen. Two hydrogenase classes, [FeFe] and [NiFe] catalyze the interconversion of dihydrogen to protons and electrons. In order to facilitate electron transfer, these enzymes contain iron-sulfur clusters. Synthetic models for both of these hydrogenases are thoroughly studied. More recently, a third class of hydrogenase, Hmd or alternatively [Fe]-hydrogenase, was discovered in methanogenic archaea. This enzyme catalyzes the heterolysis of dihydrogen to a proton with hydride transfer to a carbocation and does not require iron-sulfur clusters.

Early work on Hmd revealed the presence of iron, carbonyl ligands, and a 2-pyridinol-6-acetic acid derivative. We examined the metal coordination of a similar ligand, 4-methyl-2-hydroxypyridine-6-acetic acid ($cmhpH_2$), on the simplified platforms of Cp*Ir and Cp*Rh. We were able to show the cmhpH ligand chelates to the metal through the carboxylate oxygen and pyridine nitrogen. The hydroxyl group exhibits strong intramolecular hydrogen-bonding and also stabilizes water binding with ionization of Cl^- in water. Hydrogen transfer reactions of secondary alcohols mediated by Cp*IrCl(cmhpH) were also examined. Initial work with $cmhpH_2$ complexes of iron resulted in insoluble products.

The structure of Hmd was reported in late 2008 and revised in 2009. The revised structure is a ferrous carbonyl fragment with appended thiolate, acyl and

2-pyridone/ 2-hydroxypyridine ligands. The Fe-acyl and pyridinol derivatives are both novel to biological systems. In an effort to confirm the structure reported for Hmd, we synthesized ferrous models containing the unique acyl ligand tethered to a donor ligand. Although Hmd active site incorporates a nitrogen heterocycle, we found phosphine to be a suitable alternative.

The addition of thioesters, derived from the reaction of *o*-diphenylphosphino benzoic acid with a multitude of thiols, to Fe(0) carbonyls resulted in oxidative addition of the thioester to give complexes of the type $Fe(SR)(Ph_2PC_6H_4CO)(CO)_3$ with a chelating phosphine acyl ligand. These complexes readily lost CO to give a dimer of the type $Fe_2(SR)_2(Ph_2PC_6H_4CO)_2(CO)_3$. In two cases, where R=Et or 2,6-dimesitylphenyl, we were able to show phosphine binding, prior to oxidative addition, gave products of the formula $Fe[PPh_2(C_6H_4COSR)](CO)_4$. With the bulky R = 2,6-dimesitylphenyl thioester, the oxidative addition reaction was completely arrested.

In the case of R = Ph, we were able to carbonylate the dimer to give the tricarbonyl monomer, which exhibited a similar IR spectrum to the CO inhibited form of Hmd. The substitution reactions of this monomer with CN^- and $TsCH_2NC$ were stereoselective, similar to the enzyme. The CN^- derivative was characterized by EXAFS, XANES, and IR spectroscopy and all demonstrated a remarkable similarity to CN^- inhibited Hmd. Protonation of the thiolate in Hmd has been proposed, and we examined protonation of the tricarbonyl monomer.

The product was unstable even at -30 ºC and the IR spectrum was found to differ greatly from the Hmd active site.

A similar method to the oxidative addition of thioesters was attempted in the addition of *o*-(diphenylphosphino)benzaldehyde to Fe(0) carbonyls. Although an acyl hydride intermediate was detected, the isolated product is a result of C-C coupling of two aldehyde carbons to give a tetradentate bisphosphine-bisalkoxide ligand bound to a ferrous dicarbonyl fragment. A similar coupling reaction has been reported, but our method is superior in terms of cost and yields. The $Fe(P_2O_2)(CO)_2$ complex reacts with (ferrocenium)BF_4 to give a 50% conversion to a complex with BF_3 bound to each alkoxide. The mechanism for this reaction is proposed to involve an iron mediated F^- abstraction from BF_4^-. The binding of Lewis acids to the alkoxides was found to be general. Addition of water to a THF solution of the bis-BF_3 complex resulted in loss of the P_2O_2 ligand as a diol. The novel diphosphine diol was isolated in analytical purity.

Hydrogen transfer reactions mediated by 2-pyridone (2hpH) complexes are potentially relevant to the mechanism by which Hmd heterolytically cleaves dihydrogen. The complex Cp*IrCl(2hp) was reported to be an excellent precatalyst for direct dehydrogenation of secondary alcohols. We found this complex reacted with secondary alcohols or dihydrogen to give a transient complex (Cp*IrHCl(2hpH)), followed by formation of a 2hp bridged dimer of the formula $[Cp^*IrH)_2(2hp)]^+$. This dimer was found to be a resting state of catalysis and not the active catalyst. In the presence of Cl^-, the dimer dissociates into monomers that are highly active for dehydrogenation of secondary alcohols.

An exploratory project of TsDPENH complexes of d^8 metals, where TsDPENH = S,S-TsNHCHPhCHPhNH$_2$, was also performed. There are many reports of metal TsDPEN complexes for hydrogen transfer, but all complexes reported are pseudo-octahedral. We report new square planar Pt(II), Pd(II), Rh(I), and Ir(I) complexes containing the TsDPEN ligand which display good thermal- and air-stability.

The addition of two equivalents of TsDPEN to Pt precursors afforded two products, assigned as the *cis*- and *trans*-isomers, that do not interconvert in solution. The similar addition of two equivalents of TsDPEN to Pd precursors gave only the *trans*-amide complex, which was structurally characterized. The ^{1}H NMR spectrum of Pd(TsDPEN)$_2$ matched the ^{1}H NMR spectrum of the major product of the Pt(TsDPEN)$_2$ complex well. An (allyl)Pd(TsDPEN) complex exhibits interesting isomerization. The solid state characterization shows only one form, but in solution allyl rotation occurs to give two detectable isomers. This demonstrates the assymetric environment provided by the Pd(TsDPEN) fragment.

In all TsDPEN complexes we report, the ^{1}H NMR spectra confirm the diaxial phenyl orientation of the TsDPEN ligand, but equatorial orientation can be effected by addition of a hydrogen-bond acceptor such as acetone. This interaction was confirmed by the solid state structure of the Pd(TsDPEN)$_2$ complex.

Acknowledgments

I would like to thank a large number of people for my successes outside and inside the University. The foremost leader to my success in chemistry is my advisor, Thomas Rauchfuss, who guided me to become a skeptical, well read, and critical chemist, both with my results and the reports of others. I would like to thank the many Rauchfuss group members who taught me technique, helped early on with insightful criticism, and maintained the many instruments and computers that were vital to my work at Illinois. I would also like to thank the many full time staff members that help make this a top notch chemistry university with a large number of techniques that you can not only utilize, but be fully trained to understand the technique in order to improve data collection and understanding. I would like to thank my committee members for helpful suggestions on writing technique and editing of a much improved research proposal document. I want to thank my collaborator Professor Seigo Shima who allowed me a trip to Marburg Germany to learn a great deal about the biology side of Hmd and the cultural side a very different country. Without the guidance of my undergraduate advisor, Jeffrey Zaleski, I probably would have never chosen graduate school, or made as confident decision about attending the University of Illinois.

On a more personal side of life, I would like to thank my family for the countless number times you helped me when I asked, but mostly even when I didn't. Without your help, I never would have been able to purchase my home,

renovate it, move into the house, or fill it with the nice things that made life easier. You also provided a great sounding board for the difficult decisions throughout my time in Champaign. The Fifth Saturday group kept me grounded with some people outside of science that kept me sane and always offered a good excuse to go learn a new skill or take a trip. I would like to thank my 4 year roommate Rufus. You may have made a few messes I had to clean up, but you were always there with a smile when I came home. I have made a large number of friendships here with the many sociable chemists who have provided many hours of entertainment outside of the laboratory. Rather than list people and miss someone, I would like to thank you all collectively for the many trips, the teaching of beer brewing, the grilling and sharing of food, and the advice for the few times we talked science outside of the laboratory. I would like to thank one special friend, Liz, who made the last year of graduate school the best of all and who helped me maintain my sanity during the writing of this dissertation.

Table of Contents

Chapter 1

Transition Metal-Mediated Reactions of Thioesters

Introduction

In this thesis a significant effort is dedicated to metal-thioester interactions. This area of coordination chemistry has not been heavily studied, and for this reason, this overview is provided. In general, thioester-metal interactions have been examined in three contexts, simulation of metalloenzymatic reactions involving thioesters, synthesis of thioesters, and the use of thioesters as acylating agents in organic synthesis. These themes are surveyed in this introductory chapter. Additionally, less targeted, exploratory work on metal-thioester compounds has been investigated, and the relevant background is provided in the introductions to chapters 2 and 3.

Thioesters represent hydrolytically stable acylating agents that can be prepared from virtually all carboxylic acids.[1-4] The important role of coenzyme A in biosynthesis has encouraged much work on biomimetic processes that incorporate thioesters,[5] which for the most part operate without the participation of metal ions.[6] Multiple metalloenzymes have been discovered to be integral to the biosynthesis and biodegradation of thioesters, and their study offers a rich source for thioester-metal interactions. Herein we present a review of thioester reactions for models of the metalloenzymes acetyl-coenzyme A synthase and glyoxalase II.

Thioester-metal interactions have also been investigated in organic synthesis from several perspectives.[7] A major area of study is the metal-catalyzed use of thioesters as acylating agents. The difficulty in these transformations is the high affinity of catalytically active metals to the thiolate products that inhibit further turnovers. Studies on biological systems define three methods to activate otherwise stable metal-thiolate bonds. Zinc(II) has an affinity for thiolate second only to copper(II)[8] and can act as a stoichiometric acceptor of thiolate *in vivo*.[9] Second, S-alkylation considerably weakens the metal-sulfur bond.[10] Third, metal-disulfide interactions are considerably weaker than metal-thiolate interactions,[11] and several biological systems mobilize metals by oxidation of thiolate ligands to disulfides.[12-15] Some transition metal-catalyzed organic transformations that utilize principals inspired by biology, and might be utilized more generally are also discussed.

Ni Complexes Related to Acetyl-Coenzyme A Synthase Activity

Acetyl-coenzyme A synthase (ACS) is a metalloenzyme found in acetogenic, methanogenic, and sulfate-reducing bacteria.[9,10] The enzyme assembles/disassembles acetyl-CoA from CO, CoA (a thiol), and a methyl unit transferred from methylcobal(III)amin.[16,17] ACS contains a Ni-Fe-S core (Figure 1.1) that catalyzes the reversible acetyl-CoA assembly that enables acetogens to grow on one-carbon substrates and methanogens to utilize acetate as a substrate for methane production.[18] Detailed understanding of this process is relevant to the global carbon cycle and understanding the archaea one-carbon

transformations.[9] From an organometallic standpoint, this enzyme is interesting due to the proposed intermediates featuring Ni-CO, Ni-CH_3, and $NiC(O)CH_3$ moieties.[19,20]

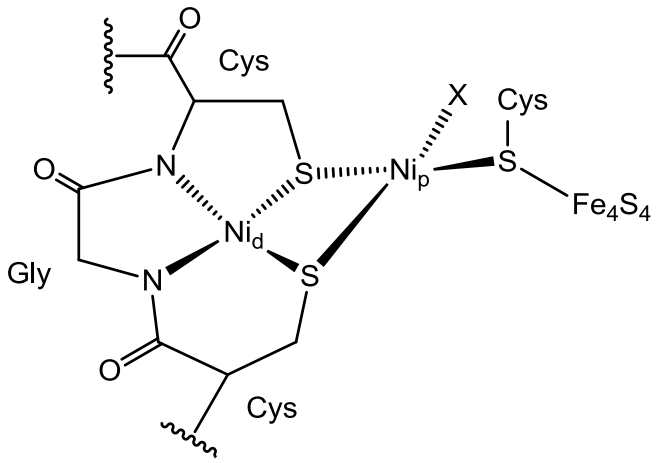

Figure 1.1. Schematic representation of the A cluster with X = a non-protein ligand.

The structure of the Ni-Fe-S cluster of ACS has been elucidated by crystallographic analysis of proteins obtained from multiple sources (Figure 1.1).[21-23] The active site features an Fe_4S_4 cluster bridged via cysteinyl sulfur to a dinickel subunit. The Fe_4S_4 cluster is believed to serve solely as an electron relay to the Ni_pNi_d cluster. The Ni_p (proximal to Fe_4S_4) center is ligated to 3 bridging Cys residues. The Ni_d (distal to Fe_4S_4) center is square planar, with coordination by the two thiolates and two amido groups provided by the CysGlyCys residues. Common mechanistic scenarios[24,25] and synthetic model complexes presented herein suggest substrate binding and transformations occur at the Ni_p site. An overview for the proposed ACS-catalyzed process is shown in Scheme 1.1.[26]

Scheme 1.1. Overview of ACS-catalyzed transformation with Ni(0) mechanism shown.

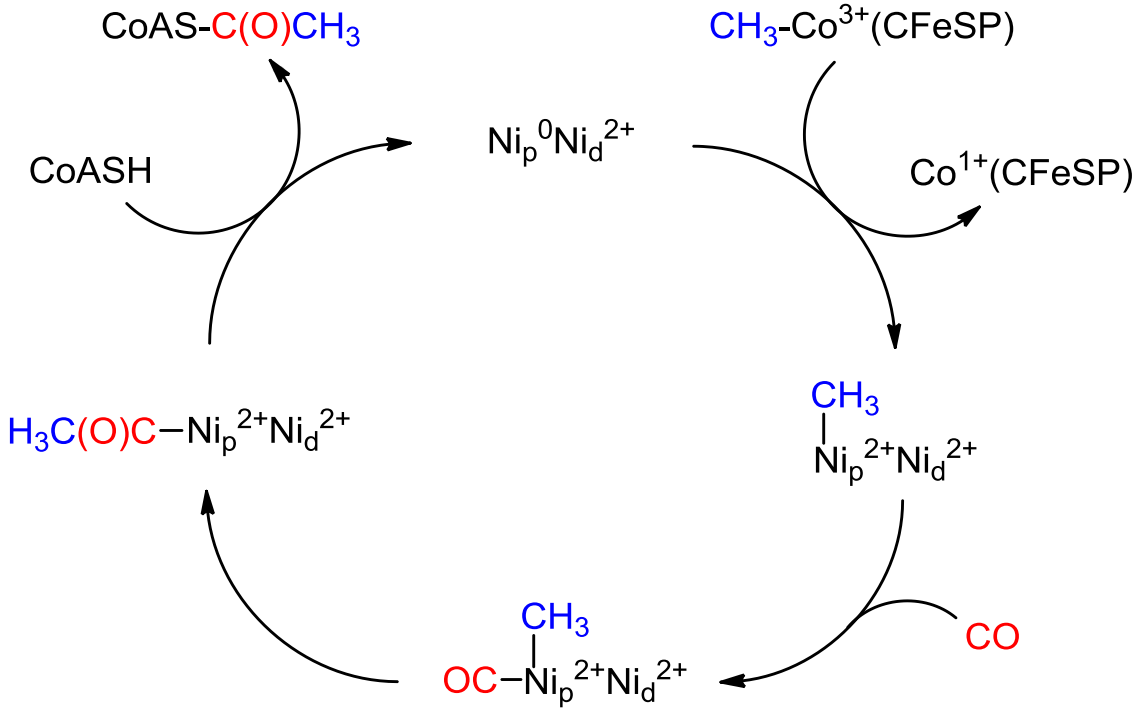

Early modeling work with monomeric nickel complexes $[Ni(NS_3^R)L]^+$ derived from the tripodal ligand $NS_3^R = N(CH_2CH_2SR)_3$ (R = *i*-Pr, *t*-Bu) was reported by Holm and coworkers.[27] These models were the first to allow stable isolation of Ni-Me species which then inserted CO to give stable acyl complexes (Figure 1.2). The thioether ligands were inert to further reaction, but addition of thiol to the acyl complexes resulted in formation of thioester with loss of protonated NS_3^R ligands and formation of a black solid attributed to Ni(0). These results were the first to mimic the overall transformation of ACS and suggested a single Ni center could catalyze the entire transformation.

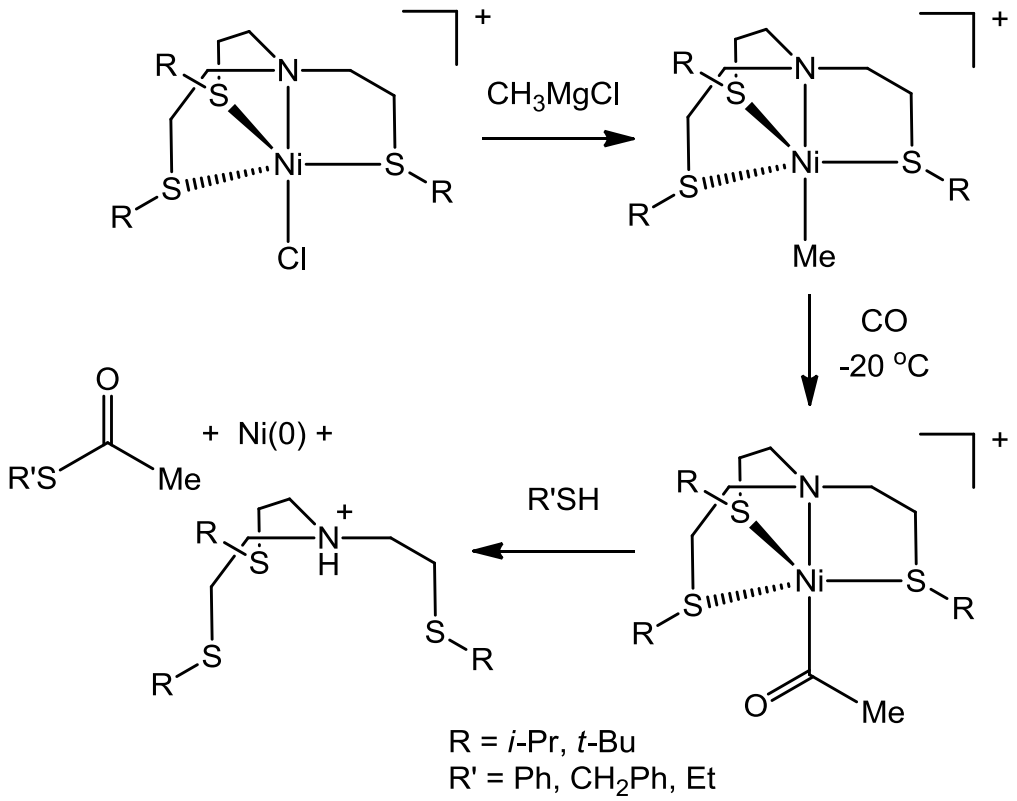

Figure 1.2. Thioester synthesis from Ni-Me followed by CO insertion and addition of thiol.

Second generation models for ACS developed by Holm integrated methyl and thiolate ligands onto monomeric Ni complexes of bpy, where bpy = 2,2'-bipyridyl.[28] The $Ni(bpy)Me_2$ reacted with aryl thiols to give isolatable Ni(bpy)Me(SR) complexes. The Me-Ni bond readily underwent CO insertion to give the acyl thiolate complexes, that could be isolated, but readily underwent reductive elimination to give free thioesters and a $Ni(bpy)(CO)_2$ complex.

A recently popularized method for the synthesis of dinickel complexes has been through the use of several Ni(N_2S_2) complexes (Figure 1.3) that act as bridging thiolate ligands to another nickel by one[29] or both[30-32] thiolates. The Ni(N_2S_2) unit has been utilized as a neutral and dianionic ligand. One potential problem with complexes of this type is the acylation of a bridging thiolate which has been reported by Riordan et al.[29]

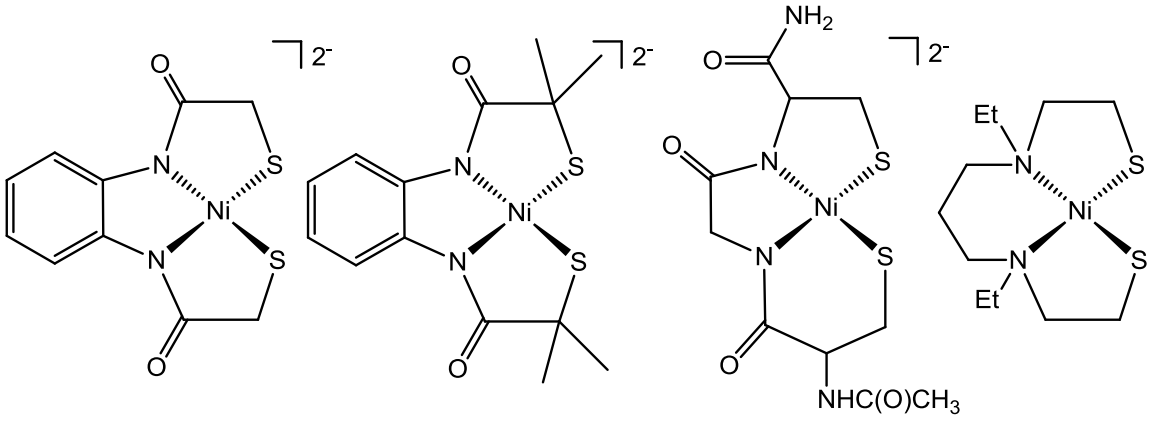

Figure 1.3. Examples of Ni(N_2S_2) complexes used to generate dinuclear complexes through bridging thiolate ligands.

Our group[31] and Tatsumi's[32] have described dinickel models formed by the reaction of a Ni(N_2S_2) complex with Ni(cod)$_2$. In one case, the unstable Ni(II)Ni(0) complex was found to react with methylcobaloxime Co(dmgBF_2)$_2$(Me)(Py) and the thiolate KSDmp, where Dmp = 2,6-dimesitylphenyl, to give a methylnickel thiolate species (Figure 1.4).[32] It is proposed that in the enzyme an oxidative addition of Me^+ is provided by methylcobalamin to a Ni_d(II)Ni_p(0) site resulting in a Ni_d(II)Ni_p(II)-Me species. Under 1 atm of CO, the methyl nickel thiolate species reductively eliminated the acetylthioester ($CH_3C(O)SDmp$) in good yield. The conversion is stoichiometric

due to the fact that CO poisons Ni products. A general consensus from modeling work is that the CO addition at the ACS active cluster must be highly regulated to avoid similar inactivation products.

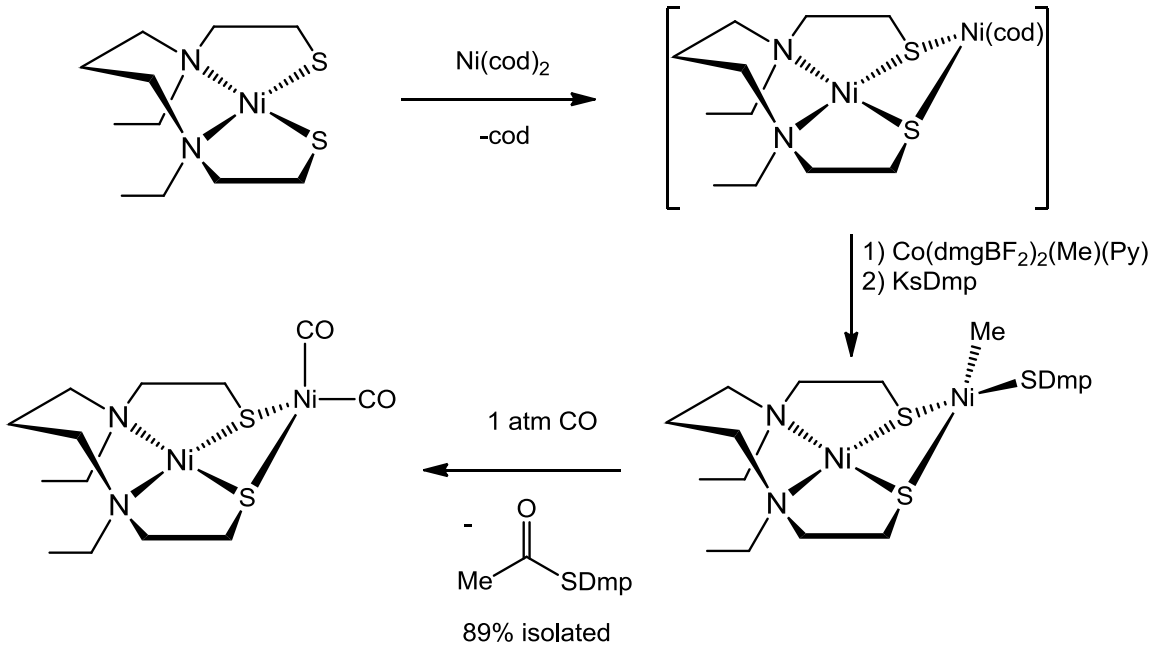

Figure 1.4. Binuclear Ni-methyl complex generated through a biomimetic synthesis and insertion of CO followed by reductive elimination of thioester to give a CO inactivated product.

In view of the potential role of Ni(0) in ACS catalysis, the oxidative addition of thioesters ($CH_3C(O)SPh$, $CH_3C(O)SC_6F_5$) to Ni(0) reagents was reported by Riordan and coworkers to give the corresponding alkylnickel(II) thiolates(Scheme 1.2).[19] Electron-rich phosphines combined with C_6F_5-derived thioesters facilitated the highest conversions. Low temperature reactions gave metastable acylnickel thiolates consistent with oxidative addition followed by decarbonylation to the stable alkylnickel thiolates. They proposed the oxidative addition of thioester to Ni(0) might also play a role in the repair of acetylated cysteine at the ACS cluster.[19]

Scheme 1.2.

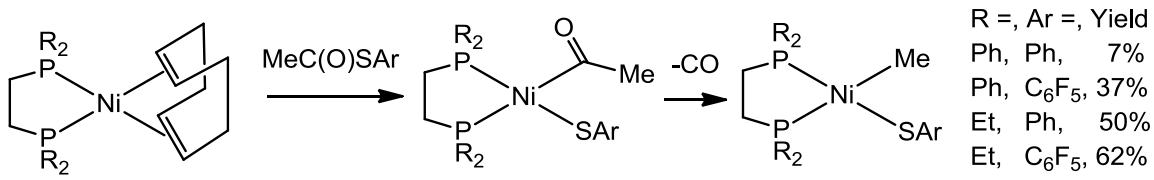

Glyoxalase Enzyme Models for Thioester Hydrolysis

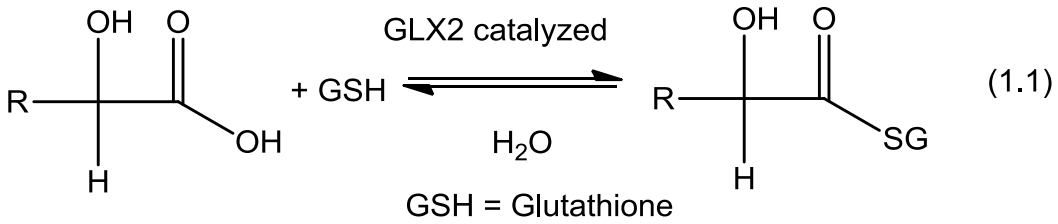

The diversity of the role of thioester-metal interactions is exemplified by the enzyme glyoxylase II (GLX2) which catalyzes hydrolysis of a 2-hydroxythioester to 2-hydroxy acid and free glutathione (eq 1.1).[33-38] This reaction is part of the overall glyoxylase pathway for the degradation of methyl glyoxal ($CH_3C(O)CHO$), a byproduct of lipid and carbohydrate metabolism, that is cytotoxic and mutagenic.[39-42] GLX2 has been crystallographically characterized from several sources, and in each case displays similar metal coordination consisting of a bimetallic iron/zinc cluster (Figure 1.5). On the basis of spectroscopic studies and metal analyses, GLX2 has been found with the following cores: Fe(III)Zn(II), Fe(II)Zn(II), Fe(III)Fe(II), Zn(II)Zn(II), Fe-(II)Fe(II), and Mn(II)Mn(II).[43-45] Crowder and co-workers recently reported that human GLX2 features a Fe(II)Zn(II) center but is catalytically active as a mononuclear zinc enzyme.[46]

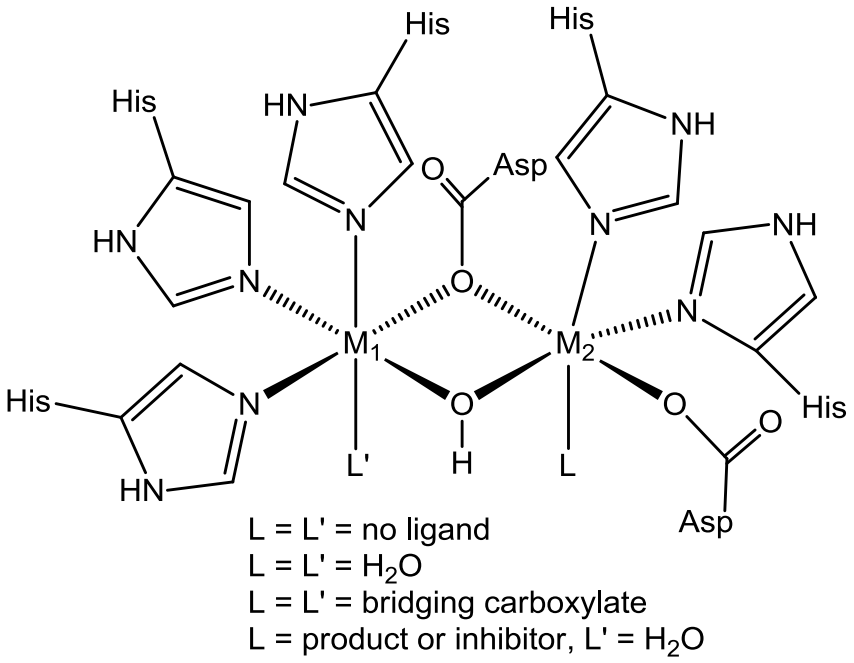

Figure 1.5. Active site structural features for crystallographically characterized GLX2.

Studies of thioester hydrolysis promoted by a metal complex have been reported by Berreau and coworkers.[47-49] Their initial finding was that a symmetric dizinc complex of 2,6-bis[(bis(2-pyridylmethyl)amino)methyl]-4-methylphenol (**L1H**), [(**L1**Zn_2)(μ-OH)]$(ClO_4)_2$ was unreactive toward hydrolysis of hydroxyphenylthioacetic acid S-methyl ester. This result was attributed to the poor nucleophilicity of the bridging hydroxide. They speculate that this system is further deactivated by the matching coordination at each zinc, which inhibits formation of a terminal hydroxide.

Binuclear zinc hydroxide complexes of N-methyl-N-((6-neopentylamino-2-pyridyl)methyl)-N-((2-pyridyl)methyl)amine (**L2**H) and N-methyl-N-((6-neopentylamino-2-pyridyl)methyl)-N-((2-pyridyl)ethyl)amine (**L3**H), abbreviated [(**L2**$Zn)_2$(μ-$OH)_2$]$(ClO_4)_2$ and [(**L3**$Zn)_2$(μ-$OH)_2$]$(ClO_4)_2$, were found to behave as

1:1 electrolytes in MeCN solution. This finding suggests that the binuclear complexes dissociate into monometallic fragments. Treatment of either complex with an equivalent of hydroxyphenylthioacetic acid S-methyl ester per zinc resulted in the formation of two equivalents of a monomeric Zn-*α*-hydroxycarboxylate complex, [(**L2** or **L3**)Zn(O_2CCH(OH)Ph)](ClO_4) and two equivalents of CH_3SH. These results suggest the potential role of a terminal hydroxide in the thioester hydrolysis step.

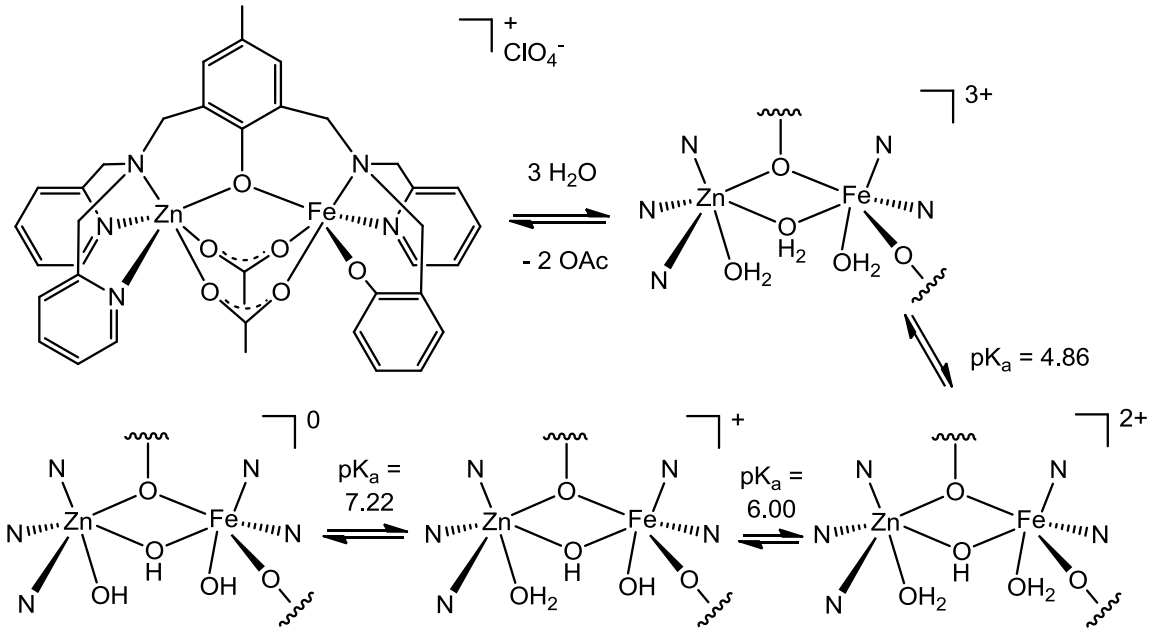

Figure 1.6. Structure of [(**L4**Fe(III)Zn(II)(μ-$O_2C_2H_3)_2$](ClO_4) and the aqua complexes formed at different pH levels for a 1:1, MeCN:H_2O solution.

The Fe(III)Zn(II) complex of 2-{[bis(2-pyridylmethyl)amino]methyl}-6-[{[2-hydroxyphenyl)methyl]-(2-pyridylmethyl)amino}methyl]-4-methylphenol (**L4**H_2), [(**L4**Fe(III)Zn(II)(μ-$O_2C_2H_3)_2$]ClO_4, was found to have a geometry remarkably similar to the proposed active site of GLX2 (Figure 1.6). This complex was active for the catalytic hydrolysis of hydroxyphenyl thioacetic acid S-methyl(d_3) ester

($PhCH(OH)C(O)SCD_3$). The deuterium labeled compound was utilized for simple analysis of products by ^2H NMR spectroscopy. Background observed rate constants for thioester hydrolysis in 1:1, MeCN:H_2O were pH-dependent, ranging from 5.7 x 10^{-8} s^{-1} at pH = 7 to 1.1(1) x 10^{-6} s^{-1} at pH = 9. In the presence of 2.5 equivalents of [(**L4**Fe(III)Zn(II)(μ-$O_2C_2H_3)_2$](ClO_4), the hydrolysis of the thioester was accelerated by up to 1000x. Under condition of 2-fold excess thioester to metal complex, hydrolysis was found to proceed to completion, suggesting catalysis.

The pH-dependent reaction results in a maximal rate enhancement above the pK_a of the $Zn(OH_2)$ moiety (pH > 8.3) (Figure 1.6). The proposed mechanism involves initial formation of a zinc alkoxide via deprotonation of the *α*-hydroxythioester[50,51] followed by Fe-OH attack at the thioester carbonyl to give the mandelate anion and CD_3S^-. This mechanism is different than the mechanism proposed for a mononuclear Zn complex in Figure 1.7. The mandelate product does not significantly interact with the Fe(III)Zn(II) complex. The CD_3S^- product is either protonated to give CD_3SH (pKa ~9.7) or undergoes a proposed Fe(III) to Fe(II) mediated disulfide (D_3CSSCD_3) formation via a Fe(III)-SCD_3 species.[52,53]

With the recent report that human GLX2 is catalytically active as a mononuclear zinc enzyme,[45] a mononuclear Zn complex, [(bpta)Zn]($ClO_4)_2$ where bpta = *N*,*N*-bis(2-pyridylmethyl)-tert-butylamine, was examined as a catalyst for thioester hydrolysis. Under identical conditions described above for the Fe(III)Zn(II) complex at pH = 9, the mononuclear Zn complex is > 17-fold slower

for thioester hydrolysis. In this reaction, no disulfide product is detected, but a Zn-SCD_3 complex is formed in equilibrium with $HSCD_3$. The kinetic data for thioester hydrolysis promoted by $[(bpta)Zn](ClO_4)_2$ revealed that the reaction is second order overall. An associative type mechanism that likely involves nucleophilic attack of the Zn-OH moiety on the thioester was proposed (Figure 1.7). The difference in mechanism between the Fe(III)Zn(II) and Zn(II) is explained by the difference in basicity of the Zn-OH. In the Zn(II) complex there is no evidence for deprotonation of the thioester *α*–hydroxyl group.

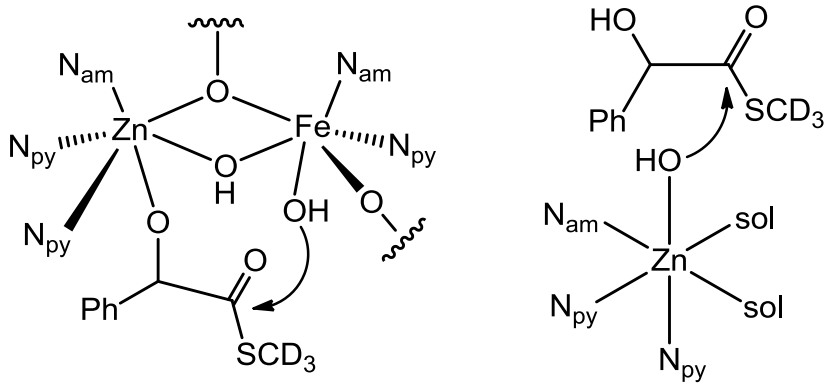

Figure 1.7. Different mechanisms for hydrolysis of $PhCH(OH)C(O)SCD_3$ in a Fe(III)Zn(II) complex and a mononuclear Zn(II) complex.

Biologically Inspired Thioesters Conversions

Thioester-metal interactions have been investigated in organic synthesis from several perspectives.[7] The area is too broad to discuss in entirety, but some basic principles from biology might be integrated generally to catalysis when the desired products include formation of a thiol. A few methods to decrease metal-thiolate interactions, and increase catalytic turnover are discussed below.

One of the most insightful themes come from the efforts of Liebeskind et al. who have examined Pd catalyzed thioester-boronic acid cross-coupling.[54] They used 4-halo-*n*-butyl thioesters to achieve alkylative conversion of the stable palladium–thiolate bond to a labile palladium–thioether bond (Scheme 1.3). The coupling reactions requires *trans*-di(μ-acetato)-bis[*o*-(di-*o*-tolylphosphino)benzyl]-dipalladium(II), NaI, and K_2CO_3. Using this mixture, various boronic acids cross-couple with thioesters to give ketones in good to excellent yields. Electron-rich boron reagents, R' = 3-methoxyphenyl, resulted in lower yields. Tetrahydrothiophene was detected by GC/MS, which supports the hypothesis of sulfur scavenging by alkylative displacement. Yields for this conversion were much higher than those achieved for similar Pd-catalyzed coupling of boronic acid with thioesters lacking the ability to S-alkylate.[55,56]

Scheme 1.3. Thioester cross-coupling with proposed Pd-thiolate and S-alkylation intermediate.

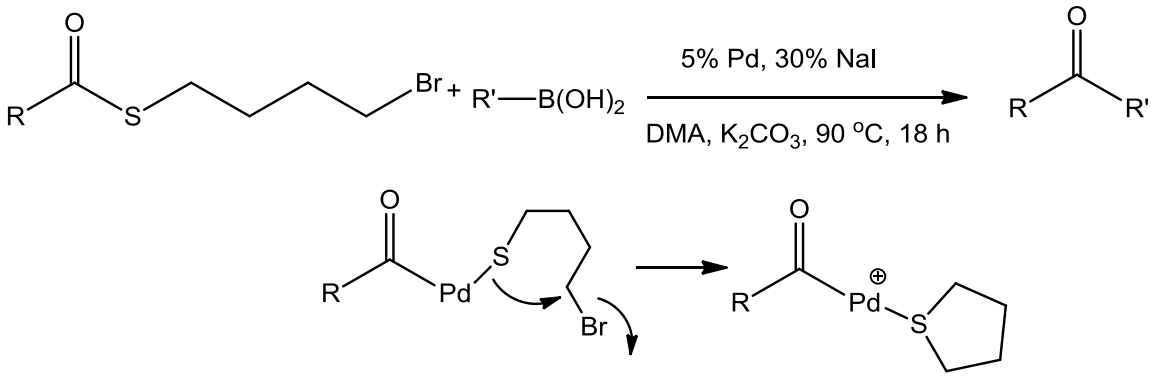

A similar Pd catalyzed thioester-boronic acid cross-coupling was achieved under nonbasic conditions utilizing a stoichiometric excess of a thiophilic metal to accept the thiolate ligand (Figure 1.8).[57] Using a precatalyst mixture consisting of

$Pd_2(dba)_3$ and tris(2-furyl)phosphine, a variety of thioesters and boronic acid were coupled in the presence of Cu(I) thiophene-2-carboxylate (CuTC) as the thiolate acceptor.

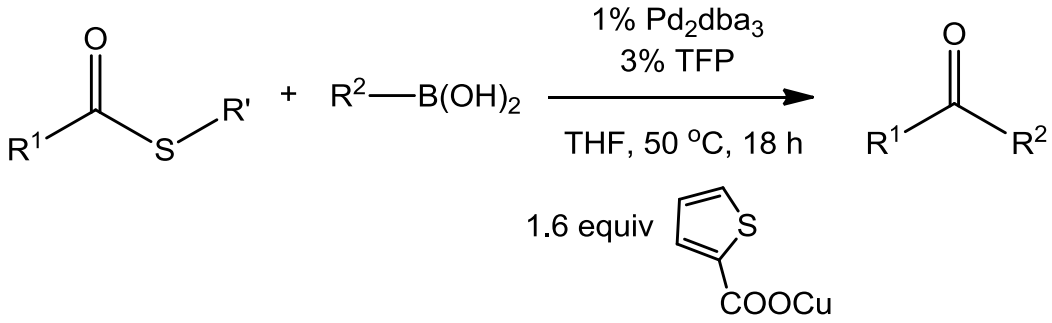

Figure 1.8. Thioester-boronic acid coupling

The choice of thiolate acceptor was critical to the reaction. Reactions with CuTC resulted in high conversion, but Cu(I) halides, CuCN, and Zn(II) carboxylates resulted in low conversion. A mechanism involving Cu(I) interaction with the thioester prior to oxidative addition at Pd(0) is proposed (Scheme 1.4). The best evidence for this interaction is the suppression of reactivity of CuTC toward naphthalene-2-boronic acid in the presence of 1 equiv of thioester.

Scheme 1.4.

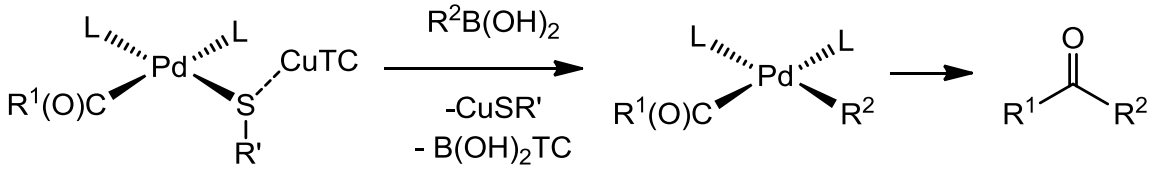

The mild reaction condition for these conversions allowed for direct preparation of a chloromethyl ketone, $R^1 = ClCH_2$, R^2 = 2-naphthyl in 57%

isolated yield. Trifluoromethyl ketones were also isolated with $R^1 = CF_3$, and R^2 = *m*-NO_2Ph (63%), (*E*)-β-styryl (93%).

This use of thioesters as acyl building blocks is similar to the use of thioesters in acetyl coenzyme A, which operates under protic conditions in the presence of oxygen- and nitrogen-based functionalities.[58] S-Acylthioglycolic acids have shown utility for metal-induced acyl transfer using Zn(II) to activate the thioester (Scheme 1.5).[59] With this procedure, a variety of esters (primary and secondary) have been prepared in good yields. This process requires a pendent carboxylate for internal activation of the thioester from a proposed metal carboxylate intermediate(Scheme 1.5). Enantiomerically pure alcohols could be used to obtained the corresponding esters without racemization, e.g. (1*R*,2*S*,5*R*)-menthol.

Scheme 1.5.

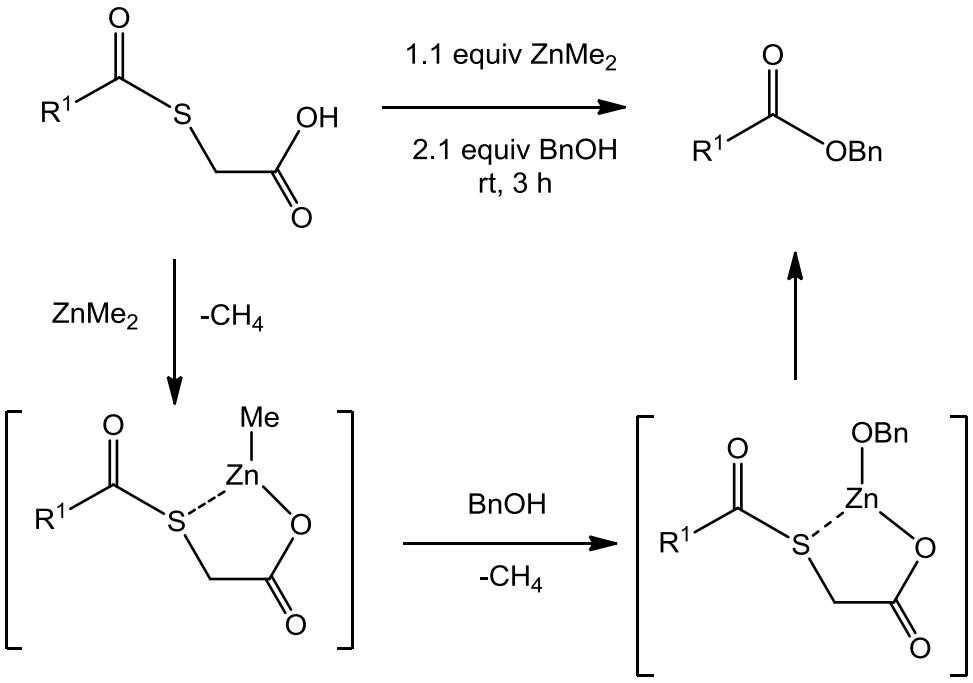

Conclusions

Models for coenzyme A synthase have shown it is possible to synthesize thioesters from the basic building blocks of a Ni-Me, CO, and a thiol. These transformations have been reported for both mononuclear and binuclear Ni complexes and suggest the transformations occur at a single nickel site in the enzyme.

The transition metal-catalyzed transformations of thioesters (or other C-S bonds) in general results in formation of intermediates containing a strong metal-thiolate bond. This strong interaction can be weakened by conversion to thioether derivatives or in the presence of an appropriate thiolate acceptor.

Oxidative addition of thioesters to Ni(0) complexes also resulted in formation of a nickel acyl thiolate.[19] A similar method has been utilized in chapters 2 and 3 with Fe(0) to install acyl and thiolate ligands to Fe(II) in a single step. By attaching a phosphine to the thioester, we will show high yields of the oxidative addition product are attained. These products are then compared to the active site of Hmd hydrogenase (Chapter 3). In a related methodology, we also examined oxidative addition of phosphine derivatized aldehydes to Fe(0) with a plan to install the thiolate in a second step (Chapter 7).

References

[1] Mukaiayama, T.; Takeda, T.; Atsumi, K. “The Reaction of Trimethylsilyl Sulfides With Carboxylic Esters. a Convenient Method for the Preparation of Thiolesters.” *Chem. Lett*., **1974**, 187-188.

[2] Yamada, S.; Yokoyama, Y.; Shioiri, T. “New synthesis of thiol esters.” *J. Org. Chem*., **1974**, *39*, 3302-3303.

[3] Masamune, S.; Kamata, S.; Diakur, J.; Sugihara, Y.; Bates, G. S. “A General, Selective Synthesis of Thiol Esters.” *Can. J. Chem.,* **1975**, *53*, 3693-3695.

[4] Neises, B.; Steglich, W. “Simple Method for the Esterification of Carboxylic Acids.” *Angew. Chem. Int. Ed.*, **1978**, *17*, 522-524.

[5] Drueckhammer, D. G. “CoA-dependent enzymes, chemistry of.” *Wiley Encyclopedia of Chemical Biology*, **2009**, *1*, 384-392.

[6] Ogino, K.; Fujihara, H., “Biochemical reactions involving thioesters.” *Org. Sulfur Chem.: Biochem. Aspects*, **1992**, 71-136.

[7] Fujiwara, S.; Kambe, N. “Thio-, Seleno-, and Telluro-Carboxylic Acid Esters.” *Top. Curr. Chem*., **2005**, *251*, 87-140.

[8] Bertini, I.; Briganti, F.; Scozzafava, A. In *Handbook of Metal-Ligand Interactions in Biological Fluids*; Berton, G.; Ed.; Marcel Dekker: New York, 1995 Vol. 1, 176.

[9] Korbashi, P.; Katzhendlers, J.; Saltman, P.; Chevion, M. “Zinc protects Escherichia coli against copper-mediated paraquat-induced damage.” *J. Biol. Chem.* **1989***, 264*, 8479-8482.

[10] Lippard, S. J.; Wilker, J. J. “Alkyl Transfer to Metal Thiolates: Kinetics, Active Species Identification, and Relevance to the DNA Methyl Phosphotriester Repair Center of Escherichia coli Ada.” *Inorg. Chem.* **1997**, *36*, 969-978.

[11] Baumgartner, M. R.; Schmalle, H.; Dubler, E. “The interaction of transition metals with the coenzyme α-lipoic acid: synthesis, structure and characterization of copper and zinc complexes.” *Inorg. Chim. Acta,***1996***, 252*, 319-331.

[12] Maret, W. “Metallothionein/disulfide interactions, oxidative stress, and the mobilization of cellular zinc.” *Neurochem. Int.* **1995**, *27*, 111-117.

[13] Maret, W.; Vallee, B. L. “Thiolate ligands in metallothionein confer redox activity on zinc clusters.” *Proc. Nat. Acad. Sci.* **1998**, *95*, 3478-3482.

[14] Jacob, C.; Maret, W.; Vallee, B. L. “Control of zinc transfer between thionein, metallothionein, and zinc proteins.” *Proc. Nat. Acad. Sci.* **1998**, *95*, 3489-3494.

[15] Tummino, P. J.; Scholten, J. D.; Harvey, P. J.; Holler, T. P.; Maloney, L.; Gogliotti, R.; Domagala, J.; Hupe, D. “The in vitro ejection of zinc from human immunodeficiency virus (HIV) type 1 nucleocapsid protein by disulfide benzamides with cellular anti-HIV activity.” *Proc. Nat. Acad. Sci.* **1996**, *93*, 969-973.

[16] Ragsdale, S. W. “Nickel and the carbon cycle.” *J. Inorg. Biochem.*, **2007**, *101*, 1657-1666.

[17] Lindahl, P. A.; Graham, D. E. Acetyl-Coenzyme A Synthases and Nickel-Containing Carbon Monoxide Dehydrogenases. In *Metal Ions in Life Sciences* Sigel, A.; Sigel, H.; Sigel, R. K. O.; Eds.; Wiley-Interscience: Chichester, UK, 2007; Vol. *2*, 357–416.

[18] Hugler, M.; Huber, H.; Stetter, K. O.; Fuchs, G. “Autotrophic CO2 fixation pathways in archaea (Crenarchaeota).” *Arch. Microbiol.*, **2003**, *179*, 160-173.

[19] Juan, B.; Thauer, R. K. Methyl-CoenzymeMReductase and Its Nickel Corphin Coenzyme F430 in Methanogenic Archaea. in *Metal Ions in Life Sciences*; Sigel, A.; Sigel, H.; Sigel, R. K. O.; Eds.; Wiley-Interscience: Chichester, UK, 2007; Vol. *2*, 323–356.

[20] Jeoung, J. H.; Dobbek, H. “Carbon Dioxide Activation at the Ni,Fe-Cluster of Anaerobic Carbon Monoxide Dehydrogenase.” *Science*, **2007**, *318*, 1461-1464.

[21] Doukov, T. I.; Iverson, T. M.; Seravalli, J.; Ragsdale, S. W.; Drennan, C. L. “A Ni-Fe-Cu Center in a Bifunctional Carbon Monoxide Dehydrogenase/ Acetyl-CoA Synthase.” *Science*, **2002**, *298*, 567-572.

[22] Darnault, C.; Volbeda, A.; Kim, E. J.; Legrand, P.; Vernede, X.; Lindahl, P. A.; Fontecilla-Camps, J. C. “Ni-Zn-[Fe_4-S_4] and Ni-Ni-[Fe_4-S_4] clusters in closed and open subunits of acetyl-CoA synthase/carbon monoxide dehydrogenase*.” Nat. Struct. Biol.*, **2003**, *10*, 271-279.

[23] Svetlitchnyi, V.; Dobbek, H.; Meyer-Klaucke, W.; Meins, T.; Thiele, B.; Romer, P.; Huber, R.; Meyer, O. “A functional Ni-Ni-[4Fe-4S] cluster in the monomeric acetyl-CoA synthase from Carboxydothermus hydrogenoformans.” *Proc. Natl. Acad. Sci. U. S. A.*, **2004**, *101*, 446-451.

[24] Lindahl, P. A. “Acetyl-coenzyme A synthase: the case for a Ni_p^0-based mechanism of catalysis.” *J. Biol. Inorg. Chem.*, **2004**, *9*, 516-524.

[25] Ragsdale, S. W. “Metals and Their Scaffolds To Promote Difficult Enzymatic Reactions.” *Chem. Rev.*, **2006**, *106*, 3317-3337.

[26] Ariyananda, P. W. G.; Kieber-Emmons, M. T.; Yap, G. P. A.; Riordan, C. G. “Synthetic analogs for evaluating the influence of N–H·····S hydrogen bonds on the formation of thioester in acetyl coenzyme a synthase.” *Dalton Trans.*, **2009**, 4359-4369.

[27] Stavropoulos, P.; Muetterties, M. C.; Carrie, M.; Holm, R. H. “Structural and Reaction Chemistry of Nickel Complexes in Relation to Carbon Monoxide Dehydrogenase: A Reaction System Simulating Acetyl-Coenzyme A Synthase Activity.” *J. Am. Chem. Soc.* **1991**, *113,* 8485-8492.

[28] Tucci, G. C.; Holm, *R.* H. “Nickel-Mediated Formation of Thioesters from Bound Methyl, Thiols, and Carbon Monoxide: A Possible Reaction Pathway of Acetyl-Coenzyme A Synthase Activity in Nickel-Containing Carbon Monoxide Dehydrogenases.” *J. Am. Chem.* Soc., **1995**,*117*, 6489-6496.

[29] Dougherty, W. G.; Rangan, K.; O’Hagan, M. J.; Yap, G. P. A.; Riordan, C. G. “Binuclear Complexes Containing a Methylnickel Moiety: Relevance to Organonickel Intermediates in Acetyl Coenzyme A Synthase Catalysis.” *J. Am. Chem. Soc.*, **2008**, *130*, 13510-13511.

[30] Song, Y.; Ito, M.; Kotera, M.; Matsumoto, T.; Tatsum, K. “ Cationic and Anionic Dinuclear Nickel Complexes $[Ni(N_2S_2)Ni(dtc)]^n$ (n = -1, +1) Modeling the Active Site of Acetyl-CoA Synthase.” *Chem. Lett.,* **2009**, *38*, 184-185.

[31] Linck, R. C.; Spahn, C. W.; Rauchfuss, T. B.; Wilson, S. R. “Structural Analogues of the Bimetallic Reaction Center in Acetyl CoA Synthase: A Ni-Ni Model with Bound CO” *J. Am. Chem. Soc.*, **2003**, *125*, 8700-8701.

[32] Ito, M.; Kotera, M.; Matsumoto, T.; Tatsumi, K. “Dinuclear nickel complexes modeling the structure and function of the acetyl CoA synthase active site.” *Proc. Natl. Acad. Sci. U. S. A.*, **2009**, *106*, 11862-11866.

[33] Zang, T. M.; Hollman, D. A.; Crawford, P. A.; Crowder, M. W.; Makaroff, C. A. “Arabidopsis glyoxalase II contains a zinc/iron binuclear metal center that is essential for substrate binding and catalysis.” *J. Biol. Chem.* **2001**, *276*, 4788-4795.

[34] Schilling, O.; Wenzel, N.; Naylor, M.; Vogel, A.; Crowder, M.; Makaroff, C.; Meyer-Klaucke, W. “Flexible Metal Binding of the Metallo-β-lactamase Domain: Glyoxalase II Incorporates Iron, Manganese, and Zinc in Vivo.” *Biochemistry* **2003**, *42*, 11777-11786.

[35] Wenzel, N. F.; Carenbauer, A. L.;Pfiester, M. P.; Schilling, O.; Meyer-Klaucke, W.; Makaroff, C. A.; Crowder, M. W. “The binding of iron and zinc to glyoxalase II occurs exclusively as di-metal centers and is unique within the metallo-ß-lactamase family.” *J. Biol. Inorg. Chem.* **2004**, *9*, 429-438.

[36] Marasinghe, G. P. K.;Sander, I. M.; Bennett, B.; Periyannan, G.; Yang, K.-W.; Makaroff, C. A.; Crowder, M. W. Structural Studies on a Mitochondrial Glyoxalase II.” *J. Biol. Chem.* **2005**, *280*, 40668-40675.

[37] Campos-Bermudez, V. A.; Leite, N. R.; Krog, R.; Costa-Filho, A. J.; Soncini, F. C.; Olivia, G.;Vila, A. J. “Biochemical and Structural Characterization of Salmonella typhimurium Glyoxalase II: New Insights into Metal Ion Selectivity.” *Biochemistry* **2007**, *46*, 11069-11079.

[38] Limphong,P.;McKinney,R.M.;Adams,N.E.;Bennett,B.;Makaroff, C. A.; Gunasekera, T.; Crowder, M. W. “Human Glyoxalase II Contains an Fe(II)Zn(II) Center but Is Active as a Mononuclear Zn(II) Enzyme.” *Biochemistry* **2009**, *48*, 5426-5434.

[39] Thornalley, P. J. “The glyoxalase system in health and disease.” *Mol. Aspects Med.* **1993**, *14*, 287-371.

[40] Vander Jagt, D. L.; Hunsaker, L. A. “Methylglyoxal metabolism and diabetic complications: roles of aldose reductase, glyoxalase-I, betaine aldehyde dehydrogenase and 2-oxoaldehyde dehydrogenase.” *Chem.-Biol. Interact.* **2003**, *143*, 341-351.

[41] Thornalley, P. J. “Advances in glyoxalase research Glyoxalase expression in malignancy, anti-proliferative effects of methylglyoxal, glyoxalase I inhibitor diesters and S-D-lactoylglutathione, and methylglyoxal-modified protein binding and endocytosis by the advanced glycation endproduct receptor.” *Crit. Rev. Oncol. Hematol.* **1995**, *20*, 99-128.

[42] Thornalley, P. J. “Methylglyoxal, glyoxalases and the development of diabetic complications.” *Amino Acids* **1994**, *6*, 15-23.

[43] Cameron, A. D.; Ridderstrom, M.; Olin, B.; Mannervik, B. “Crystal structure of human glyoxalase II and its complex with a glutathione thiolester substrate analogue.” *Structure* **1999**, *7*, 1067-1078.

[44] Crowder, M. A.; Maiti, M. K.; Banovic, L.; Makaroff, C. A. “Glyoxalase II from A. thaliana requires Zn(II) for catalytic activity.” *FEBS Lett.* **1997**, *418*, 351-354.

[45] O'Young, J.; Sukdeo, N.; Honek, J. F. "Escherichia coli glyoxalase II is a binuclear zinc-dependent metalloenzyme." *Arch. Biochem. Biophys.* **2007**, *459*, 20-26.

[46] Limphong, P.; McKinney, R. M.; Adams, N. E.; Bennett, B.; Makaroff, C. A.; Gunasekera, T.; Crowder, M. W. "Human Glyoxalase II Contains an Fe(II)Zn(II) Center but Is Active as a Mononuclear Zn(II) Enzyme." *Biochem.,* **2009**, *48*, 5426-5434.

[47] Berreau, L. M.; Saha, A.; Arif, A. M. "Thioester hydrolysis reactivity of zinc hydroxide complexes: investigating reactivity relevant to glyoxalase II enzymes." *Dalton Trans.* **2006**, 183-192.

[48] Danford, J. J.; Dobrowolski, P.; Berreau, L. M. "Thioester Hydrolysis Reactivity of an Fe(III)Zn(II) Complex." *Inorg. Chem.*, **2009**, *48*, 11352-11361.

[49] Danford, J. J.; Arif, A. M.; Berreau, L. M. **"**Thioester Hydrolysis Promoted by a Mononuclear Zinc Complex" *Inorg. Chem.*, **2010**, *49*, 778-780.

[50] Chamberlain, B. M.; Cheng, M.; Moore, D. R.; Ovitt, T. M.; Lobkovsky, E. B.; Coates, G. W. "Polymerization of lactide with zinc and magnesium β-diiminate complexes: stereocontrol and mechanism." *J. Am. Chem. Soc.* **2001**, *123*, 3229-3238.

[51] Rieth, L. R.; Moore, D. R.; Lobkovsky, E. B.; Coates, G. W. "Single-site β-diiminate zinc catalysts for the ring-opening polymerization of β-butyrolactone and β-valerolactone to poly(3-hydroxyalkanoates)." *J. Am. Chem. Soc.* **2002**, *124*, 15239-15248.

[52] Rao, T. V.; Sain, B.; Murthy, P. S.; Rao, T. S. R. P.; Joshi, G. C.; Jain, A. K. "Iron(III)-ethylenediaminetetraacetic acid mediated oxidation of thiols to disulfides with molecular oxygen." *J. Chem. Res. Synops.* **1997**, *8*, 300-301.

[53] Plietker, B. *Iron Catalysis in Organic Chemistry*; Wiley-VCH: Weinheim, Germany, 2008.

[54] Savarin, C.; Srogl, J.; Liebeskind, L. S. "Thiol Ester-Boronic Acid Cross-Coupling. Catalysis Using Alkylative Activation of the Palladium Thiolate Intermediate." *Org. Lett.* **2000***, 2*, 3229-3231.

[55] Tokuyama, H.; Yokoshima, S.; Yamashita, T.; Fukuyama, F. "A novel ketone synthesis by a palladium-catalyzed reaction of thiol esters and organozinc reagents." *Tetrahedron Lett.* **1998**, *39*, 3189-3192.

[56] Zeysing, B.; Gosch, C.; Terfort, A. "Protecting Groups for Thiols Suitable for Suzuki Conditions." *Org. Lett.* **2000**, *2*, 1843-1845.

[57] Liebeskind L. S.; Srogl, J. “Thiol Ester-Boronic Acid Coupling. A Mechanistically Unprecedented and General Ketone Synthesis.” *J. Am. Chem. Soc.* **2000**, *122*, 11260-11261.

[58] Lynen, F. In *Enzymes*; Smellie, R. M. S., Ed.; Academic: New York, 1970; 1-19.

[59] Liebeskind, L. S.; Srogl, J.; Savarin, C.; Polanco, C. “Bioinspired organometallic chemistry.” *Pure Appl. Chem.*, **2002**, *74*, 115-122.

Chapter 2

Synthesis and Oxidative Addition of Thioesters to Iron(0)

Introduction

With the recent discovery of an acyl thiolate Fe cofactor involved in a central step in the archaeal methanogenic cycle,[1] we have become interested in synthetic methods to install thiolate and acyl ligands to transition metals. One synthetic method that seemed viable and simple is the installation of both ligand sets in a single step through the oxidative addition of thioesters to low oxidation state transition metals, specifically Fe(0) carbonyls. Results in this area would incorporate C-S bond fission and also be of possible interest in the area of hydrodesulfurization.[2]

The interaction of simple thioesters with Fe(0) carbonyls has been examined by Seyferth and coworkers. They prepared a series of diiron acyl thiolates via the formal oxidative addition of alkyl and arythioesters to $Fe_2(CO)_9$ and $Fe_3(CO)_{12}$ (eq 1).[3] The results presented in this chapter suggests that these diiron compounds arise via the intermediacy of mono-iron acylthiolates. The best isolated yields of Seyferth's method were also modest (17 % with S-ethyl thiobenzoate).

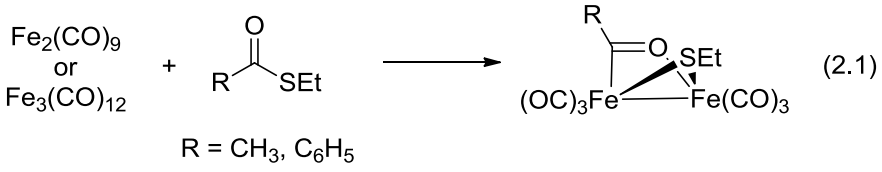

(2.1)

The oxidative addition of thioesters has also been described by Shaver and coworkers for complexes of Rh(I)[4] utilizing a chelate assisted method. In these reactions, 8-quinoline thioester derivatives C_9H_6N-8-C(O)SR (R = n-Bu, $CHMe_2$, CH_2Ph, Ph, *p*-$C_6H_4CH_3$) were found to react with $Rh(PPh_3)_3Cl$ to give thiolato-bridged dimers as a result of C-S bond cleavage (Scheme 2.1). In these reactions, the products contained one thiolate and one acyl ligand per Rh with isolated yields greater than 80%. Shaver et al.assumed the oxidative addition was preceeded by the intial binding of the quinoline nitrogen, but no evidence was presented for products prior to the cleavage of the C-S bond.

Scheme 2.1. Proposed sequence for the oxidative addition of 8-quinoline thioesters to Rh(I)

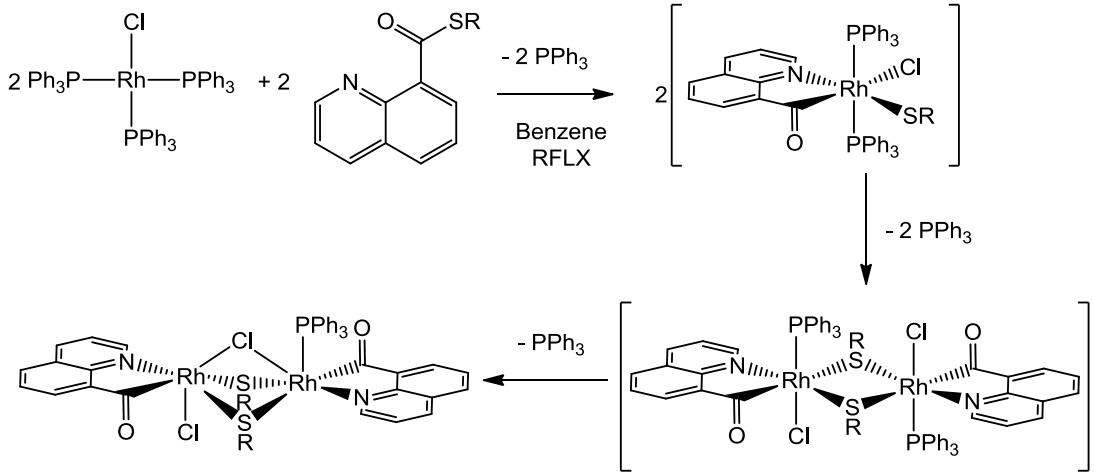

The reactions of α,β-unsaturated thioesters with Pt(0)[5] were reported with the isolation of intermediates prior to C-S bond cleavage. Addition of the α,β-unsaturated thioester to $Pt(PPh_3)_2(C_2H_4)$ quickly resulted in formation of a π-complex. At longer reaction times, an equilibrium was reached between this complex and the C-S activated $Pt(PPh_3)_2$(acyl)(thiolate) complex that also lost

PPh_3 to form a thiolate-bridged dimer (Scheme 2.2). Intramolecular attack of the C-S bond by the π-bound $Pt(PPh_3)_2$ is proposed via a S-bound intermediate. This intermediate was supported by the finding that the kinetic product of oxidative addition has *cis* phosphines. This cis complex was observed to quantitatively isomerize to the trans product. Additionally, bulky substituents at the α position significantly slow the C-S bond cleavage, but similar derivatives at the β position have little affect on C-S cleavage rates..

Scheme 2.2. α,β-unsaturated thioester addition to $Pt(PPh_3)_2(C_2H_4)$

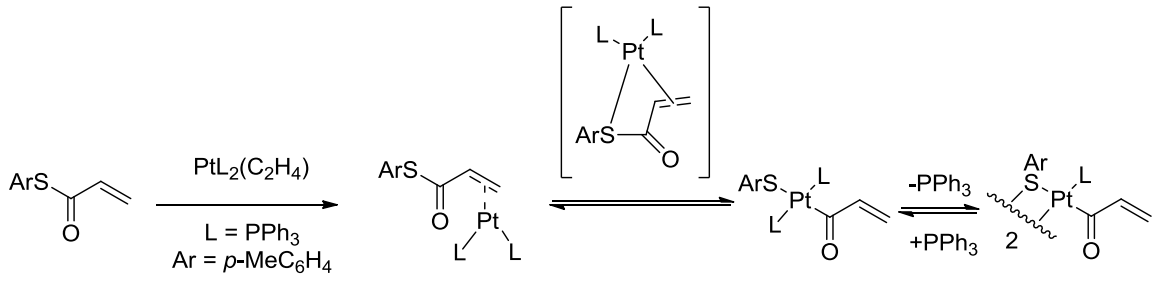

Because our targets were Fe acyl thiolates in a 1:1:1 ratio , we decided to combine the preparative routes of Seyferth with the idea of chelate-assisted oxidative addition. Herein we describe the synthesis of several thioester derivatives based on a $Ph_2P(o\text{-}C_6H_4C(O)SR)$ platform, where R = alkyl or aryl, and their reactions with Fe(0) carbonyls.

Results and Discussion

Phosphine Thioesters. Thioester phosphines containing a variety of aryl and alkylthio substituents can be prepared via carbodiimide coupling in good to

excellent yields (eq 2.1).[6] Although DMAP, 4-$Me_2NC_5H_4N$, was utilized in early preparations, we found that the addition of DMAP, which is typically required for efficient thioester conversion via DCC coupled carboxylic acids and thiols, was unnecessary and did not improve yields. This finding may suggest that the phosphine can act as a nucleophilic catalyst for this reaction. The new compounds are air-stable pale yellow to colorless crystalline solids that display a singlet in the ^{31}P NMR spectrum in the δ-4 to -10 range. Such thioesters have been previously investigated as peptide coupling reagents ($Ph_2PC_6H_4C(O)SEt$).[7] Isomeric thioesters of the type $Ph_2PC_6H_4SC(O)R$ are also known.[8]

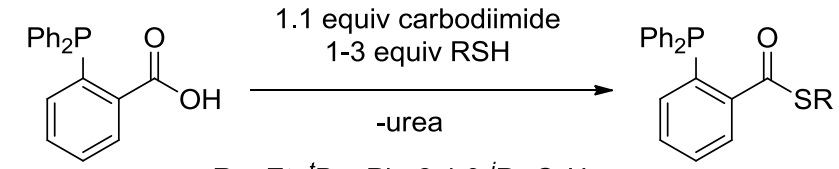

R = Et, ^{t}Bu, Ph, 2,4,6-^{i}Pr-C_6H_2, 2,6-(2,4,6-Me_3-C_6H_2)-C_6H_3, 2-NC_5H_4

(2.2)

carbodiimide = CyN=C=NCy (DCC) or $Me_2N(CH_2)_3$–N=C=NEt • HCl (EDAC)

Fe(II)-Acyl Thiolates. We found that several of the phosphine thioesters afforded iron(II) acyl thiolato derivatives. A useful iron(0) source was $Fe(bda)(CO)_3$ (bda = benzylideneacetone), but $Fe_2(CO)_9$ was also effective. The simple thioester Ph_2P-*o*-$C_6H_4C(O)SPh$ gave the cleanest and highest yielding reaction.

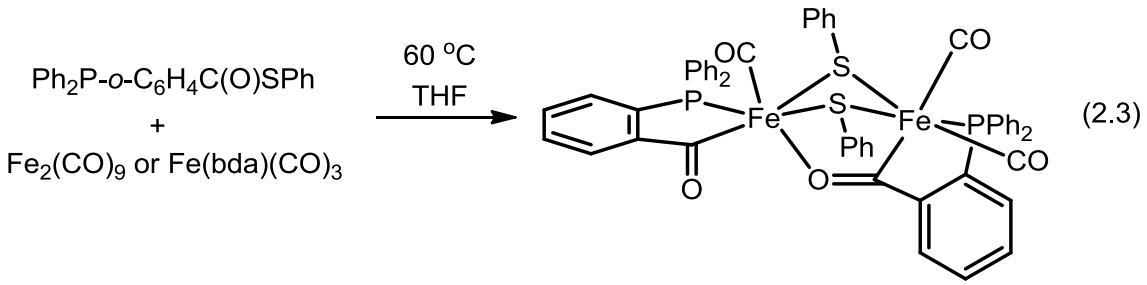

(2.3)

Treatment of a hot THF suspension of $Fe_2(CO)_9$ with Ph_2P-*o*-$C_6H_4C(O)SPh$ (eq 2.3) was found to give a dark brown product with complex IR and ^{31}P NMR signatures. Single crystals were grown from this apparent mixture and gave a simple ^{31}P NMR spectrum (Figure 2.1) indicating a pair of nonequivalent phosphine ligands. Over the course of several hours at room temperature, this initial species was found to isomerize into the other species (Figure 2.2). This pattern is understandable in light of the crystallographically determined structure of the product $Fe_2(SPh)_2[Ph_2PC_6H_4C(O)]_2(CO)_3$ (**1**) (Figure 2.3). The molecule adopts a relatively complex structure that can be related to the well-known and well studied diiron dithiolato carbonyls, e.g. $Fe_2(SPh)_2(CO)_6$.[9] Whereas compounds of the type $Fe_2(SR)_2(CO)_6$ feature a pair of $Fe^{I}L_3$ centers, **1** features a pair of $Fe^{II}L_3X$ centers. Two acyl-phosphine ligands are chelating, one on each Fe, and one acyl group is bridging.

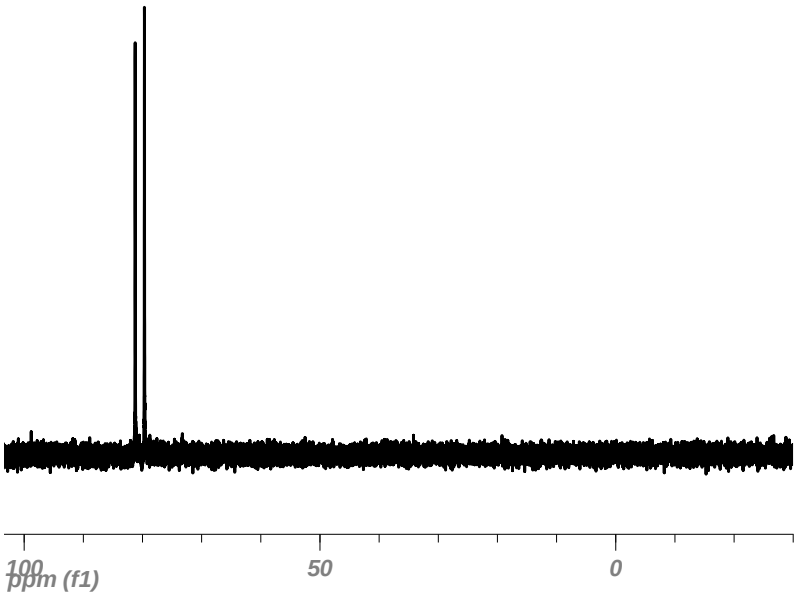

Figure 2.1. ^{31}P NMR spectrum of $Fe_2(SPh)_2[Ph_2PC_6H_4C(O)]_2(CO)_3$ (**1**) in CD_2Cl_2 solution, prepared by dissolving single crystals and recording the spectrum within 20 min.

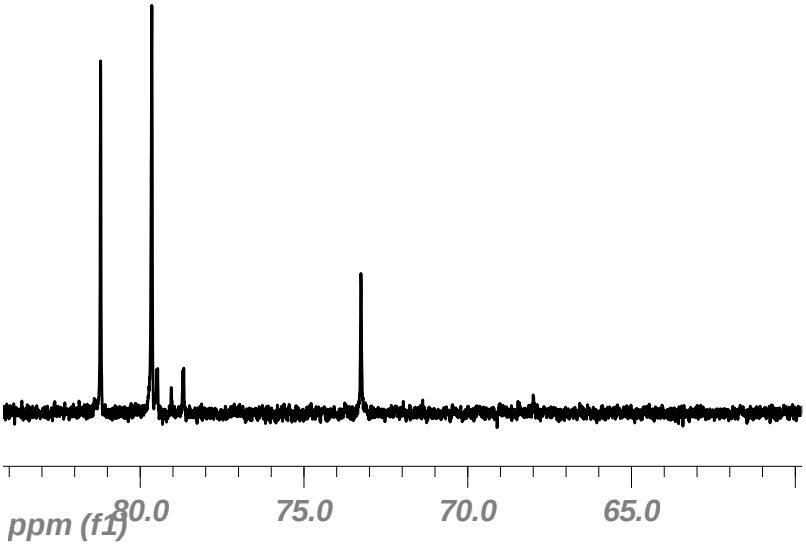

Figure 2.2. ^{31}P NMR spectrum of an equilibrated CD_2Cl_2 solution of $Fe_2(SPh)_2[Ph_2PC_6H_4C(O)]_2(CO)_3$ (**1**), recorded after ~48 hours at room temperature.

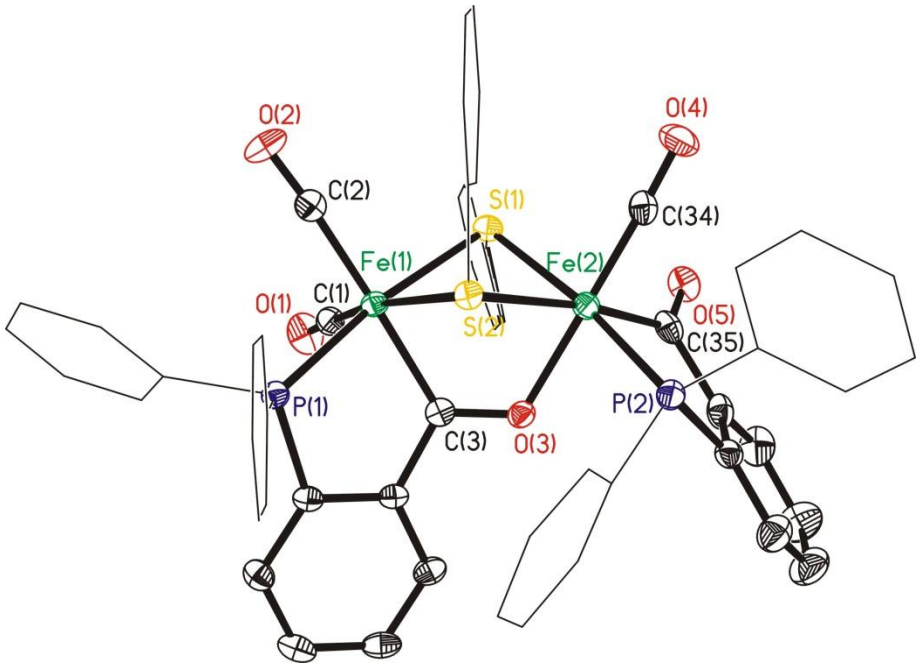

Figure 2.3. Molecular structure of **1** drawn with 35% probability ellipsoids with Fe, green; P, purple; O, red; S, yellow; C, black. Hydrogen atoms are omitted for clarity with the PPh_2 and SPh phenyl groups drawn as wires. Selected distances (Å): Fe1-C1, 1.760(3); Fe1-C2, 1.828(3); Fe1-C3, 1.963(3); Fe1-P1, 2.2115(8); Fe1-S2, 2.3258(8); Fe1-S1, 2.3581(8); Fe2-C34, 1.748(3); Fe2-C35, 1.937(3); Fe2-O3, 2.0104(18); Fe2-P2, 2.2094(8); Fe2-S1, 2.3102(8); Fe2-S2, 2.3972(8).

In light of the structure of **1**, which crystallizes as a single isomer, the solution isomerization can be explained by the reorientation of the phenyl rings on the bridging thiolate ligands (Scheme 2.3). The isomerization of bridging thiolates in diiron complexes was previously reported by King.[10] The crystallized form of **1** contains one axial and one equatorial phenyl ring. This diiron complex has no symmetry. A second isomer is possible where the axial and equatorial oriented rings are reversed. There is likely a species with two equatorial phenyl rings. The IR spectrum of **1** freshly dissolved in CH_2Cl_2 (Figure 2.4) does not change noticeably over time which shows the orientation of the thiolate phenyl rings has little effect on the electronic properties of the Fe centers.

Scheme 2.3. Different orientations of the thiolate phenyl rings looking down the Fe-Fe bond of **1**. The O is from the bridging acyl ligand and in this view the phosphines would be bound on the left side of Fe. The far left isomer is predominant in solution and the crystallized form.

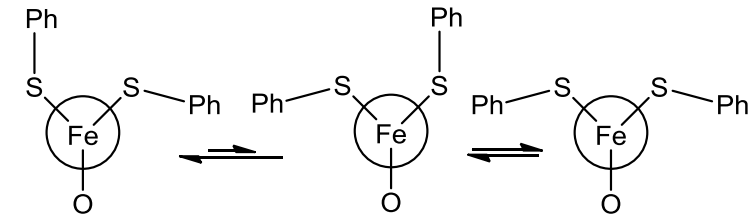

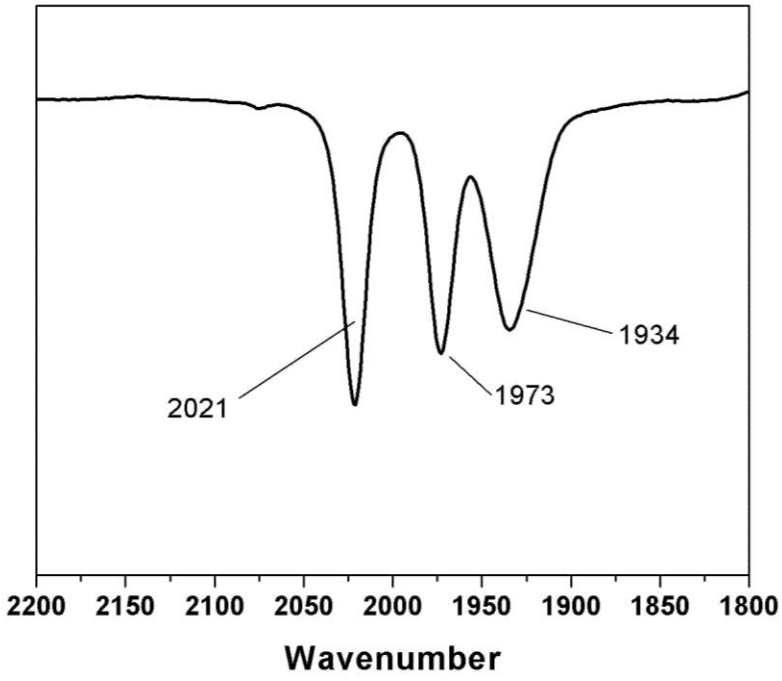

Figure 2.4. IR spectrum of **1** in CH_2Cl_2 solution.

Alkyl thioesters derived from EtSH and ^{t}BuSH gave diiron compounds spectroscopically similar to the PhS derivative, and other aryl thioesters (Ar=C_6H_4-2-OMe, 2,4,6-$^{i}Pr_3C_6H_2$) also gave derivatives of the type $Fe_2(SAr)_2(Ph_2PC_6H_4CO)_2(CO)_3$, but these yields were lower due to the formation

of othe unidentified products. Using an extremely bulky arylthioester, we were able to arrest the oxidative addition. Thus, treatment of $Fe_2(CO)_9$ with $Ph_2PC_6H_4C(O)SC_6H_4$-2,6-$(Ar^*)_2$ (Ar*=2,4,6-trimethylphenyl) gave the monophosphine adduct of $Fe(CO)_4$ (eq 2.4). The IR spectrum of this product (Figure 2.5) matches that for known derivatives of the type $Fe(CO)_4(PR_3)$.[11]

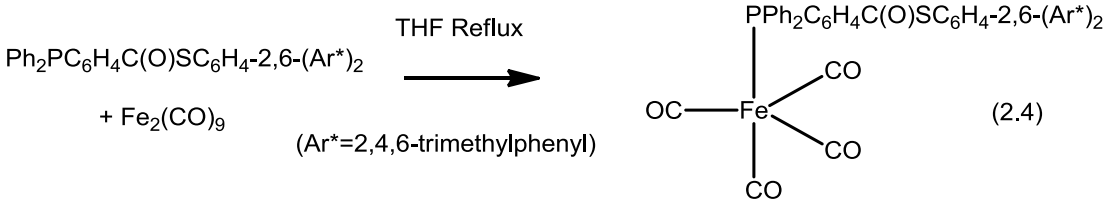

(2.4)

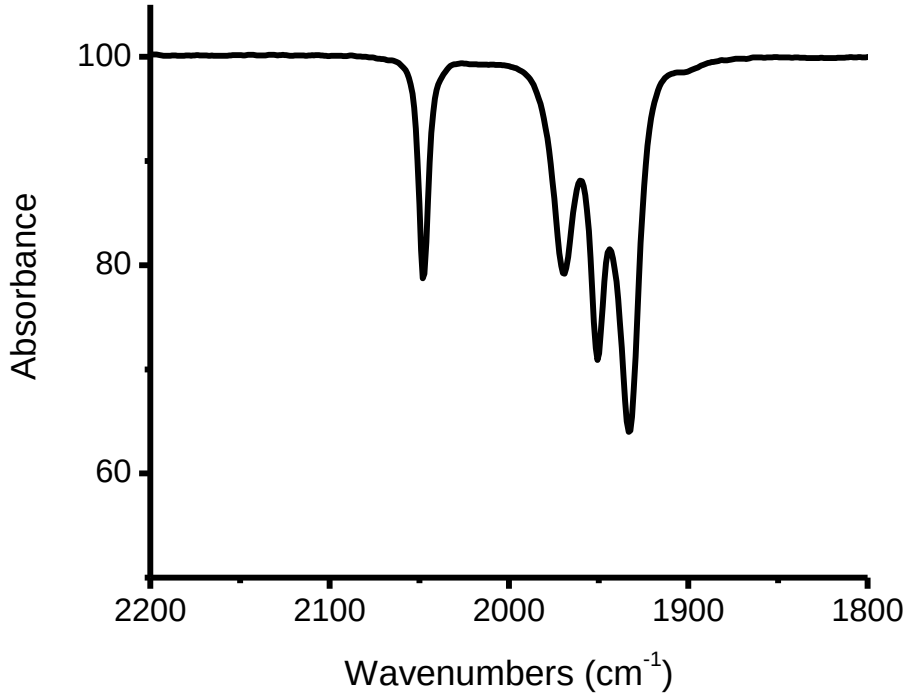

Figure 2.5. IR spectrum of $Fe(Ph_2PC_6H_4C(O)SC_6H_4$-2,6-$(Ar^*)_2(CO)_4$ (Ar* = 2,4,6-trimethylphenyl) in THF. υ_{CO} (cm^{-1}): 2049, 1972, 1951, 1933

While we could not find conditions to effect C-S bond fission in the isolated $Fe(Ph_2P$-*o*-$C_6H_4C(O)SC_6H_4$-2,6-$(Ar^*)_2(CO)_4$ (Ar* = 2,4,6-trimethylphenyl) to

prove chelate assisted oxidative addition, we were able to demonstrate the initial binding of phosphine to give a stable $Fe(CO)_4$ phosphine complex in the case of Ph_2P-*o*-$C_6H_4C(O)SEt$. The solution IR spectroscopy was again typical for a complex of the type $Fe(CO)_4(PR_3)$ (Figure 2.6).[11] Heating a solution of $Fe(CO)_4(Ph_2P$-*o*-$C_6H_4C(O)SEt)$ in THF resulted in complete conversion to a diiron complex similar to **1** with bridging SEt's instead of SPh's (Scheme 2.4). The solution IR spectroscopy for this complex closely matches the pattern for **1** (Figure 2.7).

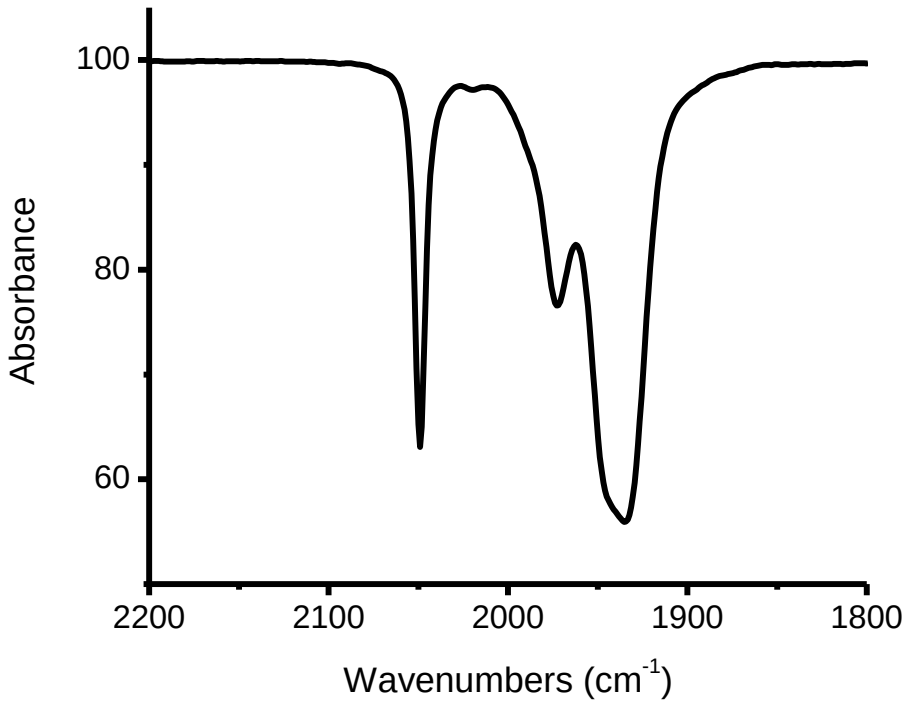

Figure 2.6. IR spectrum of $Fe(Ph_2P$-C_6H_4-$C(O)SEt)(CO)_4$ in CH_2Cl_2. υ_{CO} (cm^{-1}): 2049, 1972, 1935

Scheme 2.4.

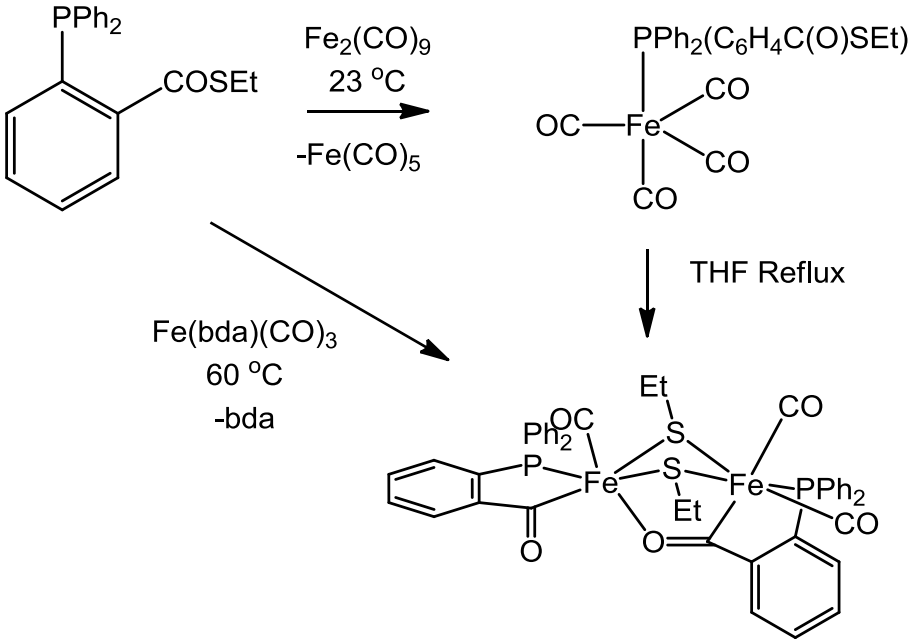

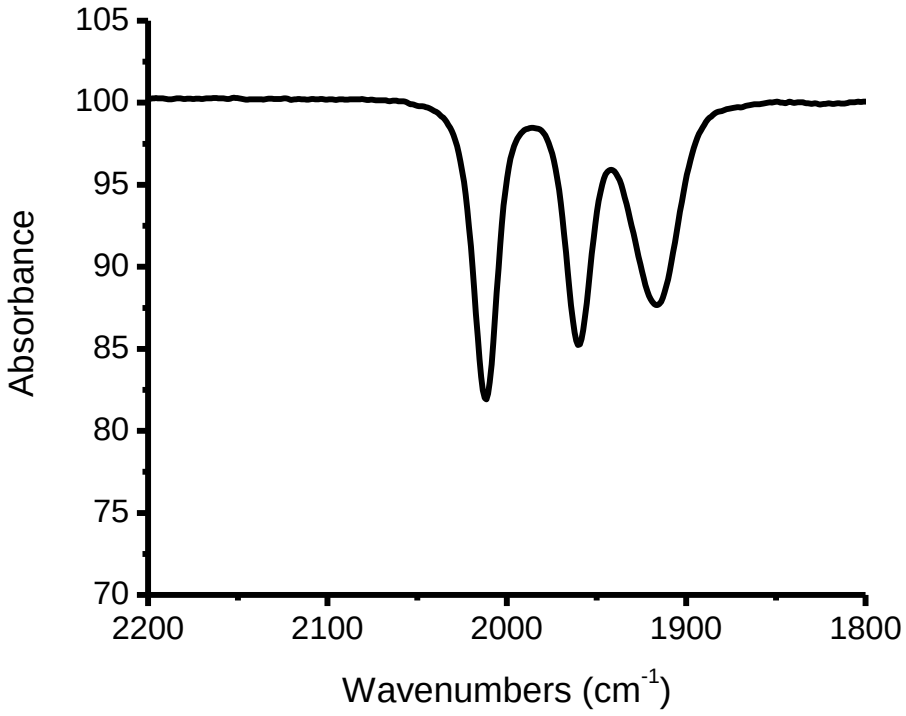

Figure 2.7. IR spectrum of $Fe_2(SEt)_2(PCO)_2(CO)_3$ in CH_2Cl_2. υ_{CO} (cm^{-1}): 2012, 1960, 1916 (SPh derivative IR υ_{CO} (cm^{-1}): 2021, 1973, 1934)

In the case of the reaction of $Fe(bda)(CO)_3$ with Ph_2P-o-$C_6H_4C(O)S(2,4,6\text{-}^iPr_3C_6H_2)$, two additional products were assigned as two isomers of $Fe(Ph_2PC_6H_4C(O))_2(CO)_2$ in a 2:1 ratio (Scheme 2.5). The major complex features a ^{31}P NMR spectrum with 2 doublets at δ67 and 57 (Figure 2.8), and CO bands in the IR spectrum at 1993 and 1926 cm^{-1}(Figure 2.9). The minor product has additional symmetry and gives only a single ^{31}P NMR signal at 60 ppm (Figure 2.8) with CO bands at 1973 and 1909 cm^{-1}(Figure 2.9). Heating the complexes in refluxing benzene for 16 hours did not change the ratio of the isomers. The symmetric product has two potential structures with cis CO's both trans to acyl or both trans to phosphine.

Scheme 2.5. Minor products isolated from thioester addition to Fe(0) carbonyls

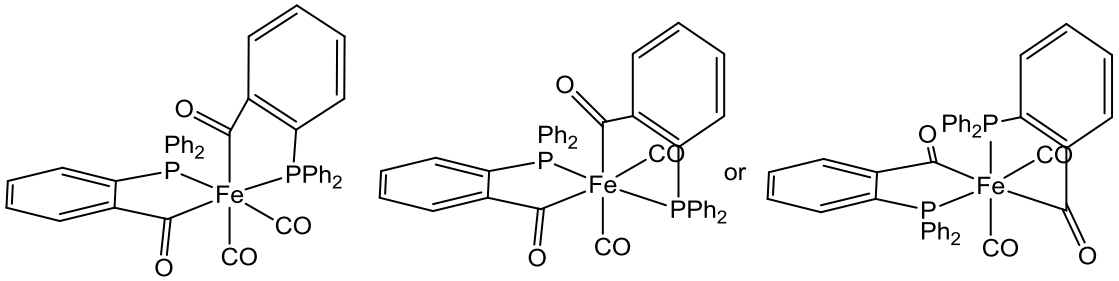

^{31}P = 2 doublet, 67, 57 ppm
V_{CO}= 1993, 1926 cm^{-1}

^{31}P = 1 singlet 60 ppm
V_{CO}= 1973, 1909 cm^{-1}

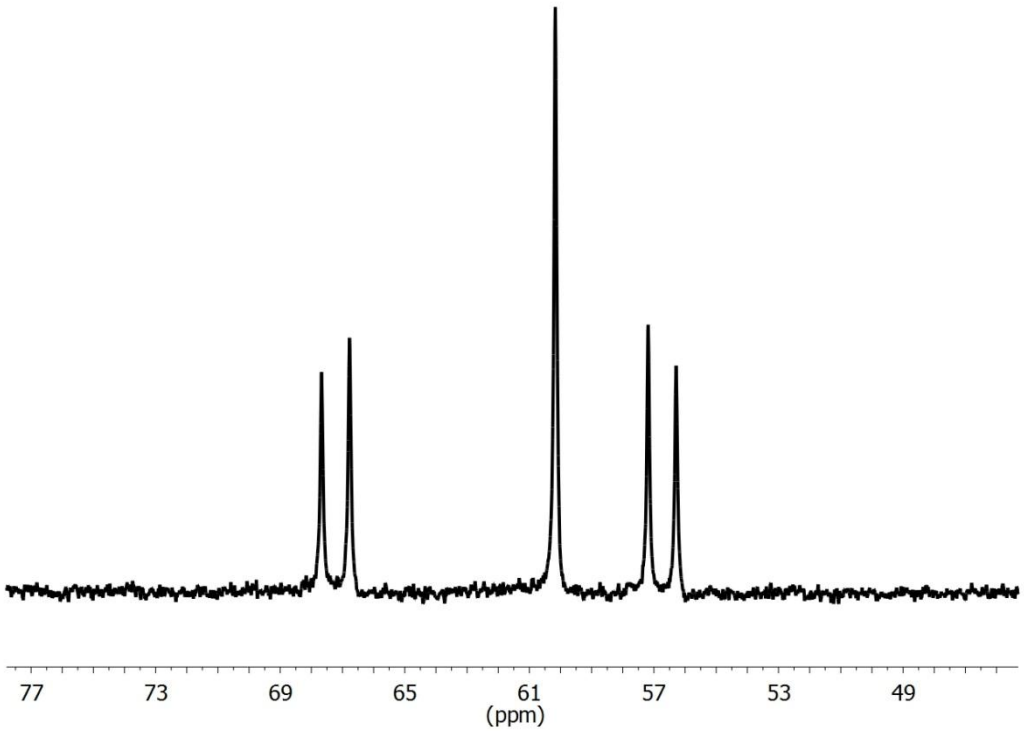

Figure 2.8. ^{31}P NMR spectrum of Fe(Ph_2P-C_6H_4-$CO)_2$ –*cis*-$(CO)_2$ in CD_2Cl_2 solution. asymmetric product: δ67.1, 56.8 doublet, $^3J_{PP}$ = 146 Hz symmetric product: δ60.2, singlet.

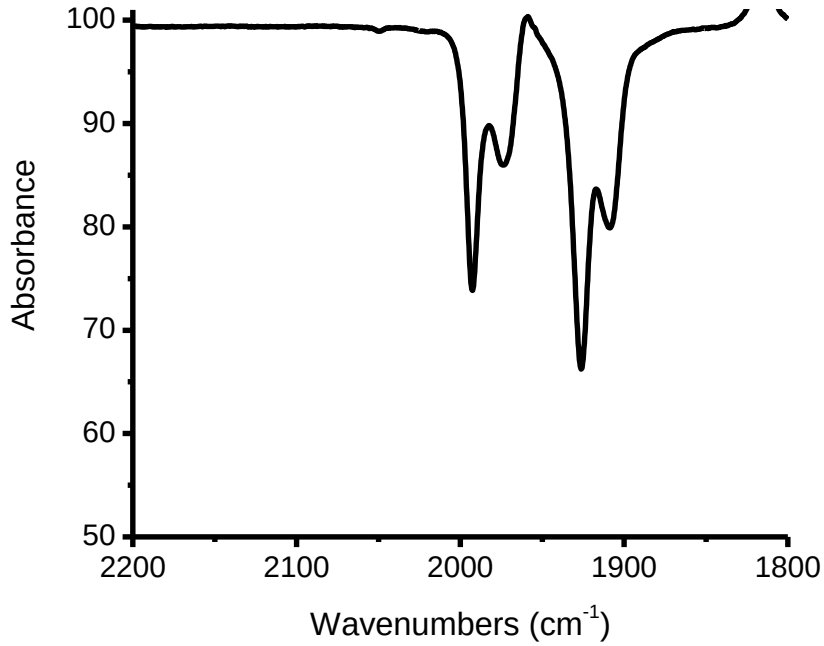

Figure 2.9. IR spectrum of Fe(Ph_2P-C_6H_4-$CO)_2$ –*cis*-$(CO)_2$ in benzene. υ_{CO} (cm^{-1}) asymmetric product:1993, 1926 υ_{CO} (cm^{-1}) symmetric product: 1974, 1909.

To gain some information on how the bis-acyl complexes were formed, we treated complex **1** with additional $Ph_2PC_6H_4$-2-C(O)SPh. No reaction occurred at room temperature. The mixture was heated to reflux in toluene for hours and the diacyl $Fe(Ph_2PC_6H_4CO)_2(CO)_2$ products were detected by IR spectroscopy. Gas chromatographic analysis of the product mixture confirmed the formation of Ph_2S_2. The reaction conditions also result in degradation of the starting material, but the products can be isolated in low yield after purification by silica gel chromatography. Thioester addition to the monomeric tricarbonyl $Fe(Ph_2PC_6H_4CO)(SPh)\ (CO)_3$ (see Chapter 3) at room temperature gave no reaction.

Thioester Derivatives of Nitrogen-based Heterocycles. We also examined reaction of thioester-functionalized *N*-heterocycles with Fe(0) reagents. The thiophenol esters of quinoline-8-carboxylic acid and 2-hydroxy-4-methyl-pyridine-6-acetic acid were synthesized by the carbodiimide coupling method used for the phosphine based thioesters (eq 2.5).

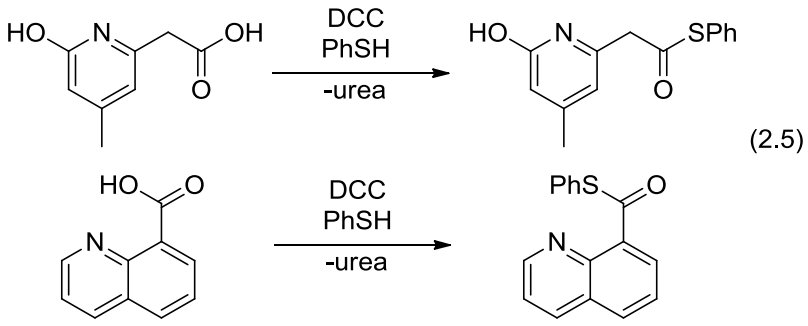

(2.5)

Both derivatives were reactive toward $Fe_2(CO)_9$ and $Fe(bda)(CO)_3$ to give products with υ_{CO} shifts similar to **1**, but the overall intensity of each CO band is quite different (Figure 2.10). The products do not feature any acyl bands in the IR spectrum, and the products for both reactions were found to be the well known

$Fe_2(SPh)_2(CO)_6$. Under the conditions (60 ºC) necessary for reasonable conversions, the nitrogen heterocycles apparently do not bind as robustly as the phosphine derivatives. We found $Fe_2(SPh)_2(CO)_6$ was also formed by the reaction of the simple thioester S-phenyl thioacetate with $Fe(bda)(CO)_3$ at 60 ºC.

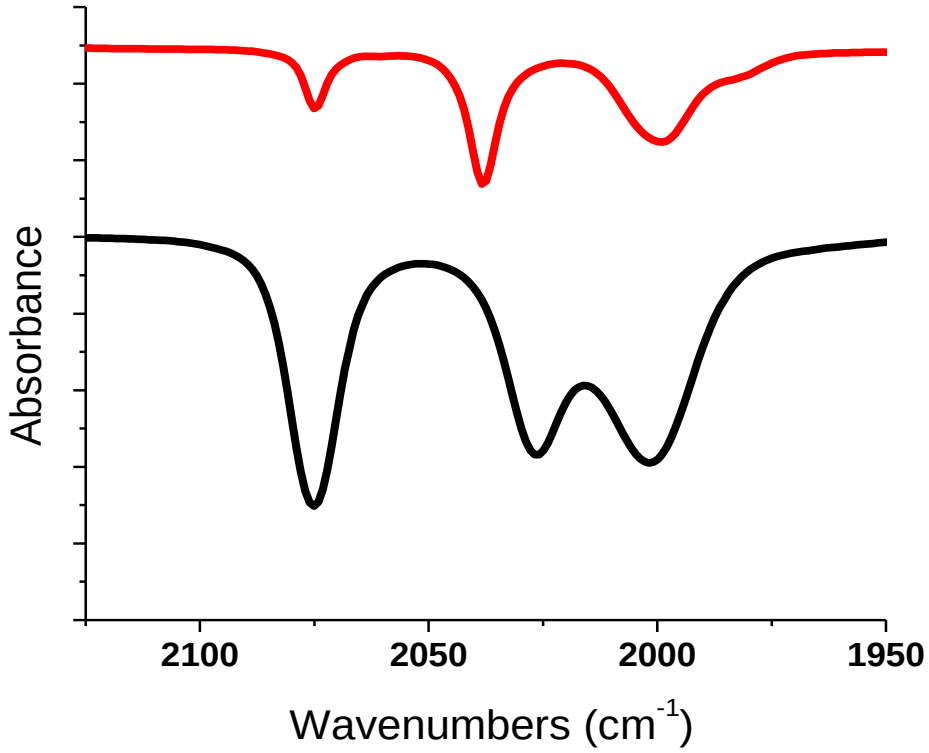

Figure 2.10. The IR spectrum of $Fe_2(SPh)_2(CO)_6$ (red) with υ_{CO} = 2075, 2039. 2001 cm^{-1} and **1** (black) with υ_{CO} = 2075, 2026, 2002 show similar shifts but different intensities for each CO band

In an effort to effect C-S cleavage at mild conditions, specifically for utilization with the nitrogen heterocycle derivatives, we synthesized the highly labile complex $Fe(CO)_3(C_8H_{14})_2$.[12] Spectroscopic analysis of its reaction with $Ph_2PC_6H_4$-2-C(O)SPh indicated displacement of only one cyclooctene (coe) ligand to give a monophosphine adduct that did not react further upon mild heating.[12] The reluctance of this species to undergo oxidative addition is attributed to strong binding of the remaining coe ligand.

Conclusions

Thioester derivatives of 2-diphenylphosphinobenzoic acid are versatile multifunctional reagents that enable easy access to phosphine-stabilized metal acyl thiolato carbonyls. The PhS derivative was examined crystallographically to show the product is a dithiolate- and acyl-bridged diiron(II) derivative $Fe_2(SPh)_2[Ph_2PC_6H_4C(O)]_2(CO)_3$.

The pathway for the oxidative addition of the thioester to Fe(0) is illuminated by the finding that a bulky phosphine thioester and nonelectrophilic analogue gave adducts of the type $Fe(Ph_2PC_6H_4COSR)(CO)_4$. The isolation of such adducts is consistent with phosphine coordination preceding a chelate-assisted oxidative addition[13] of the thioester group. The oxidative addition of the thioester can be envisioned to proceed via coordination of the thioether-like sulfur center.[14]

The overall formation of **1** from $Fe_2(CO)_9$ is proposed to proceed via descreet steps A-D (Scheme 2.6). The barrier required for the initial binding of the phosphine is probably independent of the SR derivative. The formation of the Fe-S bond (step B) is also expected to be fairly independent of the R substituent unless the steric bulk interferes. Step C is highly dependent on the substituent at sulfur. The barrier for the electron withdrawing phenyl derivative is low and we never detect a product prior to C-S bond activation. With an ethyl derivative at sulfur this barrier is higher, and we can isolate products prior to oxidative addition. The reaction also requires longer times for completion. The formation of the diiron complexes similar to **1** require one last step which is

decarbonylation. We find the decarbonylation step is faster with alkyl derivatives than the aryl derivatives, which is counterintuitive to the CO band shifts (higher in S-Aryl). This step is readily reversible in the case of SPh (see chapter 3), and our results suggest the barriers for decarbonylation may not depend strongly on the thiolate, but the barrier for the reverse reaction (carbonylation) is dependent on the thiolate derivative. Therefore, the SEt dimer is lower in overall energy than the SPh dimer.

Scheme 2.6.

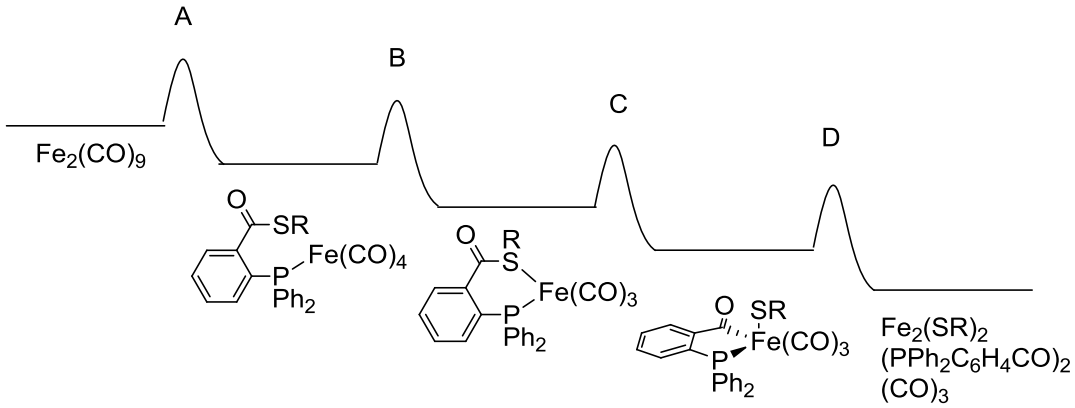

Whereas the phosphine facilitates oxidative addition of the thioester, the low affinity of Fe(0) for pyridines[15] prevented incorporation of the more Hmd-relevant *N*-heterocyclic ligand on the $Fe(CO)_3$ center.

The reaction of **1** with excess thioester phosphine gives the diacyl $Fe(Ph_2PC_6H_4CO)_2(CO)_2$ and the disulfide. This reaction, a new route to metal acyl, does not involve redox at the metal but at sulfur (Scheme 2.7).

Scheme 2.7.

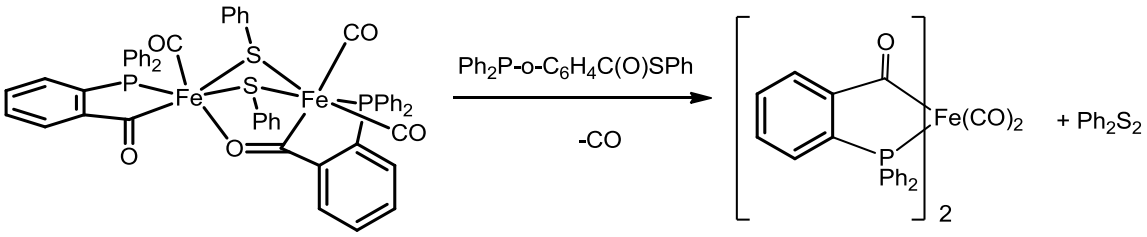

Experimental

General Considerations. Unless otherwise indicated, reactions were conducted using standard Schlenk techniques (N_2) at room temperature with stirring. All solvents were dried and degassed prior to use. Literature procedures afforded the following reagents: Ph_2P-*o*-C_6H_4COOH,[16] 2,6-dimesitylphenylthiol, 2,4,6-triisopropylthiol,[17] 2-hydroxy-4-methylpyridine-6-acetic acid,[18] $[H(Et_2O)]BAr^F{}_4$,[19] and $Fe(bda)(CO)_3$[20] followed. Benzenethiol, 2-methyl-2-propanethiol, ethanethiol, *p*-toluenesulfonylmethyl isocyanide, and Et_4NCN were purchased from Sigma-Aldrich. DCC, 2-mercaptopyridine, and DMAP were obtained from Fluka Analytical. EDAC (1-ethyl-3-(3-dimethylaminopropyl)carbodiimide hydrochloride) was purchased from Chem-Impex International. $MgSO_4$ and $NaHCO_3$ were purchased from Fisher Chemicals. $Fe_2(CO)_9$, was purchased from Strem Chemicals. Quinoline-8-carboxylic acid was purchased from Karl Industries. 2-Methoxythiophenol was obtained from SAFC Supply Solutions (St. Louis, MO). $K^{13}CN$ was purchased from Isotec. The silica gel used was 230-400 mesh Siliaflash® P60 from Silicycle. Electrospray ionization-mass spectra (ESI-MS) were acquired using a Micromass Quattro QHQ quadrupole-hexapole-quadrupole instrument. ^1H and

^{31}P NMR spectra were acquired on Varian UNITY INOVA TM 500NB and UNITY 500 NB instruments. Elemental analyses were performed by the School of Chemical Sciences Microanalysis Laboratory utilizing a Model CE 440 CHN Analyzer. In situ IR spectroscopic measurements were obtained using a ReactIR 4000 (Mettler-Toledo).

The preparation and purification of thioesters was found to be slightly less cumbersome utilizing the water soluble reagent EDAC instead of DCC.

$Ph_2PC_6H_4$-2-C(O)SPh. To a stirred solution of PhSH (870 μL, 8.475 mmol) in CH_2Cl_2 (20 mL) was added 2-diphenylphosphinobenzoic acid (2.36 g, 7.705 mmol) and DCC (1.75 g, 8.475 mmol). The reaction mixture was stirred 1 h, and the precipitated 1,3-dicyclohexylurea was filtered off. The yellow filtrate was concentrated under vacuum, and the residue was purified by column chromatography on silica gel, eluting with 50:1 hexane:ethyl acetate. The light yellow fraction was evaporated to give a crystalline solid that was dried in vacuo. Yield: 2.5 g (82%). ^{31}P NMR (202 MHz, CD_2Cl_2): δ -5.53. FDMS m/z: 398.2 (Calcd for M^+: 398.1). IR (CH_2Cl_2, cm^{-1}): ν_{CO} = 1677 (acyl). Anal. Calcd for $C_{25}H_{19}OPS$ (found): C, 75.36 (75.08); H, 4.81 (4.82); N, 0.00 (0.51).

$Ph_2PC_6H_4$-2-C(O)SEt. To a stirred solution of ethanethiol (146 μL, 1.969 mmol) in CH_2Cl_2 (25 mL) was added 2-(diphenylphosphino)benzoic acid (400 mg, 1.310 mmol), DMAP (64 mg, 0.525 mmol), and 1-EDAC (377.5 mg, 1.969 mmol) successively. The reaction mixture was stirred 1 h at 0 ºC and then warmed to room temperature with stirring 2 h. The solution was washed 3 x with 1 N HCl (30 mL), then washed 2 X with saturated aqueous $NaHCO_3$ (30 mL), and once

with water (30 mL). The CH_2Cl_2 solution was dried over $MgSO_4$. The yellow CH_2Cl_2 layer was concentrated by vacuum, and the yellow oil was recrystallized from CH_2Cl_2 /hexanes to give an oily light yellow powder. This powder was dried overnight to give a white solid. Yield: 300 mg (65% yield). ^{1}H NMR (500 MHz, CD_2Cl_2): δ 1.23 (t, 3H, CH_2CH_3, $^3J_{HH}$ = 7.4 Hz), 2.96 (q, 2H, CH_2CH_3, $^3J_{HH}$ = 7.4 Hz) 6.985 (m, 1H, aryl-H), 7.21-7.42 (m, 4H, aryl-H), 7.88 (m, 1H, aryl-H). ^{31}P NMR (202 MHz, CD_2Cl_2): δ -5.28. ESI-MS m/z: 351.4 (Calcd for MH^+: 351.1). IR (CH_2Cl_2, cm^{-1}): ν_{CO} = 1657 (acyl).

$Ph_2PC_6H_4$-2-C(O)S^{t}Bu. To a stirred solution of 2-methyl-2-propane thiol (295μL, 2.612 mmol) in CH_2Cl_2 (25 mL) was added 2-(diphenylphosphino)-benzoic acid (400 mg, 1.310 mmol), DMAP (67 mg, 0.548 mmol), and 1-EDAC (372.5 mg, 1.959 mmol) successively. The reaction was stirred 1 h at 0 ºC and then 10 h at room temperature. The solution was washed 3 x with 1 N HCl (30 mL), followed by 2 X with saturated aqueous $NaHCO_3$ (30 mL), and once with water (30 mL). The CH_2Cl_2 solution was dried over $MgSO_4$. The yellow CH_2Cl_2 layer was concentrated by vacuum, and the resulting yellow oil was crystallized from CH_2Cl_2/hexanes to give a light yellow powder. Yield: 370 mg (74.8%). ^{1}H NMR (500 MHz, CD_2Cl_2): δ = 1.433 (s, 9H, ^{t}Bu), 6.961 (m, 1H, aryl-H), 7.21-7.42 (m, 12H, aryl-H), 7.881 (m, 1H, aryl-H). ^{31}P NMR (202 MHz, CD_2Cl_2): δ = -5.92. ESI-MS m/z: 379.4 (calcd for MH^+: 379.1). IR (CH_2Cl_2, cm^{-1}): ν_{CO} = 1656 (acyl).

$Ph_2PC_6H_4$-2-C(O)S(C_6H_4-2-OMe). To a stirred solution of 2-methoxythiophenol (2 mL, 16.4 mmol) in CH_2Cl_2 (50 mL) was added 2-(diphenylphosphino)benzoic acid (4.72 g, 15.4 mmol) and DCC (3.50 g, 17.0

mmol) successively. The reaction mixture was stirred for 1.5 h, and the precipitated 1,3-dicyclohexylurea was filtered off. The filtrate was concentrated under vacuum, and residue was purified by column chromatography, eluting with 40:1 hexane/ethyl acetate. The light yellow fraction was evaporated to give a yellow crystalline solid that was dried in vacuo. Yield: 5.88 g (89% yield). ^{1}H NMR (500 MHz, C_6D_6): δ 3.21 (s, 3H, OC*H*$_3$), 6.435 (d, 1H, aryl-H), 6.71 (t, 1H, aryl-H), 6.89 (m, 2H, aryl-H), 7.01 (s, 8H, aryl-H), 7.33 (m, 4H, aryl-H), 7.405 (d, 1H, aryl-H), 8.18 (m, 1H, aryl-H). ^{31}P NMR (202 MHz, CD_2Cl_2): δ -5.13. ESI-MS m/z: 429.2 (calcd for MH^+: 429.1). IR (CH_2Cl_2, cm^{-1}): ν_{CO} = 1676 (acyl). Anal. Calcd for $C_{26}H_{21}OPS$ (found): C, 72.88 (72.49); H, 4.94 (4.82); N, 0.00 (0.41).

$Ph_2PC_6H_4$-2-C(O)SC_6H_2-2,4,6-$^{i}Pr_3$. To a stirred solution of 2,4,6-triisopropylphenylthiol (623 mg, 2.636 mmol) in CH_2Cl_2 (25 mL) was added 2-(diphenylphosphino)benzoic acid (807.5 mg, 2.636 mmol), DMAP (71.2 mg, 0.5272 mmol), and 1-EDAC (671.7 mg, 3.50 mmol) in that order. The reaction solution was stirred 6 h and then washed 3 x with 1 N HCl (30 mL), followed by 2 X with saturated aqueous $NaHCO_3$ (30 mL), and once with water (30 mL). The CH_2Cl_2 solution was dried over $MgSO_4$. The solvent was removed by vacuum. The white solid was washed with hexanes (20 mL) and dried under vacuum. Yield: 1.21 g (88% yield). ^{1}H NMR (500 MHz, CD_2Cl_2): δ 1.13 (d of d, 12H, 2,6-CH(C*H*$_3$)$_2$, $^{3}J_{HH}$ = 22.3 Hz, $^{5}J_{HH}$ = 6.5 Hz), 1.27 (d, 6H, 4-CH(C*H*$_3$)$_2$, $^{3}J_{HH}$ = 6.9 Hz), 2.92 (p, 1H, 4-C*H*(CH$_3$)$_2$, $^{3}J_{HH}$ = 6.9 Hz), 3.42 (p, 2H, 2,6-C*H*(CH$_3$)$_2$, $^{3}J_{HH}$ = 6.7 Hz), 7.02 (m, 1H, aryl-H), 7.11 (s, 2H, aryl-H), 7.21 (m, 4H, aryl-H), 7.32 (m, 6H, aryl-H), 7.44 (m, 1H, aryl-H), 7.51 (m, 1H, aryl-H), 8.23 (m, 1H, aryl-H). ^{31}P

NMR (202 MHz, CD_2Cl_2): δ -5.59. ESI-MS m/z: 525.3 (calcd for MH^+: 525.2). IR (CH_2Cl_2, cm^{-1}): ν_{CO} = 1668 (acyl). Anal. Calcd for $C_{34}H_{37}OPS$ (found): C, 77.83 (77.73); H, 7.11 (7.20); N, 0.00 (0.36).

$Ph_2PC_6H_4$-2-C(O)SC_6H_3-2,6-(C_6H_2-2,4-6-Me_3)$_2$. To a stirred solution of 2,6-dimesitylphenylthiol (1000 mg, 2.89 mmol) in CH_2Cl_2 (20 mL) was added 2-diphenylphosphinobenzoic acid (884 mg, 2.89 mmol), DMAP (35 mg, 0.29 mmol), and EDAC·HCl (830 mg, 4.33 mmol) successively. The reaction solution was stirred for 3.5 h and then washed 3x with 1 N HCl (30 mL), followed by 2 x with saturated aqueous $NaHCO_3$ (30 mL), and once with water (30 mL). After drying over $MgSO_4$, the solution was evaporated. The residue was dissolved in hexanes (8 mL) and precipitated a white solid within 15 min. The solid was collected by filtration, washed with 5 mL of hexanes, and dried under vacuum. Yield: 1.32 g (74%). ^{1}H NMR (500 MHz, CD_2Cl_2): δ 1.96 (s, 12H, mesityl-2,6-C*H*$_3$), 2.27 (s, 6H, mesityl-4-C*H*$_3$), 6.86 (s, 5H, aryl-H), 6.98-7.35 (15 H, aryl-H), 7.54 (t, 1H, aryl-H). ^{31}P NMR (202 MHz, CD_2Cl_2): δ -8.39. ESI-MS m/z: 635.6 (Calcd for MH^+: 635.3). IR (CH_2Cl_2, cm^{-1}): ν_{CO}=1674 (acyl). Anal. Calcd for $C_{43}H_{39}OPS$ (found): C, 81.36 (80.89); H, 6.19 (6.32); N, 0.00 (0.46).

$Ph_2PC_6H_4$-2-C(O)S-2-(C_5H_4N). To a stirred solution of 2-mercaptopyridine (450 mg, 4.04 mmol) in CH_2Cl_2 (20 mL) was added 2-(diphenylphosphino)benzoic acid (1.00 g, 3.27 mmol), and DCC (707 mg, 3.43 mmol) in that order. The reaction mixture was stirred 1 h, and the white precipitate of 1,3-dicyclohexylurea was filtered off. The filtrate was concentrated under vacuum, and the product was purified by column chromatography on silica

gel, eluting with hexane/ethyl acetate, (40/1). The light yellow fraction was evaporated to give a crystalline solid that was dried in vacuo. Yield: 939 mg (72% yield). ^{31}P NMR (202 MHz, CD_2Cl_2): δ -4.71. ESI-MS m/z: 400.2 (Calcd for MH^+: 400.1). IR (CH_2Cl_2, cm^{-1}): ν_{CO} = 1678 (acyl).

2-HO-4-Me-6-[$CH_2C(O)SPh$]-C_5H_2N. To a stirred solution of PhSH (61.4 μL, 0.5982 mmol) in THF (50 mL) was added 2-hydroxy-4-methylpyridine-6-acetic acid (100 mg, 0.5982 mmol), and DCC (123.4 mg, 0.5982 mmol) successively. The reaction mixture was stirred 4 days. Solvent was removed under vacuum, and CH_2Cl_2 (20 mL) was added. The precipitated 1,3-dicyclohexylurea was filtered off. The filtrate was concentrated under vacuum, and the yellow residue was washed with hexanes. The solid was extracted into ~15 mL of EtOAc, and this extract was filtered through a ~5-cm. plug of silica gel. Solvent was removed by vacuum, and the residue was recrystallized from CH_2Cl_2 by the addition of hexanes, giving a white powder. Yield: 62 mg (40%). ^{1}H NMR (500 MHz, CD_2Cl_2): δ 2.23 (s, 3H, 4-C*H*$_3$), 3.89 (s, 2H, C*H*$_2$C(O)S) 6.15 (s, 1H, pyridyl-H), 6.34 (s, 1H, pyridyl-H), 7.43 (m, 5H, SC_6*H*$_5$). ESI-MS m/z: 260.3 (Calcd for MH^+: 260.1). IR (CH_2Cl_2, cm^{-1}): ν_{CO}=1657 (acyl). Anal. Calcd for $C_{14}H_{13}NO_2S$ (found): C, 64.84 (64.96); H, 5.05 (5.61); N, 5.40 (6.14).

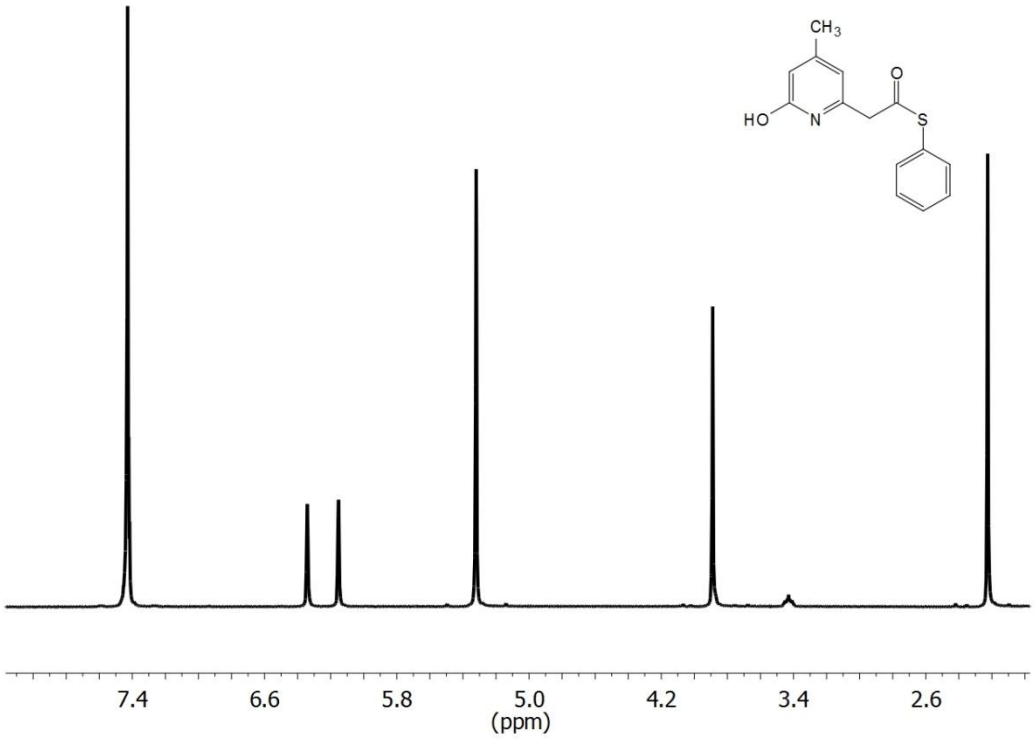

Figure 2.11. ^{1}H NMR spectrum of 2-HO-4-Me-6-[$CH_2C(O)SPh$]-C_5H_2N in CD_2Cl_2.

$Fe(Ph_2PC_6H_4C(O)SC_6H_3$-2,6-$Ar^*_2)(CO)_4$ (Ar*=2,4,6-trimethylphenyl). A solution of $Ph_2PC_6H_4C(O)SC_6H_3$-2,6-Ar^*_2 (94.2 mg, 0.148 mmol) in 20 mL of CH_2Cl_2 was transferred to a mixture 54 mg (0.148 mmol) of $Fe_2(CO)_9$ in 10 mL of CH_2Cl_2 at 0 ºC. The mixture was stirred for 15 min. and then allowed to warm to room temperature. The mixture was evaporated to dryness under vacuum, and the solid was rinsed with ~15 mL of hexanes. The solid was recrystallized from 15 mL Et_2O / 30 mL of hexanes. Yield: 90 mg (76 %). ^{31}P NMR (202 MHz, CD_2Cl_2): δ72.0 (s). IR (THF, cm^{-1}): ν_{CO}= 2048, 1969, 1950, 1933. IR spectroscopic measurements indicated that a solution of the compound in refluxing THF remained unchanged for 24 h.

Synthesis of $Fe(Ph_2PC_6H_4C(O)SEt)(CO)_4$ Prepared analogously to $Fe(Ph_2PC_6H_4C(O)SC_6H_4$-2,6-$(Ar^*)_2(CO)_4$. Yield: 95 mg (86 %) ^{31}P NMR (202 MHz, CD_2Cl_2): δ72.6 (s). IR (CH_2Cl_2, cm^{-1}): ν_{CO} = 2049, 1972, 1935. Upon reflux in THF over 8 hours $Fe_2(SEt)_2(PCO)_2(CO)_3$ was formed. This complex was independently prepared via the reaction of $Fe(bda)(CO)_3$ and $Ph_2PC_6H_4C(O)SEt$ similarly to **1**. Yield: 90 mg (25 %) IR (CH_2Cl_2, cm^{-1}): ν_{CO} = 2012, 1960, 1916.

$Fe(Ph_2PC_6H_4CO)(CO)_2$. A solution of 100.9 mg (0.187 mmol) of **1** and of 256.2 mg (0.643 mmol) of $Ph_2PC_6H_4$-2-C(O)SPh in 20 mL of toluene was heated to 95 ºC for 16 h. Solvent was removed by reduced pressure and the residue was dissolved in minimal 2:1 CH_2Cl_2:hexanes and column chromatography was performed with silica gel, eluting with CH_2Cl_2:hexanes. The first yellow band collected was unreacted $Ph_2PC_6H_4$-2-C(O)SPh, and the second yellow band was the product. Removal of solvent under reduced pressure gave a yellow powder. Yield: 18 mg (14 %). Both C_s and C_2 isomers of $Fe(Ph_2PC_6H_4CO)_2(CO)_2$ with cis CO ligands and the cis-phosphine: trans-phosphine ratio of 2:1. The isomer ratio was unaffected when by heating a sample in refluxing benzene for 24 h. ^{31}P NMR (202 MHz, CD_2Cl_2): δ67 and 57 (C_s-isomer: d, $^2J_{PP}$= 145 Hz), 60 (C_2-isomer: s) (see Figure 2.8). IR (CH_2Cl_2, cm^{-1}): ν_{CO} = 1993 and 1926 (C_2-isomer), 1973 and 1909 (C_s-isomer).

Crystallography

A structural model consisting of the host molecule and a disordered methylene chloride solvate molecule was developed. Since positions for the solvate molecule was poorly determined a second structural model was refined with

contributions from the solvate molecules removed from the diffraction data using the bypass procedure in PLATON (Spek, 1990). No positions for the host network differed by more than two su's between these two refined models. The electron count from the "squeeze" model converged in good agreement with the number of solvate molecules predicted by the complete refinement. The "squeeze" data are reported here.

References

[1] Hiromoto, T.; Ataka, K.; Pilak, O.; Vogt, S.; Stagni, M. S.; Meyer-Klaucke, W.; Warkentin, E.; Thauer, R. K.; Shima, S.; Ermler, U. "The crystal structure of C176A mutated [Fe]-hydrogenase suggests an acyl-iron ligation in the active site iron complex." *FEBS Lett.* **2009**, *583*, 585-590.

[2] Murray, S. G.; Hartley, F. R. "Coordination chemistry of thioethers, selenoethers, and telluroethers in transition-metal complexes." *Chem. Rev.* **1981,** *81,* 365-414.

[3] Seyferth, D.; Womack, G. B.; Archer, C. M.; Dewan, J. C. "A simple route to hexacarbonyldiiron complexes containing a bridging thiolate and an organic bridging ligand by means of [(m-RS)(m-CO)$Fe_2(CO)_6$]- intermediates." *Organometallics* **1989**, *8*, 430-442.

[4] Shaver, A.; Uhm, H. L.; Singleton, E.; Liles, D. C. ""Chelate-assisted" oxidative addition of the carbon-sulfur bond in 8-quinoline thioesters to chlorotris(triphenylphosphine)rhodium." *Inorg. Chem.* **1989**, *28*, 847-851.

[5] Minami, Y.; Kato, T.; Kuniyasu, H.; Terao, J.; Kambe, N. "Reactions of α,β-Unsaturated Thioesters with Platinum(0): Implication of a Dual Mechanism Leading to the Formation of Acyl Platinum." *Organometallics* **2006**, *25*, 2949-2959.

[6] Neises, B.; Steglich, W. "Simple Method for the Esterification of Carboxylic Acids." *Angew. Chem. Int. Ed.*, **1978**, *17*, 522-524.

[7] Myers, E. L.; Raines, R. T. "A Phosphine-Mediated Conversion of Azides into Diazo Compounds." *Angew. Chem., Int. Ed.* **2009**, *48*, 2359-2363.

[8] Zhang, J.; Wang, H.; Xian, M. “An Unexpected Bis-ligation of S-Nitrosothiols.” *J. Am. Chem. Soc.* **2009**, *131*, 3854-3855.

[9] Maresca, L.; Greggio, F.; Sbrignadello, G.; Bor, G. “The anti-syn equilibria of the organothio bridged derivatives of iron carbonyl, (μ -RS)$_2$Fe$_2$(CO)$_6$, and of their monosubstitution products with some phosphines, (μ -RS)$_2$Fe$_2$(CO)$_5$(PR’$_3$).” *Inorg. Chim. Acta* **1971**, *5*, 667–674.

[10] King, R. B. Organosulfur Derivatives of Metal Carbonyls. I. The Isolation of Two Isomeric Products in the Reaction of Triiron Dodecacarbonyl with Dimethyl Disulfide.” *J. Am. Chem. Soc*., 1962, 84, 2460

[11] Conder, H. L.; Darensbourg, M. Y. “The synthesis of group V substituted derivatives of iron pentacarbonyl in high yield.” *J. Organomet. Chem.* **1974**, *67*, 93-97.

[12] Fleckner, H.; Grevels, F. W.; Hess, D. “Tricarbonylbis(.eta.2-cis-cyclooctene)iron: photochemical synthesis of a versatile tricarbonyliron source for olefin isomerization and preparative applications.” *J. Am. Chem. Soc.* **1984**, *106*, 2027-2032.

[13] Landvatter, E. F.; Rauchfuss, T. B. “Chelate-Assisted Oxidative Addition of Functionalized Phosphines to Iridium(I).” *Organometallics* **1982**, *1*, 506.

[14] Looman, S. D.; Giese, S.; Arif, A. M.; Richmond, T. G. “pi-Basicity of the (diamine)tricarbonyltungsten(0) fragment stabilizing [eta]2-aldehyde complexes at tungsten(0).” *Polyhedron* **1996**, *15*, 2809-2811

[15] Boxhoorn, G.; Cerfontain, M. B.; Stufkens, D. J.; Oskam, A. “Photochemistry of [Fe(CO)$_4$L] complexes (L = NMe$_3$ or pyridine) in argon and xenon matrices. Evidence for the formation of C3v[Fe(CO)3L] and the reversible infrared-induced isomerization to Cs[Fe(CO)$_3$L].” *J. Chem. Soc., Dalton Trans.* **1980**, 1336-1341.

[16] Hoots, J. E.; Rauchfuss, T. B.; Wrobleski, D. A. “Substituted Triaryl Phosphines.” *Inorg. Syn.* **1982**, *21*, 175.

[17] Blower, P. J.; Bishop, P. T.; Dilworth, J. R.; Hsieh, T. C.; Hutchinson, J.; Nicholson, T.; Zubieta, J. “The effects of steric hindrance on the chemistry of rhenium and molybdenum nitrosyl thiolato-complexes. The structures of [Mo(SC$_6$H$_2$-iso-Pr$_3$)$_3$(NH$_3$)(NO)] and [Re(SC$_6$H$_3$-iso-Pr$_2$)$_4$(NO)].” *Inorg. Chim. Acta* **1985**, *101*, 63-65.

[18] Royer, A. M.; Rauchfuss, T. B.; Wilson, S. R. “Coordination Chemistry of a Model for the GP Cofactor in the Hmd Hydrogenase: Hydrogen-Bonding and Hydrogen-Transfer Catalysis.” *Inorg. Chem.* **2008**, *47*, 395-397.

[19] Brookhart, M.; Grant, B.; Volpe, A. F. "[(3,5-$(CF_3)_2C_6H_3)_4B$]-[$H(OEt_2)_2$]+: a convenient reagent for generation and stabilization of cationic, highly electrophilic organometallic complexes." *Organometallics* **1992**, *11*, 3920-3922.

[20] Alcock, N. W.; Richards, C. J.; Thomas, S. E. "Preparation of tricarbonyl(.eta.4-vinylketene)iron(0) complexes from tricarbonyl(.eta.4-vinyl ketone)iron(0) complexes and their subsequent conversion to tricarbonyl(.eta.4-vinylketenimine)iron(0) complexes." *Organometallics* **1991**, *10*, 231-238.

Chapter 3

Derivatives of Fe Acyl Thiolate Phosphines: Structural Models of [Fe]-Hydrogenase (Hmd)

Introduction

The conversion of carbon dioxide to methane is accomplished on a massive scale biologically, as indicated by the magnitude of the world's natural gas reserves (6,254 trillion cubic feet).[1] The means by which microorganisms carry out this conversion has been delineated over the previous few decades.[2] This conversion is catalyzed by a sequence of enzyme-catalyzed reactions, and this collection of enzymes are a particularly rich source of cofactors. For example, the biochemical cycle starts with the conversion of CO_2 to a formamide using a methanofuran cofactor and ends with the hydrogenolysis of a CH_3-S bond in coenzyme M (Scheme 3.1). For chemists seeking new ideas on catalysis, these cofactors represent tantalizing and potentially rewarding targets. The biosynthesis and mode of action are areas ripe for discovery, and perhaps applications.

Scheme 3.1. Biochemical pathway for conversion of CO_2 to CH_4

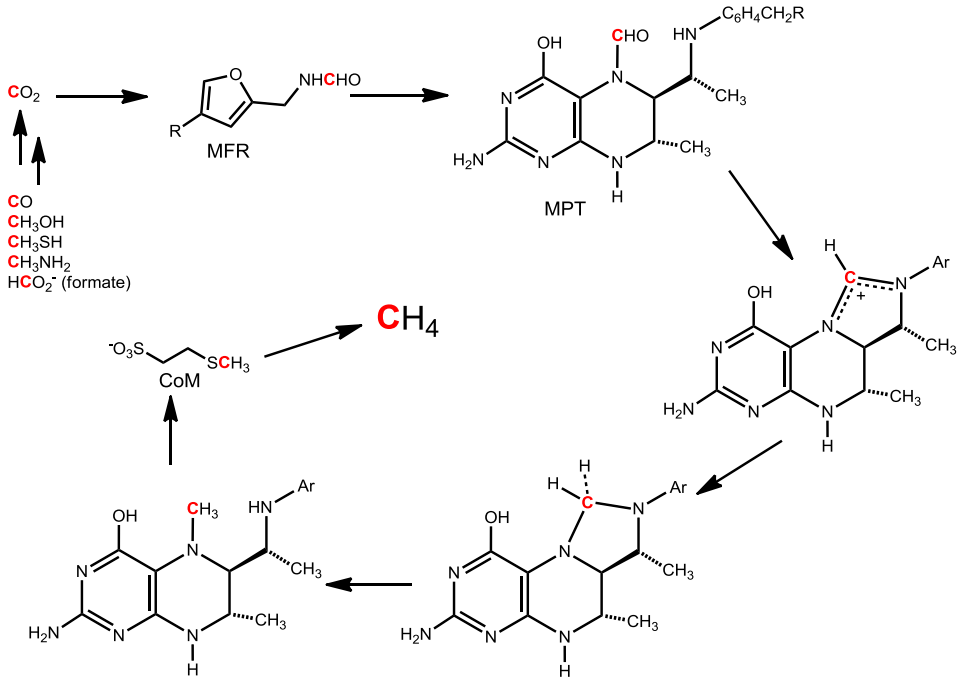

The most recently elucidated step in the archaeal methanogenic cycle is the reduction of a stabilized carbocation to the corresponding methylene derivative (eq 3.1).[3] Normally, this conversion is effected by a [NiFe]-hydrogenase in the hydrogenotrophic methanogens, but under conditions where nickel is insufficiently bioavailable, the organism up-regulates backup enzymes that catalyzes the same conversion.[4,5] The enzymes are called H_2-forming methylenetetrahydromethanopterin dehydrogenase (Hmd, PDB 3F47) and F_{420}-dependent methylene tetrahydromethanopterin dehydrogenase (Mtd, PDB 3IQF).

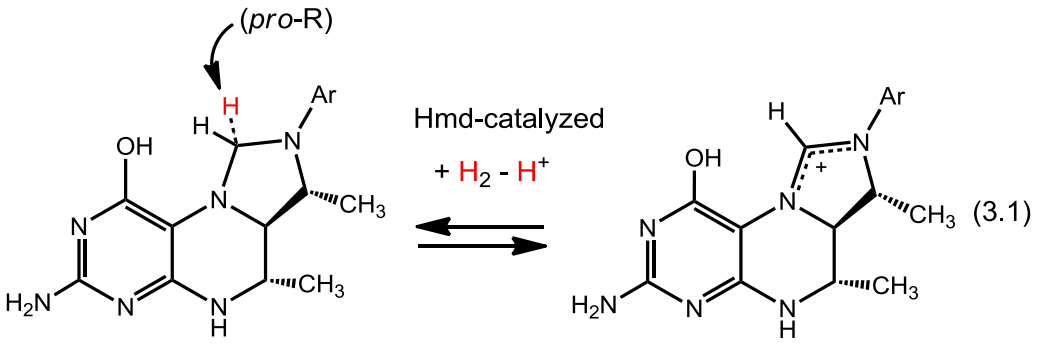

The Hmd enzyme was originally thought to be free of metals because catalysis is relatively insensitive to CO, but later Hmd was found to be an iron enzyme that is inhibited by relatively high pressures of CO.[6] Over the course of the preceding five years, the structure of the active site has been elucidated using both the native protein as well as mutants.[7-11] The protein harbors an active site consisting of the third example of a iron thiolato carbonyl center found in biology.[12,13] The fact that these Fe-SR-CO species catalyze reactions involving H_2 is an example of convergent evolution and an affirmation of their deep significance.[12]

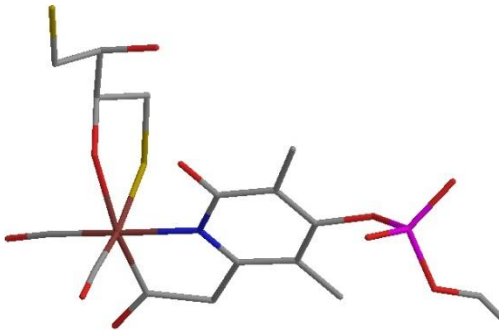

Figure 3.1. Stick model of the jHmd C176A mutant active site with dithiothreitol (DTT) replacing cys176 (PDB 3H65) (*M. jannaschi*). One OH of the DTT occupies the site trans to acyl. Color scheme: brown, Fe; blue, N; red, O; purple, P; yellow, S; grey, C.

The environment of the Fe center in Hmd is $Fe(SR)(acyl)L(CO)_2X$, where L is an N-bonded ligand that is a derivative of either 2-hydroxypyridine or 2-pyridonate and X occupies an apparently labile site. In the crystal structure X has been modeled as oxygen,[8] which is in line with the EXAFS analysis.[14] In the mutant protein, the oxygenic ligand is provided by an alcohol (Figure 3.1). Inhibited forms of the protein have been prepared where X is cyanide and CO. The cyanide derivative (Hmd^{CN}) is stable, but its formation reverses at high

dilution, whereas the CO-inhibited form (Hmd^{CO}) is highly labile, in accord with the weak inhibiting effect of this ligand.[3] These inhibited forms, especially Hmd^{CO} and Hmd^{CN} represent suitable synthetic targets, since they are coordinatively saturated. Furthermore, models for Hmd^{CO} could serve as precursors to catalytically active states.

From the structural perspective, the presence of the acyl ligand is striking. Fe-acyls are common in synthetic organometallic chemistry,[15] for example, $(C_5H_5)(CO)_2FeC(O)Me$ and $[(CO)_4FeC(O)Me]^-$, but are unusual in biology. Acyl nickel intermediate have been invoked in acetogenesis,[16] which is catalyzed by the enzyme acetyl Co-A synthase.[17,18] In Hmd, the acyl ligand may function as a trans directing group, stereoselectively labilizing the site that binds H_2. Normally, acyl ligands are cis labilizing because of the facility of the η^1- to η^2-acyl conversion,[19] but if constrained in a chelate ring as in Hmd's active site, then they may be expected to exert a trans influence comparable to that of an aryl group.[20]

For first generation models of Hmd, we sought to incorporate the most distinctive ligand, the acyl. Prior to our work, acyl thiolato *mono*iron complexes were unknown, although *di*iron complexes of the type $Fe_2(SR)(acyl)(CO)_6$ had been prepared. Thioester-iron interactions may have been involved in the origin of life.[21,22]

We have previously described the oxidative addition of thioester-modified phosphines to Fe(0) reagents to give diiron μ-thiolato species of the type $Fe_2(SPh)_2(Ph_2PC_6H_4CO)_2(CO)_3$.[23] This diferrous species carbonylates to afford the metastable monomer *fac*-$Fe(SPh)(Ph_2PC_6H_4CO)(CO)_3$ (**1**). This tricarbonyl

was found to undergo monosubstitution to give derivatives mimicking other ligand-inhibited forms of Hmd, abbreviated Hmd^{L}. Herein we describe the structural characterization of **1** and its cyanide derivative, which constitute close structural models for the active site of Hmd.

In related Hmd modeling work, Hu and coworkers have generated iron acyls stabilized by 2-mercaptopicoline derivatives. Thus, complexes of the type $Fe(S\text{-}2\text{-}C_5H_3N\text{-}6\text{-}Me)(COMe)L(CO)_2$ are generated by metathetic routes from ferrous acyl iodides to afford μ-thiolato diiron diacyl complexes. Strong field ligands cleave these dimers to give $Fe(\mu\text{-}S\text{-}2\text{-}C_5H_3N\text{-}6\text{-}Me)(COMe)(CO)_2L$ (L = CN^-, RNC, PPh_3, CO).[24] Most early modeling work, which was performed before the discovery of the acyl ligand, focused on the incorporation of pyridine and thiolate ligands to Fe(II) carbonyls (Figure 3.2).[25,26]

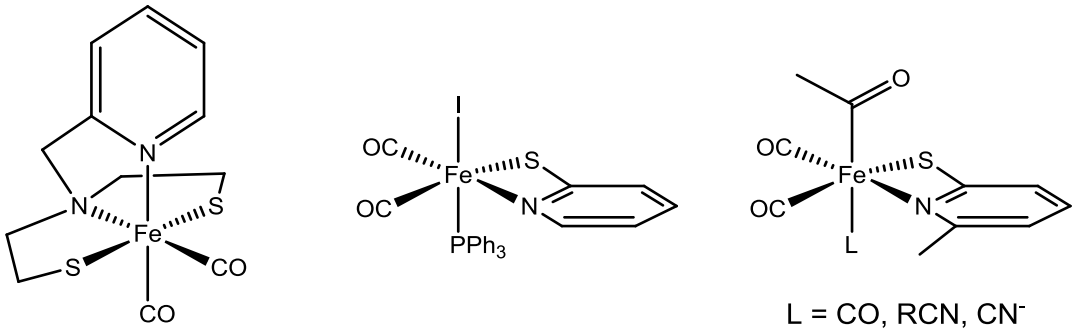

Figure 3.2. Models for the Hmd Fe cofactor.[24-26]

The most recent report in Hmd modeling is also the most similar in terms of Fe ligation and overall geometry. The addition of 2-aminopyridine to $Fe(CO)_4Br_2$ results in a pyridine carbamoyl chelated complex (Scheme 3.2).[27] Addition of mercapto ethanol or 2,6-dimethylbenzenethiol replaced the bromide

to give a bridging diiron dithiolate and Fe monomer respectively. The Iron monomer was crystallized and shown to be a close match for the overall geometry of the Hmd cofactor with a weakly bound solvent molecule trans to the acyl ligand. The one feature noticeably lacking in this model is the presence of a hydroxyl group oriented toward the solvent binding site.

Scheme 3.2. Pickett's synthesis of pyridine carbamoyl-based model for Fe cofactor of Hmd.[27]

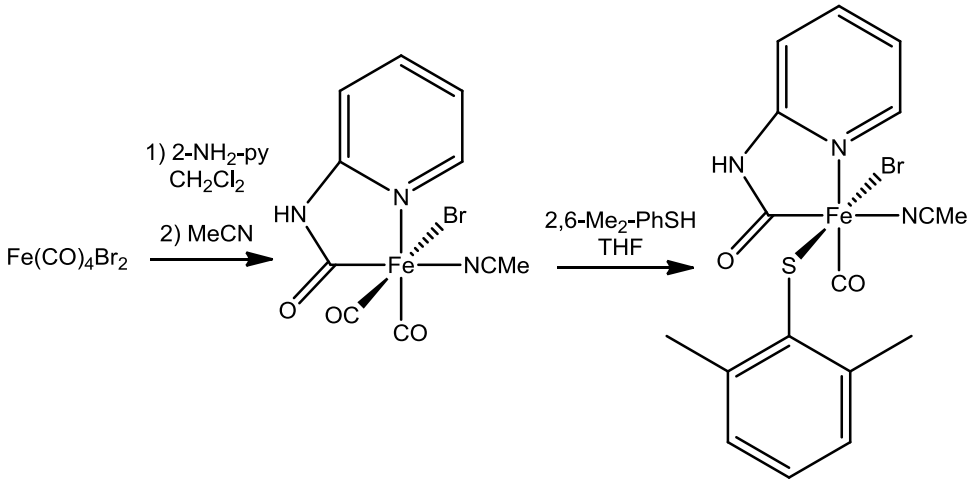

Results

$Fe(SPh)(Ph_2PC_6H_4CO)(CO)_3$. Compound **1** was obtained by high pressure carbonylation of a warm solution of the aforementioned diiron derivative (eq 3.2). Solutions of the monomer **1** were found to decarbonylate, returning to the diiron derivative, but solutions of **1** were stable for days <-20 ºC. Crystalline samples of **1** proved stable at room temperature in air for weeks.

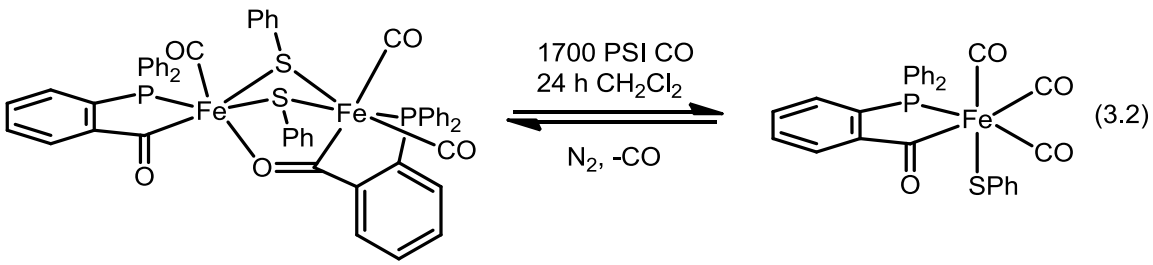

The solution IR spectra of **1** in CH_2Cl_2 and the CO-inhibited form of Hmd were found to match very closely with ν_{CO} = 2075, 2026, 2002 (2074, 2020, 1981 cm^{-1} for Hmd). We were curious about the influence of solvent on the spectrum of our model. To examine this aspect, we re-recorded the spectrum in 1:1 MeOH:CH_2Cl_2, but the spectrum was only slightly affected ($\Delta\nu$ < 4 cm^{-1}) (Figure 3.3).

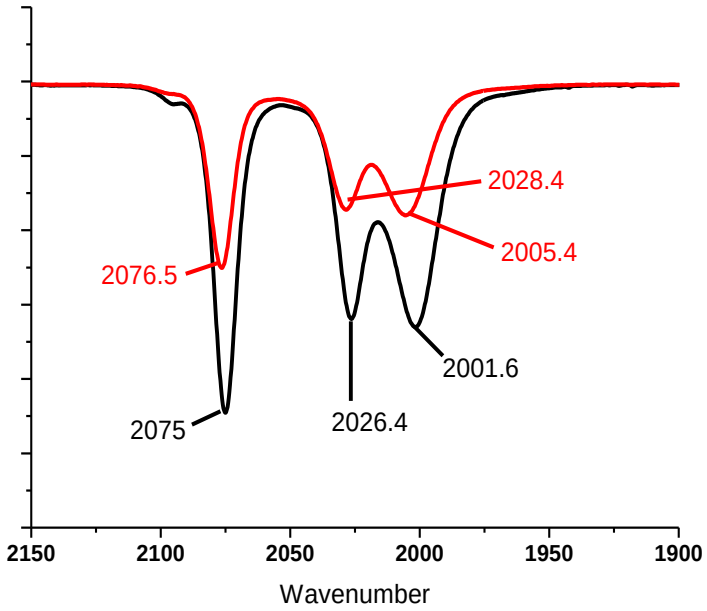

Figure 3.3. IR spectrum of Fe(SPh)[$Ph_2PC_6H_4C(O)$]$(CO)_3$ (**1**) in CH_2Cl_2 solution (black) and after dilution with an equal volume of MeOH (red).

Exposure of a solution of complex **1** to 1 atm of ^{13}CO at room temperature resulted in rapid (<5 min.) exchange of all sites to give $Fe(SPh)(Ph_2PC_6H_4CO)(^{13}CO)_3$ (eq 3.3). The ^{31}P NMR spectrum of this species confirmed the arrangement of the CO ligands, since three separate ^{13}C-^{31}P couplings are observed with J = 58, 21, and 16 Hz (Figure 3.4). In $Fe(CO)_3(PMe_3)(\eta^2\text{-}Me_3SiCCSiMe_3)$, the ^{13}CO-^{31}P coupling constants are 59 (trans) and 35 Hz (cis).[28] In contrast to our result, Hmd only exchanges CO at single site.[10]

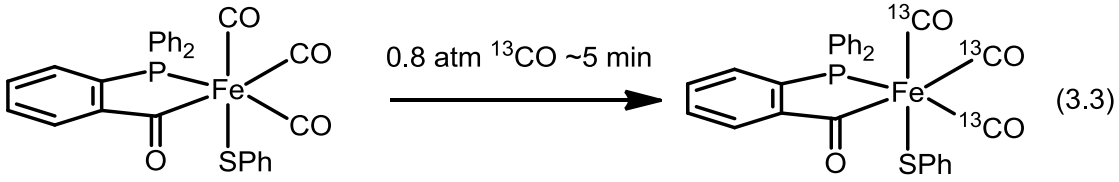

(3.3)

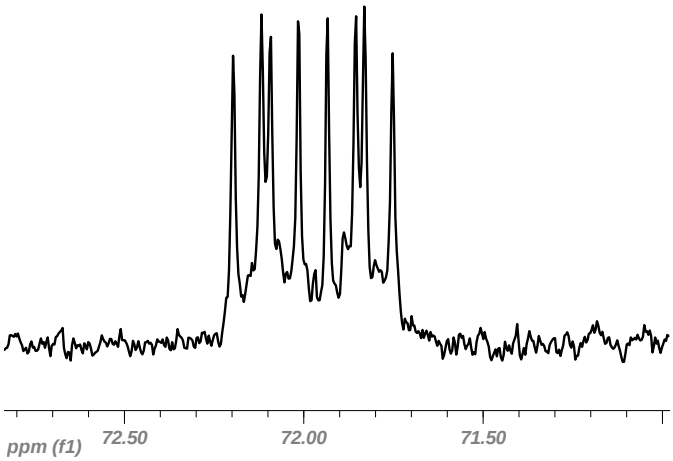

Figure 3.4. ^{31}P NMR spectrum of $Fe(SPh)[Ph_2PC_6H_4C(O)](CO)_3$ (**1**) in CD_2Cl_2 solution after stirring under 0.8 atm of ^{13}CO for ~5 min.

Structure of $Fe(SPh)(Ph_2PC_6H_4CO)(CO)_3$. The tricarbonyl monomer **1** was further characterized by X-ray crystallography (Figure 3.5). The structure of

1 confirms the facial tricarbonyl geometry and compares well with the recent structure of the C176A mutant of Hmd, which has been characterized at 2.15 Å resolution.[8] In this mutant, one cysteinyl ligand is replaced by one thiolate of dithiothreitol, which also provides an alcohol ligand in the coordination site trans to the acyl (see Figure 3.1). The bond distances (and angles) for this structure are compared to the EXAFS data for wild type Hmd in Table 3.1.

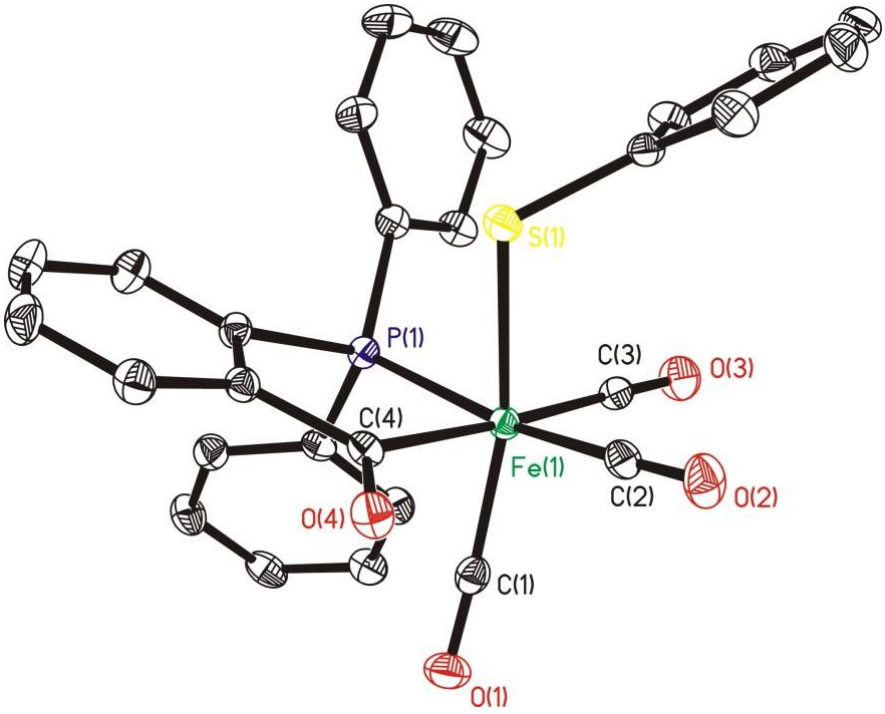

Figure 3.5. Structure of **1**, drawn with 35% probability ellipsoids with Fe, green; P, purple; O, red; S, yellow; C, black. Hydrogen atoms are omitted for clarity.

Table 3.1. Selected Bond Lengths (Å) and Angles (º) for **1** and for the Fe Center of Hmd (EXAFS analysis of sample jHmd in ref. 29).

Bond parameter for 1	Compound 1	*Hmd* *M. jannaschii*[29]
Fe1 - C1	1.7844 (0.0018)	1.769(5)
Fe1 - C2	1.8229 (0.0019)	1.769(5)
Fe1 - C3	1.8395 (0.0018)	1.769(5)
Fe1 - C4	2.0202 (0.0016)	1.88(1)
Fe1 - P1	2.2381 (0.0005)	2.052(9) (Fe-N)
Fe1 - S1	2.3457 (0.0005)	2.335(4)
C4-Fe1-P1	85.40 (0.05)	
C4-Fe1-S1	79.97 (0.05)	
P1-Fe1-S1	84.85 (0.02)	
C1-Fe1-S1	163.69 (0.06)	
C2-Fe1-P1	168.22 (0.05)	
C3-Fe1-C4	176.61 (0.07)	

$[Fe(SPh)(Ph_2PC_6H_4CO)(CN)(CO)_2]^-$. Complex **1** reacts smoothly with cyanide to afford the anion $[Fe(SPh)(Ph_2PC_6H_4CO)(CN)(CO)_2]^-$ ([**2**]$^-$), isolated as its Et_4N^+ salt (eq 3.4). The ^{13}C and ^{31}P NMR spectra for Et_4N[**2**] and its ^{13}CN-labeled derivative indicate that substitution is stereospecific. Cyanide is located cis to the phosphine ligand, on the basis of precedent: in $FeH(^{13}CN)(PPh_2CH_2CH_2PPh_2)_2$, $J(^{31}P,^{13}C)$ = 20 Hz,[3230] vs 24 Hz in Et_4N[**2**](^{13}CN) (Figure 3.6). Unlike **1**, solutions of [**2**]$^-$ are stable with respect to loss of CO as also seen for Hmd^{CN}.[10] The IR spectrum of [**2**]$^-$ and [**2**]$^-$(^{13}CN) in CH_2Cl_2 solution (Figures 3.7, 3.8) also closely match the cyanide-inhibited forms of Hmd, wherein cyanation also proceeds stereoselectively[10] (Figure 3.9, Table 3.2).

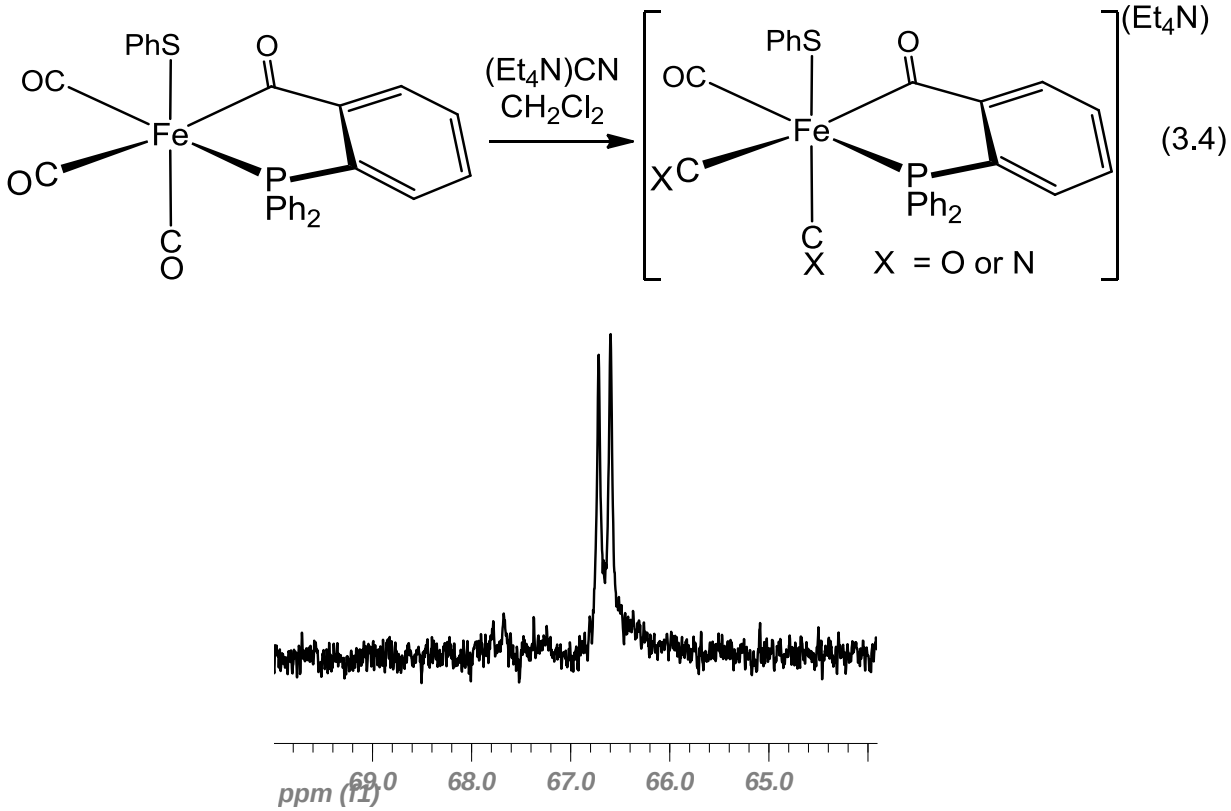

Figure 3.6. ^{31}P NMR spectrum of $Et_4N[Fe(SPh)[Ph_2PC_6H_4C(O)](^{13}CN)(CO)_2]$ Et_4N[**2**](^{13}CN) in CD_2Cl_2 solution.

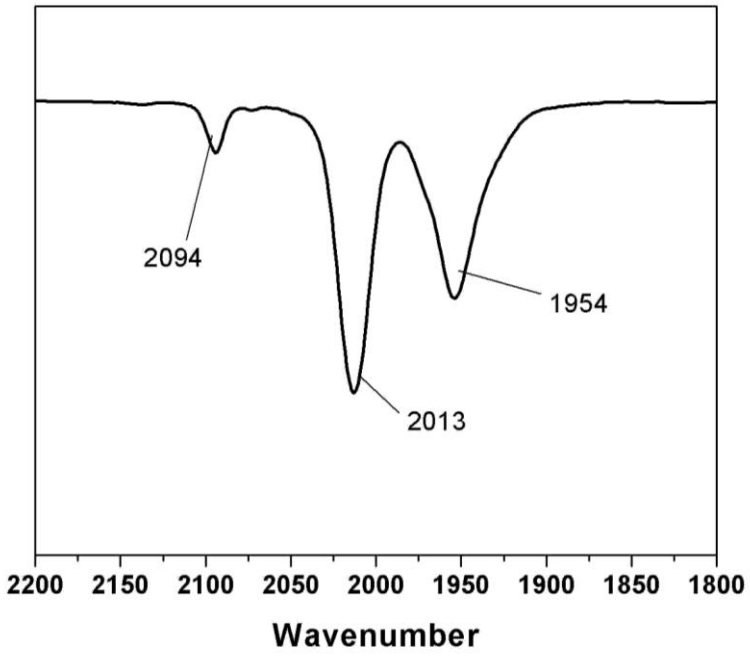

Figure 3.7. IR spectrum of $Et_4N[Fe(SPh)[Ph_2PC_6H_4C(O)](CN)(CO)_2]$ Et_4N[**2**] in CH_2Cl_2 solution.

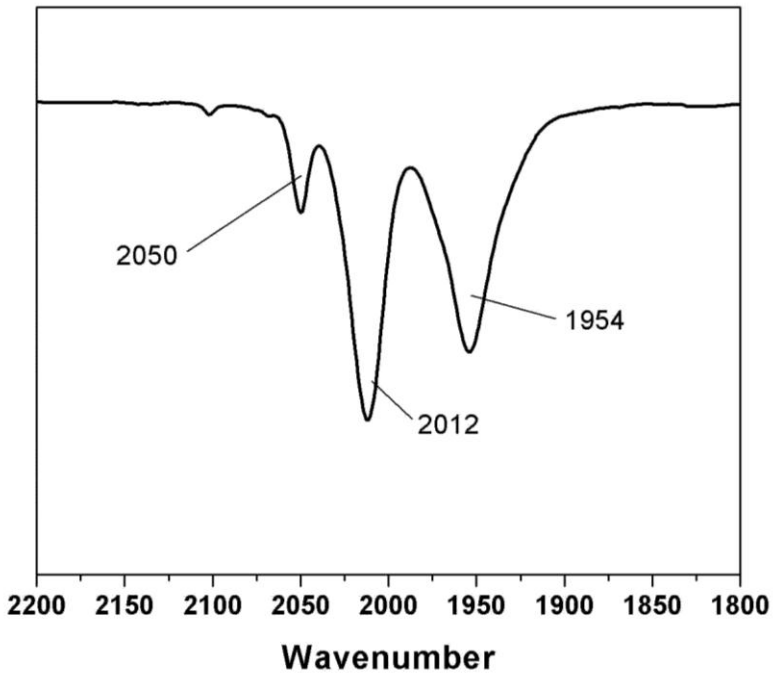

Figure 3.8. IR spectrum of $Et_4N[Fe(SPh)[Ph_2PC_6H_4C(O)](^{13}CN)(CO)_2]$ Et_4N[**2**](^{13}CN) in CH_2Cl_2 solution.

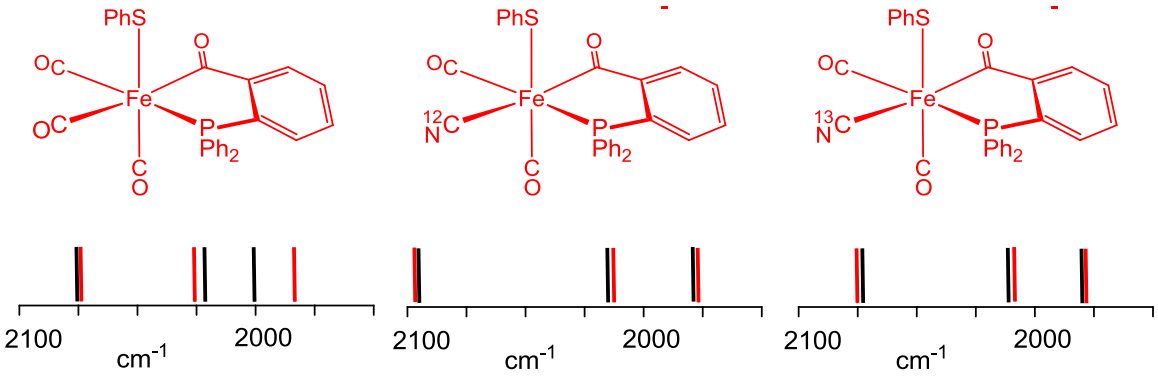

Figure 3.9. IR spectral positions for ν_{CN} and ν_{CO} for selected model compounds and Hmd^{CO} and Hmd^{CN}.

Table 3.2. Selected IR Data for Model Compounds and for Hmd from *M. marburgensis*.[10]

Sample (models in CH_2Cl_2 soln. unless otherwise indicated; enzyme in aqueous soln.)	ν_{CO} (cm^{-1})
Hmd^{CO} from *M. marburgensis*[10]	2074, 2020, 1981
$Fe(SPh)(Ph_2PC_6H_4CO)(CO)_3$ (**1**) (1:1 CH_2Cl_2:MeOH)	2075, 2025, 2001 (2077, 2028, 2005)
Hmd^{CN} from *M. marburgensis*[10]	2090 (ν_{CN}), 2020, 1956
$Et_4N[Fe(SPh)(Ph_2PC_6H_4CO)(CN)(CO)_2]$ (Et_4N[**2**]) (1:1 CH_2Cl_2:MeOH)	2093 (ν_{CN}), 2013, 1954 (2093 (br, ν_{CN}), 2026, 1973)
$Et_4N[Fe(SPh)(Ph_2PC_6H_4CO)(^{13}CN)(CO)_2]$ (Et_4N[**2**]^{13CN})	2050 (ν_{CN}), 2012, 1954
$Fe(SPh)(Ph_2PC_6H_4CO)(CNCH_2Ts)(CO)_2$	2154 (ν_{CN}), 2042, 1988

The cyanide derivative was further characterized by X-ray absorption spectroscopy. The XANES spectrum, indicative of the electronic structure of the iron site, closely matches that of the iron binding site in wild type Hmd^{CN}.[11] The intense pre-edge peak for the new complex is resolved as a doublet, assigned tentatively to the 1s-3d/4p transition(s).* The XANES spectra for both the CN-inhibited enzyme as well as Et_4N[**2**] (Figure 3.10 show) a mild shoulder in their rising edge, followed by a sharp resonance at about 7130 eV and a broad resonance at about 7150 eV. The position of the subsequent minimum at 7170

* The high resolution in the *K*-edge region was achieved with the Si(220) monochromator with an intrinsic resolution of 0.4 eV vs 0.9 eV for Si(111).

eV is mainly attributed to the distance of those ligands dominating the EXAFS pattern (Figure 3.11). The high similarity of its position indicates strong similarities in the overall geometry of the active sites.

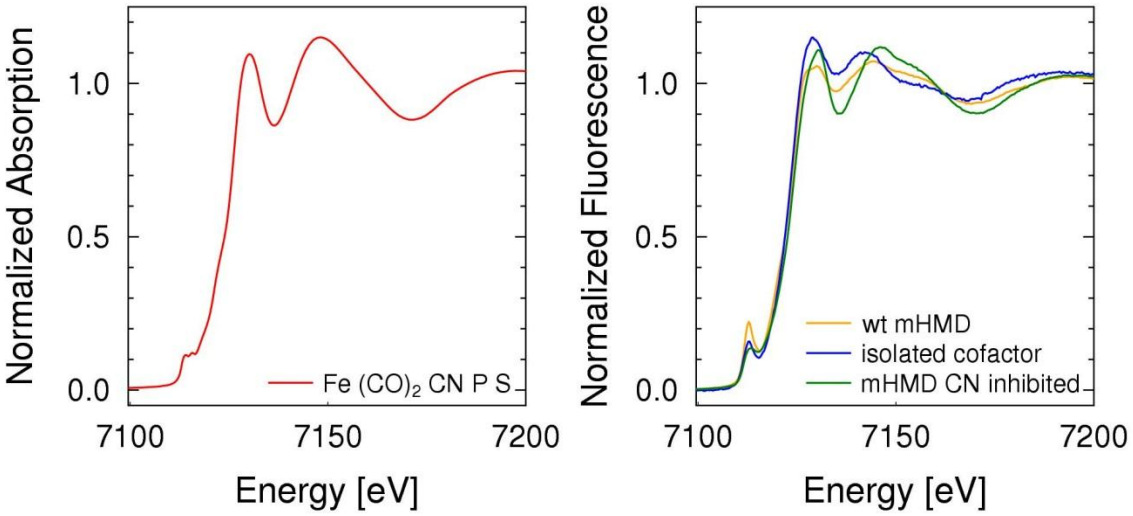

Figure 3.10. XANES spectrum of $Et_4N[Fe(SPh)(Ph_2PC_6H_4CO)(CN)(CO)_2]$ (left) and wild-type Hmd from *M. marburgensis*, the isolated Fe-GP cofactor, as well as the cyanide inhibited protein (right).

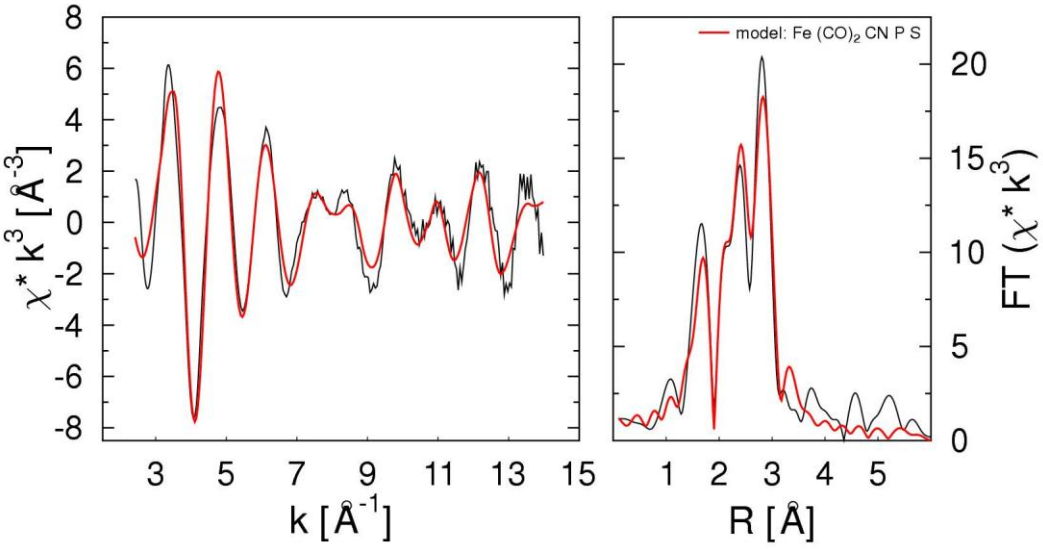

Figure 3.11. EXAFS spectrum and its Fourier transform with fits (red) for the model $Fe(CO)_3(CN)P(S)$ using the parameters in Table 3.3.

Table 3.3. Results of EXAFS Refinements for $Et_4N[Fe(SPh)(Ph_2PC_6H_4CO)(CN)(CO)_2]$ (indices a, b, and c indicate parameters that were refined jointly in order to lower the number of free parameters; Energy range 10 – 750 eV, E_f = -6.3 ± 0.3 eV, Fit index: 0.954).

ligand	*N*	*r* (Å)	$2\sigma^2$ (Å^2)
*C*O	2	1.81 ± 0.01	0.016 ± 0.003
C*O*	2	2.93 ± 0.01	0.012 ± 0.002[a]
*C*N	1	2.07 ± 0.03[c]	0.012 ± 0.004[b]
C*N*	1	3.19 ± 0.03	0.012 ± 0.002[a]
C	1	2.07 ± 0.03[c]	0.012 ± 0.004[b]
P	1	2.18 ± 0.06	0.02 ± 0.01
S	1	2.32 ± 0.02	0.008 ± 0.004

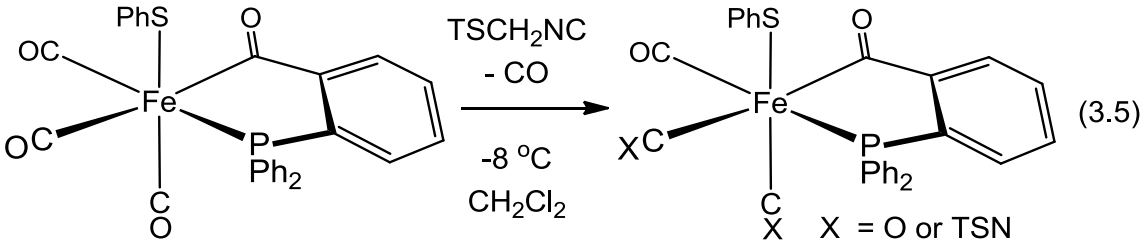

(3.5)

Adducts with $TsCH_2NC$. Reminiscent of its reactivity toward cyanide, complex **1** was found to undergo substitution by $TsCH_2NC$ under mild conditions (eq 3.5). ^{31}P NMR spectroscopic measurements show that substitution occurs in seconds at about -10 °C. The formation of a single derivative (δ70.7 vs 72.5 for **1**; see Table 3.3 or Figure 3.12 for ν_{CO} and ν_{CN}) indicates stereoselective substitution. The substituted complex is stable in solution at temperatures below -10 °C, but ^{31}P NMR measurements indicate that over the course of several

minutes at room temperature, this initial species converts to a mixture of three additional complexes, which are assumed to be isomers or the result of decarbonylation (Figure 3.13). This mixture simplifies over longer reaction times, as indicated by the appearance of two ^{31}P NMR signals in a 1:1 ratio, assigned to metastable diiron derivatives of the type $Fe_2(SPh)_2(Ph_2PC_6H_4CO)_2(CO)(RNC)_2$.

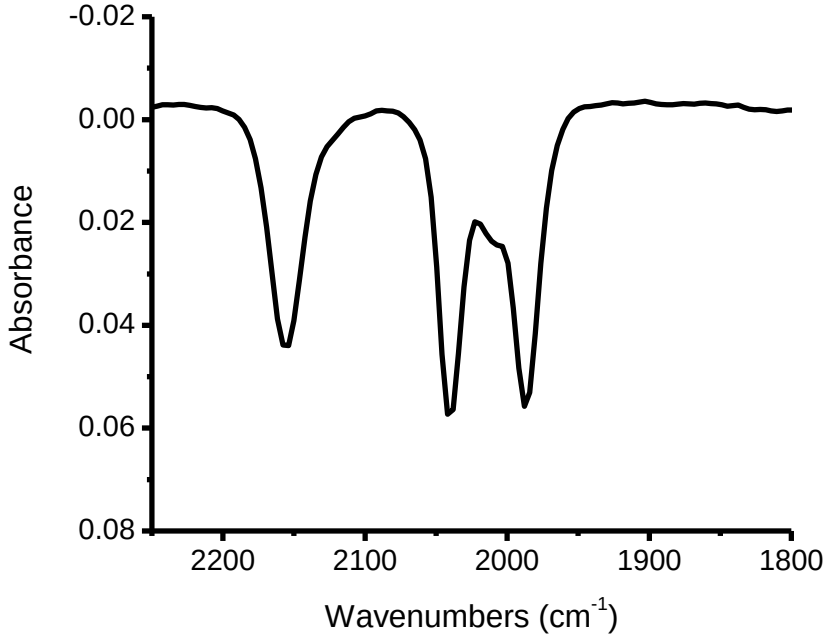

Figure 3.12. IR spectrum of $[Fe(SPh)(Ph_2PC_6H_4C(O)]_2(CNCH_2Ts)(CO)_2]$. $\nu_{CO}(cm^{-1})$: 2038, 1983 $\nu_{CN}(cm^{-1})$: 2153. Spectrum obtained on ReactIR^{TM} 4000 at -10 ºC.

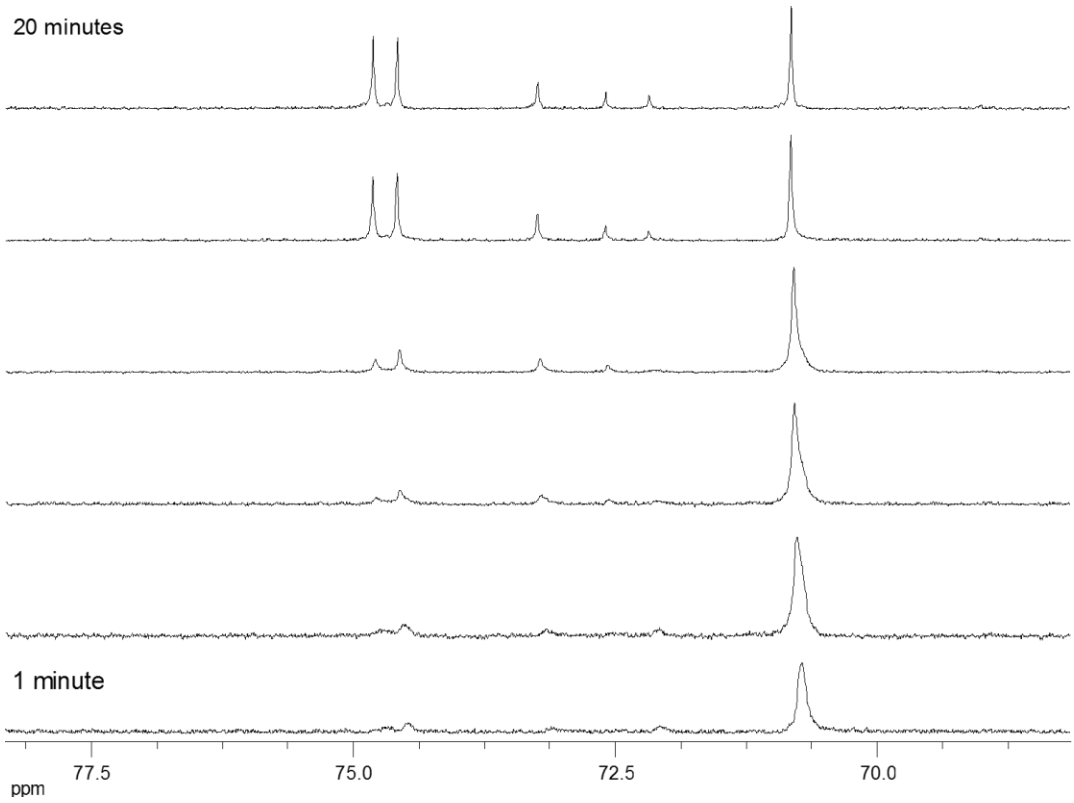

Figure 3.13. ^{31}P NMR spectrum of [Fe(SPh)($Ph_2PC_6H_4C(O)$]$_2$($CNCH_2Ts$)(CO)$_2$] in CD_2Cl_2 at room temperature at 1,4,8,12,16, and 20 minutes.

Protonation. Tricarbonyl **1** was found to undergo protonation at low temperatures to give unstable derivatives. In CH_2Cl_2 solution at –30 ºC, protonation with $H(OEt_2)_2BAr^F_4$ (Ar^F = 3,5-$(CF_3)_2C_6H_3$) afforded a single product [**1**H]$^+$ (^{31}P NMR: δ68.1, broad), which lacks apparent hydride signals in its ^{1}H NMR spectrum. The IR spectrum (-26 ºC) showed ν_{CO} bands (2090, 2041, and 2024 cm^{-1}), which are shifted by an average of 18 cm^{-1} to higher energies vs those for **1**. Addition of Et_3N to this cold solution of [**1**H]$^+$ cleanly returned **1** (IR analysis). The IR and NMR data are thus consistent with protonation at a ligand, probably the thiolate[31] or the acyl group.[32] The corresponding *S*- and *O*-protonation of the ferrous thiolate (C_5H_5)Fe(CO)$_2$*S*Ph and the ferrous acyl (C_5H_5)Fe(CO)(PPh_3)C(*O*)Me, respectively with HBF_4 and HBr induces shifts in

ν_{CO} by 40 and 32 cm^{-1}.[31,32] Upon warming its solution to 20 ºC, [**1**H]$^+$ was found to convert to a new product (^{31}P NMR: δ76.7), which decomposed over the course of a few minutes (Figure 3.14).

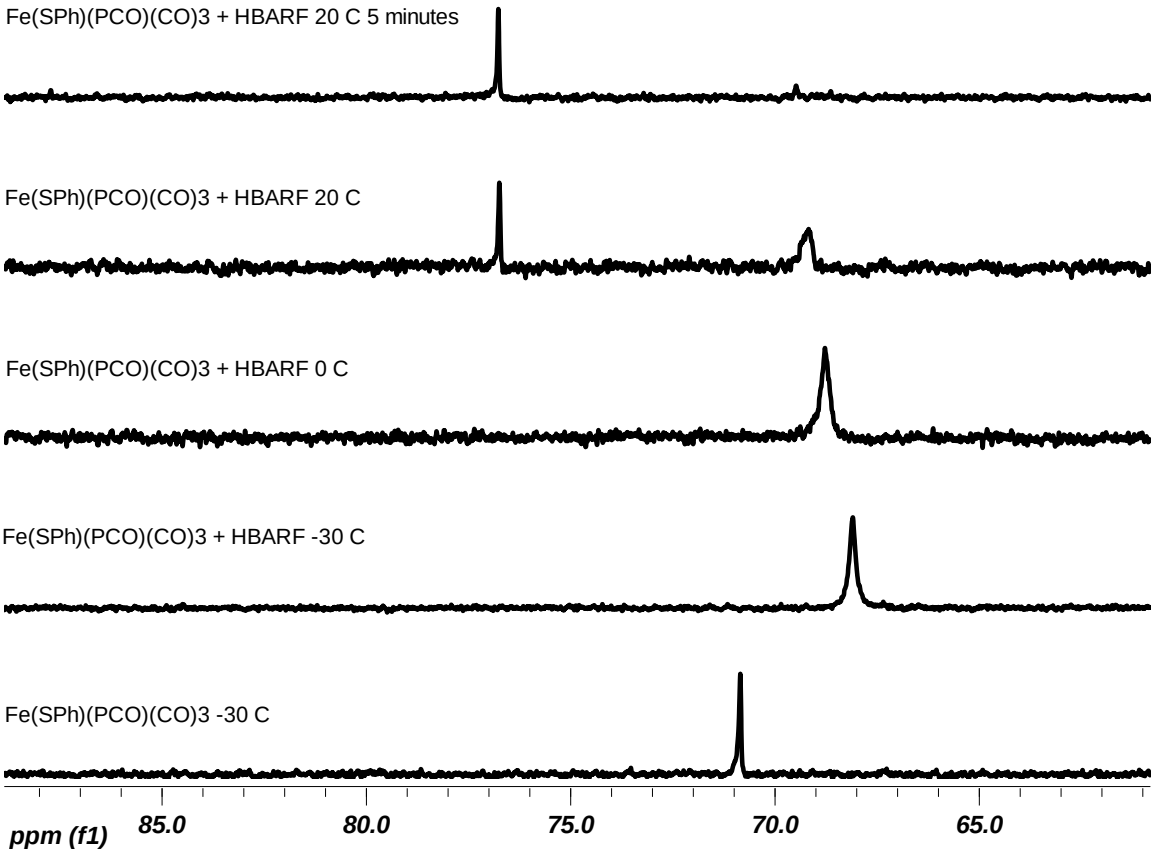

Figure 3.14. ^{31}P NMR spectrum of Fe(SPh)($Ph_2PC_6H_4C(O)$)$(CO)_3$ protonation with $H(OEt_2)_2BAr^F{}_4$ and isomerization upon warming.

Conclusions

Thioester derivatives of 2-diphenylphosphinobenzoic acid are versatile multifunctional reagents that enable easy access to phosphine-stabilized metal acyl thiolato carbonyls. The PhS derivative was examined in detail and shown to adopt a structure very similar to the one modeled for the Fe site in Hmd^{CO}.[9] The

major difference between our models and the active site is the presence of the phosphine ligand in place of the pyridyl group of the GP cofactor, but the phosphorus center offers the distinct advantage of enabling ^{31}P NMR analysis of reaction mixtures.

Whereas the phosphine facilitates oxidative addition of the thioester, the low affinity of Fe(0) for pyridines[33] prevented incorporation of the more biomimetic *N*-heterocyclic ligand on the $Fe(CO)_3$ center. Hu et al. have addressed this challenge by installing the pyridine group to preformed ferrous acyl compounds.[24]

Reactivity studies reinforce the electronic similarity between our model and the active site. Hmd stereoselectively binds ^{13}CO and CN^-.[10] ^{31}P NMR data show that **1** undergoes stereoselective substitution by both CN^- and $TsCH_2CN$, but CO is so labile in our model that stereoselective binding of ^{13}CO was not observed (Scheme 3.3). The lability of the site trans to acyl combined with the bridging tendency of thiolate ligands explains the facile conversion of **1** into the related $Fe_2(SR)_2$ derivative.[23] Our results suggest that the Fe-GP cofactor might be expected to degrade via dimerization.

Scheme 3.3. Proposed reactions of **1** involving substitution trans to the acyl ligand.

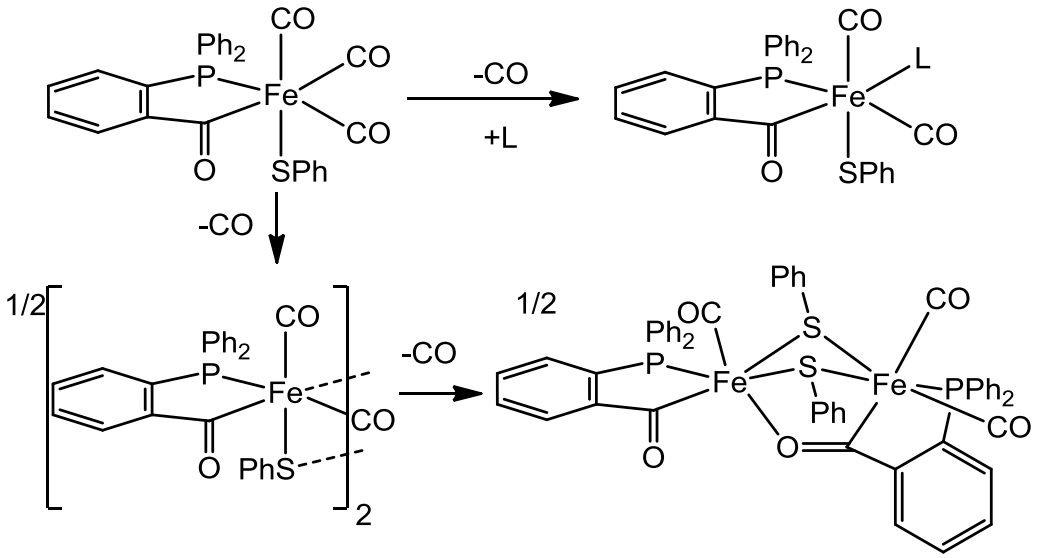

As indicated by comparisons of the XANES, EXAFS, and IR spectra for Hmd and Hmd^{CN} (*M. marburgensis*), $[Fe(SPh)(Ph_2PC_6H_4CO)(CN)(CO)_2]^-$ replicates the major details of both the electronic and geometric structure of the active site. This close match provides compelling evidence for the presence of a ferrous center in Hmd. The oxidation state of the Fe center in Hmd has been of recurring interest.[25,34]

The present results highlight the anomalous effect of cyanide on the IR spectrum of Hmd. In Hmd^{CN}, two ν_{CO} bands are shifted to higher energies by 9 and 12 cm^{-1}. In this conversion, CN^- is assumed to displace a labile ligand such as water. Nonetheless, it is extremely rare that ν_{CO} bands shift to higher energy upon installing a cyanide ligand. For example the average of the two ν_{CO} bands is 50 cm^{-1} *lower* in $[Fe(SPh)(Ph_2PC_6H_4CO)(CN)(CO)_2]^-$ than in

$Fe(SPh)(Ph_2PC_6H_4CO)(CO)_3$.[10] One possible explanation for this anomaly is that CN^- affects the second coordination sphere of the ferrous center in Hmd, such as the protonation state of the pyridone.

Our tricarbonyl model was also susceptible to reversible protonation, but only with strong acids. The ν_{CO} bands for the protonated tricarbonyl occur at 20-30 cm^{-1} above those seen for Hmd^{CO}. Furthermore, the protonated derivative is unstable at temperatures above –30 ºC. Collectively, these findings suggest that the thiol and acyl ligands are *not* protonated in Hmd^{CO} and Hmd.

Experimental

General Considerations. Unless otherwise indicated, reactions were conducted using standard Schlenk techniques (N_2) at room temperature with stirring. All solvents were dried and degassed prior to use. Literature procedures afforded the following reagents: 2-diphenylphosphinobenzoic acid,[35] $[H(Et_2O)]BAr^F{}_4$,[36] and $Fe(bda)(CO)_3$[37] followed. Benzenethiol, *p*-toluenesulfonylmethyl isocyanide, and Et_4NCN were purchased from Sigma-Aldrich. $Fe_2(CO)_9$, was purchased from Strem Chemicals. $K^{13}CN$ and ^{13}CO was purchased from Isotec. Electrospray ionization-mass spectra (ESI-MS) were acquired using a Micromass Quattro QHQ quadrupole-hexapole-quadrupole instrument. ^1H and ^{31}P NMR spectra were acquired on Varian UNITY INOVA TM 500NB and UNITY 500 NB instruments. Elemental analyses were performed by the School of Chemical Sciences Microanalysis Laboratory utilizing a Model CE

440 CHN Analyzer. In situ IR spectroscopic measurements were obtained using a ReactIR 4000 (Mettler-Toledo) instrument.

$Fe(SPh)(Ph_2PC_6H_4CO)(CO)_3$, 1. Under a stream of N_2, a solution of $Fe(bda)(CO)_3$ (445 mg, 1.55 mmol) and $Ph_2PC_6H_4C(O)SPh$ (652 mg, 1.63 mmol) in 20 mL of benzene was heated to reflux for 4 h. The solution was evaporated under vacuum and washed with a few mL of Et_2O. The brown crystalline solid was dried overnight to give 743 mg of diiron dithiolato complexes. A solution of this mixture (985 mg, 0.992 mmol) in 6 mL of CH_2Cl_2 was stirred under 1600 psi of CO at 60 ºC for 24 h to give a near quantitative conversion to **1**. Pure samples of **1** could be obtained by slow crystallization at -30 ºC (see below). For such carbonylations, the solution is first pressurized at 100-500 psi followed by careful venting. This gas-exchange procedure is repeated twice more. The bomb is then pressurized to 1400-1800 psi, with cooling of the bomb as needed to achieve the final pressure. ^{31}P NMR (202 MHz, CD_2Cl_2): δ 72.5. IR (CH_2Cl_2, cm^{-1}): ν_{CO} = 2075, 2025, 2001,1629 (acyl). Single crystals of **1** suitable for X-ray diffraction were obtained by layering hexanes over a solution of 450 mg of **1** in 5 mL of CH_2Cl_2 at –30 ºC for 96 h. Orange crystals of **1** were manually separated from a brown unidentified powder.

$Fe(SPh)(Ph_2PC_6H_4CO)(^{13}CO)_3$, 1^{13CO}. A solution of **1** (8.5 mg, 0.009 mmol) in 1 mL of CH_2Cl_2 in a J-Young NMR tube was frozen, and the tube was evacuated under vacuum. An atmosphere of 0.8 atm of ^{13}CO was introduced, and the tube was sealed. The solution was thawed and analyzed by ^{31}P NMR spectroscopy within 5 min. IR data were obtained within 25 min. ^{31}P NMR (202

MHz, CD_2Cl_2): δ72.0 (d of d of d, $^2J_{CPtrans}$ = 53, $^2J_{CPcis}$ = 21, $^2J_{CPcis}$ = 16 Hz). IR (CH_2Cl_2, cm^{-1}): ν_{CO} = 2027, 1980, 1957, 1629 (acyl).

$Et_4N[Fe(SPh)(Ph_2PC_6H_4CO)(CN)(CO)_2]$, $Et_4N[2]$. A solution of Et_4NCN (51.6 mg, 0.330 mmol) in 5 mL of CH_2Cl_2 was added to a solution of **1** (164 mg, 0.3304 mmol) in 20 mL of CH_2Cl_2. The solution was stirred 10 min. and then concentrated to 2 mL. An oil precipitated upon the addition of 10 mL of Et_2O. The oil was dissolved in THF and reprecipitated with ether. The resulting oily solid was recrystallized from THF/Et_2O twice more to give an orange tacky solid that converted to an orange powder upon vacuum drying. Yield: 115 mg (52%). ^{31}P NMR (202 MHz, CD_2Cl_2): δ66.73 (s). ESI-MS (negative mode, m/z): 536.1 (Calcd for $C_{28}H_{19}FeNO_3PS$: 536.0). IR (CH_2Cl_2, cm^{-1}): $\nu_{CN/CO}$ = 2094 (CN), 2013, 1954, 1597 (acyl). Anal. Calcd for $C_{36}H_{39}FeN_2O_3PS$. Found: C, 64.87 (64.14); H, 5.90 (5.99); N 4.20 (4.33).

$Et_4N[Fe(SPh)(Ph_2PC_6H_4CO)(^{13}CN)(CO)_2]$, $Et_4N[2]^{13CN}$. A solution of $Et_4N^{13}CN$ (17 mg, 0.108 mmol) was generated by $K^{13}CN$ and Et_4NCl in MeOH followed by filtration to remove KCl. Solvent was removed by vacuum, and the residue was dissolved in 3 mL of CH_2Cl_2 and added to a solution of **1** (54.0 mg, 0.108 mmol) in 5 mL of CH_2Cl_2. The solution was stirred 10 min. and evaporated under vacuum. Upon slurrying in Et_2O, the product converted to an oily orange powder that was dried under vacuum. ^{31}P NMR (202 MHz, CD_2Cl_2): δ66.7, doublet, $^2J_{CP}$ = 24 Hz. IR (CH_2Cl_2, cm^{-1}): ν_{CO} = 2050, 2012, 1954, 1597 (acyl).

$Fe(SPh)(Ph_2PC_6H_4CO)(CO)_2(NCCH_2Ts)$. A solution of **1** (99.6 mg, 0.185 mmol) in 3 mL of CH_2Cl_2 was cooled to –30 ºC. A background IR spectrum was

recorded in situ. A solution of $TsCH_2NC$ (36.5 mg, 0.185 mmol) in 1 mL of CH_2Cl_2 was added and IR spectra were collected every minute as the solution was allowed to warm. The CO region of the IR spectra changed cleanly between -10 to –6 ºC over the course of ~30 min. ^{31}P NMR (202 MHz, CD_2Cl_2): δ70.7 (s). IR (CH_2Cl_2, cm^{-1}): $\nu_{CN/CO}$ = 2153 (CN), 2038, 1983, 1615 (acyl). Upon warming the sample above -6 ºC, three new ^{31}P NMR signals at 73.2, 72.6, and 72.2 were initially observed before many signals appeared at further times. Upon prolonged standing at room temperature, loss of CO was observed.

Protonation of 1. A solution of **1** (30 mg, 0.056 mmol) in 3 mL of CH_2Cl_2 solution cooled to –72 ºC was examined by Ft-IR spectroscopy to confirm its integrity. A solution of $[H(Et_2O)_2]BAr^F{}_4$ (56.4 mg, 0.056 mmol) in 1 mL of CH_2Cl_2 was added with stirring. Within 5 min. the IR spectrum confirmed complete conversion to a new product (IR: 2090, 2041, 2024 cm^{-1}). Addition of Et_3N (10 μL, 0.072 mmol, –72 ºC), gave back **1**. The protonated product isomerizes slowly at –30 ºC. Protonation was also conducted in a J.Young NMR tube by adding 15.3 mg (0.028 mmol) of **1** and 30.3 mg (0.028 mmol) $[H(Et_2O)_2]BAr^F{}_4$ followed by vacuum transfer of 0.8 mL of CD_2Cl_2. The sample was warmed to -78 ºC and inserted into the NMR probe that had been precooled to -50 ºC. The sample was slowly warmed to -30 ºC and the ^{31}P NMR signal for starting material disappeared with formation of a new ^{31}P NMR signal (202 MHz, CD_2Cl_2, -30 ºC: δ68.1). The spectrum remained unchanged over the course of 30 min. Upon allowing the sample to warm to 0 ºC, no change was noted. Upon raising the sample temperature to 20 ºC, we observed rapid growth of a new singlet in the

^{31}P NMR spectrum (δ76.7). After 5 min, the signal at δ68.1 had completely disappeared. At longer times at room temperature, many new ^{31}P NMR signals were observed. The resulting solution had an odor of thiol.

XAS Data Analysis. Data were collected and analyzed by our collaborators Marco Salomone-Stagni and Wolfram Meyer-Klaucke at Wiggler station 7-3 (SSRL, Menlo Park, CA, USA) The results shown in Table 3.3 and Figures 3.10 and 3.11 are from these collaborators.

Note on High Pressure Reactions. The high pressure carbonylation reactions were performed in the 1600-1800 psi range for CO. Early in this work the carbonylation was performed at room temperature and found to require ~24 h. We then discovered the same reaction could be effected in 8 h at 60 ºC. The reaction vessel was degassed prior to heating by 3 cycles of filling the vessel to ~1800 psi CO for 5 min. and bleeding the line to ~100 PSI. After the reaction vessel was filled and heated for ~30 min., we repressurized the vessel. Initial pressure loss was attributed to gas slowly dissolving in the CH_2Cl_2 solution. The work discussed in this chapter is focused on the SPh derivative, but it is possible that other derivatives, specifically SEt, would be carbonylated to monomer in acceptable timeframes using the higher temperature method.

References

[1] Energy Information Administration *http://www.eia.doe.gov/emeu/international/reserves.html* **March 3, 2009**, World Proved Reserves of Oil and Natural Gas, Most Recent Estimates.

[2] Thauer, R. K. “Biochemistry of Methanogenesis: a Tribute to Marjory Stephenson.” *Microbiology* **1998**, *144*, 2377-2406.

[3] Shima, S.; Thauer, R. K. “A Third Type of Hydrogenase Catalyzing H_2 Activation.” *Chem. Record* **2007**, *7*, 37-46.

[4] Afting, C.; Hochheimer, A.; Thauer, R. K. “Function of H2-forming methylenetetrahydromethanopterin dehydrogenase from Methanobacterium thermoautotrophicum in coenzyme F420 reduction with H2.” *Arch. Microbiol.* **1998**, *169*, 206–210.

[5] Afting, C.; Kremmer, E.; Brucker, C.; A., H.; Thauer, R. K. “Regulation of the synthesis of H_2-forming methylenetetrahydromethanopterin dehydrogenase (Hmd) and of HmdII and HmdIII in Methanothermobacter marburgensis.” *Arch. Microbiol.* **2000**, *174*, 225-232.

[6] Lyon, E. J.; Shima, S.; Buurman, G.; Chowdhuri, S.; Batschauer, A.; Steinbach, K.; Thauer, R. K. “UV-A/Blue-Light Inactivation of the "Metal-Free" Hydrogenase (Hmd) from Methanogenic Archaea. The Enzyme Contains Functional Iron After All.” *Eur. J. Biochem.* **2004**, *271*, 195-204.

[7] Shima, S.; Pilak, O.; Vogt, S.; Schick, M.; Stagni, M. S.; Meyer-Klaucke, W.; Warkentin, E.; Thauer, R. K.; Ermler, U. “The Crystal Structure of [Fe]-Hydrogenase Reveals the Geometry of the Active Site.” *Science,* **2008**, *321*, 572-575.

[8] Hiromoto, T.; Ataka, K.; Pilak, O.; Vogt, S.; Stagni, M. S.; Meyer-Klaucke, W.; Warkentin, E.; Thauer, R. K.; Shima, S.; Ermler, U. “The crystal structure of C176A mutated [Fe]-hydrogenase suggests an acyl-iron ligation in the active site iron complex.” *FEBS Lett.* **2009**, *583*, 585-590.

[9] Hiromoto, T.; Warkentin, E.; Moll, J.; Ermler, U.; Shima, S. The Crystal Structure of an [Fe]-Hydrogenase-Substrate Complex Reveals the Framework for H_2 Activation.” *Angew. Chem. Int. Ed.* **2009**, *48*, 6457-6460.

[10] Lyon, E. J.; Shima, S.; Boecher, R.; Thauer, R. K.; Grevels, F.-W.; Bill, E.; Roseboom, W.; Albracht, S. P. J. “Carbon Monoxide as an Intrinsic Ligand to Iron in the Active Site of the Iron-Sulfur-Cluster-Free Hydrogenase H_2-Forming Methylenetetrahydromethanopterin Dehydrogenase As Revealed by Infrared Spectroscopy.” *J. Am. Chem. Soc.* **2004**, *126*, 14239-14248.

[11] Korbas, M.; Vogt, S.; Meyer-Klaucke, W.; Bill, E.; Lyon, E. J.; Thauer, R. K.; Shima, S. “The Iron-Sulfur Cluster-free Hydrogenase (Hmd) Is a Metalloenzyme with a Novel Iron Binding Motif.” *J. Biol. Chem.* **2006**, *281*, 30804-30813.

[12] Armstrong, F. A.; Fontecilla-Camps, J. C. “A Natural Choice for Activating Hydrogen.” *Science* **2008**, *321*, 498-499.

[13] Heinekey, D. M. “Hydrogenase enzymes: Recent structural studies and active site models.” *J. Organometal. Chem.* **2009**, *694*, 2671-2680.

[14] Salomone-Stagni, M.; Stellato, F.; Whaley, C. M.; Vogt, S.; Morante, S.; Shima, S.; B., R. T.; Meyer-Klaucke, W. “The iron-site structure of [Fe]-hydrogenase and model systems: an X-ray absorption near edge spectroscopy study.” *Dalton Trans.* **2010**, *39*, 3057-3064.

[15] Plietker, B., Ed. Iron Catalysis in Organic Chemistry; Wiley-VCH: Weinheim, 2008.

[16] Tucci, G. C.; Holm, R. H. “Nickel-Mediated Formation of Thioesters from Bound Methyl, Thiols, and Carbon Monoxide - a Possible Reaction Pathway of Acetyl-Coenzyme A Synthase Activity in Nickel-Containing Carbon Monoxide Dehydrogenases.” *J. Am. Chem. Soc.* **1995**, *117*, 6489-6496.

[17] Lindahl, P. A.; Graham, D. E. “Acetyl-coenzyme A synthases and nickel-containing carbon monoxide dehydrogenases.” *Met. Ions Life Sci.* **2007**, *2*, 357-415.

[18] Fontecilla-Camps, J. C.; Amara, P.; Cavazza, C.; Nicolet, Y.; Volbeda, A. “Structure-function relationships of anaerobic gas-processing metalloenzymes.” *Nature* **2009**, *460*, 814-822.

[19] Ford, P. C.; Rokicki, A. “Nucleophilic Activation of Carbon Monoxide: Applications to Homogeneous Catalysis by Metal Carbonyls of the Water Gas Shift and Related Reactions.” *Adv. Organometal. Chem.* **1988**, *28*, 139-206.

[20] Hartwig, J. F. Organotransition Metal Chemistry, from Bonding to Catalysis; University Science Books: New York, 2010.

[21] Huber, C.; Wächtershäuser, G. “Activated Acetic Acid by Carbon Fixation on (Fe,Ni)S Under Primordial Conditions.” *Science* **1997**, *276*, 245-247.

[22] Wächtershäuser, G. “From volcanic origins of chemoautotrophic life to Bacteria, Archaea and Eukarya.” *Philos. Trans Roy. Soc.* **2006**, *361*, 1787-1806.

[23] Royer, A. M.; Rauchfuss, T. B.; Gray, D. L. “Oxidative Addition of Thioesters to Iron(0): Active-Site Models for Hmd, Nature's Third Hydrogenase.” *Organometallics* **2009**, *28*, 3618-3620.

[24] Chen, D.; Scopelliti, R.; Hu, X. “Synthesis and Reactivity of Iron Acyl Complexes Modeling the Active Site of [Fe]-Hydrogenase.” *J. Am. Chem. Soc.* **2009**, *132*, 928-929.

[25] Wang, X.; Li, Z.; Zeng, X.; Luo, Q.; Evans, D. J.; Pickett, C. J.; Liu, X. “The iron centre of the cluster-free hydrogenase (Hmd): low-spin Fe(II) or low-spin Fe(0)?” *Chem. Commun.* **2008**, 3555-3557.

[26] Obrist, B. V.; Chen, D.; Ahrens, A.; Schünemann, V.; Scopelliti, R.; Hu, X. “An Iron Carbonyl Pyridonate Complex Related to the Active Site of the [Fe]-Hydrogenase (Hmd).” *Inorg. Chem.* **2009**, *49*, 3514-3516.

[27] Turrell, P. J.; Wright, J. A.; Peck, J. N. T.; Oganesyan, V. S.; Pickett, C. J. “The Third Hydrogenase: A Ferracyclic Carbamoyl with Close Structural Analogy to the Active Site of Hmd.” *Angew. Chem. Int. Ed.* **2010**, *49*, 7508-7511.

[28] Dennett, J. N. L.; Ferguson, M. J.; McDonald, R.; Takats, J. “Reaction of $[Fe(CO)_4(2\text{-}Me_3SiCCSiMe_3)]$ with PMe_3 — CO rather than alkyne substitution.” *Can. J. Chem.* **2005**, *83*, 862–868.

[29] Salomone-Stagni, M.; Vogt, S.; Shima, S.; Meyer-Klaucke, W., Extended X-ray absorption fine structure of the [Fe]-hydrogenase Hmd active site, 14th International Conference on X-Ray Absorption Fine Structure (XAFS14), 2009.

[30] Rocchini, E.; Rigo, P.; Mezzetti, A.; Stephan, T.; Morris, R. H.; Lough, A. J.; Forde, C. E.; Fong, T. P.; Drouin, S. D. “Synthesis and properties of iron-group hydrido-cyano complexes trans-[MH(CN)(L)(2)], M = Fe, Ru or Os, L = diphosphine, and their hydrogen, trifluoroboron and triphenylboron isocyanide derivatives of the type trans-$[MH(CNH)(L)(2)]O_3SCF_3$, trans-$[MH(CNBX_3)(L)(2)]$, X = F or Ph, and trans-$[M(H\text{-}2)(CNBF_3)$-(dppp)(2)$]BF_4$ [dppp = $Ph2P(CH_2)(3)PPh_2$].” *J. Chem. Soc., Dalton Trans.* **2000**, 3591-3602.

[31] McGuire, D. G.; Khan, M. A.; Ashby, M. T. “Discontinuum between a Thiolate and a Thiol Ligand.” *Inorg. Chem.* **2002**, *41*, 2202-2208.

[32] Green, M. L. H.; Hurley, C. R. “Evidence for an iron-carbene complex.” *J. Organomet. Chem.* **1967**, *10* 188-190.

[33] Boxhoorn, G.; Cerfontain, M. B.; Stufkens, D. J.; Oskam, A. “Photochemistry of $[Fe(CO)_4L]$ complexes (L = NMe_3 or pyridine) in argon and xenon matrices. Evidence for the formation of C3v[Fe(CO)3L] and the reversible infrared-induced isomerization to Cs$[Fe(CO)_3L]$.” *J. Chem. Soc., Dalton Trans.* **1980**, 1336-1341.

[34] Guo, Y.; Wang, H.; Xiao, Y.; Vogt, S.; Thauer, R. K.; Shima, S.; Volkers, P. I.; Rauchfuss, T. B.; Pelmenschikov, V.; Case, D. A.; Alp, E. E.; Sturhahn, W.; Yoda, Y.; Cramer, S. P. "Characterization of the Fe Site in Methanothermobacter marburgensis Hydrogenase (mHmd) via Nuclear Resonant Vibrational Spectroscopy (NRVS)." *Inorg. Chem.* **2008**, *47*, 3969-3977.

[35] Hoots, J. E.; Rauchfuss, T. B.; Wrobleski, D. A. "Substituted Triaryl Phosphines." *Inorg. Syn.* **1982**, *21*, 175.

[36] Brookhart, M.; Grant, B.; Volpe, A. F. "[(3,5-$(CF_3)_2C_6H_3)_4B$]-[$H(OEt_2)_2$]+: a convenient reagent for generation and stabilization of cationic, highly electrophilic organometallic complexes." *Organometallics* **1992**, *11*, 3920-3922.

[37] Alcock, N. W.; Richards, C. J.; Thomas, S. E. "Preparation of tricarbonyl(.eta.4-vinylketene)iron(0) complexes from tricarbonyl(.eta.4-vinyl ketone)iron(0) complexes and their subsequent conversion to tricarbonyl(.eta.4-vinylketenimine)iron(0) complexes." *Organometallics* **1991**, *10*, 231-238.

Chapter 4

Half-Sandwich Complexes of Hydroxypyridine Acetic Acid and Related Pyridine Ligands

Introduction

We have already described the synthesis of structural models for the Fe cofactor of Hmd, providing support for the structure reported in 2009. This structure, which features an Fe-acyl linkage, is now generally accepted (Chapter 3).[1] Prior to the revision of the structure, the best interpretation of the crystallographic results indicated that Fe was bound to a pyridine acetic acid, as supported both by the X-ray crystallography and the characterization of the isolated GP cofactor.

Early work on the nature of Hmd suggested that the enzyme was metal free. This situation changed in 2004.[2] It is only weakly inhibited by CO, This metal-free theory was further supported by the lack of acid-labile sulfur, indicating the lack of iron-sulfur clusters in the enzyme.[3] All other hydrogenases feature Fe-S clusters.

The initial information was accurate with regards to the substrate and the stereochemistry of its reactions. There is no dispute that Hmd catalyzes the reversible reduction of methenyltetrahydromethanopterin (methenyl-H_4MPT^+)[4] with H_2 to methylenetetrahydromethanopterin (methylene- H_4MPT) (eq 4.1), and in the presence of the substrates methyleneH_4MPT or methenylH_4MPT^+, Hmd also catalyzes the exchange of D_2 with H_2O. Thus, Hmd can be viewed as a

"third" hydrogenase, supplementing the well-known [NiFe]- and [FeFe]-hydrogenases.[5,6]

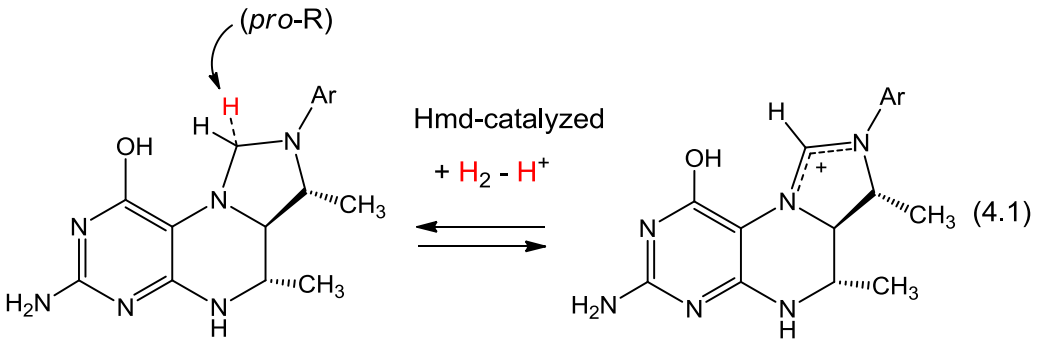

(4.1)

In more recent work, Thauer et al. demonstrated that Hmd consists of a 38000 dalton homodimeric protein containing one organometallic cofactor per subunit.[7] This cofactor features an $Fe(CO)_2$ subunit (ν_{CO} = 2011, 1944 cm^{-1})[8] bound to an organic component, guanylylpyridone (GP), which was isolated and spectroscopically characterized (Figure 1).[9] GP was isolated as a 3,5-dimethylpyrid-2-one-4-ol-6-acetic acid group conjugated to a guanidine nucleotide through the 4-position. This information was the starting point for our modeling. It is now understood that Fe is not bound to carboxylate, but to acyl. The isolated carboxylic acid is a product of the hydrolysis of the Fe-acyl bond.

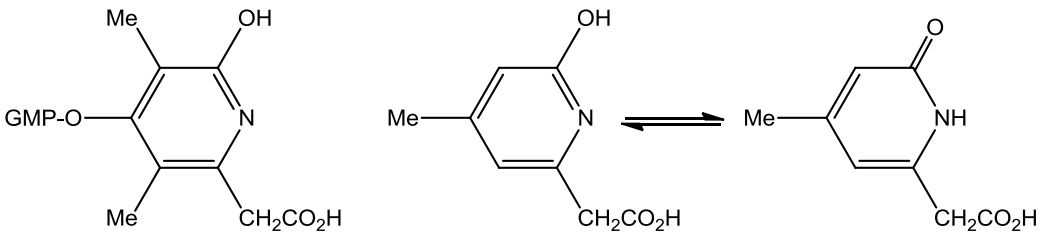

Figure 4.1. Structure of organic component, GP, of organometallic cofactor (left) and 2-hydroxypyridine/2-pyridone tautomers of the simplified analogue $cmhpH_2$ (right).

The heterocycle 6-carboxymethyl-4-methyl-2-hydroxypyridine (cmhpH_2) is known[10,11] and represents a simplified analogue of Hmd-pyridoneH_2, bearing both the 2-hydroxyl and 6-carboxymethyl functionalities (Figure 4.1). While early modeling by others focused on the formation of ferrous carbonyls with cis-CO's,[12,13] we sought to model the metal complexation of the GP cofactor. Initial attempts to form cmhp(H) complexes with Fe carbonyls, $Fe(CO)_4X_2$ where X = Br, I, proved to be difficult with the unstable initial products resulting in insoluble solids that we were unable to characterize. Herein, we describe an initial evaluation of the coordinating properties of this model cofactor using the simplified octahedral metal platforms provided by Cp^*M^{2+} (M = Rh, Ir; Cp* = C_5Me_5).[14] The resulting adducts should approximate the environment provided by low-spin ferrous iron, as were likely to exist in the enzyme.[15]

The coordination chemistry of 2-pyridones is well developed,[16] but coordination of 2-pyridones bearing functionality is generally limited. Intriguingly, Cp^*Ir^{III} complexes of 2-pyridones have recently been shown to catalyze hydrogen-transfer,[17] which is relevant to the methanogenesis pathway (eq 4.1). We were particularly interested in the role of the hydroxyl group in promoting heterolytic cleavage of H_2.

Results and Discussion

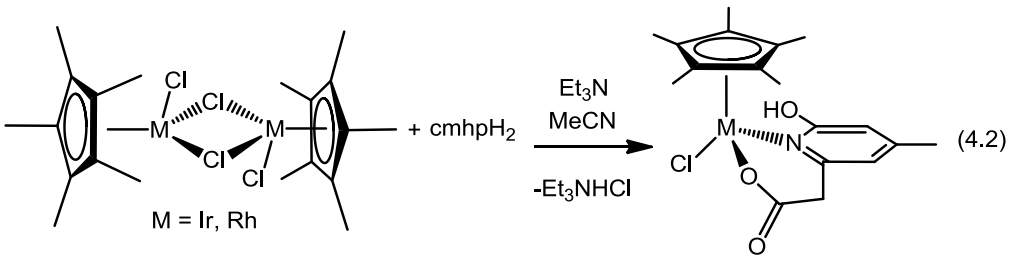

We found that treatment of $[Cp^*MCl_2]_2$ with $cmhpH_2$ and base afforded excellent yields of the air-stable solids Cp*M(Hcmhp)Cl for M = Ir (**1**) and Rh (**2**) (eq 4.2). The NMR spectra for the new complexes exhibited diastereotopic signals for the methylene group, consistent with complexation of both the heterocycle and the acetate arm. As verified crystallographically, Cp*Rh(Hcmhp)Cl adopts a chiral "piano-stool" structure with a chelating $Hcmhp^-$. The presence of the intact 2-hydroxy group on the pyridine was confirmed crystallographically, indicating that the heterocycle is bound as the 2-hydroxypyridine tautomer (Figure 4.2). The O1-C11 and N1-C11 bond distances and the O1-C11-N1, O1-C11-C12 angles of the Hcmhp ligand also confirm the pyridine form.[18] In the crystal, this hydroxy group forms an intermolecular hydrogen-bond to the carbonyl on the carboxylate of a neighboring complex with a O---O distance of 2.582(2) Å.

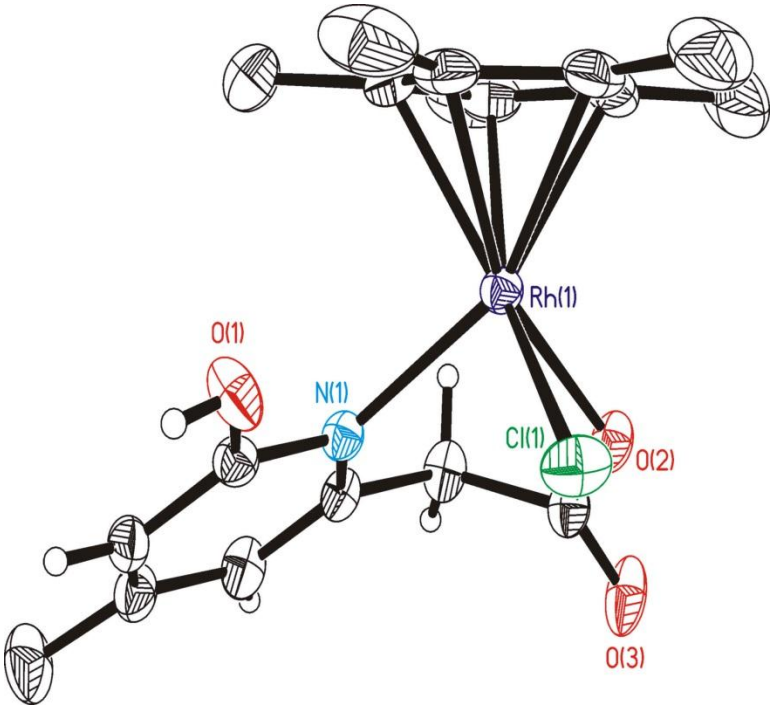

Figure 4.2. Molecular structure of **2** with thermal ellipsoids drawn at the 50 % probability level with methyl H's removed for clarity and Rh, Purple; Cl, Green; N, Blue; O, Red; C, Black. Selected bond distances and angles: Rh1-N1 2.1383(16), Rh1-O2 2.1223(14), Rh1-Cl1 2.4042(5), Rh1-Cp*(centroid) 1.771(2), O1-C11 1.326(2), N1-C11 1.349(3), O1-C11-N1 116.02(17), O1-C11-C12 121.39(18).

Complexes **1** and **2** exhibit good solubility in water and alcohols. This hydrophilicity is proposed to arise from both the solvation of the 2-hydroxyl group. Another potentially contributing factor is the ability of the hydroxyl group to stabilize ligands that can participate in hydrogen-bonding, such as water.[19] In aqueous solutions of **1**, chloride is fully ionized as indicated by the finding that the ^{1}H NMR spectrum was unaffected by the addition of $AgPF_6$, i.e. chloride is ionized prior to the addition of a Ag^{+} source. In contrast, similar complexes lacking the hydroxyl functionality Cp*Ir(paa)Cl (**3**) (paaH = 2-pyridylacetic acid) and Cp*Ir(pa)Cl (**4**) (paH = picolinic acid, C_5H_4N-2-CO_2H) require the addition of $AgPF_6$ for complete conversion to the aqua complexes (Figure 4.3). The K_{eq} for

the ionization of Cl^- for the iridium complexes in water is shown in figure 4.4. The rhodium and iridium complexes behaved similarly.

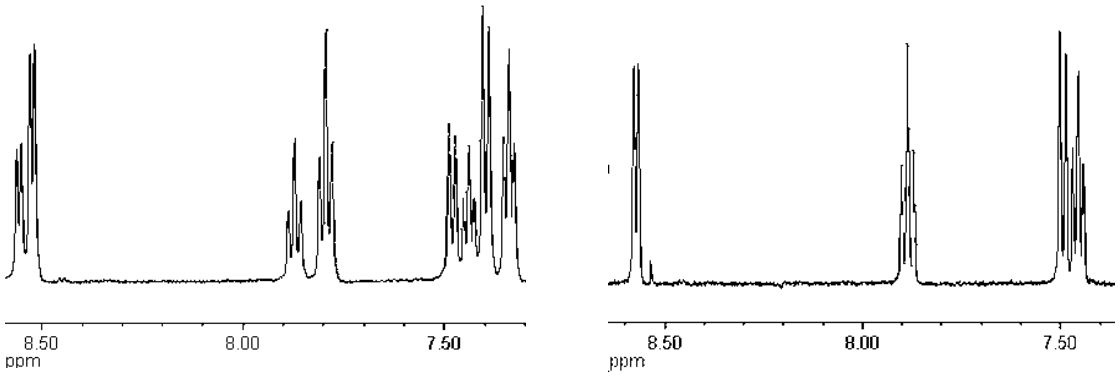

Figure 4.3. (left) ^{1}H NMR spectrum of **Cp*IrCl(paa)** in D_2O. (right) ^{1}H NMR of **Cp*IrCl(paa)** after addition of $AgPF_6$.

$$Cp^*Ir(N\text{-}O)Cl + H_2O \underset{}{\overset{K}{\rightleftharpoons}} [Cp^*Ir(N\text{-}O)(H_2O)]^+ + Cl^- \quad (2)$$

N-O	K
2-picolinate	1.4
pyridine-2-acetate	0.53
$cmhpH^-$	>30

Figure 4.4. K_{eq} values for the ionization of Cl^- in water for several Cp*Ir pyridine carboxylate complexes.

We investigated the affinity of **1** and **2** for ligands that could serve as hydrogen-bond acceptors. Treatment of **2** with 2-pyridone (hpH) in the presence of Et_3N afforded the neutral complex Cp*Rh(cmhpH)(hp) (**5**). The ^{1}H NMR spectra for **5** indicated the formation of a single species. To further investigate the potential for hydrogen bonding, single crystals were grown. Crystallographic analysis of the orange crystals revealed four molecules in the asymmetric unit, each of which was very similar exhibiting *intra*molecular hydrogen bonding

between the two pyridone-derived ligands (Figure 4.5). The O---O separations in **5** range from 2.327(18) to 2.480(17) Å, and is virtually the only difference between the four molecules (Table 4.1). The short O---O distances are indicative of a strong hydrogen bond (a "low-barrier hydrogen bond" or LBHB),[20,21] and among the shortest O---O separations reported, especially for a coordination complex.[22] Previous studies have shown that intramolecular LBHBs are favored when ΔpK_a, the difference in the acidity of the hydrogen-bond donor and hydrogen bond acceptor, is ~0. This aspect indicates, not surprisingly, that the 4-methyl and 6-carboxymethyl substituents in H_2cmhp have little effect on the pK_a of the hydroxyl group relative to the parent 2-hydroxypyridine. The C-O, N-C, and Rh-N distances, as well as the O-C-N and N-C-C angles for the 2hp and cmhp ligands are averaged between the pyridone and pyridine binding modes.

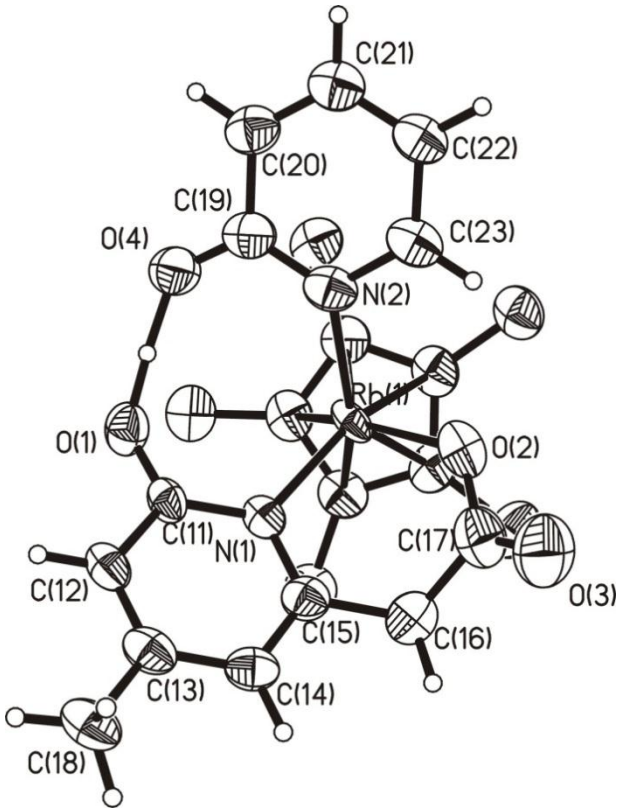

Figure 4.5. Structure of one of four similar molecules in the asymmetric unit of **5** with Cp* protons removed for clarity and 50% probability ellipsoids. Selected bond distances and angles: Rh1-N1, 2.165(6); Rh1-N2, 2.178(6); O1-C11, 1.286(9); O4-C19, 1.282(10); N1-C11, 1.357(9); N2-C19, 1.347(10); O1-C11-N1, 120.5(8); O4-C19-N2, 121.4(9); N1-C11-C12, 120.5(8); N2-C19-C20, 119.0(9). O---O distances (O--H--O angles): 2.327(18), (171(4)), 2.348(17), (159(8)), 2.384(17), (173(9)), 2.480(17), and (173(9)).

The clearest characterization technique for a LBHB in solution is ^{1}H NMR spectroscopy.REF In compounds containing LBHB's, the chemical shifts of the participating proton range from δ16 to 20. The ^{1}H NMR spectrum of **5** exhibits a singlet at δ 17.1 (CD_2Cl_2 soln) vs. δ 9.83 in **2**, which lacks an LBHB. Pyrazolate (pyz^-) also replaced the chloride in **2** to give Cp*Rh(Hcmhp)(pyz) with a similarly strong hydrogen bond (δ 16.3).

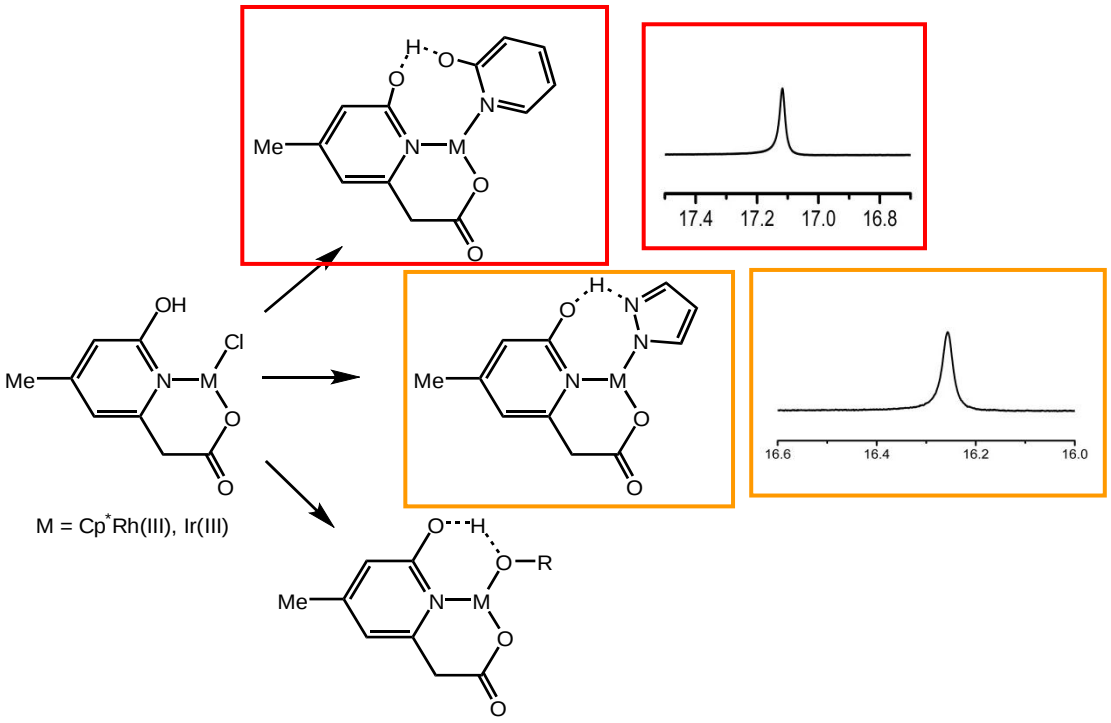

Figure 4.6. Demonstration of hydroxyl group role in hydrogen bonding with insets of the atypical shifts in the ^{1}H NMR spectrum of **5** (red border) and **6** (orange border) showing LBHB's.

In view of the ability of the 2-hydroxy group to encourage the binding of hydrogen-bond acceptors (Figure 4.6) and in view of the biological function of Hmd as a hydrogen-transfer catalyst, we examined these Hcmhp-derived complexes to promote hydrogen transfer. Iridium complexes are well known to promote hydrogen transfer reactions.[23-26] Although the rhodium complex **2** is not sufficiently robust thermally, **1** is an excellent catalyst for the dehydrogenation of PhCH(OH)Me to acetophenone (eq 4.3). In terms of TON and catalyst longevity, **1** is superior to structurally related complexes lacking the 2-OH group (Table 4.1).

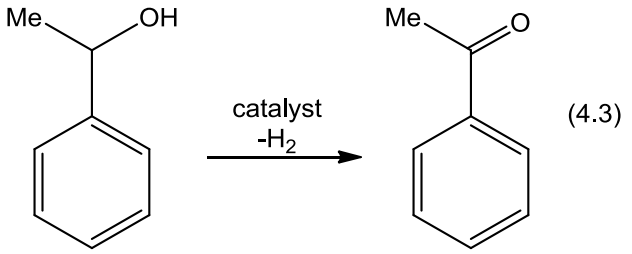

(4.3)

Table 4.1. Turn-over numbers (TON) and turn-over frequencies (TOF) for catalytic dehydrogenation of PhCH(OH)Me to PhC(O)Me (neat, 130 ºC) using 0.10 mol % of **1** as catalyst.

Catalyst precursor	TON (24 h)	TOF (2 h)
Cp*Ir(Hcmhp)Cl	169	21
Cp*Ir(C_5H_4N-2-CH_2CO_2)Cl	64	10
Cp*Ir(C_5H_4N-2-CO_2)Cl	8	Trace
$[Cp^*IrCl_2]_2$	24	2.7
Cp*Ir(Hcmhp)Cl*	339	40

* 2.4 mL 1-phenylethanol, 2.4 mL toluene, and 0.10 mol % Ir catalyst under reflux conditions

Conclusions

Our findings indicate that the 2-hydroxy substituent in $Hcmhp^-$ can significantly influence the reactivity of the sixth coordination site in octahedral complexes. Although newer information suggests an acyl rather than carboxylate attached to pyridine and chelated to the Fe center in hmd, in $Hcmhp^-$ the chelating nature of the ligand constrains the orientation of this hydroxy substituent to be adjacent to the open coordination site in a similar fashion.[27] Hcmhp is well suited for intramolecular H-bonding but the H-bond acceptor should be in the plane of the Hcmhp (as it is in Hmd), whereas the Cp*Ir system

forces these ligands to be facial. This research suggests the importance of the hydroxyl functionality should not be overlooked in newer models containing acyl ligands. Currently even the best Fe acyl thiolate models lack this potentially important component.[28-30]

Experimental Section

General considerations. Unless otherwise indicated, reactions were conducted using standard Schlenk techniques (N_2) at room temperature with stirring. cmhpH_2 was synthesized according to a modification of the literature preparation (given below).[31] The proposed structure was confirmed by ^{1}H NMR. Attempts to prepare cmhpH_2 by the method of Shaw *et al.* were unsuccessful.[32] 2-hydroxypyridine, pyrazole, Et_3N, picolinic acid, 2-pyridylacetic acid hydrochloride, and $AgPF_6$ were purchased from Aldrich. DL-1-phenylethanol was obtained from Alfa-Aesar. Electrospray ionization-mass spectra (ESI-MS) were acquired using a Micromass Quattro QHQ quadrupole-hexapole-quadrupole instrument. ^{1}H NMR was acquired on Varian UNITY INOVATM 500NB and UNITY 500 NB instruments. Elemental analyses were performed by the School of Chemical Sciences Microanalysis Laboratory utilizing a Model CE 440 CHN Analyzer.

cmhpH_2. A solution of 10 mL (79 mmol) of ethyl 3-aminocrotonate in 20 mL of Et_2O was purged with HCl at 0 °C. Upon formation of an off-white precipitate, the addition of HCl was stopped. A second 10-mL portion (79 mmol) of ethyl 3-aminocrotonate in 20 mL of Et_2O was added, and the combined slurry

was thoroughly stirred for 5 min. Ether was removed by vacuum to give a cloudy yellow oil, which was heated at 120 °C. Crystals formed (presumably NH_4Cl) and the oil thickened. The residue was washed with 40 mL of water and 40 mL of Et_2O, leaving ~7.6 g of an off-white solid. This solid residue was extracted into a solution of 1.65 g (41 mmol) of NaOH in 50 mL of H_2O. The solution was neutralized to pH 7 by the addition of HCl, whereupon a colorless precipitate formed. The precipitate was collected by filtration and washed with 30 mL of EtOH, leaving white crystals. Yield: 3.52 g (21 mmol, 26%). ^{1}H NMR (500 MHz, DMSO): δ2.04 (s, 3H, 4-C*H*$_3$), 3.14 (s, 2H, CO_2CH_2), 5.73 (s, 1H, aryl-C*H*), 5.86 (s, 1H, aryl-C*H*), 12.18 (s, 1H, O*H*) exchanged in D_2O.

Cp*IrCl(cmhpH) (1). A colorless solution of 0.109 g (0.65 mmol) of $cmhpH_2$ and 91 µL (0.65 mmol) of Et_3N in 3 mL of MeCN was transferred to an orange solution of 0.260 g (0.32 mmol) of $(Cp^*IrCl_2)_2$ in 2 mL of MeCN. The reaction solution became yellow and a yellow precipitate appeared upon stirring 1 h. The bright yellow powder was collected by filtration and washed with 5 mL cold MeCN and 5 mL Et_2O. Yield: 300 mg (0.57 mmol) (87%). ^{1}H NMR (500 MHz, CD_2Cl_2): δ1.58 (s, 15 H, Cp*), 2.39 (s, 3H, 4-C*H*$_3$), 3.64 (q, 2H, CO_2CH_2), 6.71 (s, 1H, aryl-C*H*), 6.79 (s, 1H, aryl-C*H*), 9.46 (s, 1H, O*H*) exchanged in D_2O. Anal. Calcd for $C_{18}H_{23}ClIrNO_3$ (found): C, 40.86 (40.64); H, 4.38 (4.27); N, 2.65 (2.80).

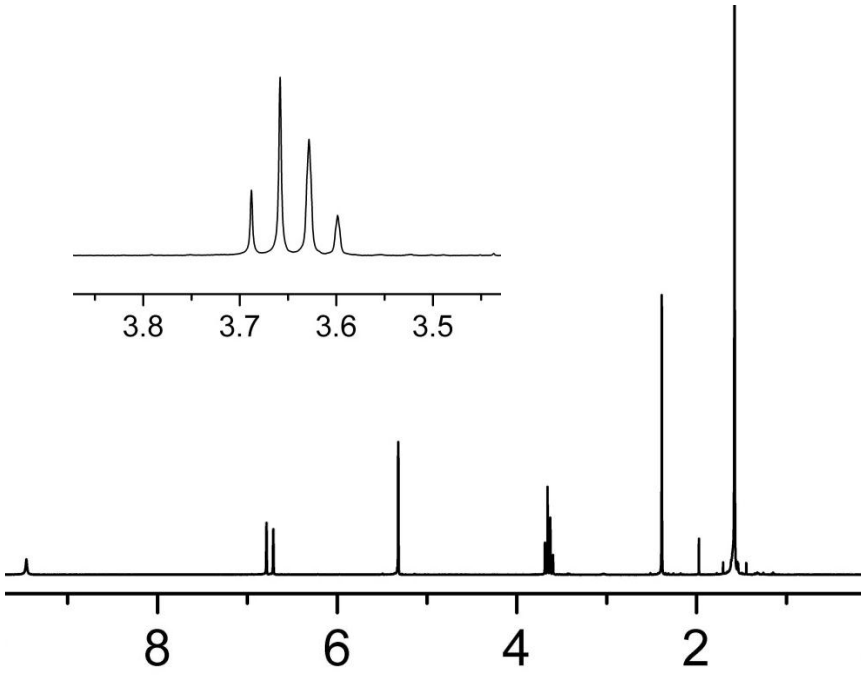

Figure 4.7. ^{1}H NMR spectrum of **1** in CD_2Cl_2. (inset) Methylene signals showing bound chelate ring.

Cp*RhCl(cmhpH) (2). This compound was prepared similarly to **1**. Orange powder. Yield: 80%. ^{1}H NMR (500 MHz, CD_2Cl_2): δ1.60 (s, 15 H, Cp*), 2.39 (s, 3H, 4-CH_3), 3.67 (q, 2H, CO_2CH_2), 6.68 (s, 1H, aryl-CH), 6.78 (s, 1H, aryl-CH), 9.83 (s, 1H, O*H*) exchanged in D_2O. Anal. Calcd for $C_{18}H_{23}ClNO_3Rh$ (found): C, 49.16 (48.96); H, 5.27 (5.27); N, 3.19 (3.37). Single crystals of **2** suitable for X-ray diffraction were obtained by diffusion of Et_2O into a concentrated solution of **2** in MeOH.

Cp*IrCl(paa), (3) paaH = 2-pyridylacetic acid. A mixture of 199 mg (0.25 mmol) of $(Cp^*IrCl_2)_2$, 86.8 mg (0.50 mmol) of paaH·HCl, and 69.1 mg (0.50 mmol) K_2CO_3 was stirred in 10 mL of 1:1 MeOH:H_2O for 45 min. by which time the orange color disappeared. Upon concentrating the solution to 2 mL, a yellow precipitate appeared. The solid was collected by filtration and washed with 5 mL

Et_2O. Yield: 191 mg (0.383 mmol, 77%). ^1H NMR (500 MHz, CD_2Cl_2): δ1.58 (s, 15 H, Cp*), 3.61 (d, 1H, 14.7 Hz, $CO_2CH\mathit{H}$), 3.77 (d, 1H, 14.7 Hz, $CO_2C\mathit{H}H$), 7.31 (d of t, 1H, 0.8 Hz, 6 Hz, NCHC*H*), 7.35 (d, 1H, 8 Hz, NCC*H*), 7.76 (d of t, 1H, 2 Hz, 8 Hz, NCCC*H*), 8.69 (d of d, 1H, 1 Hz, 6 Hz, NC*H*). Anal. Calcd for $C_{17}H_{21}ClIrNO_2$ (found): C, 40.92 (40.78); H, 4.24 (3.92); N, 2.81 (2.79).

Cp*IrCl(pa), (4) (paH = picolinic acid). A mixture of 79.7 mg (0.10 mmol) of $(Cp^*IrCl_2)_2$, 24.6 mg (0.10 mmol) of paH, and 27.6 mg (0.10 mmol) of K_2CO_3 was stirred in 8 mL of 1:1 MeOH:H_2O for 45 min. (until orange color disappeared). The solution was concentrated to 2 mL under vacuum with formation of a yellow precipitate. The solid was collected by filtration and washed with 5 mL of Et_2O. Yield: 74 mg (0.153 mmol, 76% yield). ^1H NMR (500 MHz, $CDCl_3$): δ1.70 (s, 15 H, Cp*), 7.55 (d of t, 1H, 1.5 Hz, 5.5 Hz, NCHC*H*), 7.94 (d of t, 1H, 1.4 Hz, 8 Hz, NCCC*H*), 8.13 (d of d, 1H, 0.7 Hz, 8 Hz, NCC*H*), 8.69 (d of d, 1H, 0.6 Hz, 5 Hz, NC*H*). Anal. Calcd for $C_{16}H_{19}ClIrNO_2$ (found): C, 39.62 (39.40); H, 3.95 (3.81); N, 2.89 (2.84).

General Procedure for Treatment of Cp*RhCl(cmhpH), Cp*IrCl(cmhpH), Cp*IrCl(paa), and Cp*IrCl(pa) with $AgPF_6$ in D_2O. 10 mg (0.023 mmol) Cp*RhCl(cmhpH) was dissolved 0.7 mL of D_2O in an NMR tube. The ^1H NMR spectrum was recorded. The sample was treated with 6.3 mg (0.025 mmol) of $AgPF_6$, giving an immmediate white precipitate. A ^1H NMR spectrum was recorded once more.

Cp*Rh(MeCN)(cmhpH)][PF_6]. A solution of 114 mg (0.45 mmol) of $AgPF_6$ in 8 mL of MeCN was added to a mixture of 200 mg (0.45 mmol) of **2** in 3

mL of MeCN. A white precipitate formed immediately. The orange solution was filtered, and solvent removed by vacuum. Orange microcrystals were obtained by recrystallization from 2 mL of MeCN and 10 mL of a 1:1 Et_2O: hexanes mixture. Solid was dried by vacuum. Yield: 222 mg (0.38 mmol, 85%). ^1H NMR (500 MHz, CD_3CN): δ1.625 (s, 15 H, Cp*), 1.737 (s, 3H, CH_3CN) exchanged with CD_3CN, 2.324 (s, 3H, 4-CH_3), 3.53 (d, broad, 2H, CO_2CH_2), 6.737 (s, 1H, aryl-CH), 6.797 (s, 1H, aryl-CH). ESI-MS: m/z = 445.3 ($[Cp^*Rh(MeCN)(cmhpH)]^+$), 404.3($[Cp^*Rh(cmhpH)]^+$), 401.3($[Cp^*Rh(MeCN)(cmhpH\text{-}CO_2)]^+$), 360.3($[Cp^*Rh(cmhpH\text{-}CO_2)]^+$).

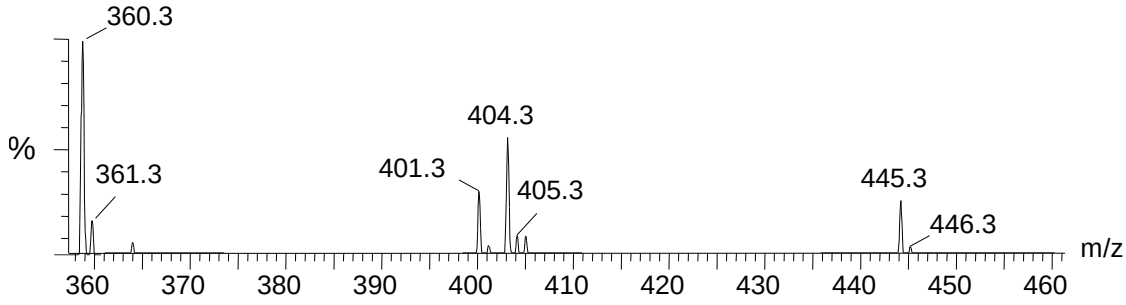

Figure 4.8. ESI-MS of **Cp* Rh(MeCN)(cmhpH)** (m/z = 445.3, $[Cp^*Rh(MeCN)(cmhpH)]^+$; 404.3, $[Cp^*Rh(cmhpH)]^+$; 401.3, $[Cp^*Rh(MeCN)(cmhpH\text{-}CO_2)]^+$; 360.3, $[Cp^*Rh(cmhpH\text{-}CO_2)]^+$) in MeCN showing signals due to fragmentation by loss of CO_2 and MeCN.

Cp*Rh(hp)(cmhpH)·1.5 MeCN (5). A solution of 19.3 mg (0.20 mmol) of 2-hydroxypyridine and 28 µL (0.20 mmol) of Et_3N in 5 mL of CH_2Cl_2 was transferred to an orange solution of 90 mg (0.20 mmol) of **2** in 3 mL of CH_2Cl_2. The solution darkened and was stirred 10 min. Et_3NHCl was removed by extraction with water 3 x 3 mL (under vigorous mixing all products dissolve in water layer). The organic phase was evaporated, and the product was extracted into 1 mL of MeCN, and this extract was diluted with 10 mL of a 1:1

Et_2O/hexanes and stored at -20 °C for 24 h. Solvent was decanted from the red crystals (some of which were suited for X-ray diffraction). Yield: 50.3 mg (0.20 mmol, 50%). ^{1}H NMR (500 MHz, CD_2Cl_2): δ1.46 (s, 15 H, Cp*), 2.16 (s, 3H, 4-CH_3), 3.50 (d, 1H, 15 Hz, $CO_2CH\mathit{H}$), 3.55 (d, 1H, 15 Hz, $CO_2C\mathit{H}H$), 6.30 (s, 1H, cmhpH-aryl-CH), 6.34 (s, 1H, cmhpH-aryl-CH), 6.61 (d of t, 1H, 6 Hz, 1 Hz, hp-NCC*H*), 6.68 (d, 1H, 8 Hz, hp-NCOC*H*), 7.461 (d of t, 1H, 7 Hz, 2 Hz, hp-NCOCC*H*), 8.32 (d, 1H, 5 Hz, hp-NC*H*) 17.1 (s, 1H, O*H*···O; this signal disappeared upon addition of D_2O).

Cp*Rh($C_3H_3N_2$)(cmhpH) (6). A solution of 8.5 mg (0.128 mmol) of pyrazole and 18 µL (0.128 mmol) of Et_3N in 5 mL of CH_2Cl_2 was transferred to an orange solution of 56.4 mg (0.128 mmol) of **2** in 5 mL of CH_2Cl_2. After stirring for 30 min. the solution was extracted three times with 5 mL of water. Solvent was removed by vacuum, and the product was extracted into ~1mL of CH_2Cl_2. The product precipitated from solution upon addition of 10 mL of 1:1 Et_2O/hexanes. Yield: 28 mg (0.059 mmol, 46 %). ^{1}H NMR (500 MHz, CD_2Cl_2): δ1.52 (s, 15 H, Cp*), 2.12 (s, 3H, 4-CH_3), 3.32 (d, 1H, 14 Hz, $CO_2CH\mathit{H}$), 3.55 (d, 1H, 14 Hz, $CO_2C\mathit{H}H$), 6.07 (s, 1H, cmhpH-aryl-C*H*), 6.15 (d, 1H, 1 Hz, cmhpH-aryl-C*H*), 6.39 (q, 1H, 2Hz, pyrazolate-CC*H*C), 7.61 (d, 1H, 1 Hz, pyrazolate-NC*H*), 7.67 (s, 1H, pyrazolate-NC*H*), 16.3 (s, 1H, O*H*···O; this signal disappeared upon addition of D_2O).

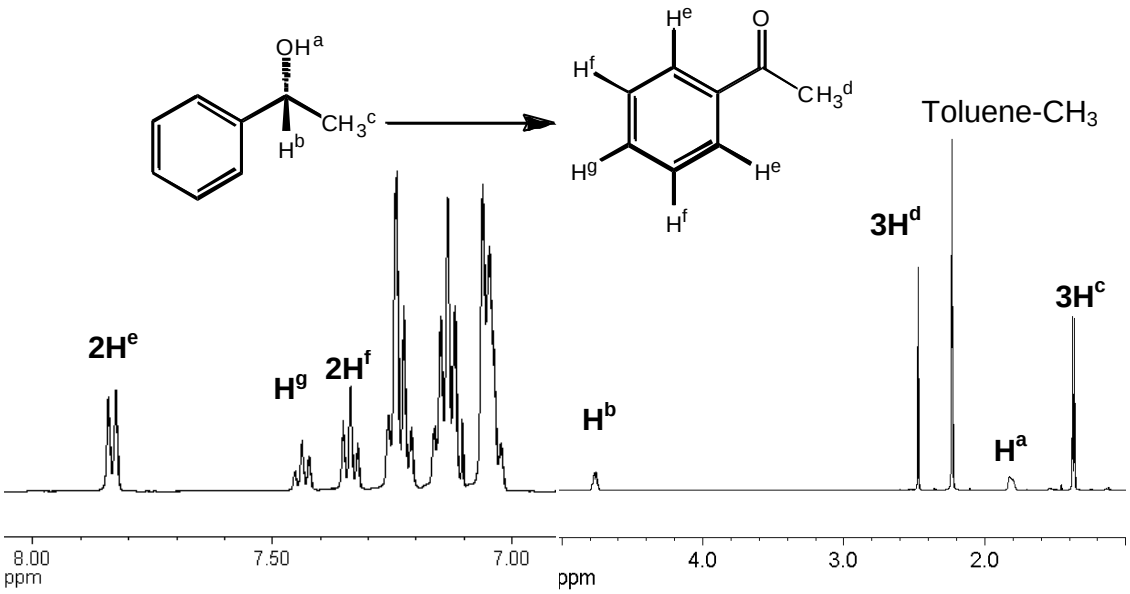

Figure 4.9. Example ^{1}H NMR spectrum for analysis of catalytic 1-phenylethanol dehydrogenation in $CDCl_3$. 0.1 mL of reaction mixture was diluted in $CDCl_3$ from reaction of 2.4 mL 1-phenylethanol, 2.4 mL toluene, and 0.10 mol % Ir catalyst under reflux conditions after 24 h.

Dehydrogenation of 1-Phenylethanol. In a typical procedure, a mixture of 3.4 mg (0.0060 mmol) of Cp*IrCl(cmhpH) in 725 µL (6.00 mmol) of DL-1-phenylethanol was heated by oil bath at 130 °C. After 2 h, 50 µL of reaction mixture was removed, diluted with $CDCl_3$ and the ratio of PhCOMe/PhCHOHMe was analyzed by ^{1}H NMR spectroscopy(See Figure 4.9).

X-ray Cystallography of compounds Cp*RhCl(cmhpH). Structure was phased by direct methods. Systematic conditions suggested the unambiguous space group Pbca. The space group choice was confirmed by successful convergence of the full-matrix least-squares refinement on F^2. The highest peaks in the final difference Fourier map were in the vicinity of atom Rh1; the final map had no other significant features. A final analysis of variance between observed and calculated structure factors showed no dependence on amplitude

or resolution. This model converged with $w_R^2 = 0.064$ and $R_1 = 0.025$ for 227 parameters with no restraints against 5794 data. The hydroxyl H atom surfaced in a late difference Fourier map and its position was refined with an independent isotropic displacement parameter. Methyl H atom positions, R-CH_3, were optimized by rotation about R-C bonds with idealized C-H, R--H and H--H distances. Remaining H atoms were included as riding idealized contributors. Methyl H atom U's were assigned as 1.5 times U_{eq} of the carrier atom; remaining H atom U's were assigned as 1.2 times carrier U_{eq}.

Crystallography of Cp*Rh(hp)(cmhpH). Structure was phased by direct methods. Systematic conditions suggested the ambiguous space group Ia. The space group choice was confirmed by successful convergence of the full-matrix least-squares refinement on F^2. The highest peaks in the final difference Fourier map were in the vicinity of the four independent Rh atoms; the final map had no other significant features. A final analysis of variance between observed and calculated structure factors showed no dependence on amplitude or resolution. The structure was refined in the alternate I-centered lattice to simplify the treatment of general and racemic twinning. The proposed model was complicated by numerous restraints, but efforts to find a super lattice were not successful. The proposed model includes four equivalent host molecules and six idealized acetonitrile solvates refined against 17651 unique unmerged reflections using general and racemic twinning in space group Ia. Owing to high correlation coefficients, the four independent host molecules were restrained to equivalent geometry using effective standard deviations of 0.01 and 0.02 % for bond lengths

and angles, respectively. Displacement parameters for atoms separated by less than 1.7 % were restrained to similar, symmetrical amplitudes (esd 0.01). Hydroxyl H atom positions, R-OH, were restrained to optimize the intramolecular hydrogen bond between atoms O1 and O4. Remaining H atoms were included as riding idealized contributors. Methyl and hydroxyl H atom U's were assigned as 1.5 times U_{eq} of the carrier atom; remaining H atom U's were assigned as 1.2 times carrier U_{eq}. The fractional contribution of the racemic twin was based on 7628 unmerged Friedels.

References

[1] Hiromoto, T.; Ataka, K.; Pilak, O.; Vogt, S.; Stagni, M. S.; Meyer-Klaucke, W.; Warkentin, E.; Thauer, R. K.; Shima, S.; Ermler, U. "The crystal structure of C176A mutated [Fe]-hydrogenase suggests an acyl-iron ligation in the active site iron complex." *FEBS Lett.* **2009**, *583*, 585-590.

[2] Lyon, E. J.; Shima, S.; Buurman, G.; Chowdhuri, S.; Batschauer, A.; Steinbach, K.; Thauer, R. K. "UV-A/Blue-Light Inactivation of the "Metal-Free" Hydrogenase (Hmd) from Methanogenic Archaea. The Enzyme Contains Functional Iron After All." *Eur. J. Biochem.* **2004**, *271*, 195-204

[3] Zirngibl, C.; van Dongen, W..; Schworer, B.; von Bunau, R.; Richter, M.; Klein, A.; Thauer, R. K. "" Eur. J. Biochem. 1992, 208, 511-

[4] Thauer, R. K. "Biochemistry of Methanogenesis: a Tribute to Marjory Stephenson." *Microbiology* **1998**, *144*, 2377-2406.

[5] Cammack, R.; Frey, M.; Robson, R. Hydrogen as a Fuel: Learning from Nature; Taylor & Francis: London, 2001.

[6] Fontecilla-Camps, J. C.; Volbeda, A.; Cavazza, C.; Nicolet, Y. "Structure/Function Relationships of [NiFe]- and [FeFe]-Hydrogenases." *Chem. Rev.* **2007**, *107*, 4273-4303.

[7] Korbas, M.; Vogt, S.; Meyer-Klaucke, W.; Bill, E.; Lyon, E. J.; Thauer, R. K.; Shima, S. "The Iron-Sulfur Cluster-free Hydrogenase (Hmd) Is a Metalloenzyme with a Novel Iron Binding Motif." *J. Biol. Chem.* **2006**, *281*, 30804-30813.

[8] Lyon, E. J.; Shima, S.; Boecher, R.; Thauer, R. K.; Grevels, F.-W.; Bill, E.; Roseboom, W.; Albracht, S. P. J. "Carbon Monoxide as an Intrinsic Ligand to Iron in the Active Site of the Iron-Sulfur-Cluster-Free Hydrogenase H_2-Forming Methylenetetrahydromethanopterin Dehydrogenase As Revealed by Infrared Spectroscopy." *J. Am. Chem. Soc.* **2004**, *126*, 14239-14248.

[9] Shima, S.; Lyon, E. J.; Sordel-Klippert, M.; Kauss, M.; Kahnt, J.; Thauer, R. K.; Steinbach, K.; Xie, X.; Verdier, L.; Griesinger, C. "Structure elucidation: The cofactor of the iron-sulfur cluster free hydrogenase Hmd: structure of the light-inactivation product." *Angew. Chem., Int. Ed.* **2004**, *43*, 2547-2551.

[10] Ahmed, S.; Lofthouse, R.; Shaw, G. "Purines, Pyrimidines, and Imidazoles. Part XL1V.l Syntheses of Some Dihydro-1.3-oxazine Derivatives and Related Substituted Uracils." *J. Chem. Soc., Perkin Trans. I* **1976**, 1969-1975.

[11] Collie, J. N. "Production of pyridine derivatives from ethylic β-amidocrotonate." *J. Chem. Soc.* **1897**, 303-311.

[12] Wang, X.; Li, Z.; Zeng, X.; Luo, Q.; Evans, D. J.; Pickett, C. J.; Liu, X. "The iron centre of the cluster-free hydrogenase (Hmd): low-spin Fe(II) or low-spin Fe(0)?" *Chem. Commun.* **2008**, 3555-3557.

[13] Guo, Y.; Wang, H.; Xiao, Y.; Vogt, S.; Thauer, R. K.; Shima, S.; Volkers, P. I.; Rauchfuss, T. B.; Pelmenschikov, V.; Case, D. A.; Alp, E. E.; Sturhahn, W.; Yoda, Y.; Cramer, S. P. "Characterization of the Fe Site in Methanothermobacter marburgensis Hydrogenase (mHmd) via Nuclear Resonant Vibrational Spectroscopy (NRVS)." *Inorg. Chem.* **2008**, *47*, 3969-3977.

[14] Severin, K. "Supramolecular chemistry with organometallic half-sandwich complexes." *Chem. Commun.* **2006**, 3859–3867.

[15] Shima, S.; Lyon, E. J.; Thauer, R. K.; Mienert, B.; Bill, E. "Mossbauer Studies of the Iron-Sulfur Cluster-Free Hydrogenase: The Electronic State of the Mononuclear Fe Active Site." *J. Am. Chem. Soc.* **2005**, *127*, 10430-10435.

[16] Rawson, J. M.; Winpenny, R. E. P. "The Coodination Chemistry of 2-Pyridones and Its Derivatives." *Coord. Chem. Rev.* **1995**, *139*, 313-374.

[17] Fujita, K.; Tanino, N.; Yamaguchi, R. "Ligand-Promoted Dehydrogenation of Alcohols Catalyzed by Cp*Ir Complexes. A New Catalytic System for Oxidant-Free Oxidation of Alcohols." *Org. Lett.* **2007**, *9*, 109-111.

[18] Almlöf, J.; Kvick, A.; Olovsson, I. "Hydrogen band studies. XLVII. Crystal structure of the intermolecular complex 2-pyridone: 6-chloro-2-hydroxypyridine." *Acta Cryst.* **1971**, *B27*, 1201-1208.

[19] Kelson, E. P.; Phengsy, P. P. “Synthesis and Structure of a Ruthenium(II) Complex Incorporating k^N Bound 2-Pyridonato Ligands; A New Catalytic System for Transfer Hydrogenation of Ketones.” *Dalton Trans.* **2000**, 4023-4024.

[20] Steiner, T. “The hydrogen bond in the solid state.” *Angew. Chem., Int. Ed.* **2002**, *41*, 48-76.

[21] Emsley, J. “Very Strong Hydrogen Bonds.” *Chem. Soc. Rev.* **1980**, *9*, 91-124.

[22] Hussain, M. S.; Schlemper, E. O. “A short and nearly symmetrical intramolecular hydrogen bond: x-ray and neutron diffraction analysis of 2,2-(1,3-diaminopropane)bis(2-methyl-3-butanone oximato)nickel(II) chloride hydrate.” *Inorg. Chem.* **1979**, *18*, 2275-2282.

[23] Goldman, A. S.; Roy, A. H.; Huang, Z.; Ahuja, R.; Schinski, W.; Brookhart, M. “Catalytic Alkane Metathesis by Tandem Alkane Dehydrogenation-Olefin Metathesis.” *Science* **2006**, *312*, 257-261.

[24] Zhu, K.; Achord, P. D.; Zhang, X.; Krogh-Jespersen, K.; Goldman, A. S. “Highly Effective Pincer-Ligated Iridium Catalysts for Alkane Dehydrogenation. DFT Calculations of Relevant Thermodynamic, Kinetic, and Spectroscopic Properties.” *J. Am. Chem. Soc.* **2004**, *126*, 13044 -13053.

[25] Murata, K.; Ikariya, T.; Noyori, R. “New Chiral Rhodium and Iridium Complexes with Chiral Diamine Ligands for Asymmetric Transfer Hydrogenation of Aromatic Ketones.” *J. Org. Chem.* **1999**, *64*, 2186-2187.

[26] Mashima, K.; Abe, T.; Tani, K. “The half-sandwich hydride and 16-electron complexes of rhodium and iridium containing (1S,2S)-N-(p-toluenesulfonyl)-1,2-diphenylethylenediamine: relevant to asymmetric transfer hydrogenation.” *Chem. Lett.* **1998**, 1201-1202.

[27] Tomon, T.; Koizumi, T.-a.; Tanaka, K. “Stabilization and destabilization of the Ru-CO bond during the 2,2'-bipyridin-6-onato (bpyO)-localized redox reaction of [Ru(terpy)(bpyO)(CO)](PF_6).” *Eur. J. Inorg. Chem.* **2005**, 285-293.

[28] Chen, D.; Scopelliti, R.; Hu, X. “Synthesis and Reactivity of Iron Acyl Complexes Modeling the Active Site of [Fe]-Hydrogenase.” *J. Am. Chem. Soc.* **2009**, *132*, 928-929.

[29] Turrell, P. J.; Wright, J. A.; Peck, J. N. T.; Oganesyan, V. S.; Pickett, C. J. "The Third Hydrogenase: A Ferracyclic Carbamoyl with Close Structural Analogy to the Active Site of Hmd." *Angew. Chem. Int. Ed.* **2010**, *49*, 7508-7511.

[30] Royer, A. M.; Rauchfuss, T. B.; Gray, D. L. "Oxidative Addition of Thioesters to Iron(0): Active-Site Models for Hmd, Nature's Third Hydrogenase." *Organometallics* **2009**, *28*, 3618-3620.

[31] Collie, J. N. "Production of pyridine derivatives from ethylic β-amidocrotonate." *J. Chem. Soc.* **1897**, *71*, 299-311.

[32] Ahmed, S.; Lofthouse, R.; Shaw, G. "Purines, Pyrimidines, and Imidazoles. Part XL1V.l Syntheses of Some Dihydro-1.3-oxazine Derivatives and Related Substituted Uracils." *J. Chem. Soc.* **1976**, *71*, 1969-1975.

Chapter 5

Organoiridium Pyridonates and Their Role in the Dehydrogenation of Alcohols

Introduction

The coordination chemistry of the tautomeric pair 2-hydroxypyridine/2-pyridone is well established[1,2] and is rich with opportunities for catalytic reactions that would benefit from the these bifunctional ligands in proton transfer reactions. Ligand facilitated proton-transfer is pervasive in bioinorganic and organometallic chemistry, being recently highlighted through studies of the [FeFe]-hydrogenases[3] and alkyne hydration,[4] respectively. The discovery of a derivative of a 2-pyridonate ligand at the active site of the hydrogenase enzyme Hmd[5] has enhanced interest in complexes containing *both* 2-pyridone and hydride ligands. Specifically, the active site of Hmd features an *N*-bonded 2-pyridone/hydroxypyridine ligand adjacent to the coordination site proposed for the hydride substrate.[6] Furthermore, the oxygen center of the pyridone/hydroxypyridine projects toward that coordination site (5.1).[7,8] It is likely that the 2-oxo functionality on the pyridyl ring participates in the hydrogen transfer reactions catalyzed by this enzyme.[9]

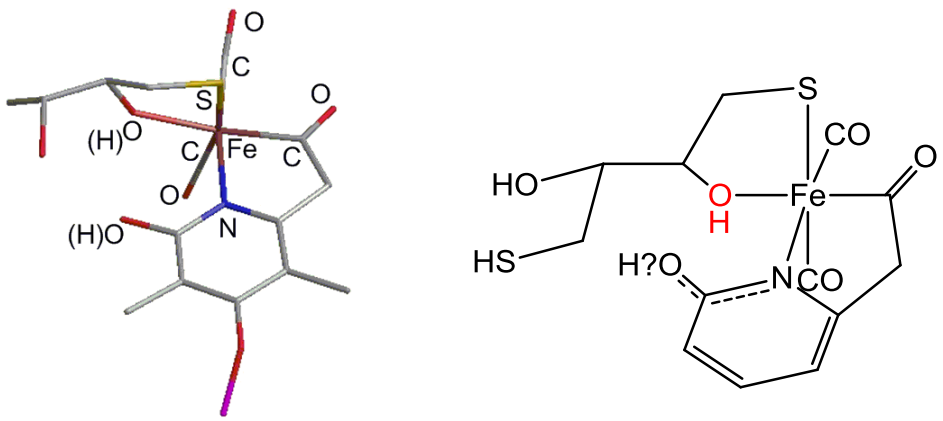

Figure 5.1. Structure of the dithiothreitol modified active site of Hmd, showing the binding of the pyridone/pyridinol cofactor.

Both members of the tautomeric pair 2-hydroxypyridine/2-pyridone are known to serve as unidentate ligands, binding metals through N or O.[2] Although complexes with O-bonding are more common with hard metals, e.g. $[Fe(O\text{-}2\text{-}C_5H_4NH)_6]^{2+}$,[10] softer metals prefer *N*-bonded 2-hydroxypyridine (2-hpH).[11] The ligand properties of the pyridonate anion are usefully referenced to the behavior of carboxylates. With a pK_a of 17.0 (DMSO),[12] 2-hydroxypyridine is much less acidic than acetic acid (pK_a 12.3, DMSO[13]). Pyridon*ate* can serve either as an *O*- or an *N*-bonded ligand,[14] the latter being more common for soft metals, e.g. $Ru(NC_5H_4O)_2(terpy)(H_2O)$.[15,16] Most commonly, pyridonates serve as *N,O*-bridging ligands in polymetallic compounds.[1,17-20] Monometallic complexes of bidentate pyridonates, i.e. κ^2-pyridonates, are rarer.[21-24]

The hydroxyl substituent of 2-pyridinols is known to interact with anionic ligands via hydrogen-bonding. For example, hydrogen-bonding between 2-pyridinol and hydride ligands is well known through the studies of Crabtree and

Morris.[25,26] 2-Hydroxypyridine is also known to form hydrogen bonds to halide and other ligands (eq 5.1).[27] More complicated ligands that incorporate the 2-pyridone functionality also participate in intramolecular H-bonding.[28-30]

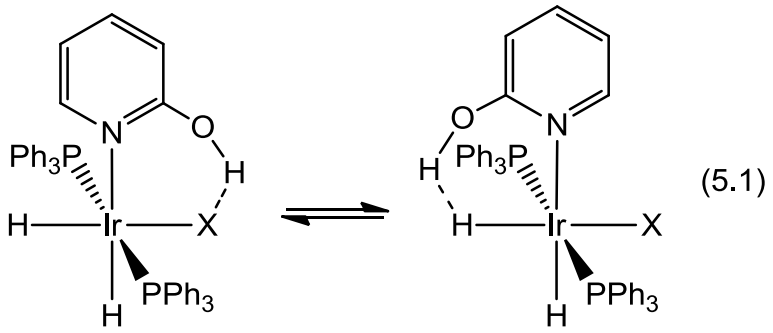

(5.1)

Yamaguchi *et al.* reported that the complex Cp*Ir(2-hp)Cl is especially active for the dehydrogenation of secondary alcohols.[31] These species were found to catalyze the (acceptorless) dehydrogenation of 1-phenylethanol with TON's of up to 700 in refluxing toluene. In terms of activity for alcohol dehydrogenation, Cp*Ir(κ^2-2-pyridone)Cl is one of the best (Table 5.1).[32-38] Dehydrogenation was proposed to proceed via ring-opening of the Ir(κ^2-2-pyridinoate) center to give a pyridinol-alkoxide complex that undergoes β-hydride elimination.[31] Pursuant to our interests in transfer hydrogenation,[39,40] we sought further insight into the Cp*Ir-2-pyridonate system with the goal of identifying intermediates and improving the efficiency of the catalyst.

Table 5.1 Reported Homogeneous Catalysts for Alcohol Dehydrogenation.[a]

Catalyst	Alcohol	TON (24h)	Special notes	Ref.
$CpRuCl(PPh_3)_2$	PhCH(OH)Me	3.2	5 mol% Ru cat. PhMe 110 °C	33
$(Indenyl)RuCl(PPh_3)_2$	PhCH(OH)Me	4.4	5 mol% Ru cat. PhMe 110 °C	33
$[(Benzene)RuCl_2]_2$	PhCH(OH)Me	4.8	5 mol% Ru cat. PhMe 110 °C	33
$[(p\text{-}Cymene)RuCl_2]_2$	PhCH(OH)Me	11.6	5 mol% Ru cat. PhMe 110 °C	33
$PhCH{=}Ru(PCy_3)_2Cl_2$	PhCH(OH)Me	14.2	5 mol% Ru cat. PhMe 110 °C	33
$Ru(Imes)(PPh_3)_2CO(H)_2$	PhCH(OH)Me	3.4	5 mol% Ru cat. PhMe 110 °C	33
$[(p\text{-}cymene)RuCl_2]_2$ + 6 PPh_3	PhCH(OH)Me	18	5 mol% Ru cat. PhMe 110 °C	33
$[Ru(u\text{-}OCO\text{-}C_2F_4\text{-}OCO)(CO)(H_2O)(dppp)]_2$	PhCH(OH)Me	197	0.4 mol% Ru cat. p-xylenes 130 °C	34
$[Ru(u\text{-}OCO\text{-}C_2F_4\text{-}OCO)(CO)(H_2O)(dppb)]_2$	PhCH(OH)Me	178	0.4 mol% Ru cat. p-xylenes 130 °C	34
$[Ru(u\text{-}OCO\text{-}C_2F_4\text{-}OCO)(CO)(H_2O)(dppf)]_2$	PhCH(OH)Me	350	0.2 mol% Ru cat. p-xylenes 130 °C	34
$[Ru(u\text{-}OCO\text{-}C_2F_4\text{-}OCO)(CO)(H_2O)(rac\text{-}BINAP)]_2$	PhCH(OH)Me	203	0.4 mol% Ru cat. p-xylenes 130 °C	34
$[Ru(u\text{-}OCO\text{-}C_2F_4\text{-}OCO)(CO)(H_2O)(PPh_3)_2]_2$	PhCH(OH)Me	50	0.4 mol% Ru cat. p-xylenes 130 °C	34
$IrH_5(iPr_3P)_2$	PhCH(OH)Me	91	1 mol% cat. 28h Me_3Si_2O 100 °C	35
$[(p\text{-}Cymene)RuCl_2]_2$ + $Me_2NCH_2CH_2OH$	PhCH(OH)Me	10.8 (6 h)	5mL alcohol 20.5 mmol cat. 90 °C	36
$[(p\text{-}Cymene)RuCl_2]_2$ + $Me_2NCH_2CH_2OH$	IPA	204 (6 h)	5mL alcohol 20.5 mmol cat. 90 °C	36
$Cp^*IrCl_2(2\text{-}hpH)$	PhCH(OH)Me	700 (20h)	0.1 mol% Ir cat. PhMe 110 °C	31

[a] Catalyst systems that require large quantities of basic or acidic media and systems for primary alcohol dehydrogenation were omitted for this comparison.[37,38]

Results

Hydrides Derived from Cp*Ir(κ^2-2-pyridonate)Cl. The relevant catalysts or precatalysts are Cp*Ir(κ^1-2-hydroxypyridine)Cl_2 and Cp*Ir(κ^2-2-pyridonate)Cl (**1**). In the presence of a base (K_2CO_3), the dichloride was found to give the same results as **1**, which was the starting point for our studies.1* Treatment of

*The related pyridonate complex (cymene)Ru(κ^2-2-pyridonate)Cl(17) Lahuerta, P.; Latorre, J.; Sanau, M.; Cotton, F. A.; Schwotzer, W. *Polyhedron* **1988**, *7*, 1311-1316. was found to be

solutions of **1** with secondary alcohols was found to give hydrides. For example, a CD_2Cl_2 solution of **1** with 5x excess PhCH(OH)Me at 25 ºC initially gives a transient hydride, previously unobserved, which converted cleanly to a more stable hydride over the course of several hours (Figure 5.2). ESI-MS analysis of reaction mixtures indicated that the stable hydride has the formula $[Cp^*_2Ir_2(\mu\text{-}H)_2(\mu\text{-}2\text{-}hp)]^+$ ($[\mathbf{2}]^+$).

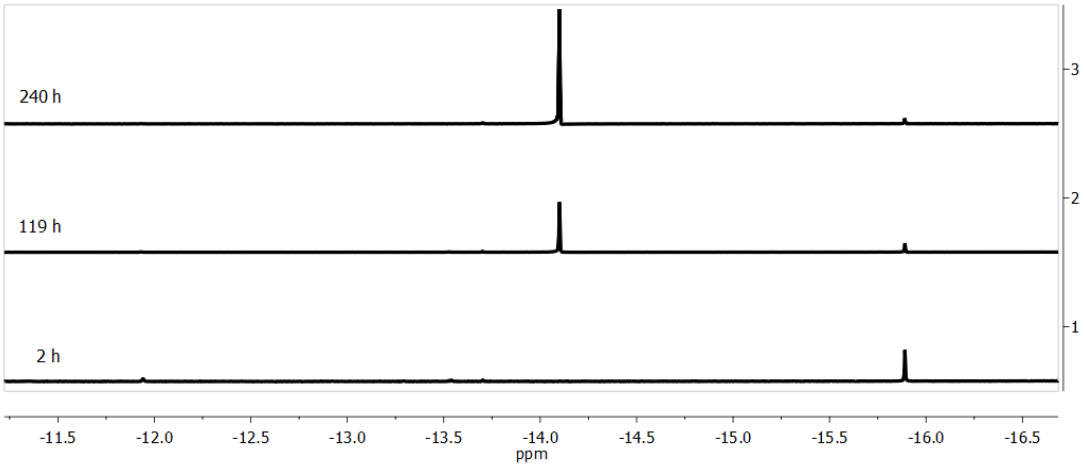

Figure 5.2. ^1H NMR spectrum in the hydride region of a CD_2Cl_2 solution of **1** and 5 equiv of PhCH(OH)Me at room temperature. The initial ^1H signal at δ-15.8 is for **3**. After 240 h, **1** is converted to give over 95% $[\mathbf{2}]^+$ (δ-15.8).

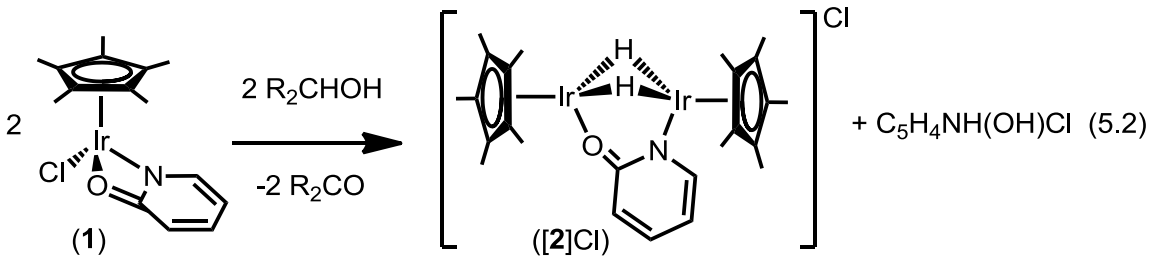

$[Cp^*_2Ir_2(\mu\text{-}H)_2(\mu\text{-}2\text{-}hp)]Cl$ ($[\mathbf{2}]Cl$) was independently generated by treatment

inactive. For the C_6H_6 derivative, see Morrison, E. C.; Palmer, C. A.; Tocher, D. A. *J. Organomet. Chem.* **1988**, *349*, 405-11.

of $Cp^*_2Ir_2H_2Cl_2$ with the Na2-hp. Its unsymmetrical structure is indicated by two equally intense ^1H NMR signals assigned to the nonequivalent Cp* ligands. Anion exchange with aqueous $NaPF_6$ converted the chloride salt into [**2**]PF_6, which was obtained in analytical purity. Crystallographic analysis confirmed that the cation in [**2**]PF_6 is unsymmetrical with the pyridonate ligand bridging the two Ir centers (Figure 5.3). The structure is related to the symmetrical compound $[Cp^*_2Rh_2H_2(\mu\text{-OAc})]PF_6$ ($r_{Rh\text{-}Rh}$ = 2.60(1) Å),[41] but the dihedral angle (between the Cp* groups) is smaller. In $[Cp^*_2Ir_2H_3]NO_3$ ([**4**]NO_3) the Cp* groups are perpendicular to the Ir---Ir vector.[42]

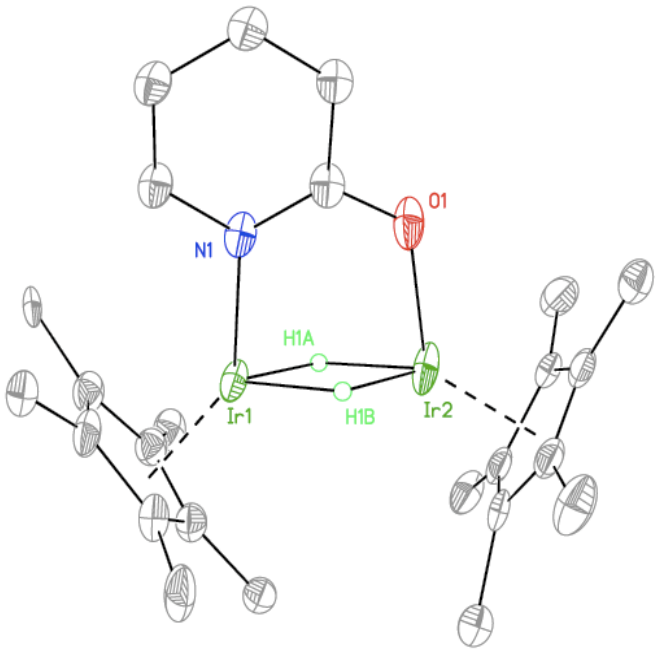

Figure 5.3. Structure of the cation in [**2**]PF_6 with methyl and aryl-H's removed for clarity: Ir, green; O, red; N, blue; C, black. Selected bond lengths [Å] and angles [°]: Ir(1)-N(1), 2.095(9); Ir(1)-N(1B), 2.101(9); Ir(1)-H(1A), 1.59(6); Ir(1)-H(1B), 1.73(7); Ir(2)-O(1), 2.033(6); Ir(2)-H(1A), 1.74(7); Ir(2)-H(1B), 1.59(6); Ir(1)-Ir(2), 2.675(3); $Cp_{centroid}$-Ir(1), 1.836; $Cp_{centroid}$(B)-Ir(1), 1.814; $Cp_{centroid}$-Ir(2), 1.807; $Cp_{centroid}$(B)-Ir(1), 1.792; Ir(1)-Ir(2)-H(1A), 35(2); Ir(1)-Ir(2)-H(1B), 38(2).

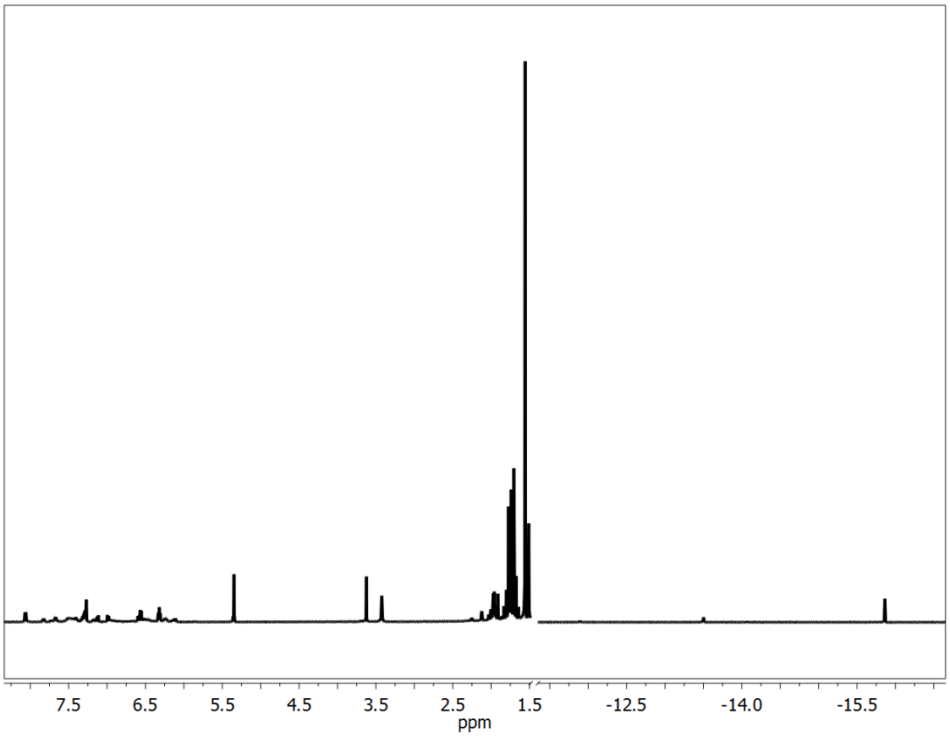

Figure 5.4. ^{1}H NMR spectrum of the products of catalytic hydrogenation of 40 equiv of **1** by Cp*Ir(TsDPEN-H) + MeOH in CD_2Cl_2 solution, after 3 weeks. The intense peak at δ1.54 corresponds to the Cp* peak of **3**, with the hydride signal at δ-15.8.

The transient hydride observed in all reactions of **1** with hydrogen donors is proposed to be the 2-hydroxypyridine complex Cp*IrHCl(2-hpH) (**3**). The compound was not isolated in pure form, but the ^{1}H NMR data are consistent with the proposed stoichiometry (Figure 5.4). Compound **3** was independently generated by treatment of **1** with the transfer hydrogenation catalyst Cp*IrH(TsDPENH).[43] This process occurs rapidly even below 0 ºC (eq 5.3). In the presence of excess MeOH, Cp*IrH(TsDPENH) (as well as (cymene)RuH(TsDPENH)) slowly catalyzes this same conversion, the slow step being the regeneration of Cp*IrH(TsDPENH). Addition of Et_3N to a solution of **3** results in its complete and immediate formation of [**2**]$^{+}$. We also found that solutions of **3** react with PPh_3 to give Cp*IrClH(PPh_3) (eq 5.4).

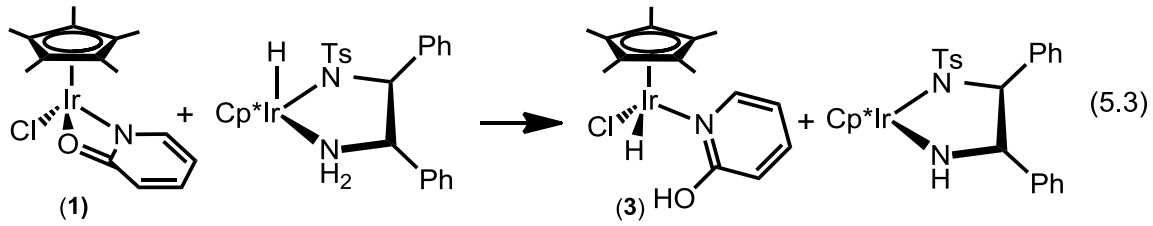

(5.3)

$$Cp^*IrClH(2\text{-}hpH) + PPh_3 \rightarrow Cp^*IrClH(PPh_3) + 2\text{-}hpH \qquad (5.4)$$

The fate of **1** was determined under conditions approaching those for catalysis (100 ºC with 5 equiv of PhCH(OH)Me vs refluxing toluene and 1000 equiv of PhCH(OH)Me) (Figures 5.5, 5.6). We observed the initial formation of a small quantity of **3** followed within minutes by the appearance of $[\mathbf{2}]^+$ as the predominant species, which persisted for hours at 100 ºC. In contrast to its rapid reaction with PhCH(OH)Me, it is interesting neither phenol nor 2,4-dinitrophenol react with **1**, thus proton-induced ring-opening is not facile. Similarly, **1** is unreactive toward methanol (25 ºC, 24 h).

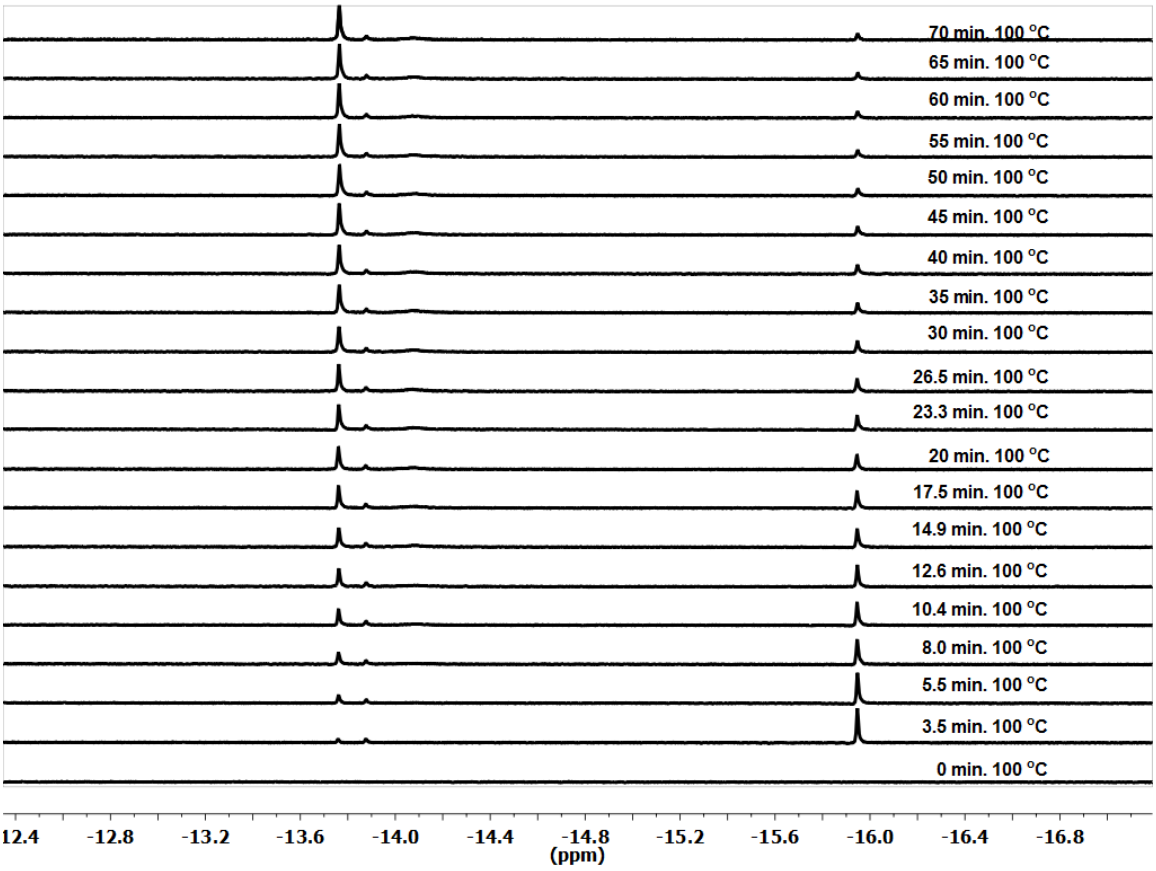

Figure 5.5. ^{1}H NMR spectrum in the hydride region for a toluene-d^{8} solution of **1** + 5 1-phenylethanol at 100 ºC over 70 minutes. The initial hydride signal at δ-15.9 is from **3**. The signal at δ-13.8 is from [**2**]$^{+}$ and is the largest signal after 15 minutes. Under normal catalytic conditions, the 5 equivalents of 1-phenylethanol would be dehydrogenated after ~ 6 minutes.

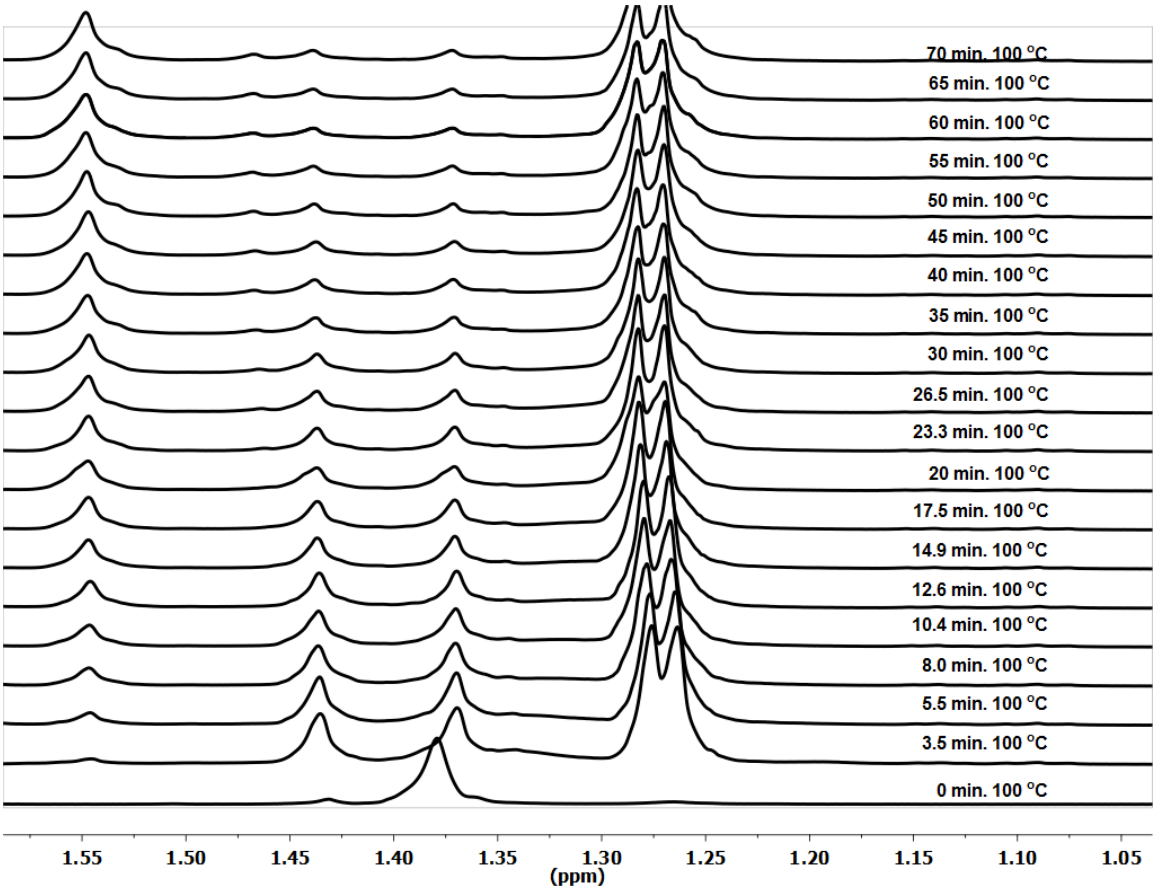

Figure 5.6. ^{1}H NMR spectra in the Cp* region for a toluene-d_8 solution of **1** + 5 1-phenylethanol at 100 ºC. The large doublet near δ1.27 is the methyl signal for 1-phenylethanol. The Cp* signal for **3** is under this methyl signal. The signals at δ1.44 and 1.37 are from $[2]^+$, which is precipitating due to low solubility in toluene and low alcohol concentration. The large signal at δ1.55 is from the formation of $Cp^*Ir(2hp)_2$. The formed solids were collected and shown to be $[2]^+$.

Solutions of **1** in CD_2Cl_2 were also found to react readily with H_2, **3** again being the first detectable hydride, which was observed after a few seconds at -30 ºC and 1 atm H_2. Conversion of **1** was complete within minutes at room temperature, the main product being $[\mathbf{2}]^+$ together with a trace of $Cp^*_2Ir_2H_2Cl_2$, as observed by Yamaguchi under similar conditions.[44] Upon prolonged exposure of these solutions to H_2, only $[\mathbf{2}]^+$ and $[Cp^*_2Ir_2H_3]^+$ ($[\mathbf{4}]^+$) (δ-15.5, s) were observed (Figure 5.7, 5.8).

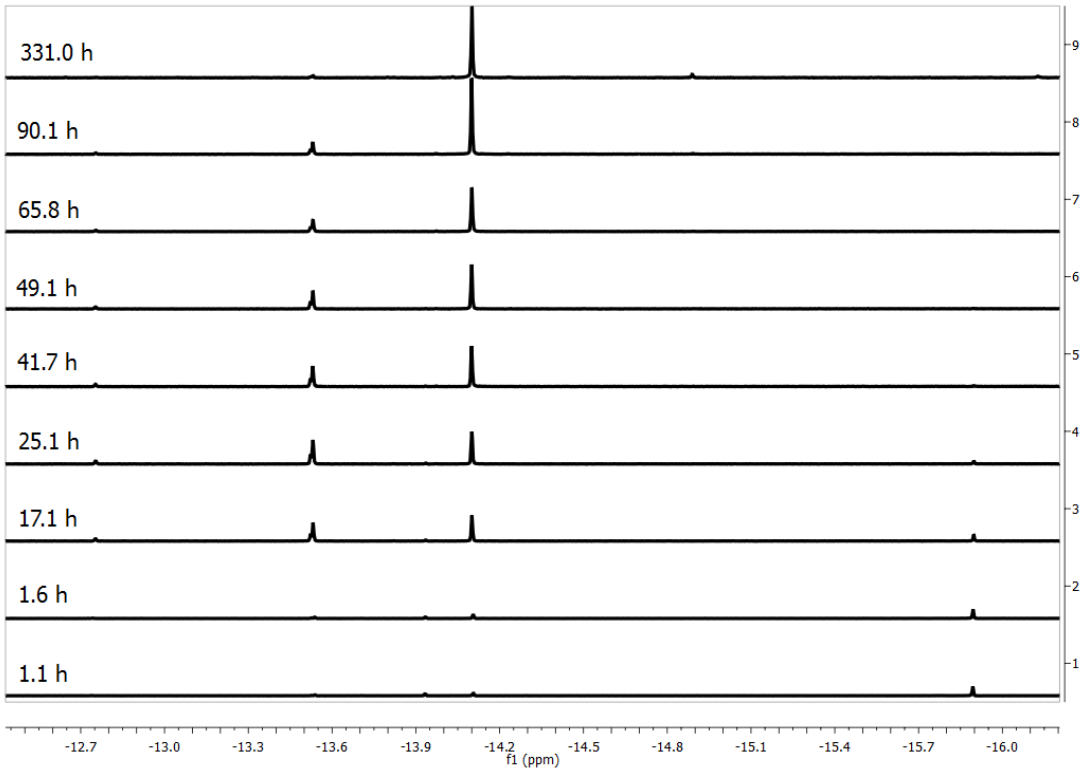

Figure 5.7. ^{1}H NMR spectra in the hydride region for a CD_2Cl_2 solution of **1** with 66 mm Hg of H_2 at room temperature. The initial signal at δ-15.8 is for **3**. After 330 h, the major hydride signal (δ-14.1) corresponds to [**2**]$^{+}$.

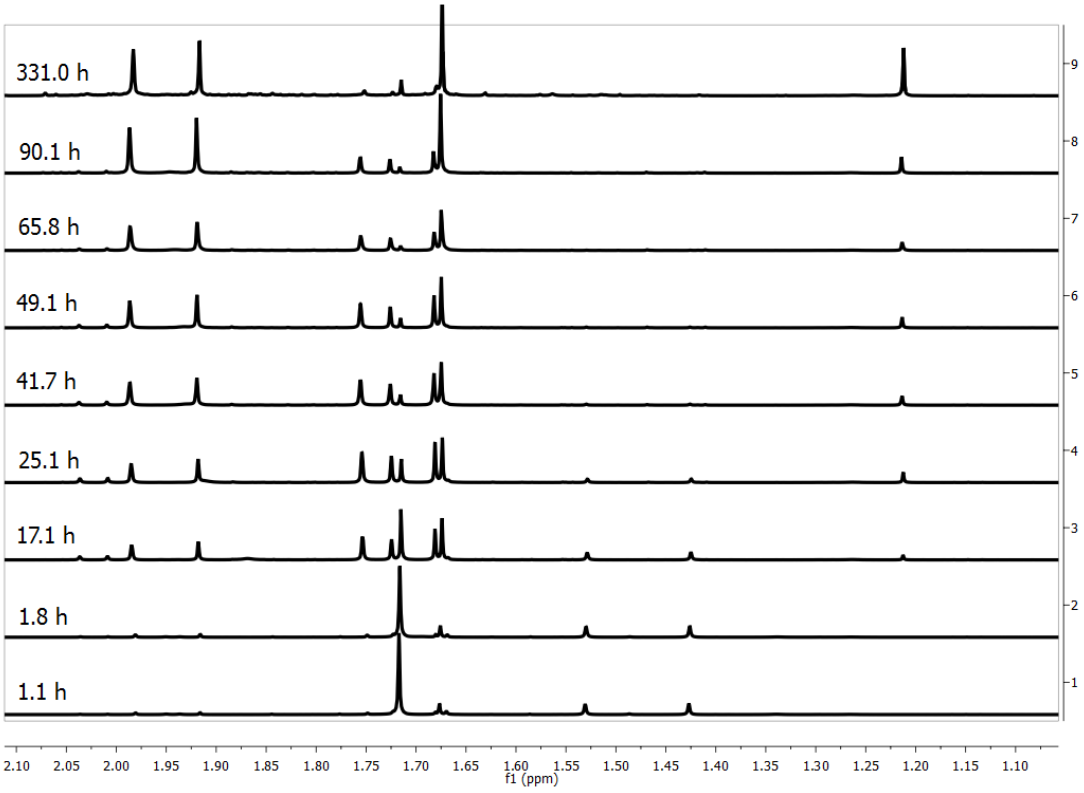

Figure 5.8. Cp* region of ^{1}H NMR spectra of **1** under 66 mm Hg H_2 at room temperature. The initial ^{1}H signal at δ1.72 is for **1**. The signal at δ1.54 cooresponds to **3**. After 330 h, the major Cp* signals at δ1.92 and 1.98 correspond to [**2**]$^{+}$. The intense signal at δ1.67 is from to Cp*Ir(2hp)$_2$, which arises from the reaction of 2-hpH + **1.**

Catalytic Role of 2^{+}. We assessed the relative activity of several Cp*Ir-hp complexes for the catalytic dehydrogenation of PhCH(OH)Me (Table 5.2). Compound **1** was found to be superior to [**2**]Cl, but both were far more active than related compounds. Striking was the finding that [**2**]PF_6 is a very poor catalyst, even though [**2**]$^{+}$ is the dominant species in solutions of active catalysts (see above). ^{19}F NMR analysis of a catalytic run after 21 h verified that the majority (~95%) of the PF_6^{-} remained intact, thus the inactivity of [**2**]PF_6 is not attributable to degradation of the counterion. Addition of PPNCl (PPN^{+} = N(PPh$_3$)$_2^{+}$) to this solution gave activity comparable to [**2**]Cl

(Table 5.2)(Figure 5.9).

Table 5.2. Turnover Numbers (TON) for Various Catalysts for Conversion of PhCH(OH)Me into PhC(O)Me. *Conditions:* 6 mL of toluene, 2.4 mL of 1-phenylethanol, 0.1 mol% Ir complex, reflux.

Catalyst	TON 5 h	TON 21 h
Cp*IrCl(2-hp) (**1**)	237	571
Cp*IrCl(2-hp) (**1**) + 5 equiv 2-hpH	253	640
$[(Cp^*IrH)_2(2\text{-hp})]Cl$ ([**2**]Cl)	167	408
$[(Cp^*IrH)_2(2\text{-hp})]PF_6$ ([**2**]PF_6)	7	107
$[(Cp^*IrH)_2(OAc)]PF_6$	38	83
$[(Cp^*Ir)_2H_3]PF_6$ ([**4**]PF_6)	57	130
$Cp^*{}_2Ir_2H_2Cl_2$	44	114
$Cp^*Ir(2\text{-hp})_2$	23	167

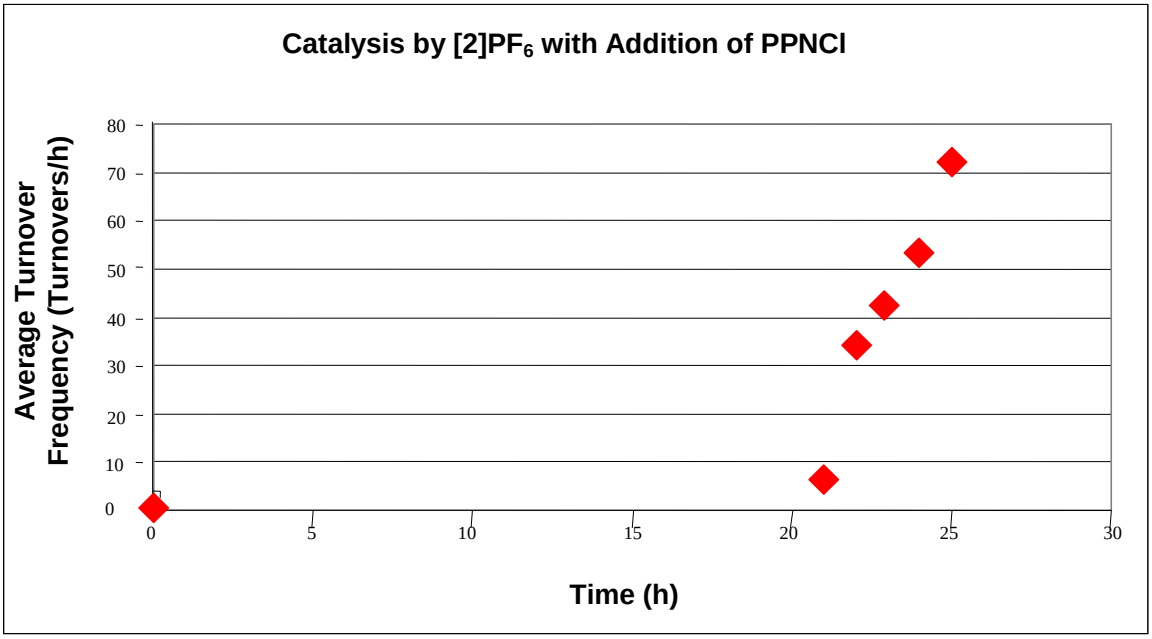

Figure 5.9. TON (h^{-1}) vs time for the dehydrogenation of PhCH(OH)Me (0.1 mol % Ir, refluxing toluene) by [**2**]PF_6 before and after addition of 2 equiv of PPN^+Cl^- (at 21 h).

The addition of further equivalents of PPNCl, which has good solubility under catalytic conditions, had only a modest effect on catalysis by **1**. The addition of a five equiv excess of 2-hpH to **1**, however, improves the stability of the catalyst system. Greater excess of 2-hpH was found to suppress activity, which is consistent with our finding that the bis(pyridonate) Cp*Ir(κ^2-2-hp)(κ^1-2-hp) is a poor catalyst (Figure 5.10).

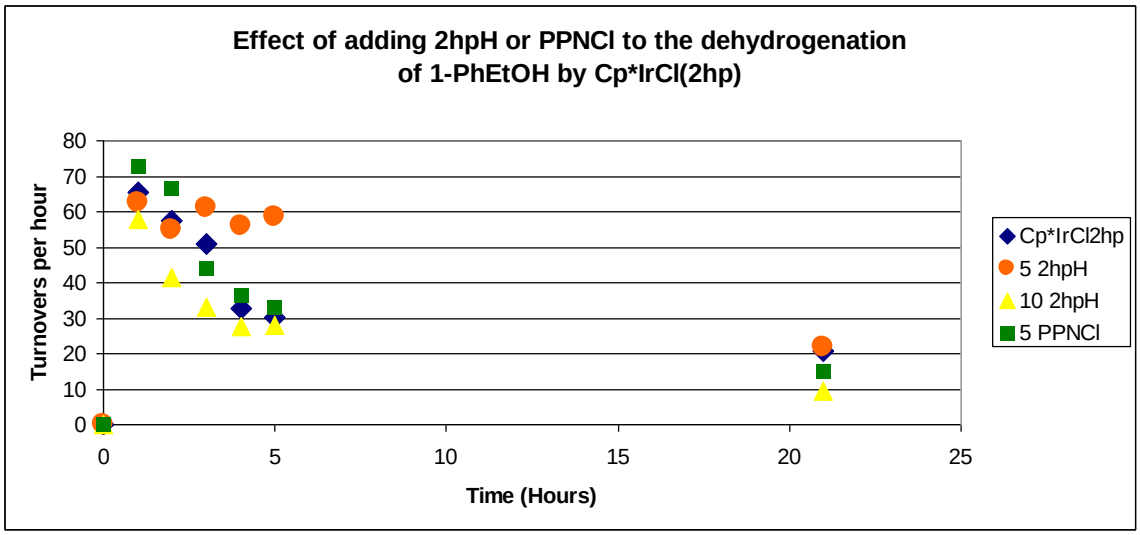

Figure 5.10. Effects of the addition of PPNCl and 2hpH on the TON for dehydrogenation of PhCH(OH)Me by **1**.

PPh_3 Derivatives. Phosphine adducts of **1** were examined in order to expand the range of these unusual catalysts and prevent dimerization to species like **2**$^+$. We found that Cp*$IrCl_2$(2-hpH) reacts with PPh_3 to give Cp*$IrCl_2(PPh_3)$, consistent with the high lability of the κ^1-hpH ligand. Treatment of **1** with PPh_3 cleanly gave Cp*$IrCl(PPh_3)$(κ^1-2-hp) (**5**). The ^{1}H NMR signals at δ5.6, 5.87, 6.78, and 8.12 are diagnostic for a *N*-bonded pyridonoate.[45,46] Treatment of **5** with

$AgPF_6$ effected closure of the pyridonate chelate ring to give [Cp*Ir(κ^2-2-hp)(PPh_3)]PF_6 (**6**, eq 5.5). Neither **5** nor **6** showed any reactivity toward H_2 or toward PhCH(OH)Me.

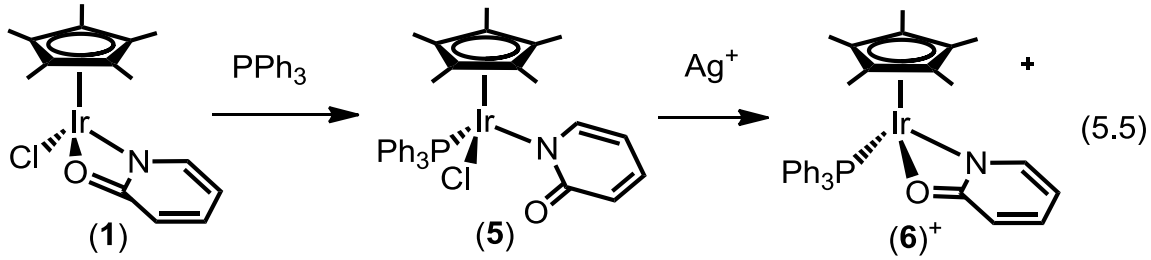

(5.5)

The above experiments showed that PPh_3 efficiently (i) replaces 2-hydroxypyridine and (ii) opens the Ir(κ^2-2-hp) chelate ring to produce stable adducts. In view of these results, we repeated the experiments involving hydrogenation of **1** (-25 ºC, 1 atm H_2) followed by quenching the mixtures with PPh_3 after several minutes. ^{31}P NMR analysis of these reaction mixtures revealed the presence of significant amounts of Cp*IrHCl(PPh_3) (Figure 5.11). This hydrido chloride is derived from displacement of κ^1-hydroxypyridine in the transiently formed **3**, not by the relatively slow reaction of $Cp^*_2Ir_2H_2Cl_2$ with PPh_3.[47] We also observed Cp*IrCl_2(PPh_3) as well as Cp*IrCl(2-hp)(PPh_3)(**5**), the latter arising from **1**. These same species were observed by addition of PPh_3 to a cooled catalytic reaction mixture. In such a case, a large amount of unreacted PPh_3 was detected, reflecting the nonreactivity of $\mathbf{2}^+$ toward PPh_3.

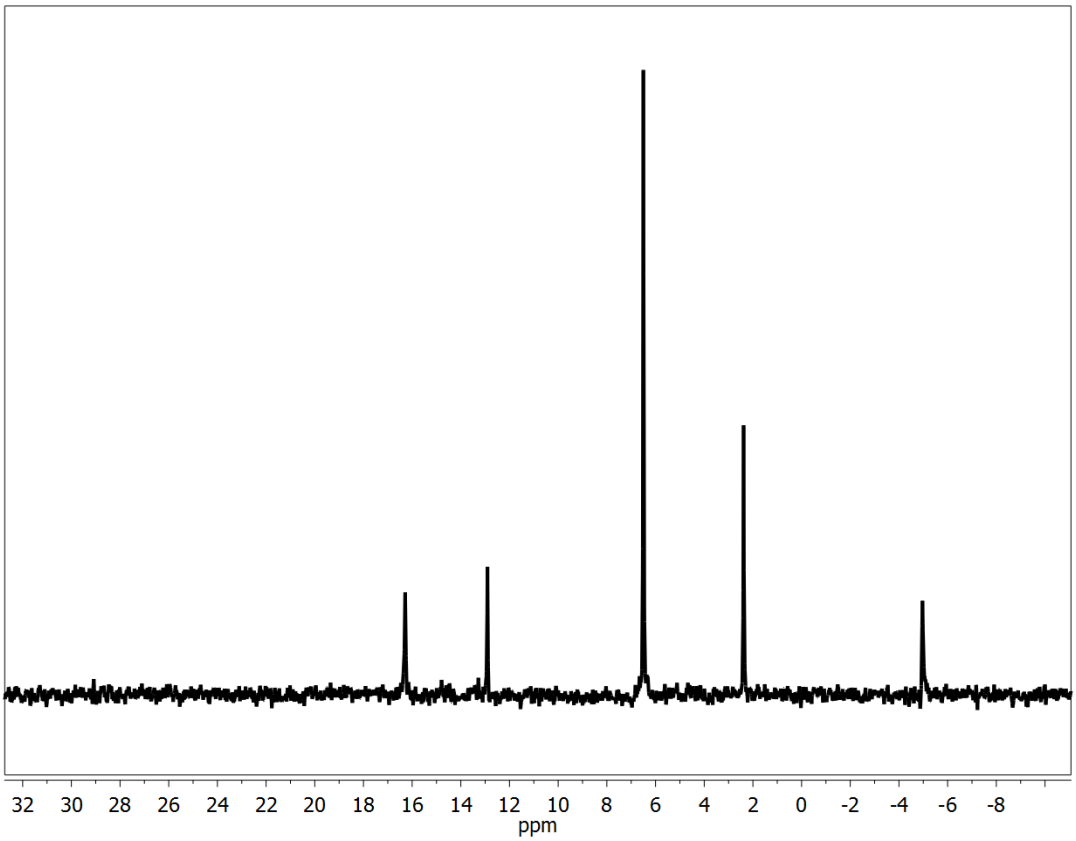

Figure 5.11. ^{31}P NMR spectrum of the PPh_3 trapped products obtained by the addition of 1 equiv of PPh_3 to the reaction of **1** + H_2 at -25 ^oC in CH_2Cl_2 solution. PPh_3 was added after 40 minutes and solution was stirred 20 min before a 0.8 mL sample was removed and analyzed at room temperature .

Complexes of Other Pyridones. Given the high catalytic activities seen for **1**, we examined related complexes using 6-methyl-2-hydroxypyridine (6-mhpH) and 2,6-dihydroxypyridine. The new complexes were prepared by combining $Cp^*_2Ir_2Cl_4$ with the sodium salts of these pyridonates. The complex $Cp^*Ir(\kappa^2$-6-mhp)Cl (**7**)(Figure 5.12) was found to be spectroscopically similar to **1**. We were unable, however, to prepare $Cp^*Ir(\kappa^1$-6-mhpH)Cl_2, the analogue of $Cp^*Ir(\kappa^1$-2-hpH)Cl_2, via cleavage of $Cp^*_2Ir_2Cl_4$ by 6-mhpH. We conclude that the increased steric bulk of this ligand precludes κ^1-coordination. Furthermore, **7**

proved to be a poor catalyst for dehydrogenation of PhCH(OH)Me.

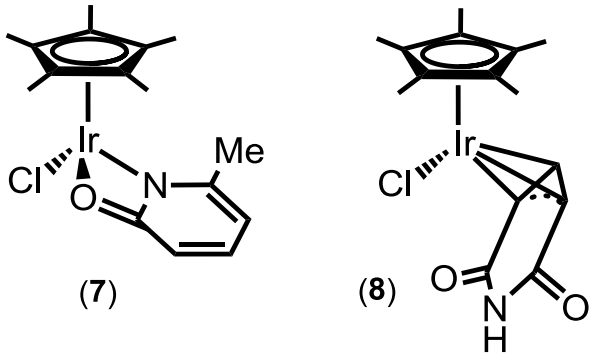

Figure 5.12. Molecular structures of complexes **7** and **8**.

Via a salt-elimination route, we prepared a species with the nominal formula Cp*Ir($C_5H_4NO_2$)Cl (**8**). ^{1}H NMR spectra even at –60 ºC indicated a symmetrical structure with signals at δ4.36, 5.61, and 6.69 (Figure 5.13). The low-field signal was found to rapidly exchange with D_2O. Single crystal X-ray diffraction of the derivative (CpMe$_4$Et)Ir analogue of **8** established that this complex is better described as the allyl derivative Cp*Ir(η^3-2,6-pyridione)Cl (Figure 5.14). The Ir1-C13 and Ir1-C16 distances of 2.219 and 2.227 Å are within the normal distances for an Ir(III)-allyl complex. The Ir1-C12 distance of 2.081 Å is the shortest Ir(III)-C bond among these structures, the closest example being Ir(η^3-C3H5)I[N($SiMe_2CH_2PPh_2)_2$] with a C2-Ir 2.113 Å.[48] With a TON of 230 (standard conditions, 21 h), complex **8** is an effective catalyst (or precatalyst) for the dehydrogenation of PhCH(OH)Me, but it is inferior to **1**.

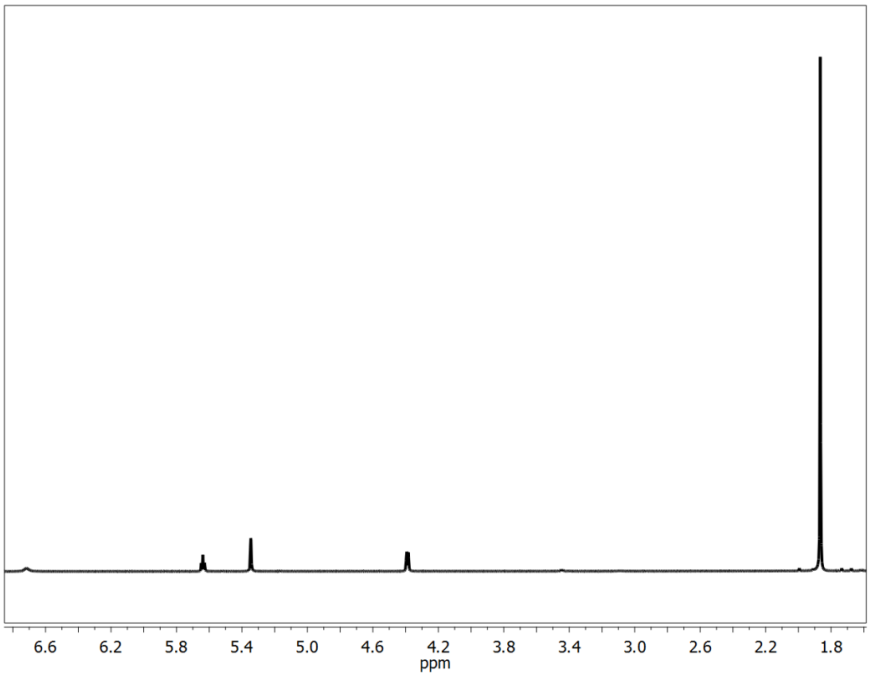

Figure 5.13. ^{1}H NMR spectrum of **8** in CD_2Cl_2 solution.

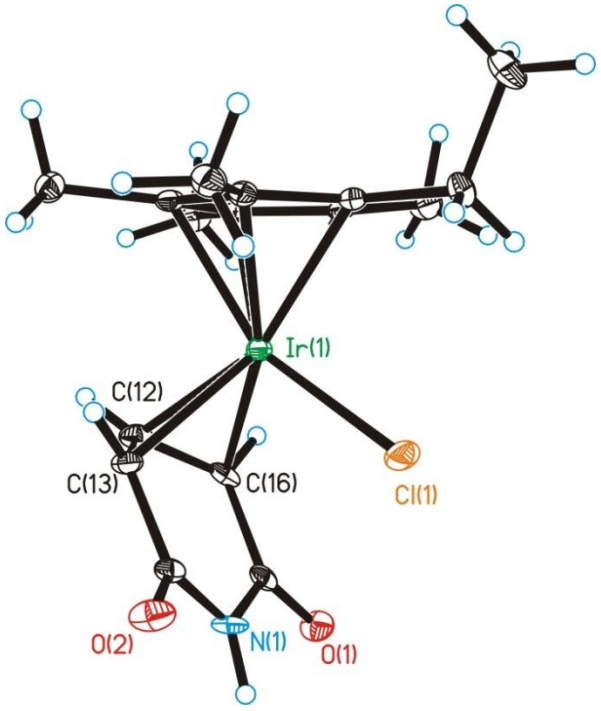

Figure 5.14. Crystallographically determined structure of ($CpMe_4Et$)IrCl(η^3-2,6-dhpH) with Ir, green; Cl, orange; O, red; N, blue, C, black. Selected bond distances (Å): Ir1-Cl1, 2.3919(12); Ir1-C12, 2.081(42); Ir1-C13, 2.219(4); Ir1-C16, 2.227(4); C12-C13, 1.436(5); C12-C16 1.417(5); C13-C14 1.464(5); N1-C14 1.387(5); N1-C15 1.391(4); C15-C16 1.463(5); C14-O2, 1.228 (4); C15-O1, 1.229 (4); Cp Centroid – Ir1, 1.833

Conclusions

The 2-pyridone ligand gives Cp*Ir(III) complexes that are highly active for homogeneous catalytic dehydrogenation of alcohols.[31] In this work we searched for the catalytically active species. Our results show that the κ^2-pyridonate complex Cp*IrCl(κ^2-2-hp) is highly reactive toward hydrogen donors, often under very mild conditions. Under catalytic conditions, the dominant species in solution is the μ-pyridonato salt [$Cp^*_2Ir_2H_2$(2-hp)]Cl. The pathway to [**2**]$^+$ presented in eq 5.6 is consistent with our results.

$$2\ Cp^*IrHCl(\kappa^1\text{-2-hpH}) \rightarrow [Cp^*_2Ir_2H_2(\text{2-hp})]Cl + [\text{2-hpH}_2]Cl \quad (5.6)$$

3 [**2**]Cl

Required for this conversion is the high substitutional lability of the 2-hpH ligand in Cp*IrHCl(κ^1-2-hpH) (**3**) as indicated in PPh_3-trapping experiments. Further evidence for the identity of **3** is provided by its formation by direct hydrogenation of **1**, both catalytically and stoichiometrically, concomitant with the conversion of Cp*IrH(TsDPENH) into Cp*Ir(TsDPEN). This conversion provides an unusual example of transfer of H_2 between metal complexes.

Although [$Cp^*_2Ir_2H_2$(2-hp)]$^+$ is the dominant complex in solution during catalysis, it is catalytically inactive. Instead, in the presence of chloride, this diiridium cation converts to a highly active long-lived dehydrogenation catalyst.

Experimental

General considerations. Unless otherwise indicated, reactions were conducted using standard Schlenk techniques (N_2) at room temperature with stirring. Solvents were dried and degassed prior to use. The following were prepared according to literature methods: Cp*Ir(κ^2-2-hp)Cl,[31] $[Cp^*_2Ir_2H_3]PF_6$,[49] $Cp^*_2Ir_2H_2Cl_2$,[47] $[Cp^*_2Ir_2H_2(\mu\text{-OAc})]PF_6$,[47] $Cp^*IrCl_2(PPh_3)$,[50] and $Cp^*_2Ir_2Cl_4$.[51] The reaction of $Cp^*_2Ir_2H_2Cl_2$ with PPh_3 to produce $Cp^*IrClH(PPh_3)$ is much slower than originally described,[47] requiring about 24 h for completion. 2-Hydroxypyridine, 6-methyl-2-hydroxypyridine, 2,6-dihydroxypyridine hydrochloride, NaOMe, Et_3N, and $AgPF_6$ were purchased from Aldrich. Racemic 1-phenylethanol was obtained from Alfa-Aesar.

Electrospray ionization-mass spectra (ESI-MS) were acquired using a Micromass Quattro QHQ quadrupole-hexapole-quadrupole instrument. ^1H, ^{19}F, and ^{31}P NMR spectra were acquired on Varian UNITY INOVA TM 500NB and UNITY 500 NB instruments. Elemental analyses were performed by the School of Chemical Sciences Microanalysis Laboratory utilizing a Model CE 440 CHN Analyzer.

$[Cp^*_2Ir_2H_2(\mu\text{-2-hp})]X$ ([2]Cl and [2]PF_6). A solution of 400 mg (7.4 mmol) of NaOMe in 5 mL of MeOH was transferred to a solution of 704 mg (7.4 mmol) of 2-hpH in 5 mL of MeOH to give a clear, colorless solution. Solvent was removed under vacuum at 60 ºC overnight to give an air-stable hygroscopic white powder, which was stored in a desiccator. Yield: 774 mg (6.6 mmol, 89%). ^1H NMR (500 MHz, CD_3OD): δ 6.33 (t, 1H, 6.2 Hz, aryl-C*H*), 6.40 (d, 1H, 8.5 Hz,

aryl-C*H*), 7.35 (t, 1H, 8 Hz, aryl-C*H*), 7.67 (d, 1H, 5.4 Hz, aryl-C*H*). A solution of 24 mg (0.205 mmol) of Na2-hp in 2 mL of MeOH was transferred to a blue solution of 150 mg (0.205 mmol) of $Cp^*_2Ir_2H_2Cl_2$ in 10 mL of CH_2Cl_2 to give an immediate red solution. After stirring 5 min., the solvent was removed under vacuum. The product was extracted into 10 mL of CH_2Cl_2, and the slurry cannula-filtered to remove NaCl. The filtrate was concentrated to about 3 mL and diluted with hexanes to produce a brown powder. Yield: 138 mg (0.176 mmol, 86%). ^{1}H NMR (500 MHz, CD_2Cl_2): δ -14.10 (s, 2H, Ir-*H*-Ir) 1.92 (s, 15 H, Cp*), 1.99 (s, 15 H, Cp*'), 6.57 (t of d, 1H, 2 Hz, 6 Hz aryl-C*H*), 7.28 (m, 2H, aryl-C*H*, aryl-C*H*'), 8.33 (d, 1H, 6 Hz, aryl-C*H*). ESI-MS: m/z = 750.2 ($[Cp^*_2Ir_2H_2(2\text{-}hp)]^+$). Red crystals of $[Cp^*_2Ir_2H_2(\mu\text{-}2\text{-}hp)]PF_6$ precipitated upon the addition of 0.5 mL saturated aqueous solution of $NaPF_6$ to an acetone solution of [**2**]Cl. The solid was filtered off, washed with water, and dried under vacuum overnight. Yield: 350 mg (0.39 mmol, 68%). ^{1}H NMR (Figure 5.15) (500 MHz, CD_2Cl_2): δ -14.10 (s, 2H, Ir-*H*-Ir), 1.92 (s, 15 H, Cp*), 1.99 (s, 15 H, Cp*'), 6.57 (t of d, 1H, 2 Hz, 6 Hz aryl-C*H*), 7.28 (m, 2H, aryl-C*H*, aryl-C*H*'), 8.33 (d, 1H, 6 Hz, aryl-C*H*). ESI-MS: m/z = 750.2 $[Cp^*_2Ir_2H_2(2\text{-}hp)]^+$). Anal. Calcd for $C_{25}H_{36}F_6Ir_2NOP$ (found): C, 33.51 (33.37); H, 4.05 (3.97); N, 1.56 (1.63). Crystals suitable for X-ray diffraction were obtained by layering a solution of 60 mg of [**3**]PF_6 in 2 mL of CH_2Cl_2 with 30 mL of Et_2O. Crystals grew over the course of 2 h at room temperature.

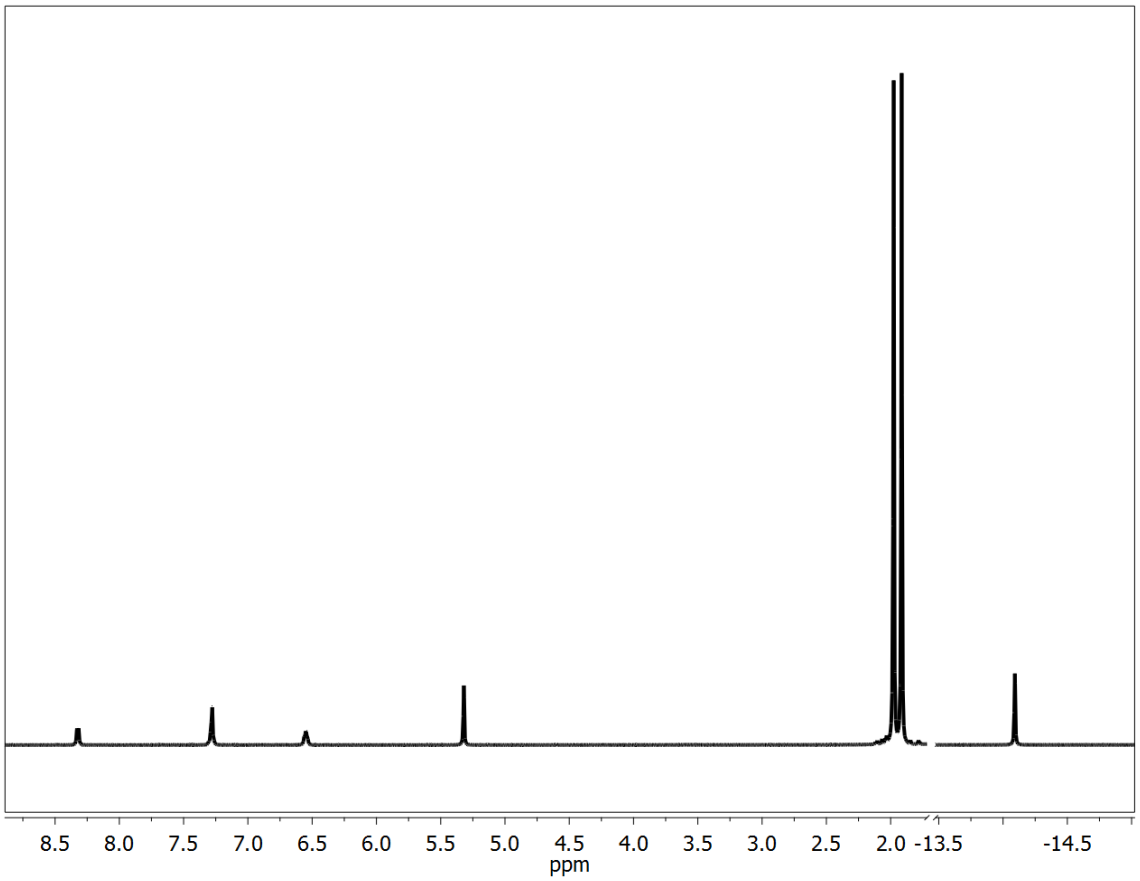

Figure 5.15. ^{1}H NMR spectrum of a solution of [**2**]PF_6 in CD_2Cl_2 solution.

Cp*IrH(Cl)(2-hpH) (3). To a solution of 7.9 mg (0.017 mmol) of **1** in 0.8 mL of CD_2Cl_2 was added 12.0 mg (0.017 mmol) of Cp*IrH(TsDPENH). NMR analysis revealed the formation of Cp*Ir(TsDPEN) and an intense set of signals assigned to Cp*IrH(Cl)(2-hpH). ^{1}H NMR (500 MHz, CD_2Cl_2): δ -15.8 (s, 1H, Ir-H), 1.54 (s, 15H, Cp*), 6.29 (t, 1H, 6 Hz, aryl-C*H*), 6.54 (d, 1H, 8 Hz, aryl-C*H*), 7.24 (m, 1H, aryl-C*H*), 8.03 (d of d, 1H, 2 Hz, 6 Hz aryl-C*H*).

Cp*Ir(2-hp)$_2$. A colorless solution of 88.2 mg (0.753 mmol) of Na2-hp in 6 mL of MeOH was transferred to an orange solution of 150 mg (0.188 mmol) of $(Cp^*IrCl_2)_2$ in 5 mL of CH_2Cl_2. After stirring 1 h the solvent was removed by

vacuum. The product was dissolved in 5 mL CH_2Cl_2 and filtered via filter cannula to remove NaCl. The reaction solution was diluted with 25 mL of hexanes, and volume of the mixture was concentrated under vacuum to 10 mL to produce a yellow powder. The product was collected by filtration over a medium glass frit in air and washed with 5 mL hexanes. Yield: 142 mg (0.274 mmol) (73 %). ^{1}H NMR (Figure 5.16) (500 MHz, CD_2Cl_2 25 ºC): $\delta =$ 1.68 (s, 15 H, Cp*), 5.97 (d of d, 1H, 2 Hz, 18 Hz, aryl-C*H*), 6.15 (t of d, 1H, 2 Hz, 13 Hz aryl-C*H*), 7.13 (t of d, 1H, 5 Hz, 15 Hz, aryl-C*H*), 7.75 (d of d, 1H, 3 Hz, 12 Hz, aryl-C*H*).

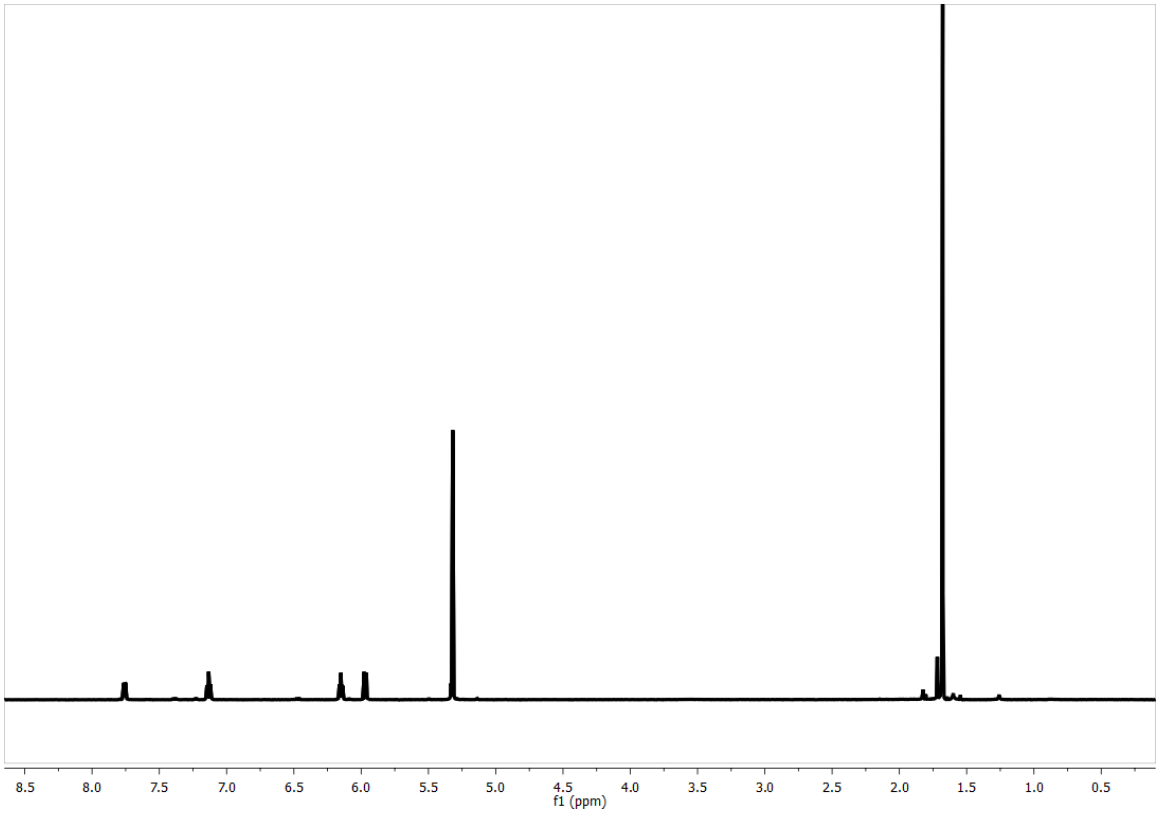

Figure 5.16. ^{1}H NMR spectrum of Cp*Ir(2hp)$_2$ at 22 °C in CD_2Cl_2 solution.

Cp*Ir(2-hp)Cl(PPh_3) (5). A colorless solution of 329 mg (1.26 mmol) of PPh_3 in 5 mL of CH_2Cl_2 was transferred to a clear orange solution of 574 mg

(1.26 mmol) of **1**. After stirring for 10 min, the reaction solution was concentrated under vacuum and diluted with hexanes to precipitate yellow crystals, which were dried under vacuum. Yield: 721 mg (1.01 mmol, 81%). Alternatively, the product could be obtained by reaction of $Cp^*IrCl_2(PPh_3)$ with Na2-hp in similar yield. ^1H NMR (500 MHz, CD_2Cl_2): δ 1.35 (d, 15 H, 2 Hz, Cp*), 5.60 (d of d, 1H, 1.5 Hz, 8.7 Hz, pyr-aryl-C*H*), 5.87 (t of d, 1H, 1.5 Hz, 6.5 Hz, pyr-aryl-C*H*), 6.78 (t of d, 1H, 2.2 Hz, 7.5 Hz, pyr-aryl-C*H*), 7.00 (m, 2H, Ph-C*H*), 7.14 (m, 3H, Ph-C*H*) , 7.33 (m, 4H, Ph-C*H*), 7.45 (m, 4H, Ph-C*H*) , 7.97 (m, 2H, Ph-C*H*), 8.12 (d of d, 1H, 2 Hz, 6 Hz, pyr-aryl-C*H*). ^{31}P NMR (202 MHz, CD_2Cl_2): δ 6.53 (s, Ir-*P*Ph_3). Anal. Calcd for $C_{33}H_{34}ClIrNOP$ (found): C, 55.10 (54.96); H, 4.76 (4.71); N, 1.95 (2.10).

$[Cp^*Ir(\kappa^2\text{-}2\text{-hp})(PPh_3)]PF_6$ (6). A solution of 40 mg (0.158 mmol) of $AgPF_6$ in 3 mL of CH_2Cl_2 was transferred to an orange solution of 114 mg (0.158 mmol) of **5** in 4 mL of CH_2Cl_2 to give an immediate colorless precipitate. The solution mixture was filtered via filter cannula to give a light orange solution, which was concentrated. Yellow crystals were obtained upon addition of hexanes and were dried under vacuum. Yield: 103 mg (0.125 mmol, 79%). ^1H NMR (500 MHz, CD_2Cl_2): δ 1.45 (d, 15 H, x Hz, Cp*), 5.46 (d , 1H, 9 Hz, pyr-aryl-C*H*), 6.52 (t of d, 1H, 1 Hz, 6.5 Hz, pyr-aryl-C*H*), 7.11 (t of d, 1H, 1.3 Hz, 8 Hz, pyr-aryl-C*H*), 7.41 (m, 12H, Ph-C*H*), 7.49 (m, 3H, Ph-C*H*), 7.77 (d of d, 1H, 0.8 Hz, 5.8 Hz, pyr-aryl-C*H*). ^{31}P NMR (202 MHz, CD_2Cl_2): δ 15.72 (s, Ir-*P*Ph_3), -145.20 (p, 710 Hz, *P*F_6) ESI-MS: m/z = 684.4 $[Cp^*Ir(2\text{-hp})(PPh_3)]^+$, 625.3 $[Cp^*IrCl(PPh_3)]^+$, 589.3 $[Cp^*Ir(PPh_3)]^+$. Neither **5** nor **6** showed any reactivity toward 1 atm H_2 or toward PhCH(OH)Me under the standard catalytic conditions.

Na6-Me-2-hp. Synthesized similar to Na2-hp. Yield: 115 mg (8.75 mmol, 96%). ^{1}H NMR (500 MHz, CD_3OD): δ 2.24 (s, 3H, C*H*$_3$), 6.18 (d, 1H, 7 Hz, aryl-C*H*), 6.24 (d, 1H, 8 Hz, aryl-C*H*), 7.30 (t, 1H, 7.8 Hz, aryl-C*H*).

Cp*IrCl(6-Me-2-hp) (7). A colorless solution of 110 mg (0.656 mmol) of Na6-mhp in 5 mL of MeOH was transferred to an orange solution of 261 mg (0.328 mmol) of $Cp^*_2Ir_2Cl_4$ in 10 mL of CH_2Cl_2. After the solution was stirred for 1 h, the solvent was removed by vacuum. The product was extracted into 5 mL of CH_2Cl_2, and this extract was filtered to remove NaCl. The filtrate was concentrated to ~2 mL and then diluted with 10 mL of hexanes to produce a yellow precipitate. Yield: 101 mg (0.213 mmol, 65%). ^{1}H NMR (500 MHz, CD_2Cl_2): δ 1.72 (s, 15 H, Cp*), 2.28 (s, 3H, 6-C*H*$_3$), 5.87 (d, 1H, 8 Hz, aryl-C*H*), 6.34 (d, 1H, 7 Hz, aryl-C*H*), 7.29(t, 1H, 8 Hz, 4-C*H*). Anal. Calcd for $C_{16}H_{21}ClIrNO$ (found): C, 40.81 (40.58); H, 4.49 (4.43); N, 2.97 (3.02). A CH_2Cl_2 solution of **8** was treated with 1 atm of H_2 at room temperature over 24 h; ^{1}H NMR analysis revealed a small amount of free 6-Me-hpH but mostly (~95%) unreacted starting material.

(C_5Me_4R)IrCl(η^3-2,6-dhpH) (R = Me (8), and R = Et). A solution of 562 mg (10.41 mmol) of NaOMe in 5 mL of MeOH was transferred to a solution of 768 mg (5.2 mmol) of 2,6-dhpH_2·HCl in 5 mL of MeOH to give a clear, colorless solution. Solvent was removed under vacuum at 60 ºC overnight to give an air reactive hygroscopic white powder stored under an Ar atmosphere in a dry box. Yield of Na2,6-dhpH·NaCl: 945 mg (4.94 mmol, 95%). ^{1}H NMR (500 MHz,

CD_3OD): δ 5.40 (d, 2H, 8 Hz, aryl-C*H*), 7.23 (t, 1H, 8 Hz, aryl-4-C*H*). A solution of 151.5 mg (0.791 mmol) of Na2,6-dhpH·NaCl in 3 mL of MeOH was added to a solution of 300 mg (0.377 mmol) of $Cp^*_2Ir_2Cl_4$ in 3 mL of CH_2Cl_2. After stirring for 1 h, the solution was concentrated under vacuum. The residue was extracted into 5 mL of CH_2Cl_2, and this extract was cannula-filtered to remove NaCl. The filtrate was concentrated to a small volume and diluted with hexanes to produce a yellow powder, which was dried under a vacuum. Yield: 280 mg (0.592 mmol, 79%). ^{1}H NMR (500 MHz, CD_2Cl_2): δ 1.84 (s, 15 H, Cp*), 4.36 (d, 2H, 5 Hz, aryl-C*H*) exchanged in D_2O, 5.61 (t, 1H, 5 Hz, 4-aryl-C*H*), 6.69 (s, 1H, N*H*) exchanged in D_2O. Anal. Calcd for $C_{15}H_{19}ClIrNO_2$ (found): C, 38.09 (38.30); H, 4.05 (4.47); N, 2.96 (2.56). $(C_5Me_4Et)IrCl(\eta^3$-2,6-dhpH) was obtained similarly to Cp*IrCl(2,6-dhpH) utilizing $(CpMe_4Et)_2Ir_2Cl_4$. Yield: 128 mg (0.263 mmol, 79%). ^{1}H NMR (500 MHz, $CDCl_3$): δ = 1.14 (t, 3 H, 8 Hz, Cp-CH_2C*H*$_3$),1.86 (s, 6 H, Cp-C*H*$_3$), 1.90 (s, 6 H, Cp-C*H*$_3$), 2.17 (q, 2 H, 8 Hz, Cp-C*H*$_2CH_3$),4.44 (d of d, 2H, 1.6 Hz, 5 Hz, aryl-C*H*) exchanged in D_2O, 5.62 (t, 1H, 5 Hz, 4-aryl-C*H*), 6.69 (s, 1H, N*H*) exchanged in presence of D_2O. Single crystals of suitable for X-ray diffraction were obtained by diffusion of Et_2O into a concentrated solution of $(CpMe_4Et)IrCl(2,6\text{-}dhpH)$ in CH_2Cl_2.

Catalytic Dehydrogenation of 1-Phenylethanol (See Table 5.2). In a 100-mL 3-necked flask equipped with a nitrogen inlet, reflux condenser, and rubber septum, 6 mL of toluene, 2.4 mL of 1-phenylethanol, 0.5 mL of CH_2Ph_2, and 0.1 mol% (Ir) catalyst were heated at a vigorous reflux in a 130 ºC oil bath. Samples of 100 μL were withdrawn at hourly intervals for the first 5 h, and a final

sample was removed after 21 h. Conversions were determined by ^{1}H NMR analysis using CH_2Ph_2 as an internal integration standard. ESI-MS analysis of all catalysts after 21 h (130 ºC) showed the presence of significant amounts of $[Cp^*_2Ir_2H_3]^+$. The ESI-MS spectra of the catalytic runs using **2**, [**4**]Cl, and [**4**]PF_6 after 21 h were nearly identical with the major peak at m/z = 750 corresponding to $[Cp_2^*Ir_2H_2(2\text{-hp})]^+$**.**

5 equivs of 2-hydroxypyridine. Using standard conditions for 1-phenylethanol dehydrogenation with the addition of 9.5 mg (0.099 mmol) 2-hydroxypyridine before heating.

10 equivs of 2-hydroxypyridine. Using standard conditions for 1-phenylethanol dehydrogenation with the addition of 19.4 mg (0.204 mmol) 2-hydroxypyridine before heating.

5 equivs of Bis(triphenylphosphine)iminium chloride (PPNCl). Using standard conditions for 1-phenylethanol dehydrogenation with the addition of 57 mg (0.099 mmol) PPNCl before heating.

Chloride Rescue of Catalysis by [2]PF_6. *Reaction Conditions:* 6 mL toluene, 2.4 mL PhCH(OH)Me, 0.1 mol% Ir catalyst, and 0.5 mL CH_2Ph_2 at reflux in a 130 ºC oil bath. After 21 h, 0.7 mL of reaction mixture was removed and the ^{19}F NMR spectrum was obtained of the neat solution. Spectra showed minimal ~5 % decomposition of the PF_6^-. Solid PPNCl 11.4 mg (0.020 mmol) was added to the mixture. To evaluate the effect of PPNCl on activity, 0.1 mL samples were withdrawn from the reaction mixture over the next 4 h, diluted with $CDCl_3$, and assayed by ^{1}H NMR spectroscopy in the usual manner.

Room Temperature Reaction of 1 with PhCH(OH)Me. Solid **1** (13 mg, 0.028 mmol) was added to a J.Young NMR tube followed by addition of 16.9 µL (0.14 mmol) of 1-phenylethanol in a drybox. CD_2Cl_2 was added and the solution was immediately shaken to give a homogeneous mixture. ^1H NMR data were obtained over the course of 240 h to give predominately $[\mathbf{2}]^+$.

Low Pressure Reaction of 1 with H_2. Solid **1** (20 mg, 0.044 mmol) was added to a J.Young NMR tube and CD_2Cl_2 (0.9 mL) was vacuum transferred. The solution was kept frozen in liquid N_2, and (H_2 66 mmHg) was admitted to the head space (~1.7 mL). The tube was sealed and warmed to 22 ºC. ^1H NMR data were obtained over the course of 240 h to initially give **3** followed by predominately $[\mathbf{2}]^+$ over longer reaction times. Three other unidentified hydrides are detected, but only after the formation of complex $[\mathbf{2}]^+$.

Low Temperature Reaction of 1 with ~1 atm of H_2. In order to observe early intermediates in the conversion of **1** to $[\mathbf{2}]^+$, a J.Young NMR tube was charged with solid **1** (9.7 mg, 0.021 mmol) and CD_2Cl_2 (0.8 mL), which was vacuum transferred. The solution was kept frozen in liquid N_2 and (H_2 437 mmHg) was added to the head space (~1.8 mL). The tube was sealed and warmed to –78 ºC. The NMR tube was warmed to -50 ºC in the instrument and ^1H NMR was obtained. After 10 minutes the solution was warmed to -40 ^oC and a spectrum was obtained. This was repeated until reaction was noticed at -20 ^oC. Spectra were collected every 5 min. for 1 h. The intermediates detected were identical to the low pressure reaction at room temperature.

Reaction of 1 with Cp*IrH(TsDPENH). Solutions containing a large quantity of **3** were obtained by transfer hydrogenation from Cp*IrH(TsDPENH) to **1**. In a typical reaction, 5.7 mg of **1** (0.012 mmol) and 4.3 mg of Cp*IrH(TsDPENH) were combined in 1 mL of CD_2Cl_2 at -27 ^oC then allowed to warm to room temperature to give a dark red solution. ^1H NMR data showed the reaction was complete within 5 minutes. Upon longer reaction times, the ^1H NMR spectrum showed very little change. The reaction was slowed by the presence of excess MeOH, which is unreactive toward **1** at room temperature.

Cp*IrH(TsDPEN)-Catalyzed Hydrogenation of 1. A solution of 5.5 mg of Cp*Ir(TsDPEN-H) (0.008 mmol) and 150.5 mg of **1** (0.329 mmol) in 15 mL of CH_2Cl_2 and 5 mL of MeOH was stirred at room temperature. ^1H NMR analysis showed nearly all **1** had reacted after 3 weeks. When the reaction mixture was warmed above 40 ºC, the Cp*IrH(TsDPEN) converted to the cyclometalated product, and H_2 transfer to **1** was stopped. ^1H NMR solutions were prepared by removal of ~1 mL of solution from the reaction. Solvent was removed under vacuum and the solid was dissolved in CD_2Cl_2.

Addition of Base to *In Situ* Formed 3. A solution of Cp*IrH(TsDPENH) (11.2 mg, 0.016 mmol) in 0.8 mL of CD_2Cl_2 was cooled in a J.Young tube to –27 ºC in a freezer inside a dry box. Solid **1** (6 mg, 0.013 mmol) was added and the solution was stored at –27 ºC 18 h until a dark red color was noted. The ^1H NMR spectrum was recorded at room temperature and again after 2 h at room temperature. The solution contained a large amount of **3**, which did not change over the 2 h. Solid proton sponge, 1,8 bisdimethylaminonaphthalene, (1.8 mg,

0.008 mmol) was added to the J. Young tube in a dry box. ^{1}H NMR obtained within 10 min. showed complete conversion of **3** to [**2**]$^+$.

High Temperature ^{1}H NMR study of 1 + PhCH(OH)Me, In Situ Analyses. A solution of **1** (10.4 mg, 0.023 mmol) in 1 mL of d^8-toluene was added to a J. Young tube, and a ^{1}H NMR spectrum was collected at 22 ºC. 13.7 µL (0.114 mmol) of PhCH(OH)Me was added to the solution, and a ^{1}H NMR spectrum was recorded immediately (22 ºC). The sealed tube was heated at 95.6 ºC, and ^{1}H NMR data were collected over 80 min. The solution initially has a small quantity of **3**, but quickly the solution is predominantly **2**$^+$. Over the course of 1 h, **2**$^+$ remains the dominant (NMR-detectable) species in solution.

PPh_3 Trapping Experiments.

Low Temperature H_2 reaction. A yellow solution of 81 mg (0.18 mmol) of **1** in 5 mL of CH_2Cl_2 at -25 ºC was flushed with 1 atm H_2. After 40 min, the solution becomes a deep red color and was treated with 46 mg (0.18 mmol) of PPh_3. The flask was flushed with N_2. After stirring the solution for 20 min. at -25 ºC, 0.8 mL of sample was removed and analyzed by ^{31}P NMR spectroscopy: Cp*IrHCl(PPh_3) (δ12.9, 9.4%), Cp*IrCl$_2$(PPh_3) (δ2.4, 19%), PPh_3 (δ-4.96, 12%), as well as Cp*IrCl(2-hp)(PPh_3) (δ6.5, 47%). A signal at δ16.3 (14%) could not be assigned.

High Temperature PhCH(OH)Me reaction. A solution of 53 mg (0.12 mmol) of **1** in 2 mL of toluene in a three-necked flask fitted with a condenser was heated in a 130 ºC oil bath then treated with 0.7 mL (5.8 mmol) of PhCH(OH)Me. After 30 min, the red solution was cooled in an ice bath and treated with 33.5 mg

(0.128 mmol) of PPh_3. After 20 min. stirring, 0.7 mL of solution was removed and analyzed by ^{31}P NMR spectroscopy was collected. The following species were observed (% relative amounts based on ^{31}P NMR analysis: Cp*IrHCl(PPh_3) (δ12.5, 4.2%), Cp*$IrCl_2$(PPh_3) (δ2.1, 18%), PPh_3 (δ-4.8, 70%) , as well as Cp*IrCl(2-hp)(PPh_3) (δ6.3, 4.9%). A peak at δ19.0 (2.8%) could not be assigned.

X-ray Cystallography of compounds [2]PF_6 and (CpMe$_4$Et)IrCl(η^3-2,6-dhpH). The crystallographic analysis of [**2**]PF_6 and (C_5Me_4Et)IrCl(η^3-2,6-dhpH) were conducted in the usual way (Supporting Information) but the cation $\mathbf{2}^+$ suffered from severed disorder in the ligands and PF_6 anion. Our model converged with w_R^2 = 0.0914 and R_1 = 0.0548 for 631 parameters with 1198 restraints against all 6133 data. The main residue had both Cp* ligands positionally disordered. The Ir-C distances between an individual Ir-Cp* ligand were constrained to be similar (esd 0.01). The pyrdinate ligand was also positionally disordered. Like C-O and Ir-N distances on the pyrdinate ligand were restrained to be similar (esd 0.01). Rigid-bond restraints (esd 0.01) were imposed on displacement parameters for all disordered sites and similar displacement amplitudes (esd 0.01) were imposed on disordered sites overlapping by less than the sum of van der Waals radii. Methyl H atom positions, R-CH_3, were optimized by rotation about R-C bonds with idealized C-H, R-C and H···H distances. Both hydride, H-Ir, atoms were located in the difference map in asymmetric positions. Full positional refinement of the hydride atoms was not possible because of the heavy Ir atoms and the sever disorder in the structure so restraints had to be applied. The short Ir1-H1a and Ir2-H1b

distances were restrained to be similar (esd 0.01) as well as the longer Ir1-H1b and Ir2-H1a distances (esd 0.01). The remaining H atoms were included as riding idealized contributors. Methyl H atom U's were assigned as 1.5 times U_{eq} of the carrier atom, hydride H atom U's assigned as 1.5 times U~eq~ of the carrier Ir atom (the carrier atom being the Ir atom that H shared the shortest bond distance with), and remaining H atom U's were assigned as 1.2 times carrier U_{eq}.

References:

[1] Sadimenko, A. P. "Organometallic complexes of polypyridine ligands V: their analogs, and N,O(S)-chelating pyridines." *Adv. Heterocycl. Chem.* **2009**, *98*, 225-306.

[2] Rawson, J. M.; Winpenny, R. E. P. "The Coodination Chemistry of 2-Pyridones and Its Derivatives." *Coord. Chem. Rev.* **1995**, *139*, 313-374.

[3] Barton, B. E.; Olsen, M. T.; Rauchfuss, T. B. "Aza- and Oxadithiolates Are Probable Proton Relays in Functional Models for the [FeFe]-Hydrogenases." *J. Am. Chem. Soc.* **2008**, *130*, 16834-16835.

[4] Grotjahn, D. B. "Heteroatoms moving protons: synthetic and mechanistic studies of bifunctional organometallic catalysis." *Pure Appl. Chem.* **2010**, *82*, 635-647.

[5] Shima, S.; Lyon, E. J.; Sordel-Klippert, M.; Kauss, M.; Kahnt, J.; Thauer, R. K.; Steinbach, K.; Xie, X.; Verdier, L.; Griesinger, C. "Structure elucidation: The cofactor of the iron-sulfur cluster free hydrogenase Hmd: structure of the light-inactivation product." *Angew. Chem., Int. Ed.* **2004**, *43*, 2547-2551.

[6] Heinekey, D. M. "Hydrogenase enzymes: Recent structural studies and active site models." *J. Organometal. Chem.* **2009**, *694*, 2671-2680.

[7] Hiromoto, T.; Ataka, K.; Pilak, O.; Vogt, S.; Stagni, M. S.; Meyer-Klaucke, W.; Warkentin, E.; Thauer, R. K.; Shima, S.; Ermler, U. "The crystal structure of C176A mutated [Fe]-hydrogenase suggests an acyl-iron ligation in the active site iron complex." *FEBS Lett.* **2009**, *583*, 585-590.

[8] Hiromoto, T.; Warkentin, E.; Moll, J.; Ermler, U.; Shima, S. “The Crystal Structure of an [Fe]-Hydrogenase-Substrate Complex Reveals the Framework for H_2 Activation.” *Angew. Chem. Int. Ed.* **2009**, *48*, 6457-6460.

[9] Shima, S.; Thauer, R. K. “A Third Type of Hydrogenase Catalyzing H_2 Activation.” *Chem. Record* **2007**, *7*, 37-46.

[10] Reedijk, J.; Smit, J. A. “Ligand properties of hydroxypyridines. II. Metal(II) nitrates containing coordinated 2-pyridone.” *Recl. Trav. Chim. Pays-Bas* **1972**, *91*, 681-687.

[11] Hollis, L. S.; Lippard, S. “Mononuclear complexes of cis-diammineplatinum(II) and -(IV) with .alpha.-pyridone. Structures of cis-$[Pt(NH_3)_2(C_5H_4NOH)_2]Cl_2$, mer-$[Pt(NH_3)_2(C_5H_4NO)Cl_3]$, and cis-$[Pt(NH_3)_2(C_5H_4NOH)Cl](NO_3)$.” J. *Inorg. Chem.* **2002**, *22*, 2708-2713.

[12] Bordwell, F. G. “Equilibrium acidities in dimethyl sulfoxide solution.” *Acc. Chem. Res.* **1988**, *21*, 456-463.

[13] Bordwell, F. G.; Algrim, D. “Nitrogen acids. 1. Carboxamides and sulfonamides.” *J. Org. Chem.* **1976**, *41*, 2507-2508.

[14] Angus, P. M.; Jackson, W. G. “Linkage isomerism in cobalt(III) pentaammine complexes of 2-pyridone.” *Inorg. Chem.* **1994**, *33*, 477-483.

[15] Kelson, E. P.; Dean, N. S.; Algarin, E. “Aquabis(3-methoxy-2-pyridonato)(2,2':6',2''-terpyridine)ruthenium(II)-acetonitrile-water (1/1/1).” *Acta Crystallogr.* **2007**, *C63*, m108-m110.

[16] Kelson, E. P.; Phengsy, P. P. “Synthesis and Structure of a Ruthenium(II) Complex Incorporating k^N Bound 2-Pyridonato Ligands; A New Catalytic System for Transfer Hydrogenation of Ketones.” *Dalton Trans.* **2000**, 4023-4024.

[17] Cotton, F. A.; Kim, Y.; Ren, T. “Compounds containing linked, multiply-bonded dimetal units. 1. Tetrakis-(Œ°-6-chloro-2-hydroxypyridinato)diruthenium(II,III) cations linked axially by pyrazine. Comparison with a single molecule axially coordinated by pyridine.” *Inorg. Chem.* **1992**, *31*, 2608-2612.

[18] Ichieda, N.; Kamimura, T.; Wasada-Tsutsui, Y.; Funahashi, Y.; Ozawa, T.; Jitsukawa, K.; Masuda, H. “Metal-metal bond formed in tetrakis(2-pyridonato)copper(II)-platinum(II)/palladium(II) complexes.” *Chem. Lett.* **2008**, *37*, 1220-1221.

[19] Andreu, P. L.; Cabeza, J. A.; Carriedo, G. A.; Riera, V.; GarcÌa-Granda, S.; Van der Maelen, J. F.; Mori, G. “The chemical and electrochemical oxidation of

pyridonate-bridged ruthenium(I) dimers. X-Ray structure of [Ru_2([mu]-pyO)$_2$(CO)$_4$(pyOH)$_2$] (pyOH = 2-pyridone)." *J. Organomet. Chem.* **1991**, *421*, 305-314.

[20] Cadiou, C.; Helliwell, M.; Winpenny, R. E. P. "Synthesis and structural study of two decanuclear cobalt(II) cages incorporating pyridonates and benzoate-based carboxylates." *Comptes Rendus Chim.* **2003**, *6*, 241-247.

[21] Grotjahn, D. B.; Lo, H. C.; Groy, T. L. "Chlorohydrido[2(1H)-pyridonato-N,O]bis[tris(1-methylethyl)phosphine]iridium(III)." *Acta Crystallogr., Sect. C* **1996**, *C52*, 300-302.

[22] Grotjahn, D. B.; Joubran, C. "Facile Oxidative Addition of Rhodium(I) to the Acyl-Oxygen Bond of 2-((Diphenylphosphino)methyl)quinolin-8-ol Acetate." *Organometallics* **1995**, *14*, 5171-5177.

[23] Flood, T. C.; Lim, J. K.; Deming, M. A. "Generation of Coordinative Unsaturation at Osmium via Ring-Opening Equilibration of a 2-Pyridonato Chelate Complex." *Organometallics* **2000**, *19*, 2310-2317.

[24] Lauhuerta, P.; Latorre, J.; Sanau, M.; Cotton, F. A.; Schwotzer, W. "Synthesis of ruthenium(II) compounds with ortho-oxypyridinate ligands (hp). Crystal structure characterization of [Ru(η^6-p-$CH_3C_6H_4CH(CH_3)_2$)Cl(hp)]." *Polyhedron* **1988**, *7*, 1311-1316.

[25] Peris, E.; Lee, J. C., Jr.; Rambo, J. R.; Eisenstein, O.; Crabtree, R. H. "Factors Affecting the Strength of N-H¨H-Ir Hydrogen Bonds." *J. Am. Chem. Soc.* **1995**, *117*, 3485-3491.

[26] Park, S. H.; Lough, A. J.; Yap, G. P. A.; Morris, R. H. "The effect of ancillary ligands on intramolecular proton-hydride (NH...HIr) bonding in complexes of iridium(III)." *J. Organomet. Chem.* **2000**, *609*, 110-122.

[27] Ragaini, F.; Gallo, E.; Cenini, S. "Promotion of the [PPN][$Rh(CO)_4$]-catalysed carbonylation of nitrobenzene by 2-hydroxypyridine and related molecules: an apparent bifunctional activation." *J. Organomet. Chem.* **2000**, *593-594*, 109-118.

[28] Miyabayashi, T.; Hara, T.; Yamagata, T.; Mashima, K. "Chlorido(6-diphenylphosphino-2-pyridonato-j2P,N)-(6-diphenylphosphino-2-hydroxypyridine-j2P,N)- hydridoiridium(III) chloroform 1.896-solvate." *Acta Crystallographica Section E* **2007**, *E63*, m576–m578.

[29] Tomon, T.; Koizumi, T.-a.; Tanaka, K. "Stabilization and destabilization of the Ru-CO bond during the 2,2'-bipyridin-6-onato (bpyO)-localized redox reaction of [Ru(terpy)(bpyO)(CO)](PF_6)." *Eur. J. Inorg. Chem.* **2005**, 285-293.

[30] Royer, A. M.; Rauchfuss, T. B.; Wilson, S. R. “Coordination Chemistry of a Model for the GP Cofactor in the Hmd Hydrogenase: Hydrogen-Bonding and Hydrogen-Transfer Catalysis.” *Inorg. Chem.* **2008**, *47*, 395-397.

[31] Fujita, K.; Tanino, N.; Yamaguchi, R. “Ligand-Promoted Dehydrogenation of Alcohols Catalyzed by Cp*Ir Complexes. A New Catalytic System for Oxidant-Free Oxidation of Alcohols.” *Org. Lett.* **2007**, *9*, 109-111.

[32] Zhao, J.; Hartwig, J. F. “Acceptorless, Neat, Ruthenium-Catalyzed Dehydrogenative Cyclization of Diols to Lactones.” *Organometallics* **2005**, *24*, 2441-2446.

[33] Adair, G. R. A.; Williams, J. M. J. “Oxidant-free oxidation: ruthenium catalysed dehydrogenation of alcohols.” *Tetrahedron Lett.* **2005**, *46*, 8233-8235.

[34] van Buijtenen, J.; Meuldijk, J.; Vekemans, J. A. J. M.; Hulshof, L. A.; Kooijman, H.; Spek, A. L. “Dinuclear Ruthenium Complexes Bearing Dicarboxylate and Phosphine Ligands. Acceptorless Catalytic Dehydrogenation of 1-Phenylethanol.” *Organometallics* **2006**, *25*, 873-881.

[35] Lin, Y.; Ma, D.; Lu, X. “Iridium pentahydride complex catalyzed dehydrogenation of alcohols in the absence of a hydrogen acceptor.” *Tetrahedron Lett.* **1987**, *28*, 3115-3118.

[36] Junge, H.; Loges, B.; Beller, M. “Novel improved ruthenium catalysts for the generation of hydrogen from alcohols.” *Chem. Commun.* **2007**, 522–524.

[37] Johnson, T. C.; Morris, J. D.; Wills, M. “Hydrogen generation from formic acid and alcohols using homogeneous catalysts.” *Chem. Soc. Rev.* **2010**, *39*, 81-86.

[38] Friedrich, A.; Schneider, S. “Acceptorless Dehydrogenation of Alcohols: Perspectives for Synthesis and H_2 Storage.” *Chem. Cat. Chem* **2009**, *1*, 72-73.

[39] Heiden, Z. M.; Rauchfuss, T. B. “Proton-Induced Lewis Acidity of Unsaturated Iridium Amides.” *J. Am. Chem. Soc.* **2006**, *128*, 13048-13049.

[40] Heiden, Z. M.; Rauchfuss, T. B. “Proton-Assisted Activation of Dihydrogen: Mechanistic Aspects of Proton-Catalyzed Addition of H_2 to Ru and Ir Amido Complexes.” *J. Am. Chem. Soc.* **2009**, *131*, 3593–3600.

[41] Nutton, A.; Bailey, P. M.; Maitlis, P. M. “Pentamethylcyclopentadienyl-rhodium and -iridium complexes : XXVIII. Properties and x-ray crystal structures of $[(RhC_5Me_5)_3(H)_3O]+$ and $[(RhC_5Me_5)_2(H)_2OAc]+$ prepaerd from reactions of $[RhC_5Me_5)_2(OH)_3]+$ with alcohols.” *J. Organomet. Chem.* **1981**, *213*, 313-332.

[42] Ogo, S.; Nakai, H.; Watanabe, Y. “pH-Dependent H_2-Activation Cycle Coupled to Reduction of Nitrate Ion by Cp*Ir Complexes.” *J. Amer. Chem. Soc.* **2002**, *124*, 597-601.

[43] Ikariya, T.; Blacker, A. J. “Asymmetric Transfer Hydrogenation of Ketones with Bifunctional Transition Metal-Based Molecular Catalysts.” *Acc. Chem. Res.* **2007**, *40*, 1300-1308.

[44] Yamaguchi, R.; Ikeda, C.; Takahashi, Y.; Fujita, K. “Homogeneous Catalytic System for Reversible Dehydrogenation,àíHydrogenation Reactions of Nitrogen Heterocycles with Reversible Interconversion of Catalytic Species.” *J. Am. Chem. Soc.* **2009**, *131*, 8410-8412.

[45] Grotjahn, D. B.; Lo, H. C. “Fragmentation of 2-Pyridyl Esters Gives both Œ-2(C,O)- and Œ∑2(C,C)-Bound Ketene Ligands on ClIr[P(^{i}-Pr)$_3$]$_2$.” *Organometallics* **1995**, *14*, 5463-5465.

[46] Chuchuryukin, A. V.; Chase, P. A.; Mills, A. M.; Lutz, M.; Spek, A. L.; van Klink, G. P. M.; van Koten, G. “Hydroxy- and Mercaptopyridine Pincer Platinum and Palladium Complexes Generated by Silver-Free Halide Abstraction.” *Inorg. Chem.* **2006**, *45*, 2045-2054.

[47] Gill, D. S.; Maitlis, P. M. “Pentamethylcyclopentadienylrhodium and -iridium complexes. VIII. Di-m-hydridobis[chloro(pentamethylcyclopentadienyl)iridium] and related compounds.” *J. Organomet. Chem.* **1975**, *87*, 359-364.

[48] Fryzuk, M. D.; Huang, L.; McManus, N. T.; Paglia, P.; Rettig, S. J.; White, G. S. “Synthesis and reactivity of the iridium vinylidene Ir:C:CH_2[N($SiMe_2CH_2PPh_2$)$_2$]. Formation of carbon-carbon bonds via migratory insertion of a vinylidene unit.” *Organometallics* **1992**, *11*, 2979-2990.

[49] Gilbert, T. M.; Bergman, R. G. “Synthesis of trimethylphosphine-substituted (pentamethylcyclopentadienyl)iridium hydride complexes; protonation and deprotonation of (pentamethylcyclopentadienyl)(trimethylphosphine)iridium dihydride.” *J. Am. Chem. Soc.* **1985**, *107*, 3502-3507.

[50] Kang, J. W.; Moseley, K.; Maitlis, P. M. “Pentamethylcyclopentadienylrhodium and -iridium halides. I. Synthesis and properties.” *J. Am. Chem. Soc.* **1969**, *91*, 5970-5977.

[51] White, C.; Yates, A.; Maitlis, P. M. “(η^5-PentamethylCyclopentadienyl)Rhodium and -Iridium Compounds.” *Inorg. Synth.* **1992**, *29*, 228-234.

Chapter 6

Synthesis of new Pt and Pd complexes of TsDPEN

Introduction

In recent years, bidentate amido-amines have been popularized as supporting ligands for homogenous transfer hydrogenation catalysts.[1-3] The ligands offer several features that are relevant to the efficient and selective behavior of these catalysts, including their bidentate anionic nature that ensures tight binding to most metals. The wide availability of chiral 1,2-diamines is convenient, and the presence of a primary amine serves as a proton donor in catalysis.

Almost all such complexes are quasi-octahedral containing one chelating, monoanionic amino-amido ligand. Given the success of the amino-amide platform, we decided to investigate the coordination of these ligands to square planar centers provided by Pt(II), Pd(II), Rh(I), and Ir(I). Related ligand sets Tsen and (±)-TsDACH, (Figure 6.1), were not investigated.

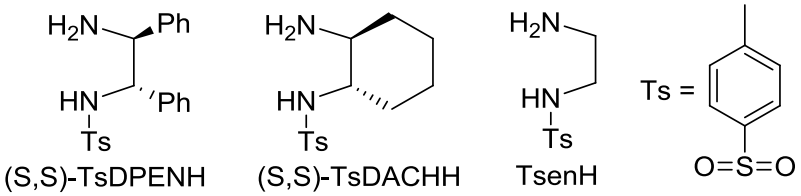

Figure 6.1. Common monotosylated diamines used for transfer hydrogenation catalysis.

Several reports have discussed amido complexes of platinum and palladium where amide is deprotonated amine, deprotonated amide ($RC(O)NH_2$), and deprotonated sulfonamide (RSO_2NH_2), but the hydrogen transfer properties of these complexes have not been reported.[4-10] In general, nitrogen-based ligands have been shown to enable the formation of Pt(IV) through oxidative addition of group 14 halides, whereas similar complexes with phosphine ligands are unstable.[11,12] These results have been attributed to stabilization of the harder Pt(IV) center with the hard nitrogen donor set.[11,12]

Scheme 6.1. Equilibrium experiments between sulfonamide and alkoxide ligands in Pt^{+2} shows a strong preference for the amide coordination.

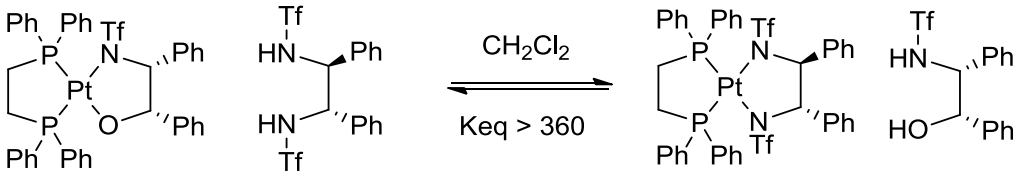

Gagne and coworkers have made a series of bisphosphine bis-sulfonamide and sulfonamide alkoxide complexes.[4] Through competition reactions (example Scheme 6.1) they showed that Pt formed more stable complexes with the series trend of NTf > NSO_2-Ar > OR. They also showed crystallographically the phenyl group α to N adopted an axial orientation in all of their complexes.

Bercaw and coworkers synthesized Pt^{+2} complexes from 2-(N-arylimino)pyrrolide (^{Ar}NNH) ligands and found the stereochemistry of the complexes was strongly influenced by both steric and electronic factors (Scheme 6.2).[5] With Ar = 4-CF_3-Ph or 4-OMe-Ph (Scheme 6.2), a Pt(^{Ar}NN)(CD_3)(SMe_2) complex displayed only *cis*-imine-SMe_2 geometry. A similar complex,

Pt(^{Ar}NN)(C_6D_5)(SMe_2) with Ar = 2,6-Me_2-Ph and 2,6-$^{i}Pr_2$-Ph, resulted in *trans*-imine-SMe_2 geometry. In the Ar = 2,6-$^{i}Pr_2$-Ph derivative, the SMe_2 ligand could be quantitatively replaced by MeCN to give a Pt(^{Ar}NN)(CD_3)(MeCN) complex with MeCN *cis* to imine.

Scheme 6.2. Effects of steric and electronic factors in the stereochemistry of some Pt (N-arylimino)pyrrolide complexes.

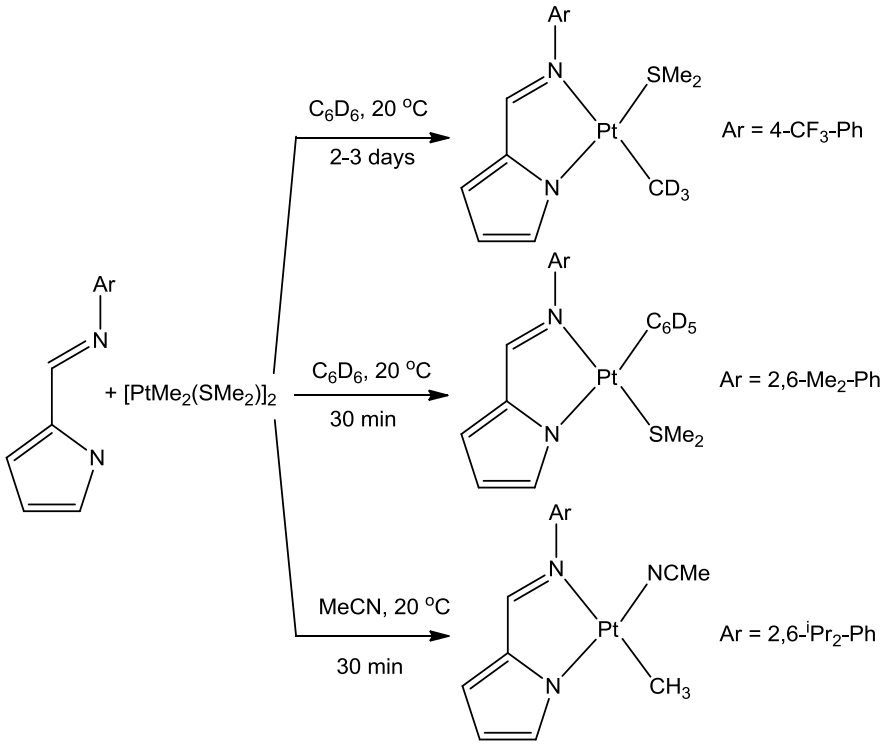

Recent work has utilized derivatives of 2-(2'-pyridyl)indolide (PyInd)[13] and 2-(2'-pyridyl)pyrrolide (PyPyr)[14,15] as monoanionic bidentate NN ligands on Pt(II). A sterically congested Pt(PyPyr)$_2$ derivative was found to be substitutionally labile at one Pt-py bond (Scheme 6.3).[15] The carbonyl derivative reacted with alcohols to reversibly give alkoxycarbonyl complexes. In this conversion the pyrrolide acts as an internal base and the free pyridine binds to Pt. The PyInd ligand was found to stabilize a rare five-coordinate Pt(IV)-silyl complex and was also

proposed to stabilize a neutral 14-electron complex implicated as an intermediate in the catalytic hydroarylation of norbornene.[13]

Scheme 6.3. Pt(PyPyr)$_2$ complex reversibly forms an alkoxycarbonyl complex

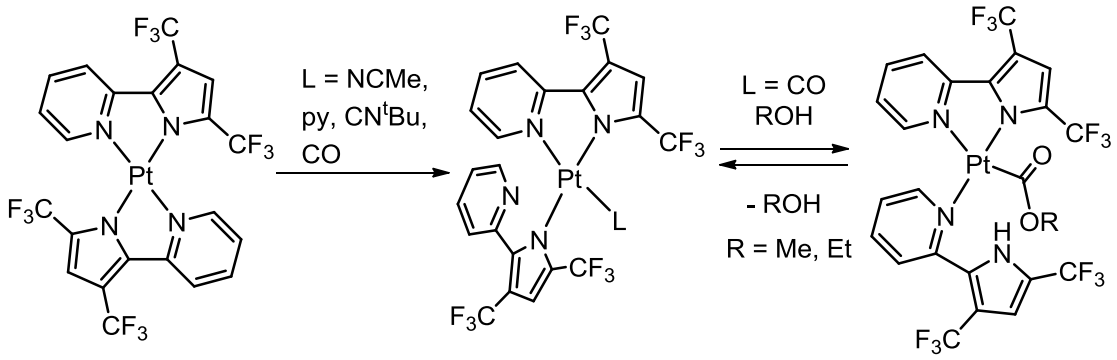

Results

Preparation of M((*S,S*)-TsDPEN)$_2$ (M = Ni, Pd, Pt). These complexes were prepared by treatment of the metal halides with TsDPENH in the presence of triethylamine as a proton acceptor. Pt(*S,S*-TsDPEN)$_2$ gave two isomers (Scheme 6.4). Both isomers display poor solubility except in DMF or DMSO, although satisfactory ^{1}H NMR spectra could be obtained on CD_2Cl_2 solutions. Upon heating in DMSO solution at 140 ºC, the platinum complexes did not noticeably isomerize, instead it was observed to slowly decompose at a rate of ~10% over 300 h. The ^{1}H NMR signals for the two diastereomers were well resolved (Figure 6.2).

Scheme 6.4. Bis-TsDPEN complexes of Pt^{+2} and Pd^{+2}

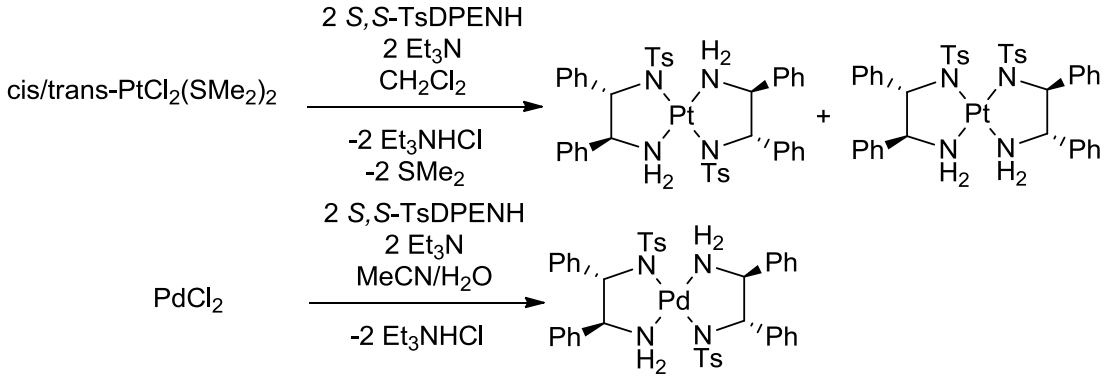

The palladium complex, Pd(*S,S*-TsDPEN)$_2$, was found to be soluble in a variety of organic solvents. Only a single isomer was observed in solution by ^{1}H NMR spectroscopy. Crystallographic analysis of Pd(*S,S*-TsDPEN)$_2$·[$(CH_3)_2CO$]$_2$ confirmed the presence of trans tosylated amides (Figure 6.3). The more abundant isomer of Pt(*S,S*-TsDPEN)$_2$ matches the ^{1}H NMR spectrum of the Pd spectrum well (Figure 6.2). Attempted preparation of Ni(*S,S*-TsDPEN)$_2$ from $NiCl_2$ and [Ni(acac)$_2$]$_3$ gave a grayish purple colored product that was insoluble in all common solvents. Considering the difference in solubility between the Pt and Pd complexes, we are not sure if this difference is due to a structure containing bridging amide-amine with multiple metal centers, or a structure similar to that of the Pt and Pd derivatives.

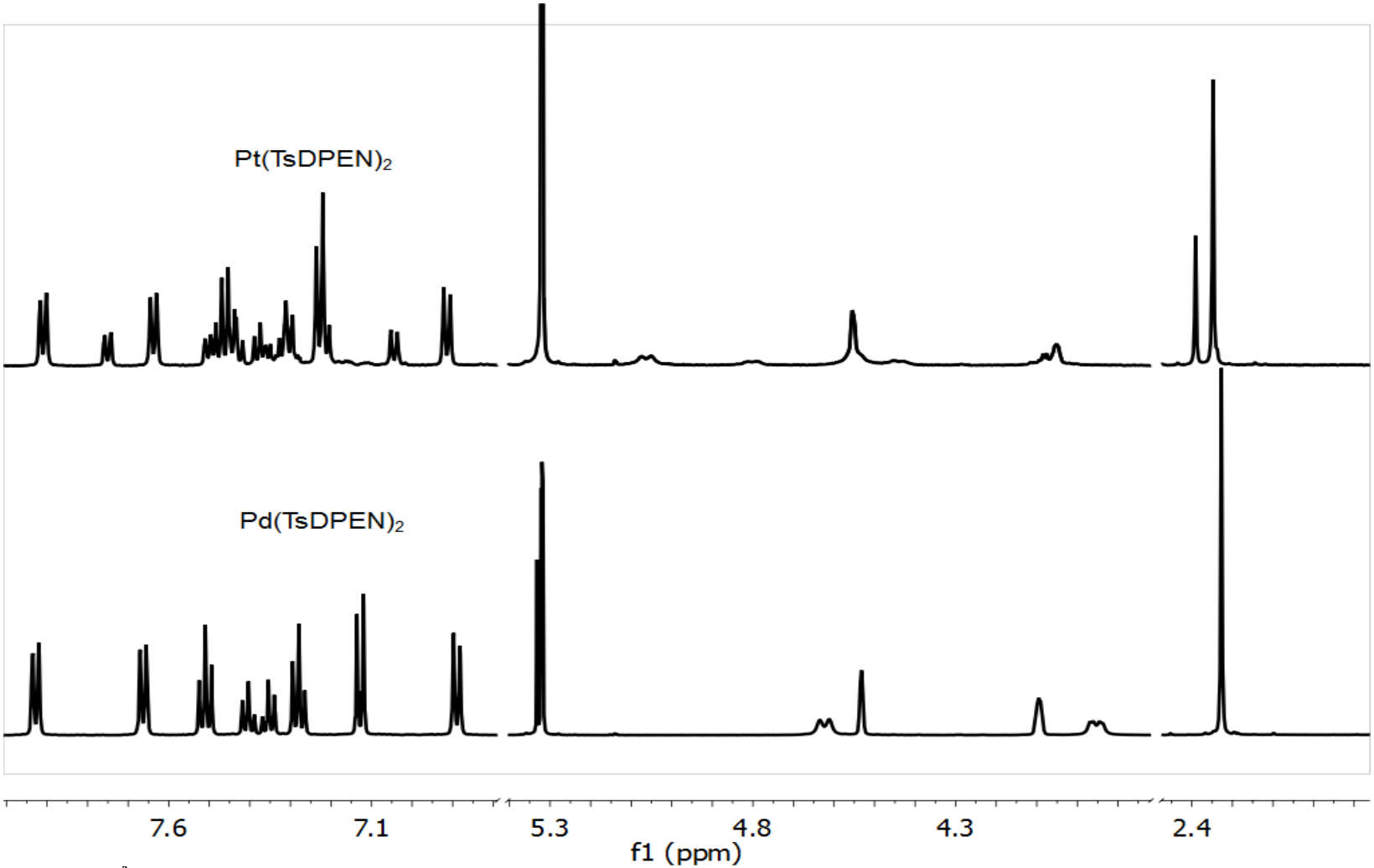

Figure 6.2. ^{1}H NMR spectrum in CD_2Cl_2 of Pd(*S,S*-TsDPEN)$_2$ bottom and Pt(*S,S*-TsDPEN)$_2$ top showing the similarity of the major Pt isomer to the trans- only structure of Pd(*S,S*-TsDPEN)$_2$ including the Ts-Me, ethylene backbone, and aryl signal regions. The NH protons show significantly differing shifts.

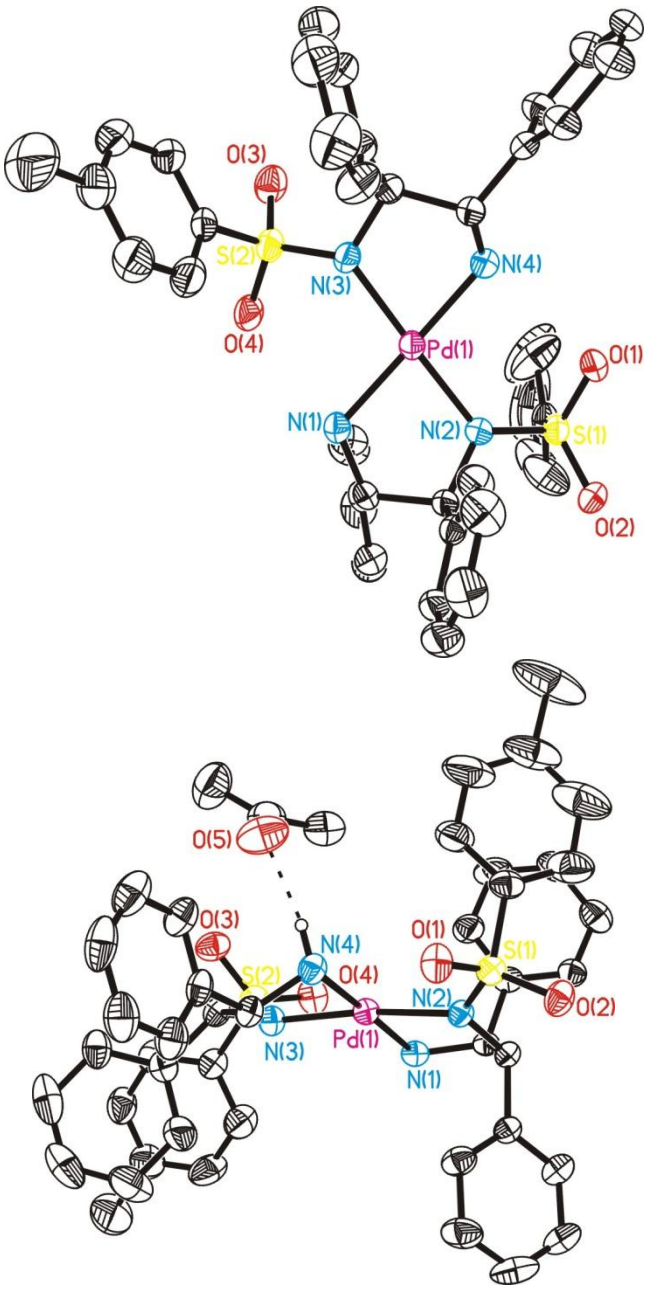

Figure 6.3. Molecular structure of the nonhydrogen atoms of Pd((*S,S*)-TsDPEN)$_2$ with Pd, pink; N, blue; S, yellow; O, red; C, black. The thermal ellipsoids are shown at 35% probability. The top view highlights the square planar geometry with trans-amine coordination. The bottom view has one NH shown to highlight hydrogen bonding to an acetone molecule. This TsDPEN ligand displays diequatorial phenyl groups, and the TsDPEN without shows the more common diaxial configuration of the phenyl groups on the ethylene backbone. Selected bond lengths (Å) and angles (^{o}): Pd-N1, 2.0458(0.0026); Pd-N2, 2.0288(0.0028); Pd-N3, 2.0486(0.0029); Pd-N4, 2.0164(0.0027); N1-Pd1-N2, 80.98 (0.10); N3-Pd1-N4, 79.48 (0.11); N2-Pd1-N4, 99.82 (0.11); N1-Pd1-N3, 99.56 (0.11)

PtCl(SMe_2)((*S,S*)-TsDPEN). Chloroplatinate derivatives of TsDPEN were of interest because they potentially could dehydrohalogenate, affording unsaturated diamido Pt(II) compounds. The reaction of *cis/trans*-$PtCl_2(SMe_2)_2$ and K(*S,S*)-TsDPEN was found to give PtCl(SMe_2)(*S,S*-TsDPEN). This species was obtained as a single isomer. We tentatively assign the SMe_2 *trans* to the amide due to bulk of the tosyl group. Two SMe signals were observed in the ^{1}H NMR spectrum, consistent with the chirality of the complex and the inertness of the Pt-S bond toward exchange. The complex was unreactive toward MeCN. Dehydrohalogenation by MeONa was unsuccessful. Attempted reaction of PtCl(SMe_2)(*S,S*-TsDPEN) and $NaBH_4$ also failed to yield a hydride signal in the ^{1}H NMR spectrum. Addition of $AgPF_6$ effected Cl^- abstraction to give the cationic MeCN complex, [Pt(NCMe)(SMe_2)(*S,S*-TsDPEN)][PF_6], but attempts to form a hydride from this complex were unsuccessful.

PtMe(MeCN)((*S,S*)TsDPEN). Platinum methyl complexes of TsDPEN were obtained using $[PtMe_2(\mu\text{-}SMe_2)]_2$, which has been used as a source of "$PtMe^+$".[5] Condensation of this platinum methyl compound with (*S,S*)-TsDPENH indeed proceed with with loss of one equiv of methane. Reaction in CH_2Cl_2 was slow and resulted in a large number of ^{1}H NMR signals in the Pt-Me region, but the same reaction in MeCN solution cleanly resulted in displacement of SMe_2 by MeCN. This product was obtained as a single stereoisomer, but the structure was not assigned. In Scheme 6.2, a Pt(Me)(MeCN) complex is shown to have a geometry with the MeCN trans to an amide ligand and Me trans to imine, although in this case the bulky aryl group is attached to the imine. The MeCN

ligand was found to be labile and could be replaced by CO to give an equilibrium mixture of both *trans*- and *cis*-stereoisomers (scheme 6.5), with υ_{CO} = 2023, 1994 cm^{-1} (Figure 6.4). The addition of CO is reversible: evaporation of a MeCN solution reformed PtMe(MeCN)((*S,S*)TsDPEN).

Scheme 6.5. Reaction of PtMe(MeCN)(*S,S*-TsDPEN) with CO.

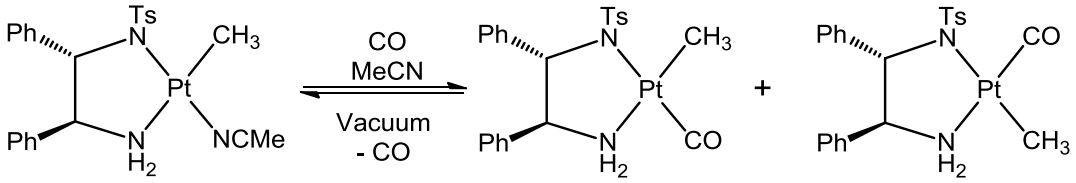

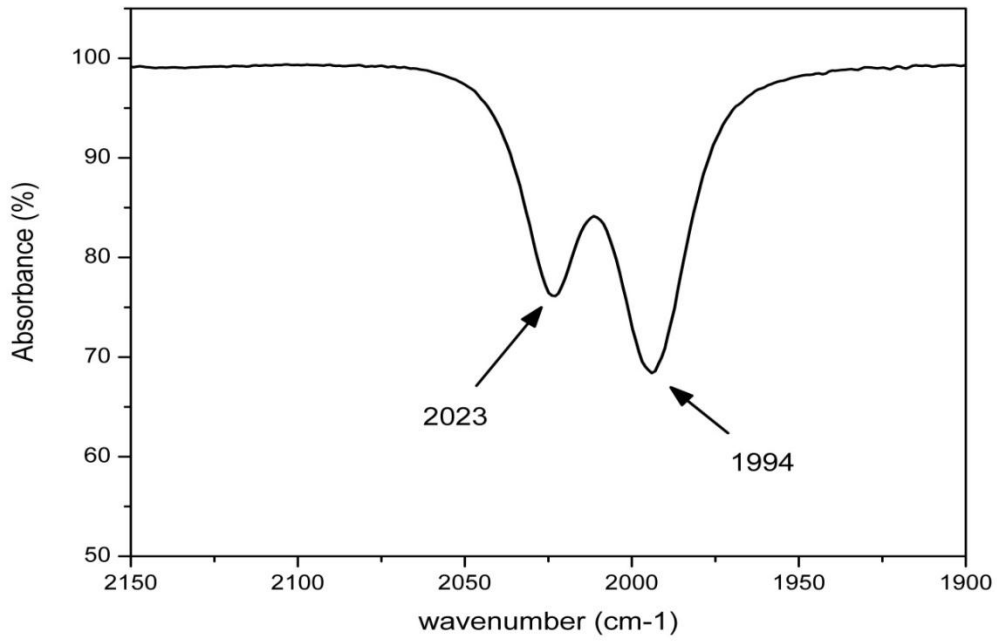

Figure 6.4. IR spectrum of the solution obtained by treating a CH_2Cl_2 solution of PtMe(MeCN)(*S,S*-TsDPEN) with one atmosphere of CO.

Pd(allyl)(*S,S*-TsDPEN). Treatment of allyl palladium chloride dimer with "(*S,S*)-$TsDPEN^-$" afforded the monomeric Pd(allyl)((*S,S*)-TsDPEN). This

colorless air-stable complex exhibited an interesting ^{1}H NMR spectrum consisting of two subspectra (Figure 6.6). The isomer ratio was solvent-dependent (Figure 6.5). A ^{1}H COSY experiment (Figure 6.13, 6.14) confirmed the presence of two subspectra. We propose that isomerism arises from slow rotation of the η^3-allyl ligand.

Solvent	K_{eq}
DMSO-d_6	0.37
CD_2Cl_2	0.55

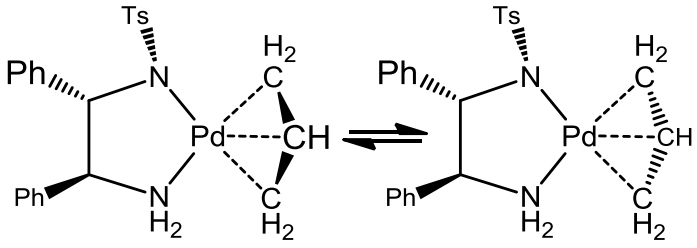

Figure 6.5. Left: K_{eq} of the steroisomers in different solvents, with drawing of possible rotational structures on right.

In order to provide further evidence for the existence of rotational isomerization in solution, crystals of Pd(allyl)((*S,S*)TsDPEN) suitable for X-ray diffraction were grown. The solid state structure (Figure 6.7) shows only one configuration for the allyl ligand. The phenyl groups on the ethylene backbone are in a diaxial position and the tosyl group protrudes toward the allyl ligand. After analysis by X-ray diffraction, the same batch of crystals were examined by ^{1}H NMR spectroscopy as a CD_2Cl_2 solution. These measurements confirmed the rapid isomerization with the presence of two unique sets of signals in the same ratio as before.

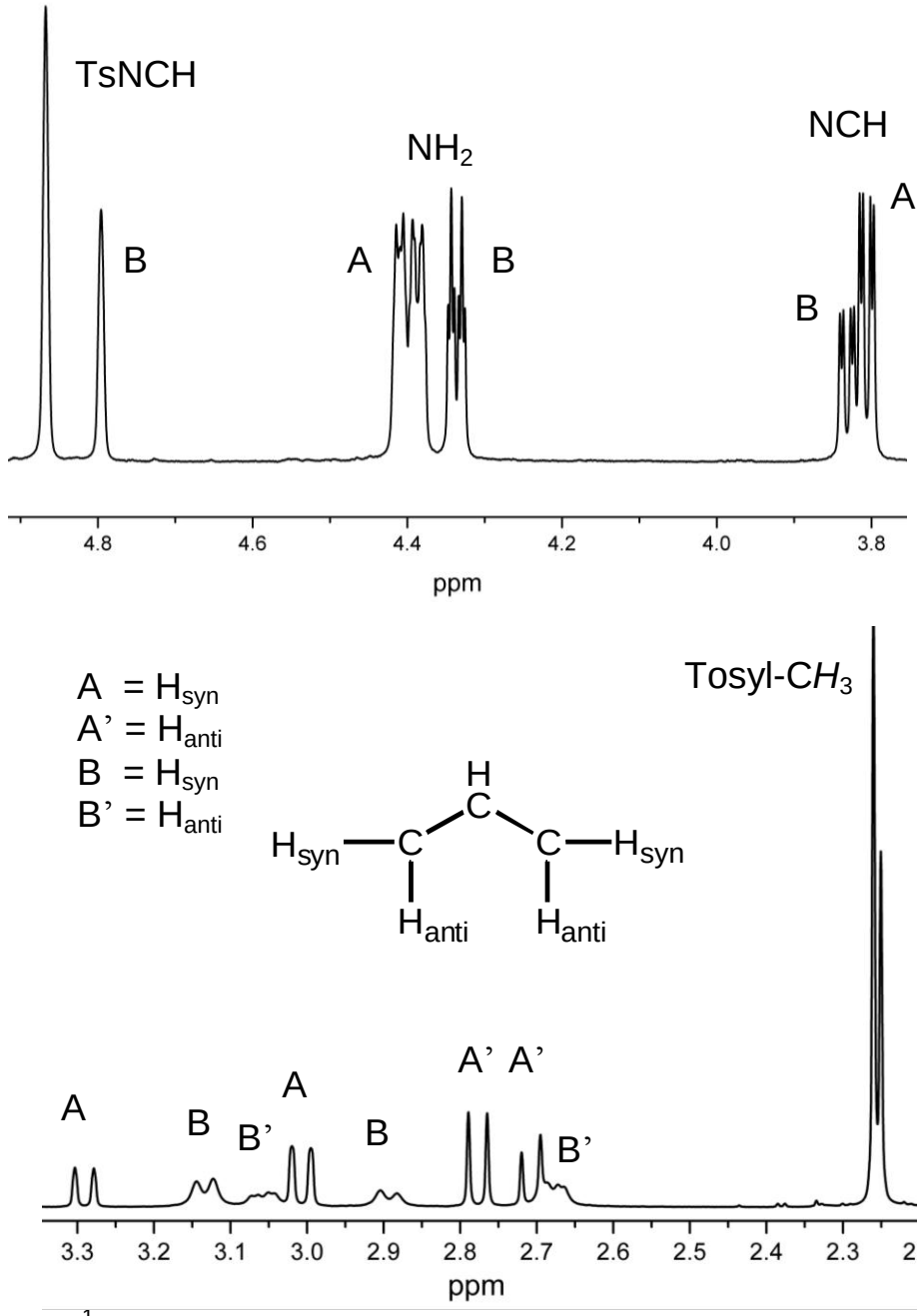

Figure 6.6. ^{1}H NMR spectrum of Pd(allyl)(*S,S*-TsDPEN) in CD_2Cl_2 solution. Top: Closeup of N*H*$_2$ and NC*H*PhC*H*PhN signals. Bottom: Closeup of allyl signals showing rotamers. Connectivity was established by ^{1}H COSY experiments.

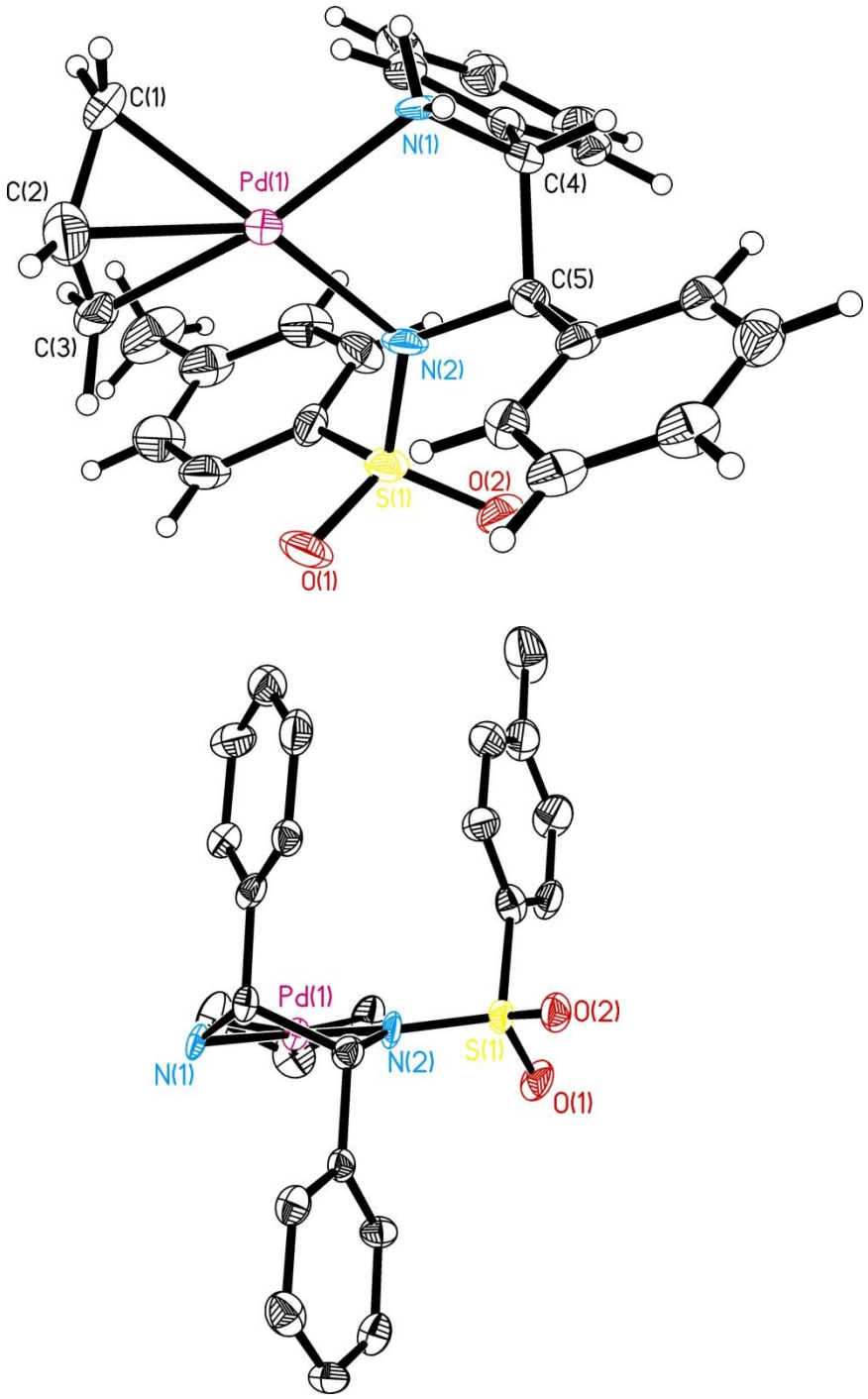

Figure 6.7. Molecular structure of the nonhydrogen atoms of Pd(allyl)((*S,S*)-TsDPEN) with Pd, pink; N, blue; S, yellow; O, red; C, black. The thermal ellipsoids are shown at 35% probability. The top view highlights the close approach of the tosyl ring and the allyl ligand. The bottom view highlights the diaxial configuration of the phenyl groups on the ethylene backbone. Selected bond lengths (Å): Pd-C1, 2.112; Pd-C3, 2.101; Pd-N1, 2.126; Pd-N2, 2.073.

Scheme 6.6. Synthesis of Rh^{I} and Ir^{I} complexes of TsDPEN.

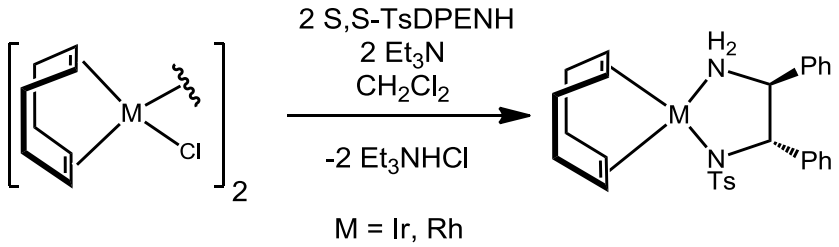

Ir(cod)(*S,S*-TsDPEN) and Rh(cod)(*S,S*-TsDPEN). The M(cod)((*S,S*)-TsDPEN) (M = Ir, Rh) complexes were prepared by treatment of $[M(cod)Cl]_2$ with two equiv each of (*S,S*)-TsDPENH and Et_3N. The products are air-stable yellow solids (Scheme 6.6). The ^1H NMR spectra each showed 12 unique signals for the 1,5-cyclooctadiene ligands. These compounds were unreactive toward H_2 (1 atm) and HCl (2 equiv).

Discussion

The goal of this exploratory effort was to discover the scope of the monoanionic bidentate ligand TsDPEN. We confirmed our hypothesis that it is compatible with a wide range of metal centers and is thus well suited for further exploratory studies. The new d^8 complexes of TsDPEN enjoy good thermal stability, at least compared to the Cp*Ir(TsDPEN) and (cymene)Ru(TsDPEN) complexes where cyclometalation of the Ph rings can be problematic.[16] In general, all complexes reported in this chapter were air stable for several weeks (Pd metal formed during longer storage in some cases). The disadvantage of square-planar TsDPEN complexes, at least with respect to asymmetric catalysis, is that the chiral information in the pseudo-C_2 symmetric backbone is well

positioned for interaction with axial ligands, but is not well suited for interaction with ligands that are quasi-coplanar with the M(TsDPEN) chelate ring.

The J_{HH} value in the ^{1}H NMR spectrum for the C*H*PhC*H*Ph group in all complexes in this chapter indicate diaxial phenyl rings of the TsDPEN ligand. In the case of equatorial phenyl groups, the J_{HH} would be expected to be 8-13 Hz.[17-20] Diaxial phenyl groups is consistent with the square planar arrangement around the metal. In contrast, ligands in the axial coordination sites would provide steric bulk to push the phenyl groups into diequatorial positions. This concept was previously demonstrated on the Cp*Ir(TsDPEN-H) system.[17] The diaxial phenyl groups induce the tosyl ring to project toward the site *cis* to the sulfonamide (Figure 6.8). In cases where the phenyl groups are diaxial, the tolyl group within the Ts substituent tends to orient equatorially. This spacial arrangement is demonstrated in the crystal structure of Pd(allyl)(*S,S*-TsDPEN).

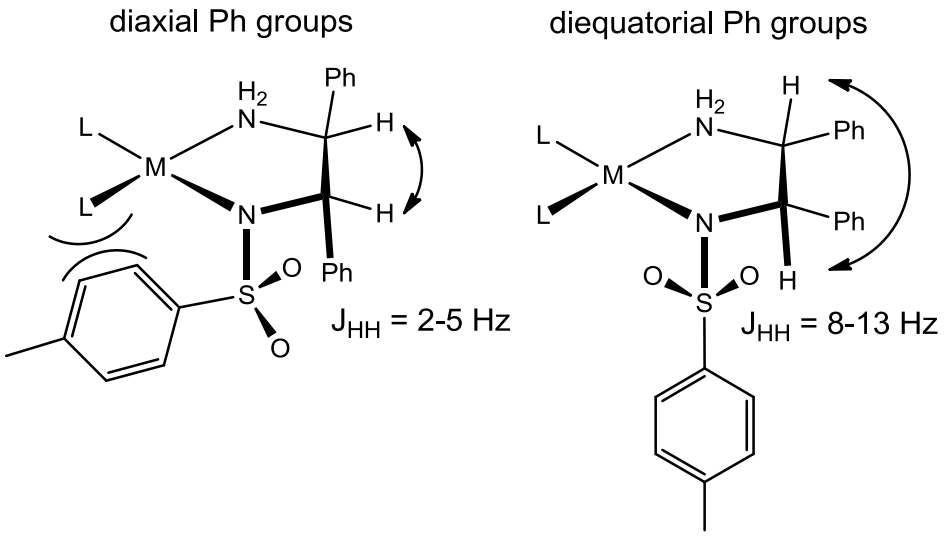

Figure 6.8. Diaxial and diequatorial conformations of TsDPEN complexes, with expected J_{HH} values for the C*H*PhC*H*Ph group. Figure also shows proposed "knock-on effect" on the Ts group for the diaxial conformation.

The geometry around the metal atoms in the $M(TsDPEN)_2$ complexes is tentatively proposed to be determined by steric factors caused by the bulky tosyl group. The Pt complex was isolated as 2 geometries, detected by ^1H NMR spectroscopy, attributed to kinetic trapping of *cis* and *trans* stereoisomers in a 1:4 ratio, respectively. The ratio was invariant to temperature and attempts to alter the isomer ratio were unsuccessful even up to its decomposition temperature of 140 ºC (DMSO solution). The $Pd(TsDPEN)_2$ complex was isolated as only one isomer, as determine by NMR spectroscopy. It is typical for Pd(II) to be more substitutionally labile and hence more configurationally labile than Pt(II). The sulfonamido ligands are mutually trans, as determined crystallographically. The major isomer of $Pd(TsDPEN)_2$ displays a ^1H NMR spectrum that is very similar to that for the Pd complex and is assigned the same trans geometry.

Single crystals of $Pd(TsDPEN)_2$ were grown in acetone and the X-ray structure contains a hydrogen bond from one amine NH to an acetone O. The TsDPEN ligand containing the hydrogen bonded amine has equatorial phenyl rings. The other TsDPEN ligand does not contain a hydrogen bond and has the usual diaxial phenyl conformation. We were able to show this hydrogen-bonding effect in solution by ^1H NMR spectroscopy. Addition of acetone-d_6 to a CD_2Cl_2 solution of $Pd(TsDPEN)_2$ resulted in a shift for the NH signal and increased coupling values for the C*H*PhC*H*Ph signals in the ^1H NMR spectrum. The increased coupling values suggest the phenyl rings rapidly isomerize between the diaxial and diequatorial positions in the presence of a hydrogen bond acceptor.

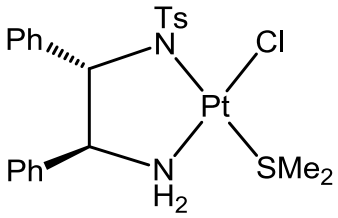

Figure 6.9. Proposed geometry of PtCl(TsDPEN)(SMe_2) due to steric interaction of the Ts-group.

Exploiting the convenient SMe_2-stabilized precursors,[21] several Pt complexes were prepared with a single TsDPEN ligand. The PtCl(SMe_2)(*S,S*-TsDPEN) complex was isolated as a single isomer. As in The Pt((*S,S*)-TsDPEN)$_2$, it is possible that this isomer is thermodynamically favored or kinetically too inert to isomerize. Steric interactions between the tosyl and SMe_2 ligand would be expected to favor the *cis* SMe_2 amine isomer (Figure 6.9). In this complex, the Pt-SMe_2 bond was found to be inert with respect to substitution by MeCN. Removal of the chloride ligand using Ag^+ in MeCN solution gave [Pt(NCMe)(SMe_2)(*S,S*-TsDPEN)]$^+$.

In contrast to PtCl(SMe_2)((*S,S*)-TsDPEN), the related complex PtMe(MeCN)(*S,S*-TsDPEN) proved to undergo rapid ligand exchange. The stereochemistry of this methyl complex was not unequivocally assigned. In one precedent, the case of PtMe(MeCN)(2-(N-arylimino)pyrrolide), MeCN was found to be trans to amide.[5] This complex did reversibly bind CO to give 2 isomers in a ratio that did not change over time at room temperature, but the rapid loss of CO prohibited isolation. The thermal[22] and photochemical[23] isomerization of Pt(II) carbonyls of the type Pt(CO)(PR_3)X_2 have been shown to involve dissociation of CO as the first step. In these studies the thermal isomerization proceeded from

trans to cis only, but the irradiated solutions proceeded to a photostationary combination of both isomers. In our case, the binding of CO is proposed to be sufficiently weak that rapid CO exchange allows easy approach to equilibrium. Pt(II) carbonyls have been reported for several β-diiminate complexes[24,25] as well as tris(pyrazolyl) borate[26] and diimine[27] complexes. Collectively, these studies suggest the PtMe(MeCN)(*S,S*-TsDPEN) would also bind ethylene or other olefins.

Interesting isomerism was also identified for Pd(allyl)(*S,S*-TsDPEN). A single isomer crystallized and was identified crystallographically, but two distinct isomers are evident in solution at room temperature. The ratio of solution isomers was found to be dependent on solvent. The different solution geometries were assigned to a rotation of the allyl ligand, which was previously demonstrated on bis-allyl complexes of Ni, Pd, and Pt at low temperatures (Figure 6.10).[28,29] For these complexes, the π–allyl rotation occurs at a lower temperature (between -30 and 0 ºC) and is preferred over a π-σ allyl arrangement (>0 ºC).[30] A large number of other transition metals with M-η^3-C_3H_5 coordination have established π-allyl rotation through NMR line shape analysis and magnetization transfer techniques.[31-38]

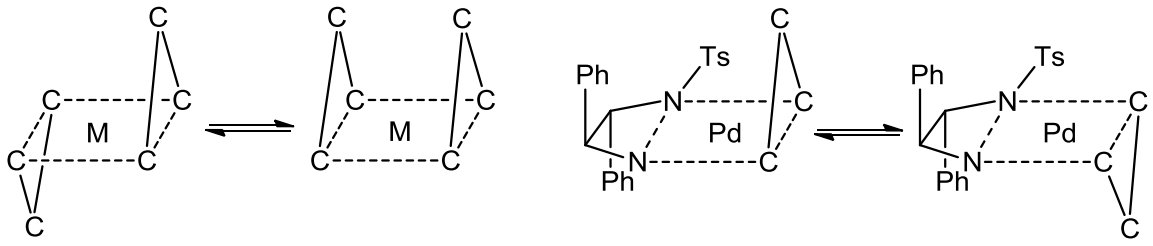

Figure 6.10. Isomeric forms of Ni, Pd, and Pt $(allyl)_2$ (left) and proposed isomers of Pd(allyl)(TsDPEN) (right).

The presence of two allyl orientations at room temperature for (π-allyl)palladium(II) complexes of N^{21},N^{22}-etheno-bridged porphyrins has also been reported (Figure 6.11).[39] The isomers could be assigned in these complexes due to the strong ring current effects of porphyrin in the ^{1}H NMR signals of the allyl group. For example, the *cis* isomer with R' = H gave a signal at δ-4.55 and the *trans* isomer gave a signal at δ-1.25 for the central CH.

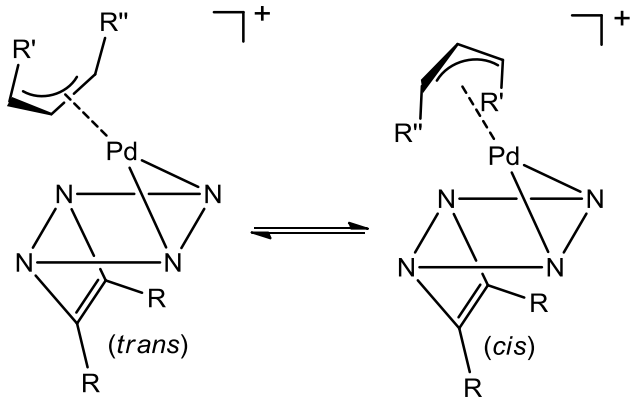

Figure 6.11. *cis-trans* isomers proposed in Pd(allyl)(porphyrin) complexes

In work related to our synthesis of Ir(TsDPEN)(cod), Tilley and coworkers recently reported complexes of the monoanionic bidentate 2-(2'-pyridyl(indolide) (PyInd) ligand with both cod or two monoalkene co-ligands. The Ir and Rh complexes containing the bidentate cod ligand were inert toward trialkylsilanes even at high temperatures. In contrast, the Rh bis-ethylene complex and an in situ formed Ir bis-cyclooctene complex reacted with 4 (2 for Ir) equivalents of Et_3SiH to give the Rh(V) and Ir(V) bis(silyl)dihydride complexes and two equivalents of $SiEt_4$ in the Rh case (Figure 6.12). These results suggest we

might see additional reactivity by integrating bis-monodentate olefin complexes of Ir and Rh with TsDPEN.

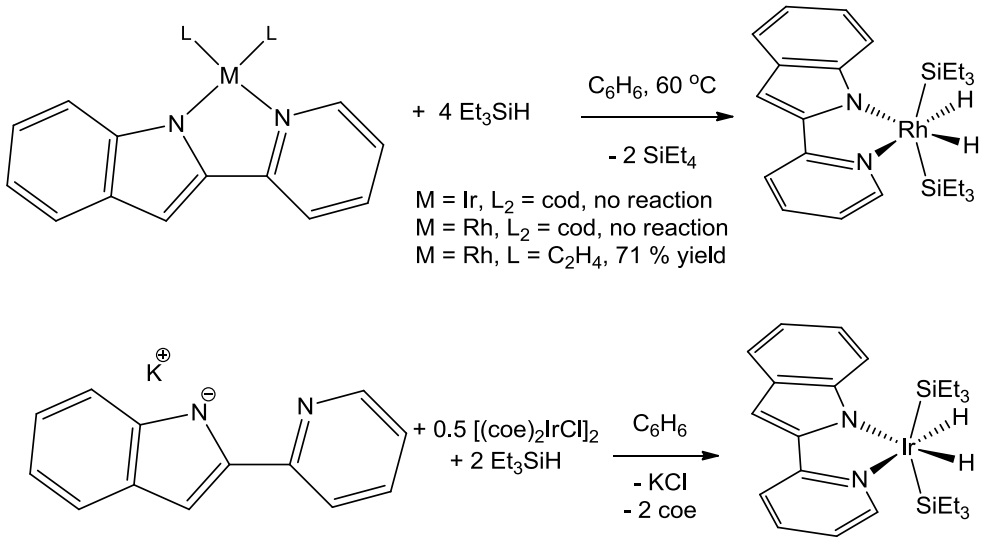

Figure 6.12. Rh and Ir complexes of PyInd are inert toward silanes with a bidentate bis-olefin ligand, but react when monodentate olefins are used.

Experimental

General Considerations. Unless otherwise indicated, reactions were conducted using standard Schlenk techniques (N_2) at room temperature with stirring. Tosyl chloride (Aldrich) was purified by recrystallization from diethyl ether. (*S,S*)-DPEN (TCI America) was used as received. (*S,S*)-TsDPEN was prepared according to Noyori et al[40]. $PtCl_2(SMe_2)_2$ (mixture of isomers)[41], $[PtMe_2(SMe_2)]_2$,[13] $[(cod)IrCl]_2$[42], and $[(cod)RhCl]_2$[43] were synthesized according to literature preparations. $PdCl_2$ and K_2PtCl_4 were obtained from Pressure Chemical Company. $Ni(acac)_2$ and $NiCl_2$ were obtained from Strem Chemicals. Et_3N and NaOMe were used as recieved from Aldrich. ESI-MS were acquired

using a Micromass Quattro QHQ quadrupole-hexapole-quadrupole instrument. ^{1}H NMR was acquired on Varian UNITY INOVA 500NB and UNITY 500 NB instruments. Elemental analyses were performed by the School of Chemical Sciences Microanalysis Laboratory utilizing a Model CE 440 CHN Analyzer.

Pt((*S,S*)-TsDPEN)$_2$. A solution of 73.3 mg (0.20 mmol) of (*S,S*)-TsDPENH in 2 mL of MeOH was deprotonated by addition of a solution of 23.7 mg (0.44 mmol) of NaOMe in 2 mL of MeOH via cannula. After stirring for 5 min., a colorless solution was obtained. This solution was added via cannula to a yellow solution of 39 mg (0.10 mmol) of *cis,trans*-$PtCl_2(SMe_2)_2$ in 2 mL of MeOH. Within minutes, the solution was colorless with formation of a white precipitate. The solvent was removed by vacuum, and the complex was extracted into 150 mL of CH_2Cl_2. This extract was filtered and then evaporated, leaving a white oily solid, which was washed with diethyl ether (3 X 10 mL). The resulting white powder was dried by vacuum. Yield: 78.7 mg(85%). The same product could be obtained using K_2PtCl_4 instead of *cis,trans*-$PtCl_2(SMe_2)_2$ in ~60% isolated yields. ^{1}H NMR analysis indicates that the sample consists of a 4:1 isomer ratio. ^{1}H NMR (500 MHz, DMSO-d^6): δ 2.29 major (s, 3H, $SO_2C_6H_4$-4-C*H*$_3$), 2.36 minor (s, 3H, SO_2C6H4-4-C*H*$_3$), 3.95 minor (m, 1H, HHNC*H*PhCHPhNTs), 4.01 major (d, 1H, 4 Hz, HHNC*H*PhCHPhNTs), 4.39 minor (d, 1H, 7.7 Hz, HHNCHPhC*H*PhNTs), 4.50 major (d, 1H, 4 Hz, HHNCHPhC*H*PhNTs), 5.23 major (d of d, 1H, 11.7 Hz, 4 Hz, H*H*NCHPhCHPhNTs), 5.29 minor (br d of d, 1H, 9.5 Hz, H*H*NCHPhCHPhNTs), 5.87 minor (br t, 1H, 10 Hz *H*HNCHPhCHPhNTs),

5.94 minor (d of d, 1H, 11.5 Hz, 4 Hz, *H*HNCHPhCHPhNTs), 6.91-7.68 major and minor (14 H). Anal. Calcd: theoretical (found) for $C_{42}H_{42}N_4O_4PtS_2$:

Isomerization of Pt((*S,S*)-TsDPEN)$_2$. A solution of 8.1 mg Pt((*S,S*)-TsDPEN)$_2$ was dissolved in 0.8 mL of DMSO-d^6 was prepared in a J. Young NMR tube. The solution was heated at 70 ºC for 24 h, but no change was observed in the ^{1}H NMR spectrum. The solution was then warmed to 110 ºC for 24 h with no change. At 140 ºC over the course of 300 h, we observed decomposition of about 10% to give new signals in the methyl region. But the isomer ratio did not change.

Pd((*S,S*)-TsDPEN)$_2$. A mixture of 366.5 mg (1.0 mmol) of (*S,S*)-TsDPENH, 88.5 mg (0.5 mmol) of $PdCl_2$, and 0.5 mL (3.6 mmol) of Et_3N in 8 mL MeCN and 5 mL water was heated to reflux for 6 h to give a yellow solution with some gray solid. The solid was removed by filtration via cannula. Solvent was removed and the yellow residue was dissolved in 10 mL of CH_2Cl_2. This solution was washed with water 3 X 5 mL. The organic layer was dried over $MgSO_4$ and filtered. Solvent was removed by vacuum, and the dirty yellow solid was recrystallized from CH_2Cl_2/hexanes to give a light yellow powder. Yield: 250 mg, (60%). ^{1}H NMR (500 MHz, CD_2Cl_2): δ 2.33 (s, 6H, SO_2C6H4-4-C*H*$_3$), 3.94 (d of d, 2H, 7.6 Hz, 2 Hz, H*H*NCHPhCHPhNTs), 4.23 (d, 2H, 2 Hz, HHNC*H*PhCHPhNTs), 4.53 (s, 2H, HHNCHPhC*H*PhNTs), 4.62 (br d, 2H, 11.5 Hz *H*HNCHPhCHPhNTs), 6.88-7.94 (28 H). Anal. Calcd: theoretical (found) for $C_{42}H_{42}N_4O_4PdS_2 \cdot 0.5\ CH_2Cl_2$: C, 58.02 (57.94); H, 4.93 (5.09); N, 6.37 (6.39).

Crystals suitable for X-ray diffraction were obtained by slow solvent evaporation of an acetone solution of Pd((*S,S*)-TsDPEN)$_2$.

"Ni((*S,S*)-TsDPEN)$_2$". The synthesis of this compound was attempted 2 different ways. First by treatment of $NiCl_2 \cdot 6H_2O$ and 2 equiv of K(*S,S*)-TsDPEN in MeOH, and a second with Ni(acac)$_2$ and 2 equiv of (*S,S*)-TsDPENH. Both reactions resulted in a light purplish gray solid that was not found to be soluble in any common solvent.

PtCl(SMe$_2$)((*S,S*)-TsDPEN). A solution containing 140 mg (0.38 mmol) of (*S,S*)-TsDPENH and 54 μL (0.38 mmol) Et_3N in 3 mL of CH_2Cl_2 was added to a solution of 150 mg (0.38 mmol) of $PtCl_2(SMe_2)_2$ in 5 mL of CH_2Cl_2. Upon stirring 16 h at room temperature, Et_3NHCl was removed by washing the organic layer with water (3 x 5 mL). The organic solution was dried with $MgSO_4$. Solvent was removed under reduced pressure, resulting in a light yellow powder. The product was recrystallized from CH_2Cl_2/diethyl ether twice. Yield: 205 mg (82%). ^{1}H NMR (500 MHz, CD_2Cl_2): δ 2.38 (s, 3H, $SO_2C_6H_4$-4-C*H*$_3$), 2.53 (s, 3H, SC*H*$_3$), 2.59 (s, 3H, SC*H*$_3$), 3.53 (br t, 1H, 8.7 Hz, *H*$_2$NCHPhCHPhNTs), 4.07 (br d, 1H, 8.5 Hz *H*$_2$NCHPhCHPhNTs), 4.23 (ddd, 1H, 13.5 Hz, 7.1 Hz, 3.6 Hz, HHNC*H*PhCHPhNTs), 4.62 (d, 1H, 7.3 Hz HHNCHPhCHPhNTs), 7.08-7.30 (12 H, aryl), 7.77 (d, 2H, 8.4 Hz, H_2NCHPhCHPhN*Ts*). Anal. Calcd: theoretical (found) for $C_{23}H_{27}ClN_2O_2PtS_2$: C, 41.97 (41.78); H, 4.14 (4.06); N, 4.26 (4.25).

[Pt(NCMe)(SMe$_2$)((*S,S*)-TsDPEN)]PF$_6$. A solution of 30.5 mg (0.12 mmol) $AgPF_6$ in 5 mL of MeCN was added via cannula to a solution of 79.5 mg (0.12 mmol) of PtCl(SMe$_2$)((*S,S*)-TsDPEN) in 5 mL of MeCN. No precipitate formed

within 30 min., so the flask was wrapped with foil to prevent light exposure, and the solution was stirred 24 h. A white precipitate formed. The supernatant solution was filtered via cannula, and the solvent was removed by vacuum. The solid residue was recrystallized from CH_2Cl_2/hexanes. After drying under vacuum at ambient temperature for 4 hours, the solid was collected. Yield: 74.8 mg (77%). ^{1}H NMR (500 MHz, CD_2Cl_2): δ 2.41 (s, 3H, SO_2C6H4-4-C*H*$_3$), 2.55 (s, 3H, NCC*H*$_3$), 2.61 (s, 3H, SCH_3C*H*$_3$), 2.66 (s, 3H, SC*H*$_3CH_3$), 3.80 (br t, 1H, 8.2 Hz, H*H*NCHPhCHPhNTs), 4.25 (m, 1H, HHNC*H*PhCHPhNTs), 4.58 (d, 1H, 7.9 Hz HHNCHPhC*H*PhNTs), 4.95 (br d, 1H, 9.0 Hz *H*HNCHPhCHPhNTs), 6.98-7.33 (12 H, aryl), 7.74 (d, 2H, 8.1 Hz, H_2NCHPhCHPhN*Ts*). ESI-MS m/z = + 663.3, ([Pt(TsDPEN)(MeCN)(SMe_2)]$^+$).

PtMe(MeCN)((*S,S*)-TsDPEN). A solution of 212 mg (0.578 mmol) of (*S,S*)-TsDPEN in 5 mL of MeCN at 0 ºC was transferred via cannula to a solution of 166 mg (0.289 mmol) of [$PtMe_2(SMe_2)]_2$ in 5 mL of MeCN at 0 ºC. After being maintained for 15 min. at 0 ºC, the solution was warmed to 0 ºC and stirred 1 h. A small amount of gas evolved. The solvent was removed by vacuum and the white colored solid was washed twice with 5 mL of diethyl ether. The residue was recrystallized from MeCN/Et_2O to give a white solid that was dried under vacuum overnight. Yield: 303 mg (85 %). ^{1}H NMR (500 MHz, CD_2Cl_2): δ 0.468 (s-Pt satellites, $J_{Pt\text{-}H}$ = 74 Hz, Pt-C*H*$_3$), 2.29 (s, 3H, $SO_2C_6H_4$-4-C*H*$_3$), 2.40 (s, 3H, PtNCC*H*$_3$), 3.28 (br d, 1H, 11.5 Hz, H*H*NCHPhCHPhNTs), 3.73 (br d, 1H, 9.5 Hz *H*HNCHPhCHPhNTs), 4.18 (m, 1H, HHNC*H*PhCHPhNTs), 4.80 (s, 1H, HHNCHPhC*H*PhNTs), 6.80-7.77 (14 H, aryl). ESI-MS m/z = + 617.2

([Pt(TsDPEN)(MeCN)MeH]$^+$). Elemental Analysis %CHN theoretical (found) for $C_{24}H_{27}N_3O_2PtS{\cdot}H_2O$: C, 45.42 (45.46); H, 4.61 (4.38); N, 6.62 (6.46).

PtMe(MeCN)((*S,S*)-TsDPEN) + CO. A solution of 11.5 mg (0.0187 mmol) of PtMe(MeCN)((*S,S*)-TsDPEN) in 5 mL of CH_2Cl_2 was stirred under 1 atm of CO. An IR spectrum of solution was collected after 45 min. and 1.5 h., showing no change in the IR spectrum upon longer reaction times. Solution was evaporated under vacuum, and the ^{1}H NMR spectrum of the sample dissolved in CD_2Cl_2 showed only starting PtMe(MeCN)((*S,S*)-TsDPEN). The IR spectrum of this solution exhibited no ν_{CO} bands. The solution was again purged with CO to give the same IR bands in the same ratio. IR spectrum (CH_2Cl_2): ν_{CO} = 1994, 2023 cm^{-1}.

Pd(C_3H_5)((*S,S*)-TsDPEN). A solution of 40 mg (0.11 mmol) of (*S,S*)-TsDPENH and 15 μL (0.11 mmol) of Et_3N in 2 mL CH_2Cl_2 was added to a solution of 20 mg (0.055 mmol) of [(allyl)PdCl]$_2$ in 2 mL of CH_2Cl_2. Solution was stirred 18 h, followed by extraction with CH_2Cl_2/water (3 x 3 mL). The colorless organic layer was dried over $MgSO_4$. Removal of solvent under vacuum gave a white powder. The product was recrystallized from CH_2Cl_2/Et_2O and dried under vacuum. Yield: 42 mg (74 %). Ratio of major to minor isomer in CD_2Cl_2 = 1.8:1, in DMSO-*d*^{6} = 2.7:1. ^{1}H NMR (500 MHz, CD_2Cl_2): δ 2.25 minor (s, 3H, SO_2C6H4-4-C*H*$_3$), 2.26 major (s, 3H, $SO_2C_6H_4$-4-C*H*$_3$), 2.68 minor (d of d, 1H, 10.5 Hz, 4 Hz, anti-C*H*HCHCH$_2$), 2.71 major (d, 1H, 12.3 Hz, anti-C*H*HCHCH$_2$), 2.77 major (d, 1H, 12.2 Hz, anti-C*H*HCHCH$_2$), 2.89 minor (d, 1H, 10.7 Hz, syn-C*H*HCHCH$_2$), 3.00 major (d, 1H, 12.3 Hz, syn-C*H*HCHCH$_2$), 3.05 minor (d of d,

1H, 10.7 Hz, 4 Hz, anti-C*H*HCHCH$_2$), 3.13 minor (d, 1H, 10.7 Hz, syn-C*H*HCHCH$_2$), 3.29 major (d, 1H, 12.4 Hz, syn-C*H*HCHCH$_2$), 3.81 major (d of d, 1H, 7 Hz, 2.2 Hz, HHNC*H*PhCHPhNTs), 3.83 minor (d of d, 1H, 7 Hz, 2.2 Hz HHNC*H*PhCHPhNTs) 4.34 minor (d of t, 2H, 6.9 Hz, 2 Hz, *H*$_2$NCHPhCHPhNTs), 4.40 major (m, 2H, *H*$_2$NCHPhCHPhNTs), 4.80 minor (s, 1H, HHNCHPhC*H*PhNTs), 4.87 major (s, 1H, HHNCHPhC*H*PhNTs), 5.42 major (t of q, 1H, Hz, C*H*HCHCH$_2$), 5.47 minor (t of q, 1H, Hz, C*H*HCHCH$_2$), 6.80-7.66 major and minor(14 H, aryl). ESI-MS m/z = + 617.2 ([Pt(TsDPEN)(MeCN)MeH]$^+$). Anal. Calcd: theoretical (found) for $C_{24}H_{26}N_2O_2PdS$: C, 56.19 (55.55); H, 5.11 (5.16); N, 5.46 (5.37). Crystals suitable for X-ray diffraction were grown over the course of two days from a concentrated sample in CH_2Cl_2 solution that was maintained at -20 ºC.

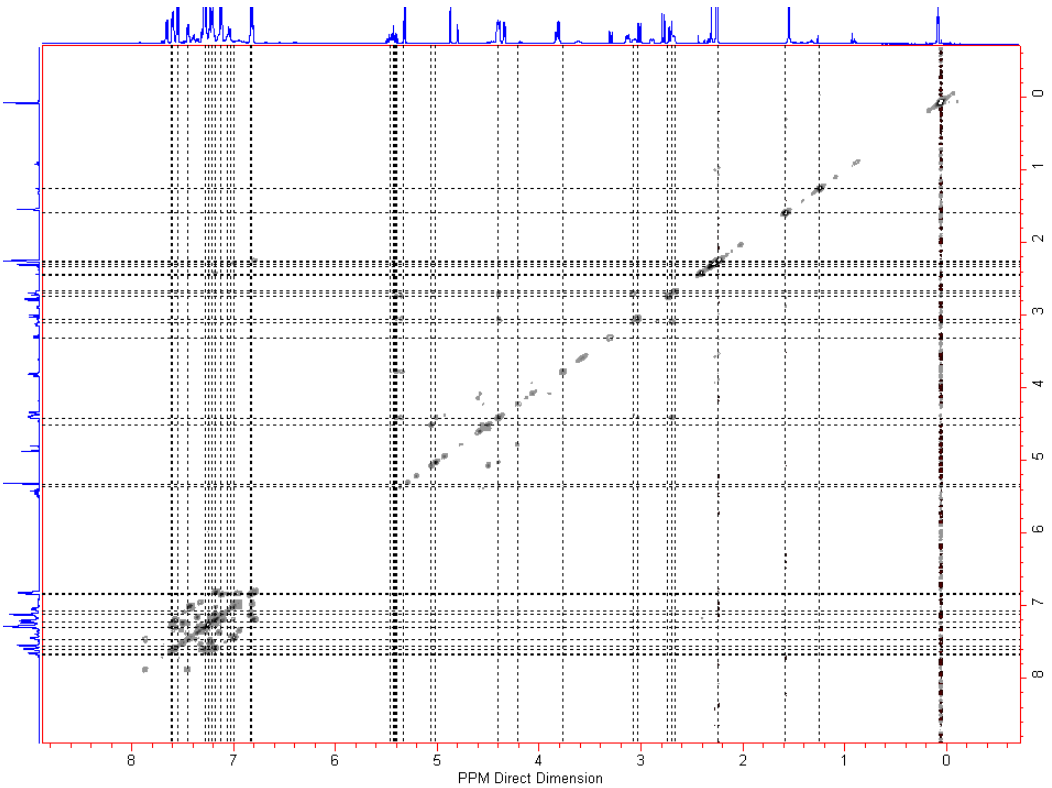

Figure 6.13. ^{1}H COSY spectrum of Pd(allyl)(*S,S*-TsDPEN) in CD_2Cl_2.

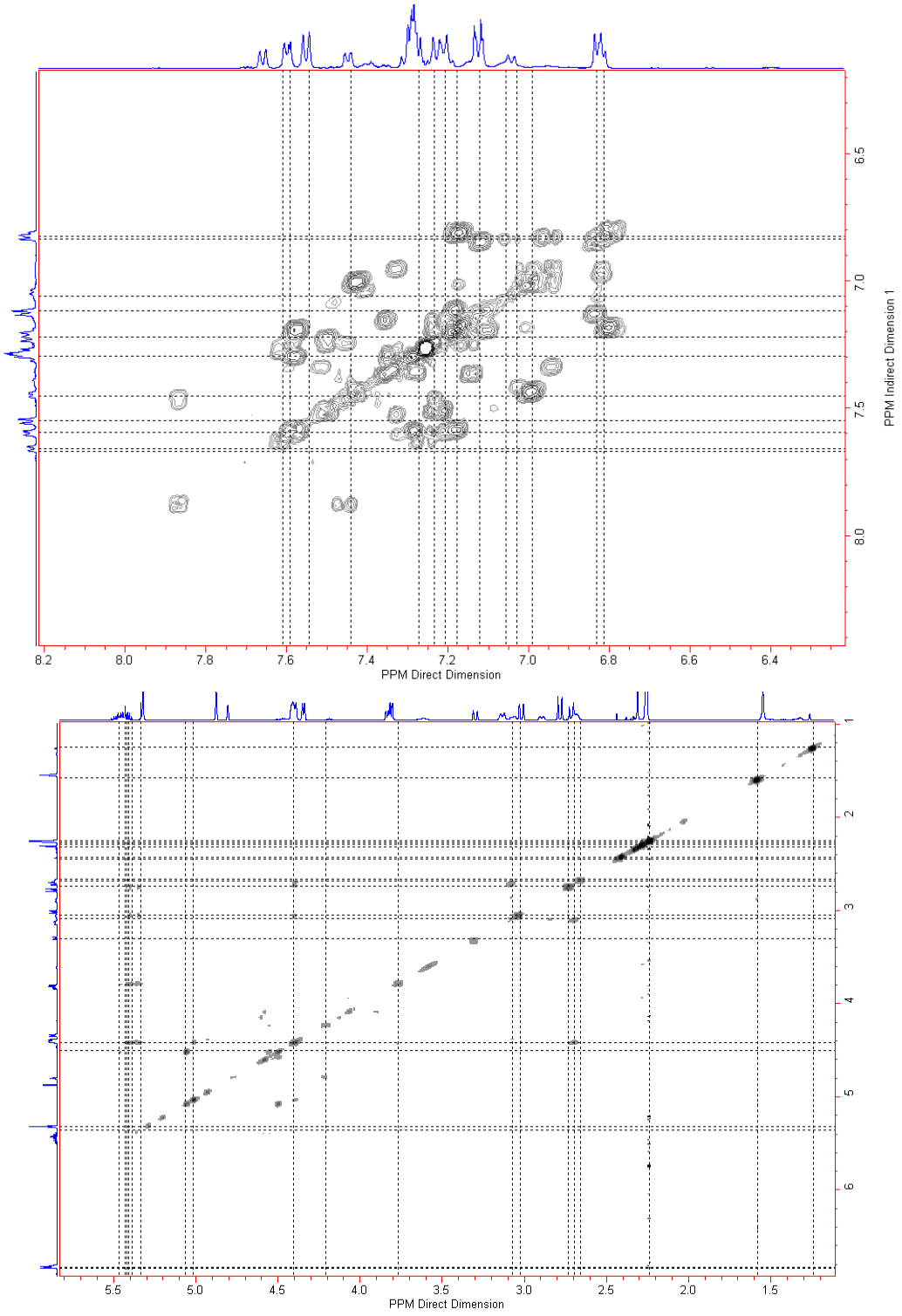

Figure 6.14. ^{1}H COSY spectrum of Pd(allyl)(*S,S*-TsDPEN) in CD_2Cl_2. Closeup view of allylic H (top) and closeup view of allylic H, amine H, and NC*H*PhC*H*PhNTs signals (bottom).

Ir(cod)((*S,S*)-TsDPEN). A solution of 219 mg (0.60 mmol) of (*S,S*)-TsDPEN and 167 µL (1.2 mmol) of Et_3N in 10 mL of CH_2Cl_2 was transferred via cannula to a solution of 201 mg (0.30 mmol) of $[(cod)IrCl]_2$ in 10 mL of CH_2Cl_2. After stirring 1 h, the solution was extracted with H_2O (3 X 5 mL). The organic layer was dried over $MgSO_4$ and filtered. Solvent was removed by vacuum, and the brown solid was recrystallized from 1:3 CH_2Cl_2/hexanes and filtered. The product must be recrystallized from 5 mL MeCN/ 15 mL Et_2O to remove a dark brown impurity. The solid is dried under vacuum. Yield: 239 mg (60 %). ^1H NMR (500 MHz, CD_2Cl_2): δ 1.44 (m, 1H, cod-C*H*H), 1.57 (m, 1H, cod-C*H*H), 1.79 (m, 1H, cod-C*H*H), 2.02 (m, 1H, cod-C*H*H), 2.14 (m, 1H, cod-C*H*H), 2.22 (m, 1H, cod-C*H*H), 2.26 (s, 3H, SO_2C6H4-4-CH_3), 2.38 (m, 1H, cod-C*H*H), 2.45 (m, 1H, cod-C*H*H), 2.97 (d, 1H, cod=C*H*), 3.09 (t of d, 1H, cod=C*H*), 3.26 (t of d, 1H, cod=C*H*), 3.32 (d of d, 1H, cod=C*H*), , 4.25 (d, 1H, 4.7 Hz, HHNC*H*PhCHPhNTs), 4.71 (s, 1H, HHNCHPhC*H*PhNTs), 4.82 (t of d, 1H, 7.5 Hz, 4.7 Hz, H*H*NCHPhCHPhNTs), 5.36 (t of d, 1H, 7.5 Hz, 2.5 Hz *H*HNCHPhCHPhNTs), 6.78-7.91 (14 H). Anal. Calcd: theoretical (found) for $C_{29}H_{33}IrN_2O_2S$: C, 52.31 (52.96); H, 5.00 (5.24); N, 4.21 (4.28).

Rh(cod)((*S,S*)-TsDPEN). A solution of 290 mg (0.792 mmol) of (*S,S*)-TsDPEN and 220 µL (1.59 mmol) of Et_3N in 15 mL of MeCN was transferred via cannula to a mixture of 195 mg (0.396 mmol) of $[(cod)IrCl]_2$ in 8 mL of MeCN. After stirring the solution for 20 h, a light yellow precipitate had formed. The solid was removed by filtration and washed with 5 mL of MeCN and 10 mL of diethyl ether. The filtrate was evaporated under vacuum, and the residue was extracted

into 5 mL of CH_2Cl_2. This solution was washed with about 6 mL of H_2O. The organic layer was dried over $MgSO_4$ and filtered. Solvent was removed by vacuum, and the solid was recrystallized from 1:3 CH_2Cl_2/hexanes. The solid was dried under vacuum. Yield: 371 mg (81%). ^{1}H NMR (500 MHz, CD_2Cl_2): δ 1.81 (m, 1H, cod-C*H*H), 1.88 (m, 1H, cod-C*H*H), 2.01 (m, 2H, cod-C*H*H), 2.11 (m, 1H, cod-C*H*H), 2.26 (s, 3H, SO_2C6H4-4-CH_3), 2.36 (m, 1H, cod-C*H*H), 2.43 (m, 1H, cod-C*H*H), 2.55-2.71 (m, 3H, 1 cod-*H*H, 2 cod=C*H*), 3.49 (br q, 1H, cod=C*H*), 3.60 (br t , 1H, cod=C*H*), 4.10 (d, 1H, 4 Hz, HHNC*H*PhCHPhNTs), 4.47 (s, 1H, HHNCHPhC*H*PhNTs), 5.17 (q, 1H, 7 Hz, H*H*NCHPhCHPhNTs), 5.54 (t, 1H, 7 Hz *H*HNCHPhCHPhNTs), 6.76-8.08 (14 H).

General Conditions to Examine H_2 Reactivity. A solution of 8 to 10 mg of the complex was prepared in a J. Young NMR tube with ~0.8 mL CD_2Cl_2 that was vacuum transferred. The tube was pressurized to about 1 atm of H_2, and the cap was sealed. The presence of H_2 in solution was also always confirmed by ^{1}H NMR spectroscopy.

References

[1] Fulton, J.R; Holland, A.W.; Fox, D.J.; Bergman, R.G. “Formation, Reactivity, and Properties of Nondative Late Transition Metal-Oxygen and –Nitrogen Bonds.” *Acc. Chem. Res*. **2002**, *35*, 44-56.

[2] Ikariya, T.; Murata, K.; Noyori, R. “Bifunctional Transition Metal-Based Molecular Catalysts for Assymetric Syntheses.” *Org. Biomol. Chem*. **2006**, *4*, 393-406.

[3] Noyori, R.; Hashiguchi, S. “Asymmetric Transfer Hydrogenation Catalyzed by Chiral Ruthenium Complexes.” *Acc. Chem. Res*. **1997**, *30*, 97-102.

[4] Becker, J. J.; White, P. S.; Gagne, M. R. “Synthesis and Characterization of Chiral Platinum(II) Sulfonamides: (dppe)Pt(NN) and(dppe)Pt(NO) Complexes.” *Inorg. Chem.* **1999**, *38*, 798-801.

[5] Iverson, C. I.; Carter, C. A. G.; Baker, R.T.; Scollard, J. D.; Labinger, J. A.; Bercaw, J. E. **"**C-H Bond Activation by Unsymmetrical 2-(N-Arylimino)pyrrolide Pt Complexes: Geometric Effects on Reactivity." *J. Am. Chem. Soc.* **2003**, *125*, 12674-12675.

[6] Zhang, J.; Liu, Q.; Duan, C.; Shao, Y.; Ding, J.; Miao, Z. You, X. Z.; Guo, Z. "Structural evidence for the facile chelate-ring opening reactions of novel platinum(II)–pyridine carboxamide complexes." *J. Chem. Soc., Dalton Trans*., **2002**, 591-597

[7] Evans, C.; Henderson, W.; Nicholson, B. K. "Metallacyclic platinum(II) bis(sulfonamides)." *Inorganica Chim. Acta* **2001**, *314*, 42-48.

[8] Li, J. J.; Li, W.; James, A. J.; Holbert, T.; Sharp, T. P.; Sharp, P. R. "Phosphine-Based Dinuclear Platinum(II) Diamido, Amido-Hydroxo, Oxo-Amido, Oxo-Imido, Diimido, and Dihydrazido Complexes." *Inorg. Chem.* **1999**, *38*, 1563-1572.

[9] Xia, A.; Sharp, P. R. "Diphosphazane supported platinum(II) triflate, amine, and amido complexes: synthesis and X-ray crystal structures." *Polyhedron,* **2002**, *21*, 1305-1310.

[10] U. Anandhi, Todd Holbert, Dennis Lueng, and Paul R. Sharp, "Platinum and Palladium Imido and Oxo Complexes with Small Natural Bite Angle Diphosphine Ligands." *Inorg. Chem.*, **2003**, *42*, 1282–1295.

[11] Rendina, L. M.; Puddephatt, R. J. "Oxidative Addition Reactions of Organoplatinum(II) Complexes with Nitrogen-Donor Ligands." *Chem. Rev.* **1997**, *97*, 1735-1754.

[12] van Asselt, R.; Rijnberg, E.; Elsevier, C. J. "Rigid bidentate nitrogen ligands in organometallic chemistry and homogeneous catalysis. 7. Stabilization of high oxidation states by rigid bidentate nitrogen ligands: synthesis and characterization of diorgano- and triorganopalladium(IV) and cationic triorganoplatinum(IV) complexes." *Organometallics* **1994**, *13*, 706-720.

[13] Karshted, D.; McBee, J. L.; Bell, A. T.; Tilley, T. D. **"**Stoichiometric and Catalytic Arene Activations by Platinum Complexes Containing Bidentate Monoanionic Nitrogen-Based Ligands." *Organometallics* **2006**, *25*, 1801-1811.

[14] McBee, J. L.; Tilley. T. D. "Nucleophilic Attack of Amides onto Coordinated Ethylene in Platinum Complexes Supported by a Chelating Pyridyl−Pyrrolide Ligand: Azaplatinacyclobutane and Vinylamine Complexes." *Organometallics*, **2010**, *29*, 184–192.

[15] Chen, J. L.; Lin, C. H.; Chen, J. H.; Chi, Y.; Chiu, Y. C.; Chou, P. T.; Lai, C. H.; Lee, G. H.; Carty, A. J. "Reactions of the (2-Pyridyl) Pyrrolide Platinum(II) Complex Driven by Sterically Encumbered Chelation: A Model for the Reversible Attack of Alcohol at the Coordinated Carbon Monoxide." *Inorg. Chem.* **2008**, *47*, 5154-5161.

[16] Heiden, Z. M.; Rauchfuss, T. B. "Proton-Induced Lewis Acidity of Unsaturated Iridium Amides." *J. Am. Chem. Soc.* **2006**, *128*, 13048–13049.

[17] Zachariah M. Heiden, Bradford J. Gorecki and Thomas B. Rauchfuss, "Lewis Base Adducts Derived from Transfer Hydrogenation Catalysts: Scope and Selectivity." *Organometallics*, **2008**, *27*, 1542–1549.

[18] Pouzard, G.; Rajzmann, M.; Bodot, H.; Pujol, L. "intramolecular interactions. XVII. Calculation of NMR coupling constants of cyclohexane and substituted cyclohexanes. Comparison of Pople and Santry's method and the finiteperturbation method.: *Org. Magn. Reson.* **1973**, *5*, 209–214.

[19] Sudmeier, J. L.; Blackmer, G. L. "Conformational analysis of diamagnetic tris-ethylenediamine complexes by proton magnetic resonance. Spectra of tris(ehtylenediamine) rhodium(III)." *Inorg. Chem.* **1971**, *10*, 2010–2018.

[20] Tormena, C. F.; Vilcachagua, J. D.; Karcher, V.; Rittner, R.; Contreras, R. H. "Experimental and theoretical investigation of NMR 2JHH coupling constants on six-membered ring systems containing oxygen or sulfur atoms." *Magn. Reson. Chem.* **2007**, *45*, 590–594.

[21] Hill, G. S.; Irwin, M. J.; Levy, C. J.; Rendina, L. M.; Puddephatt, R. J. "Platinum(II) complexes of dimethyl sulfide." *Inorg. Syn.* **1998**, *32*, 149-153.

[22] Anderson, G. K.; Cross, R. J. "Preparation of the complexes trans-[PtX_2(CO)L] and their isomerisation to cis isomers." *J. Chem. Soc., Dalton Trans.* **1980**, 1988-1991.

[23] Mok, C. Y.; Tan, S. G.; Chan, G. C. "Photochemical isomerization of Platinum(II) complexes containing phosphine and carbonyl ligands: Pt(CO)(PR_3)X_2 (X = Cl, Br, I)." *Inorg. Chim. Acta* **1990**, *176*, 43-48.

[24] West, N. W.; White, P. S.; Templeton, J. L. "Facile Dehydrogenation of Ethers and Alkanes with a β-Diiminate Pt Fragment." *J. Am. Chem. Soc.* **2007**, *129*, 12372-12373.

[25] West, N. W.; White, P. S.; Templeton, J. L. "Alkyne Insertion into the Pt−H Bond of Pt(H)(1-pentene)(β-diiminate) Initiates a Reaction Cascade That Results in C−H Activation or C−C Coupling." *Organometallics*, **2008**, *27*, 5252-5262.

[26] Reinartz, S.; White, P. S.; Brookhart, M.; Templeton, J. L. “Acid-Assisted Reductive Elimination as a Route to Platinum(II) Products from Platinum(IV) Tris(pyrazolyl)borate Reagents.” *Organometallics*, **2000**, *19*, 3854-3866.

[27] Baar, C. R.; Jennings, M. C.; Puddephatt, R. J. “Electrophilic Binuclear Methylplatinum(II) Complexes.” *Organometallics*, **1999**, *18*, 4373–4379

[28] Becconsall, J. K.; O’Brien, S. “Temperature dependence of the nuclear magnetic resonance spectrum of di-π-allylpalladium.” *J. Organometallic Chem.* **1967**, *9*, P27-P29.

[29] O’Brien, S. “The Nuclear Magnetic Resonance Spectra of Some Platinum and Palladium π-Allyl Complexes and their Reactions with Sulphur Dioxide.” *J. Chem. Soc. A.* **1970**, 9-13.

[30] Benn, R. Habilitationsschrift, Universität Siegen, Germany, 1984

[31] Davison, A.; Rode, W. C. “Stereochemically nonrigid organometallic compounds. VI. Configurational equilibria of .pi.-C5H5Mo(CO)2-allyl complexes.” *Inorg. Chem.* **1967**, *6*, 2124-2125.

[32] Faller, J. W.; Incorvia, M. J. “Steric effects in organometallic conformational equilibria. I. Allylic complexes of molybdenum.” *Inorg. Chem.* **1968**, *7*, 840-842.

[33] Nesmeyanov, A. N.; Ustynyuk, Y. A.; Kritskaya, I. I.; Shchembelov, G. A. “Proton magnetic resonance spectra and structure of iron pi.-allyl complexes.” *J. Organomet. Chem.* **1968**, *14*, 395-403.

[34] Holloway, C. E.; Kelly, J. D.; Stiddard, M. H. B. “Halogeno-π-allyl(carbonyl) complexes of tungsten.” *J. Chem. Soc. A* **1969**, 931-935.

[35] Faller, J. W.; Chen, C.-C.; Mattina, M. J.; Jakubowski, A. “Organometallic conformational equilibriums XVI. Steric effects on p-allyl and p-indenyl orientation in molybdenum and tungsten complexes.” *J. Organomet. Chem.* **1973**, *52*, 361-386.

[36] Faller, J. W.; Adams, M. A. “The rearrangement mechanism of η^3-allyliron tricarbonyl halides.” *J. Organomet. Chem.* **1979**, *170*, 71-80.

[37] Benn, R.; Rufinska, A.; Schroth, G. “Fluxional behaviour in η^3-allyl complexes of cr, mo and w as shown by magnetisation transfer difference spectroscopy (MTDS).” *J. Organomet. Chem.* **1981**, *217*, 91-104.

[38] Mann, B. E.; Shaw, S. D. “Mechanism of fluxionality of (1,2,7-eta.3-2-methylbenzyl)(h5-C5H5)Mo(CO)2.” *J. Organomet. Chem.* **1987**, *326*, C13-C16.

[39] Takao, Y.; Takeda, T.; Watanabe, J.; Setsune, J. “Isomerization Behavior in the (π-Allyl)palladium(II) Complexes with N^{21},N^{22}-Bridged Porphyrin Ligands.” O*rganometallics*, **2003**, *22*, 233–241

[40] Ikariya, T.; Haskiguchi, S.; Murata, K.; Noyori, R. Wipf, P.; Amantini, D. “Preparation of optically active (R,R)-hydrobenzoin from benzoin or benzyl.” *Org. Syn.* **2005***, 82,* 10-17.

[41] Hill, G. S.; Irwin, M. J.; Levy, C. J.; Rendina, L. M.; Puddephatt, R. J. “Platinum(II) complexes of dimethyl sulfide.” *Inorg. Syn.* **1998**, *32*, 149-153.

[42] Herde, J. L.; Lambert, J. C.; Senoff, C. V. “Cyclooctene and 1,5-cyclooctadiene complexes of iridium(I).” *Inorg. Syn*. **1974**, *15*, 18-20.

[43] Giordano, G.; Crabtree, R. H. “Di-μ-chloro-bis(η4-1,5-cyclooctadiene) dirhodium(I).” *Inorg. Syn.* **1990**, *28*, 88-90.

Chapter 7

Reductive Coupling of $Ph_2P(o\text{-}C_6H_4CHO)$ on Fe(0) to Form a Tetradentate P_2O_2 Ligand

Introduction

We previously reported the utility in installing chelated phosphine acyl ligands to Fe(II) carbonyls by the oxidative addition of phosphine thioester compounds to Fe(0) carbonyls.[1] This method was found to give varying yields depending on the identity of R in the case of $Ph_2P(C_6H_4C(O)SR)$.[2] One significant limitation of this method was the low reactivity when R was sterically encumbering, i.e. 2,6-dimesitylphenyl or ^{t}Bu.

In an effort to expand the methods for installing phosphine acyl chelates to Fe(II), we have examined the addition of $Ph_2P(o\text{-}C_6H_4CHO)$ to Fe(0) carbonyls. The coordination chemistry of this ligand is already well established, although mainly with 2nd and 3rd row metals.[3]

Scheme 7.1. Common coordination products from reaction of late transition metal complexes with $Ph_2P(o\text{-}C_6H_4CHO)$.

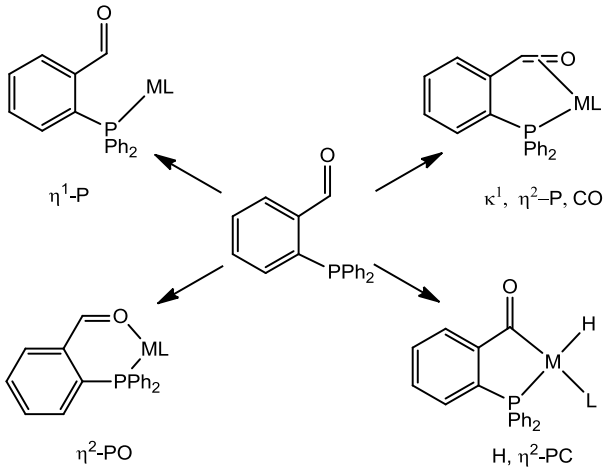

o-Diphenylphosphinebenzaldehyde has been shown to react with metals in four common ways (Scheme 7.1). The simplest is a η^1-P phosphine metal bond with no significant interaction of the aldehyde. This type of structure is the first step in the formation of the 3 other coordination modes and is generally observed in complexes that are coordinately saturated such as $W(CO)_5(PPh_2(o\text{-}C_6H_4CHO))$[4], or in square planar d^8 complexes such as *cis*-$[MCl_2(PPh_2(o\text{-}C_6H_4CHO))_2]$ where M = Pt(II)[5] or Pd(II)[6] and several Rh(I)[7,8] complexes are reported. An alternative synthesis route of the η^1-P binding mode was reported by Barbaro *et al* in which the ligand is synthesized by hydrolysis of an imino group of an $Ir(PPh_2(o\text{-}C_6H_4CH{=}NEt))$ complex to give an $Ir(PPh_2(o\text{-}C_6H_4CHO))$ complex.[9]

After initial binding of the phosphine, the ligand can then chelate by either of two routes involving σ bond formation by O to give a η^2-PO coordination, which is reported for $Re(CO)_3Cl(PPh_2(o\text{-}C_6H_4CHO))$[10] and $RuCl_2(PPh_2(o\text{-}C_6H_4CHO))_2$,[5] or by binding to the CO double bond in π fashion to give a κ^1, η^2-P,CO coordination. The κ^1, η^2-P,CO coordination mode was first proposed to explain NMR data in $Cp^*Co(PPh_2(o\text{-}C_6H_4CHO))$[11] and later established by X-ray crystallography in two W(0) complexes.[12]

The addition of *o*-diphenylphosphinebenzaldehyde to electron rich late transition metals, such as Rh(I),[13,14] Ir(I),[5,15-16] Pt(0),[17-18] Co(I),[19] frequently results in chelate-assisted C-H bond activation to give a phosphine acyl η^2-P-C complex. Usually a metal hydride is isolated (Scheme 7.2), but some metal halide complexes have been shown to eliminate HX. It is not known whether this

occurs by oxidative addition of the C-H bond followed by reductive elimination of HX, or direct electrophilic attack on the formyl group by the metal with displacement of a proton.

Scheme 7.2. C-H bond activation of $Ph_2P(o\text{-}C_6H_4CHO)$ with late transition metals to give acyl hydride complexes. (i) $[Pt(C_2H_4)n(PR_3)_{3-n}]$ (R = C_6H_4, n =1; R = cyclohexyl, n = 2), (ii) $[CoCl(PMe_3)_3]$, (iii) trans-$[IrCl(CO)(PPh_3)_2]$, (iv) $[Rh(X(CH_2CH_2PPh_2)_3]^+$ (X = N or P), (v) [RhCl(cod)(NN)] (cod = 1,5-cyclooctadiene)(NN = bypyridines), (vi) [RhCl(cod)(NN)] PPh_3.[3]

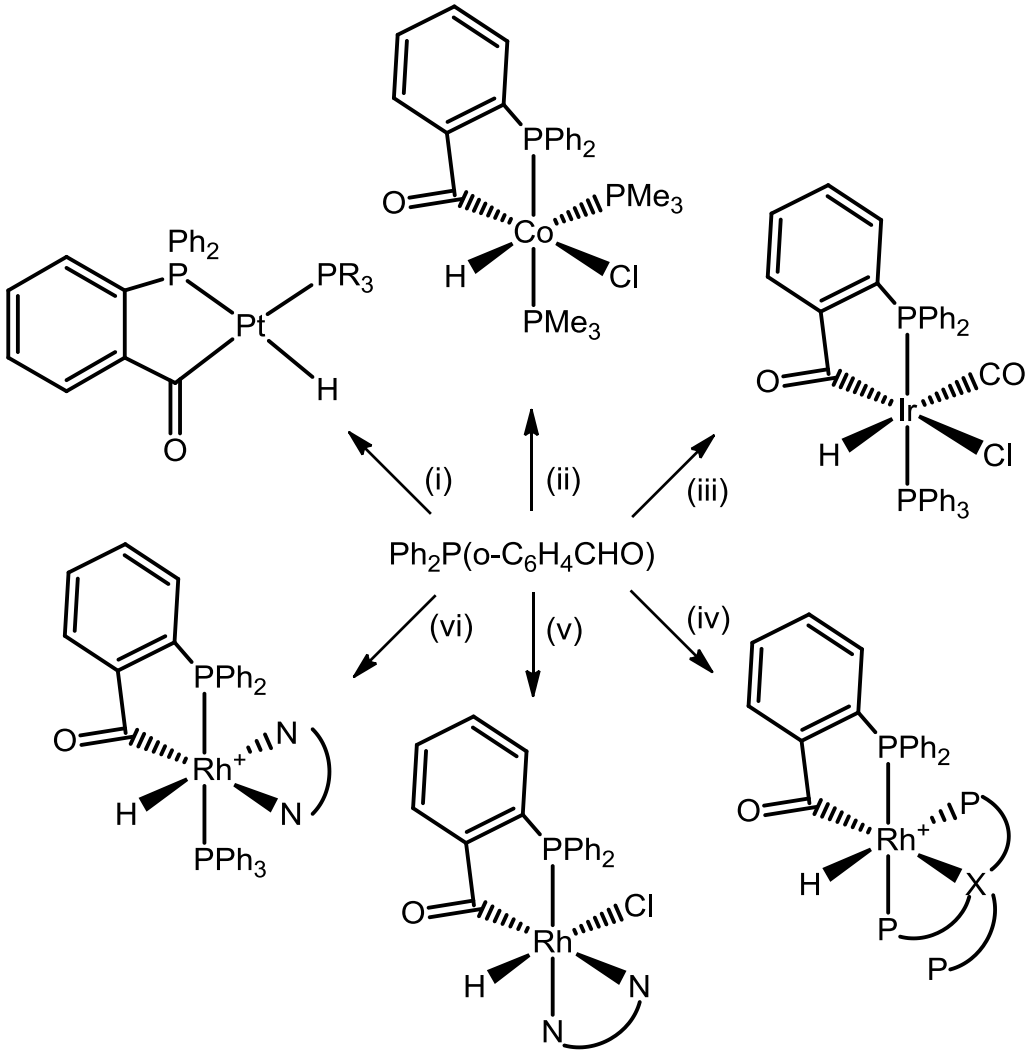

In two examples, the addition of $Ph_2P(o\text{-}C_6H_4CHO)$ to a transition metal results in C-C bond formation to give a dioxyl derivative. The synthesis and final structures of the W[12] and Tc[20] complexes are shown in Scheme 7.3.

Scheme 7.3. C-C coupling reactions of $Ph_2P(o\text{-}C_6H_4CHO)$.

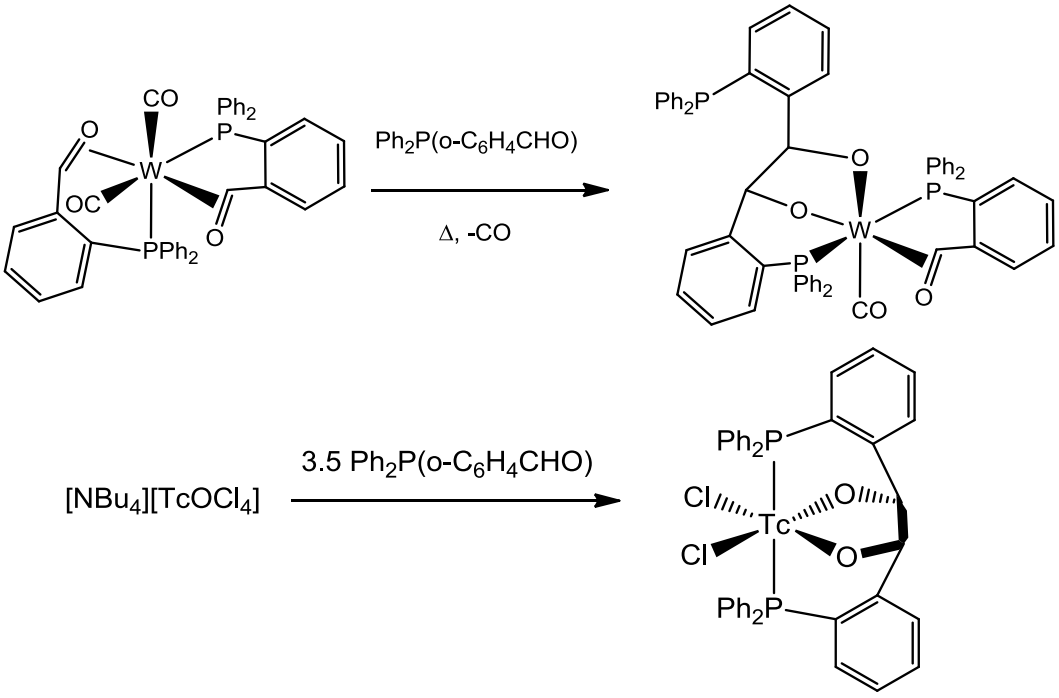

Results

Formation of $Fe(P_2O_2)(CO)_2$. Heating a THF solution of $Fe(bda)(CO)_3$, bda = benzylideneacetone, in the presence of $Ph_2P(o\text{-}C_6H_4CHO)$ gave a yellow solution and yellow precipitate. IR and NMR spectra for the solution and the solid products were found to be identical. The solution IR spectrum featured comparably intense CO bands at 1965 and 2025 cm^{-1}. The ^{31}P NMR spectrum featured a single peak at δ 21.1. The ^{1}H NMR spectrum contained a single signal outside of the phenyl proton range at δ 4.49 ppm that integrated in a 1:14

ratio to the phenyl signals. This complex is the only phosphine-containing complex detected for Fe:$Ph_2P(o\text{-}C_6H_4CHO)$ ratios of 1:1 and 1:2 Fe:P at 60 ºC .

Scheme 7.4. Formation of $Fe(P_2O_2)(CO)_2$ from $Ph_2P(o\text{-}C_6H_4CHO)$.

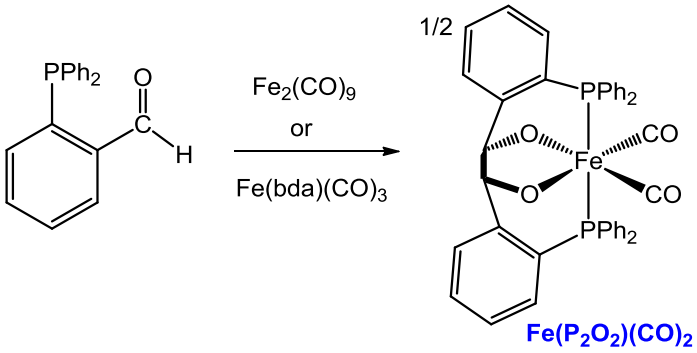

Single crystal X-ray diffraction confirmed that the product is a ferrous complex of a bisphosphine bisalkoxide ligand (Figure 7.1). Apparently the two formyl groups underwent C-C coupling (Scheme 7.4). The octahedral ferrous complex has *cis* alkoxide ligands both *trans* to CO. The phosphines are mutually trans with a P-Fe-P angle of 167°.

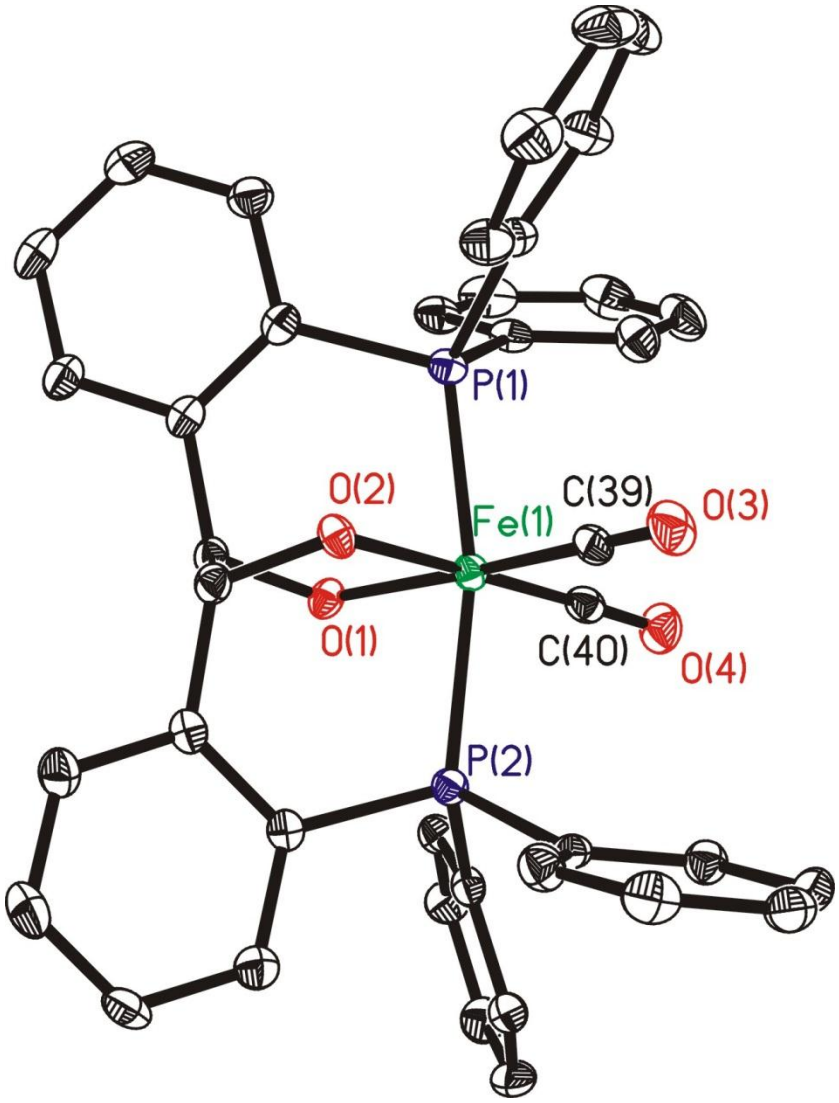

Figure 7.1. Molecular structure of $Fe(P_2O_2)(CO)_2$ with H's removed for clarity. The thermal ellipsoids are shown at 35% probability with Fe, green; P, blue; C, black; O, red. Selected Bond Lengths (Å) and Angles (°): Fe(1)-P(1) 2.2496(9), Fe(1)-P(2) 2.2395(10), Fe(1)-O(1) 1.945(2), Fe(1)-O(2) 1.954(2), Fe(1)-C(39) 1.774(3), Fe(1)-C(40) 1.754(3), C(40)-Fe(1)-C(39) 92.64(14), C(40)-Fe(1)-O(1) 96.01(12), C(39)-Fe(1)-O(2) 86.26(12), O(1)-Fe(1)-O(2) 85.07(8), P(2)-Fe(1)-P(1) 167.44(4).

The $Fe(P_2O_2)(CO)_2$ product is also obtained by the reaction of $Ph_2P(o\text{-}C_6H_4CHO)$ with $Fe_2(CO)_9$ at 60 ºC in THF. We isolated a probable intermediate in this conversion, $Fe[(PPh_2(o\text{-}C_6H_4CHO)](CO)_4$. This species was obtained in 49 % yield by addition of $Ph_2P(o\text{-}C_6H_4CHO)$ to $Fe_2(CO)_9$ at 23 ºC in THF followed

by removal of the majority of $Fe(CO)_5$ under reduced pressure, any additional $Fe(CO)_5$ was removed by washing the solid with hexanes. This complex displays an IR spectrum typical of phosphine adducts of the type $(PR_3)Fe^{(0)}(CO)_4$. For example, the ν_{CO} = 1943, 1978, 2052 cm^{-1} (Figure 7.2) compare well for the related PPh_3 derivative.[21] The ^{31}PNMR spectrum also featured a singlet at δ 68.2. Photolysis of this complex in toluene-d_8 at 23 ºC resulted initially in the formation of a κ^1, η^2-P,CO Fe complex followed by formation of an Fe hydride, which were detected by NMR spectroscopy. The κ^1, η^2-P,CO intermediate displays a singlet at δ 58.2 in the ^{31}P NMR spectrum and the aldehyde H shifts to 5.91 in the ^{1}H NMR spectrum, which is typical for η^2-C=O coordination.[12] The hydride complex displays doublets at δ -7.7 (d) and at δ 89.5 in the ^{1}H and ^{31}P NMR spectra, respectively. At 23 ºC, in the absence of light, the signal for the hydride disappears concomitant with formation of the $Fe(P_2O_2)(CO)_2$ product.

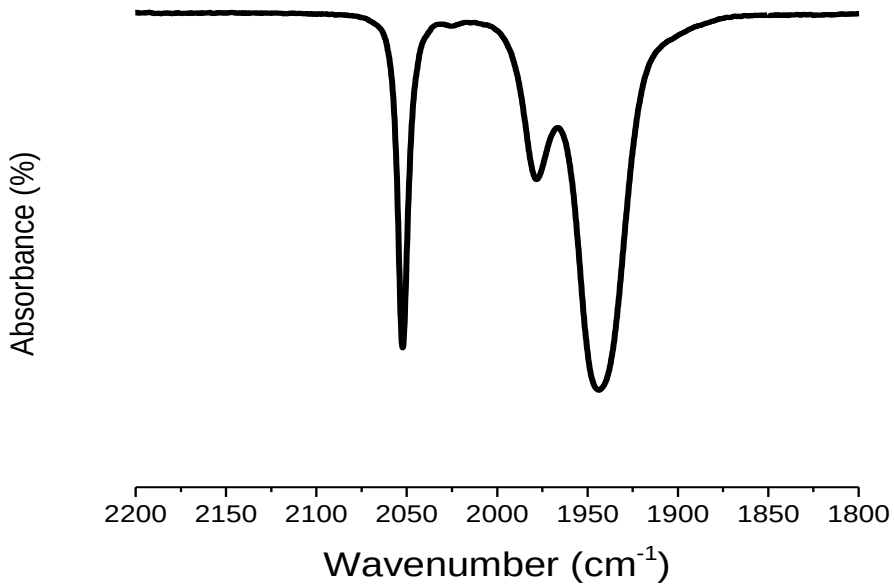

Figure 7.2. CO region of IR spectrum of $Fe[(PPh_2(C_6H_4CHO)](CO)_4$ in CH_2Cl_2 solution with ν_{CO} = 1943, 1978, 2052 cm^{-1}.

Reaction of $Fe(P_2O_2)(CO)_2$ with Ferrocenium Salts. We attempted to remove the CO ligands in $Fe(P_2O_2)(CO)_2$ by photolysis in MeCN solution. The reaction mixture was examined by IR and ^{31}P NMR spectroscopy. After 1 h, the MeCN solution contained a small amount of starting material with a minor CO band in the IR spectrum at 1937 cm^{-1}. After 5 hours, no CO bands were detected in the IR spectrum. The ^{31}P NMR spectrum showed ~90% conversion to free $Ph_2P(o\text{-}C_6H_4CHO)$ (δ -11). An alternative method for removal of CO was then attempted by addition of (ferrocenium)PF_6 ($FcPF_6$).

Scheme 7.5. Reaction of $Fe(P_2O_2)(CO)_2$ with $FcBF_4$

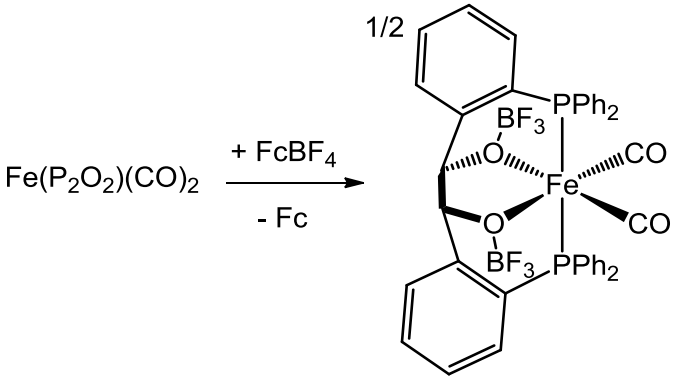

The oxidations of $Fe(P_2O_2)(CO)_2$ in CH_2Cl_2 solution by $FcPF_6$ and by $FcBF_4$ were followed by IR spectroscopy (Scheme 7.5). At room temperature, these reactions required ~20 minutes for consumption of the starting dicarbonyl complex. Surprisingly, the reaction required one equiv. of ferrocenium for complete conversion of the dicarbonyl precursor, yet the intensities of the ν_{CO} bands of the products were approximately half that of the starting material. Only final product and starting were detected in the CO region of the IR spectrum

during the reaction. The reaction with $FcPF_6$ gave a final product with an IR spectrum in CH_2Cl_2 solution with ν_{CO} = 2052, 2002 cm^{-1} (Figure 7.3), and the reaction with $FcBF_4$ gave a similar IR spectrum with ν_{CO} = 2053, 2004 cm^{-1} (Figure 7.4). The IR spectrum of the reaction of $Fe(P_2O_2)(CO)_2$ with 0.9 equivs. of $FcBF_4$ was obtained after 1 h of stirring and still featured ~10% unreacted $Fe(P_2O_2)(CO)_2$. The overall change for ν_{CO} in both anions (PF_6^- = 27, 37 cm^{-1}; BF_4^- = 28, 39 cm^{-1}) was smaller than that expected for oxidation from a ferrous dicarbonyl to a ferric dicarbonyl. The $FcBF_4$ reaction was followed by ^1H NMR with the use of CH_2Ph_2 as an internal standard. Upon completion of the reaction, ~40% of the intensity of the phenyl H was lost, presumably due to formation of a paramagnetic product. No solids were observed.

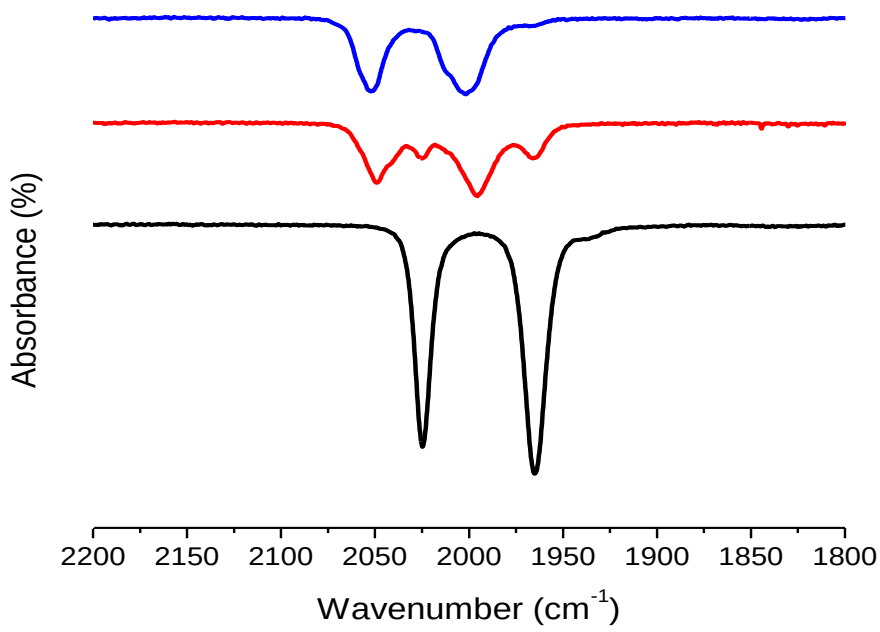

Figure 7.3. νCO region of IR spectrum of a solution of $Fe(P_2O_2)(CO)_2$ + before (black), 10 minutes after addition of 1 equiv. $FcPF_6$ (red), and 25 minutes after addition (blue).

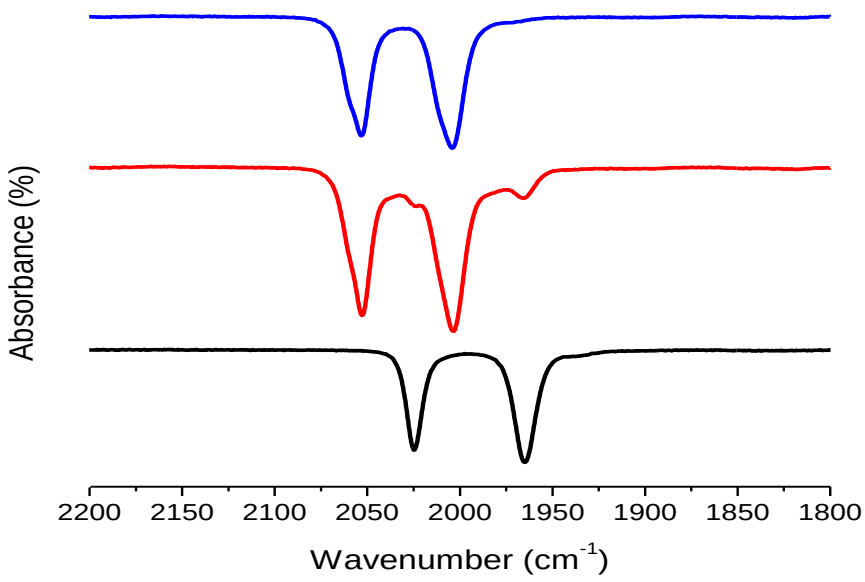

Figure 7.4. ν_{CO} region of IR spectrum of $Fe(P_2O_2)(CO)_2$ + $FcBF_4$ in CH_2Cl_2 before $FcBF_4$ addition (black), after 1 h stirring with 0.9 equivs. of $FcBF_4$ (red), and 20 minutes after addition of 1 equiv. of $FcBF_4$ (blue).

Single crystals of the diamagnetic product from reaction of $Fe(P_2O_2)(CO)_2$ and $FcBF_4$ were obtained and examined by X-ray crystallography. The product contains two molecules of BF_3 bound to the alkoxide centers (Figure 7.5.). The coordination at Fe is relatively unchanged. Changes in ligand bond distance to Fe and ligand angles are shown in Table 7.1. The greatest change is a small expansion of the P-Fe-P angle from 167.4^o to 171.8^o.

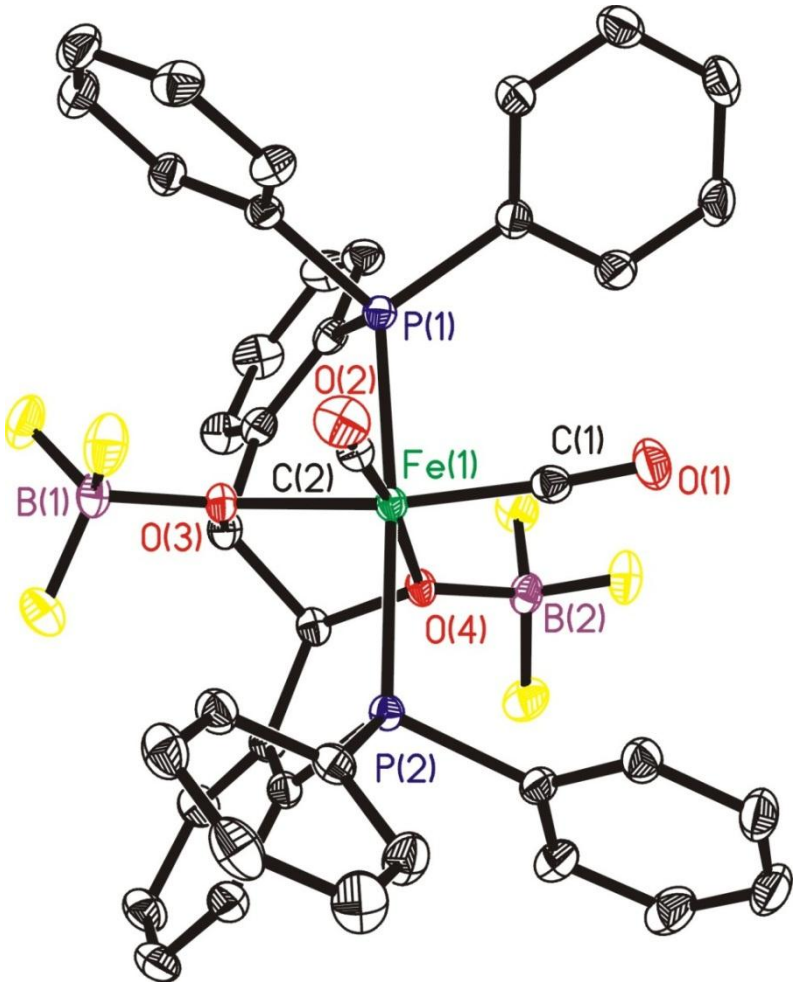

Figure 7.5. Molecular structure of $Fe(P_2O_2)(CO)_2(BF_3)_2$. The thermal ellipsoids are shown at 35% probability probability with Fe, green; P, blue; C, black; O, red. B, purple; F, yellow. Selected Bond Lengths (Å) and Angles (°) Fe(1)-P(1) 2.3136(11), Fe(1)-P(2) 2.3119(11), Fe(1)-O(3) 2.011(3), Fe(1)-O(4) 2.016(3), Fe(1)-C(1) 1.782(4), Fe(1)-C(2) 1.777(4), C(1)-Fe(1)-C(2) 85.59(18), C(1)-Fe(1)-O(4) 96.95(15), C(2)-Fe(1)-O(3) 98.20(15), O(3)-Fe(1)-O(4) 80.84(10), P(2)-Fe(1)-P(1) 171.81(4).

Table 7.1. Change in Fe ligand distances and angles upon BF_3 binding.

Bond	Avg. Change in Bond Distance (Å) Upon BF_3 Binding	Bond	Change in Bond Angle (°) Upon BF_3 Binding
Fe-CO	0.0155	C-Fe-C	-7.05
Fe-O	0.064	O-Fe-O	-4.23
Fe-P	0.0682	P-Fe-P	4.37

We wanted to investigate $Fe[P_2O_2(BF_3)_2](CO)_2$ by an independent synthesis method. Indeed, $Fe(P_2O_2)(CO)_2$ was found to react with 2 equivs. of BF_3OEt_2 in CH_2Cl_2 (Scheme 7.6). The IR spectrum of this product matched closely (but not exactly) that obtained by reaction with $FcBF_4$. In this reaction, we were able to identify the 1:1 adduct, which was not detected in the $Fe(P_2O_2)(CO)_2$ + $FcBF_4$ reaction. The 1:1 complex is characterized by ν_{CO} = 2048, 1995 cm^{-1}. The change in ν_{CO} of 23 and 30 cm^{-1} is just greater than half the overall ν_{CO} change from $Fe(P_2O_2)(CO)_2$ to $Fe[P_2O_2(BF_3)_2](CO)_2$ of 41 and 58 cm^{-1} (Figure 7.6.). The $Fe[P_2O_2(BF_3)_2](CO)_2$ complex has an IR spectrum in CH_2Cl_2 with ν_{CO} = 2066, 2023 cm^{-1}.

Reaction Scheme 7.6. Binding of Lewis Acids to $Fe(P_2O_2)(CO)_2$.

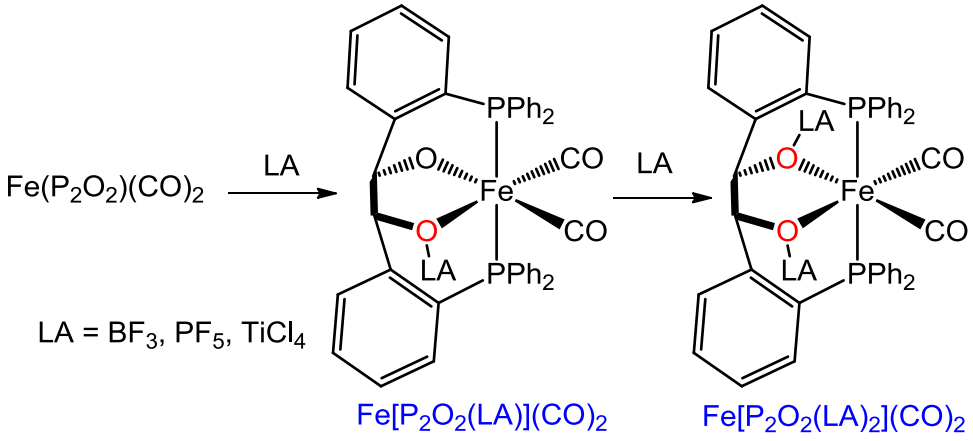

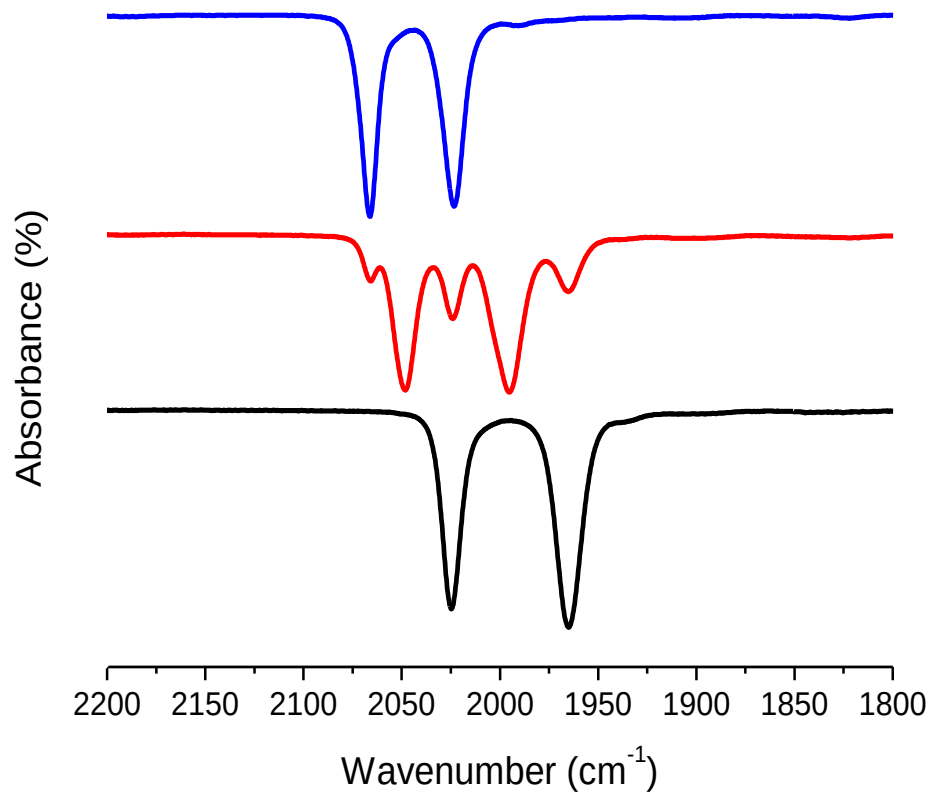

Figure 7.6. CO stretch region of IR spectrum of $Fe(P_2O_2)(CO)_2$ + BF_3 in CH_2Cl_2 before BF_3 addition (black), immediately after addition of 1 equiv. BF_3 (red), and after addition of 2 equivs. BF_3 (blue).

The generality of the binding of Lewis acids to the alkoxide ligands in $Fe(P_2O_2)(CO)_2$ was tested using $TiCl_4$. The addition of one equivalent $TiCl_4$ to a CH_2Cl_2 solution of $Fe(P_2O_2)(CO)_2$ immediately produced a large quantity of yellow precipitate. The solution IR spectrum obtained immediately after the addtiion matched the spectrum obtained for the addition of two equivalents of BF_3 with ν_{CO} = 2069, 2025 cm^{-1} (Figure 7.7). After stirring 10 minutes, the precipitate dissolved and the IR spectrum of the resulting solution mainly

featured a single dicarbonyl (ν_{CO} = 2050, 2000 cm^{-1}), which we assign to $Fe[P_2O_2(TiCl_4)](CO)_2$. This sample also contained a smaller amount of the proposed bis-$TiCl_4$ adduct. This spectrum remained unchanged over the course of 24 h in solution.

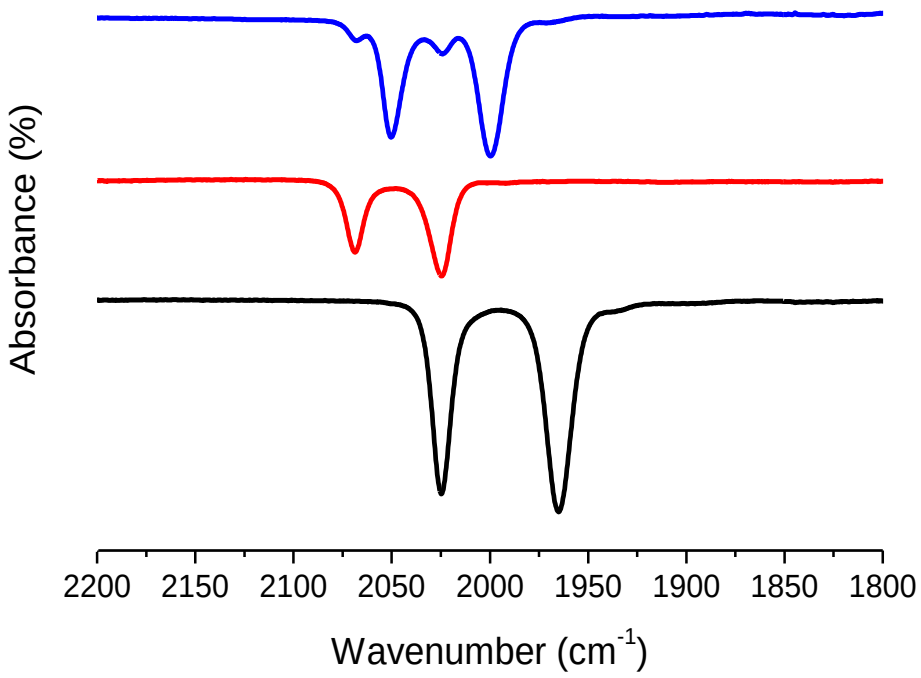

Figure 7.7. CO region of IR spectrum of $Fe(P_2O_2)(CO)_2$ + $TiCl_4$ in CH_2Cl_2 before addition of the $TiCl_4$ (black), immediately after addition of 1 equiv. of $TiCl_4$ (accompanied by a large quantity of precipitate, red), and after solution had reached equilibrium with no remaining solids (blue). The latter spectrum was shown to remain unchanged

A solution of $Fe[P_2O_2(BF_3)_2](CO)_2$ in wet THF decomposed over the course of 24 hours to give a gray precipitate. The IR spectrum of the filtrate showed no bands in the carbonyl region. The ^{31}P NMR spectrum of this solution featured a single peak at δ -16.3 (Figure 7.8). ESI-MS of the solution exhibited an intense envelop centered at m/z = 583, which corresponds to $HP_2(OH)_2^+$. This peak was not detected in pure samples of $Fe[P_2O_2(BF_3)_3](CO)_2$. These

experiments indicate that the diphosphine-diol can be removed intact from Fe (Scheme 7.7). After filtration through silica gel, the extract showed no signals in the ^{19}F NMR spectrum. The ligand was found to react with dichloromethane, but is stable in ethers.

Scheme 7.7. Preparation of free $P_2(OH)_2$.

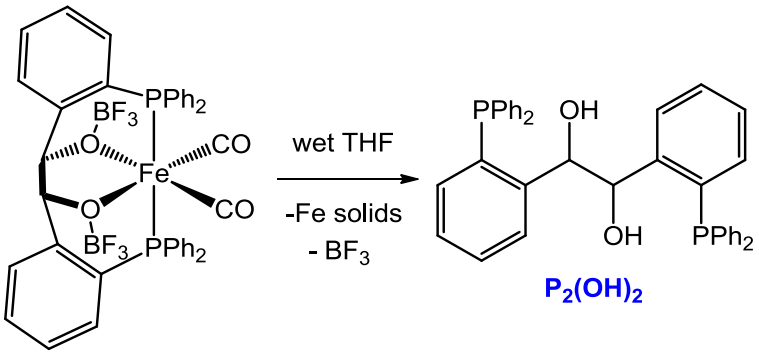

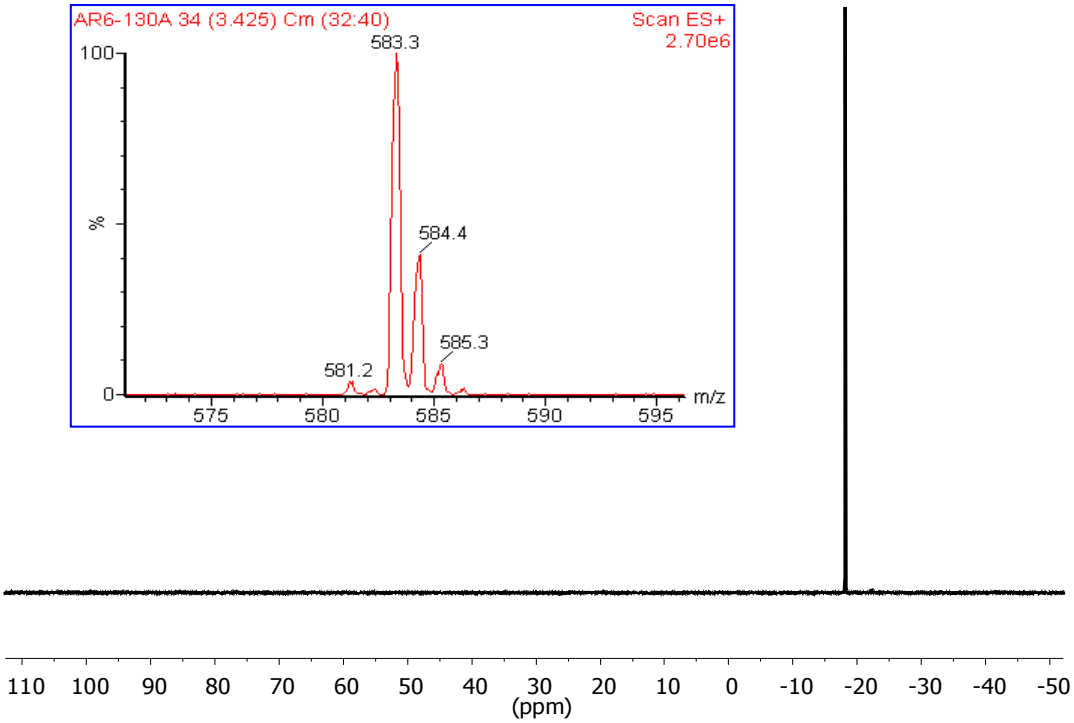

Figure 7.8. ^{31}P NMR spectrum of isolated $P_2(OH)_2$ (δ -16.3) with inset spectrum of ESI-MS of $HP_2(OH)_2^+$.

Discussion

Synthesis of $Fe(P_2O_2)(CO)_2$. The addition of 2 equivs. of $Ph_2P(o\text{-}C_6H_4CHO)$ to Fe(0) carbonyls resulted in reductive coupling of the formyl groups affording a ferrous dicarbonyl complex of an unusual diphosphine dialkoxide in high yield. The solid state structure showed the tetradentate P_2O_2 ligand with the trans phosphines. The same coupling reaction had been reported for W[12] and Tc[20] complexes. The previous reports did not give any detail beyond the crystallography. The discovery of an efficient and inexpensive coupling reaction offers the prospect that the coordination chemistry of this novel platform could be further developed.

The P_2O_2 ligand formed by our method is superior to the previous examples using Tc and W templates in several ways. One obvious reason is the use of cheap Fe starting materials. The $Fe(P_2O_2)(CO)_2$ complex is isolated in 89 % yield based on the phosphine ligand. In contrast, the Tc complex is isolated in 54 % based on phosphine (Tc is the limiting reagent) and the W complex requires multiple steps with an overall yield of 6.1 % based on phosphine. The W complex also contains a η^1-P bound $Ph_2P(C_6H_4CHO)$ ligand that might complicate isolation of metal-free $P_2(OH)_2$.

Relevant to the mechanism for C-C bond formation, we investingated the likely intermediate $Fe(PPh_2(C_6H_4CHO)$. UV-irradiation appears to induce formation of a κ^1, η^2-P,CO complex followed by oxidative addition of the aldehyde C-H bond to give an observable but unstable acyl hydride. This acyl

hydride is believe to be a precursor to $Fe(P_2O_2)(CO)_2$ via the addition of a second equivalent of $Ph_2P(o\text{-}C_6H_4CHO)$.

Scheme 7.8. Mechanism for typical pinacol coupling[22]

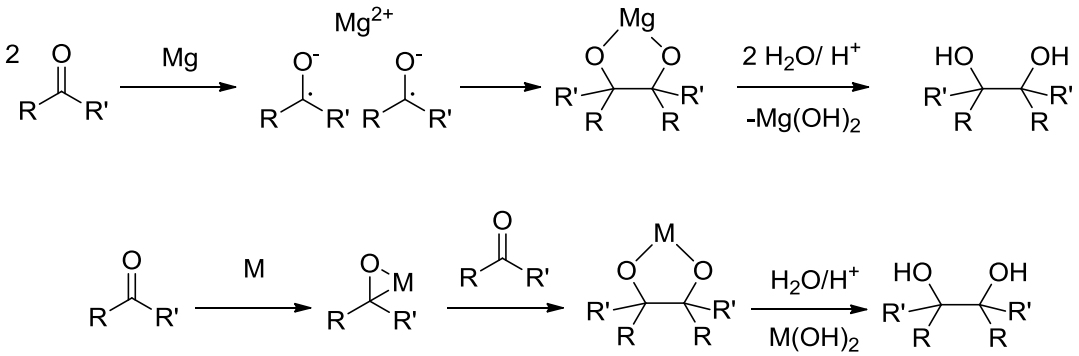

The formation of a metal acyl hydride is a different mechanism than invoked in typical pinacol coupling reactions in which a one-electron reduction of the carbonyl group of an aldehyde gives a ketyl radical anion that couples to another ketyl to give the 1,2 diolate. The other common mechanism involves metal insertion into the carbonyl group to form an oxirane that is then susceptible to attack by another formyl (Scheme 7.8). Further evidence for a novel mechanism is the reversibility of the pinacol coupling. We found that irradiation of $Fe(P_2O_2)(CO)_2$ in MeCN resulted in efficient conversion to free $Ph_2P(C_6H_4CHO)$. Reverse pinacol coupling has been reported for tetraarylethanediols with weak C-C bonds, but is generally rare.[23] The isomerization of 1,2 diols has been discussed and one possible pathway involves loss of metal hydride from the diolate to form a ketone.[24] A possible pathway for the C-C bond formation leading to $Fe(P_2O_2)(CO)_2$ is shown in Scheme 7.9.

Scheme 7.9. Possible routes to form $Fe(P_2O_2)(CO)_2$.

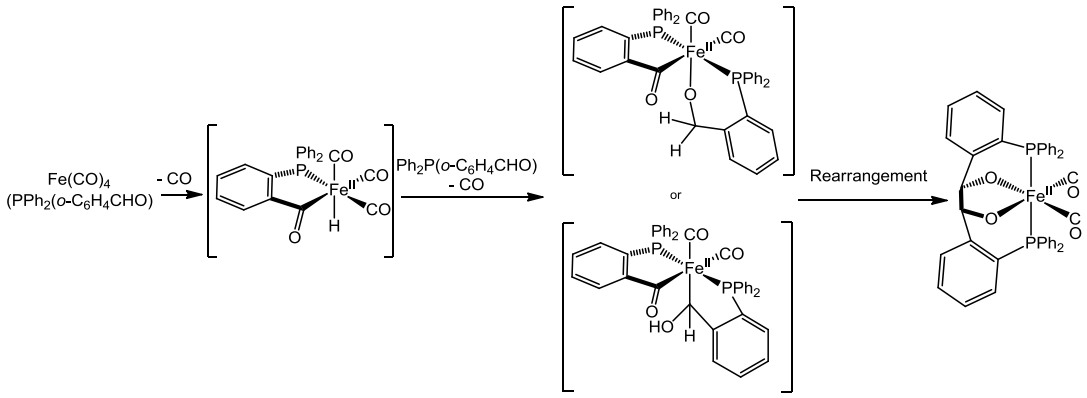

Fomation of an Fe-F Complex From BF_4^- and PF_6^- Salts. We discovered the $Fe(P_2O_2)(CO)_2$ complex reacted with both $FcBF_4$ and $FcPF_6$ to give an ~50% conversion. We attribute our observations to the formation of Lewis acid adducts with BF_3 and PF_5 attached to the alkoxide ligands. Such adducts would be expected to resist oxidation. The ferrocenium transformations require B-F or P-F bond activation to form the Lewis acid that subsequently forms adducts of the alkoxide ligand. In situ ^1H NMR showed the signal intensity decreases which suggests formation of a paramagnetic complex. We have not yet isolated the other product(s) from these reactions, but we suggest a possible route to the Lewis acid complexes also results in the formation of a paramagnetic $Fe(P_2O_2)F_2$ complex (Scheme 7.10). Only a single example of an Fe-F-phosphine complex, $Fe(CO)_2(PMe_3)_2F_2$, has been reported and the supporting data were underwhelming.[25] There are several examples of crystallographically characterized Fe-FBF_3 bonds with both mono[26,27] and bis[28] BF_4 complexation reported. In our case, we propose the B-F bond is broken to give an Fe-F bond

and BF_3. The abstraction of fluoride from BF_4^- has been reported for bis(pyrazolyl)methane complexes of Fe, Co, Ni, Cd, or Mn[29] and Zn[30] and more recently with Schiff base expanded porphyrin complexes of Zn and Cd.[31] These complexes generally were generated from unsaturated metal centers and were isolated as the bimetallic bridging difluoride complexes. The reverse reaction has been reported by Holland *et al* in which an Fe diketiminate fluoride reacts with BF_3 to form BF_4.[32]

Scheme 7.10. Possible reaction scheme of $Fe(P_2O_2)(CO)_2$ with $FcBF_4$.

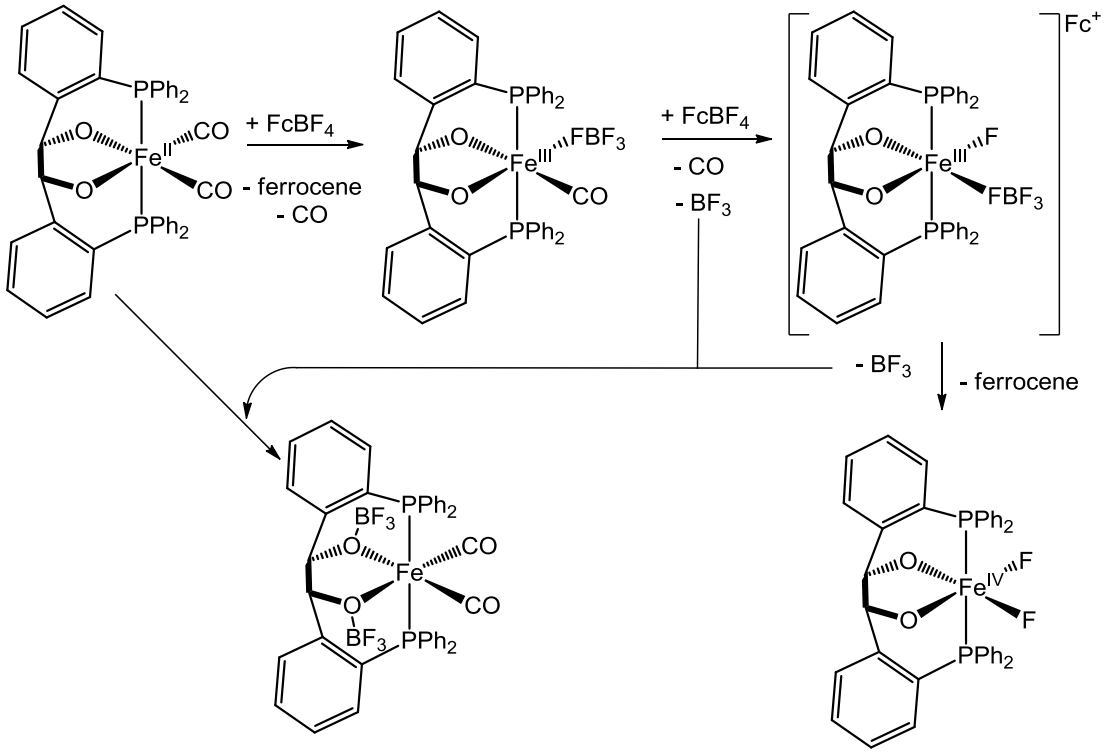

Basicity of Fe(II) alkoxides. The $Fe(P_2O_2)(CO)_2$ complex can bind one or two Lewis acids to the alkoxides with $\Delta\ \nu_{CO}$ of 23, 30 and 18, 28 cm^{-1} for the first and second BF_3 additions respectively. The small change in CO stretching

frequencies suggests the loss in electron density at Fe upon Lewis acid binding to the alkoxides is potentially less than a single electron oxidation at the metal. For comparison, oxidation of the diiron carbonyl, $[Fe(Cp)(CO)(SPh)]_2$, from Fe(II)Fe(II) to Fe(II)Fe(III) gave a $\Delta\ \nu_{CO}$ of 43, 25 cm^{-1} and second oxidation to Fe(III)Fe(III) resulted in a further $\Delta\ \nu_{CO}$ of 53, 64 cm^{-1}.[33] The solid state structure of $Fe[P_2O_2(BF_3)_3](CO)_2$ showed there is little change in Fe ligand bond distances upon binding of the Lewis acid binding at the alkoxides, although bond angles did show a significant change (Table 7.1.). The Lewis acid adducts from PF_5, BF_3, and $TiCl_4$ showed similar changes in to CO stretching frequency.

In the reaction of $Fe(P_2O_2)(CO)_2$ with $TiCl_4$, we were interested in the possibility of transmetallation to give $Ti(P_2O_2)Cl_2$, but no such transmetalation occurred. The immediate precipitate formed in this reaction suggests potential formation of small oligomers with Ti-bridged alkoxides, but the precipitate was short lived (Scheme 7.11). The precipitation of small oligomers would also explain why the IR spectrum of the solution matches the spectrum of complexes with 2 Lewis acids bound to each Fe bis-alkoxide complex when only a single equivalent of $TiCl_4$ was added. After the precipitate dissolved, the IR spectrum was typical for a single bound Lewis acid. The small amount of bis-Lewis acid complex that remains could be from $TiCl_4$ connected to multiple alkoxides.

Scheme 7.11. Potential oligomers formed in $TiCl_4$ reaction.

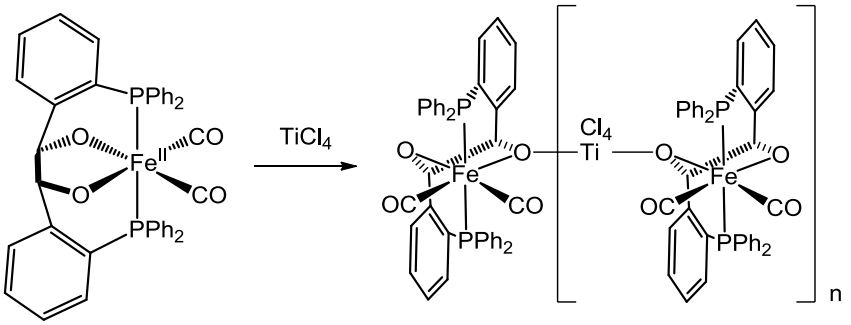

Isolation of (±)$P_2(OH)_2$. Treatment of $Fe[P_2O_2(BF_3)_2](CO)_2$ complex with wet THF liberated the free diphosphine ligand. The C_2 diastereoisomer is isolated with no formation of the meso *R,S* diastereomer (Scheme 7.12). The *R,R*- and *S,S*-$P_2(OH)_2$ diastereomers are capable of binding to the metal in the tetradentate fashion we demonstrated on Fe. The *R,S* ligand would be incapable of such coordination with one phosphine pointed away from the metal center. We should be able to take advantage of the basicity of the Fe alkoxides and bind chiral Lewis acids to separate the *R,R* and *S,S* diastereomers.

Scheme 7.12. Stereochemistry effects on Fe coordination of P_2O_2.

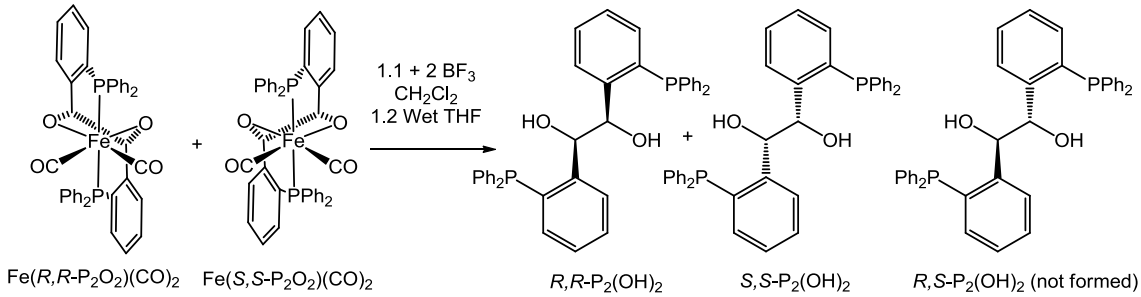

In future studies, it will be fruitful to examine the coordination of the bisphosphine diol ligand. The reaction of $Ph_2P(o\text{-}C_6H_4CHO)$ with sources of $Fe(CO)_4^{2+}$ are also promising routes to allow isolation of Fe-acyl complexes. We are also interested in the potential for Fe mediated reverse pinacol coupling which might be applicable to biomass degradation or a more general synthetic tool.

Experimental

General Considerations. Unless otherwise indicated, reactions were conducted using standard Schlenk techniques (N_2) at room temperature with stirring. $Ph_2P(o\text{-}C_6H_4CHO)$[34] and $Fe(bda)(CO)_3$[35] were synthesized according to literature preparations. $Fe_2(CO)_9$ (Strem Chemicals), 1 M $TiCl_4$ in CH_2Cl_2 (Aldrich), and BF_3OEt_2 (Aldrich) were used as received. $FcPF_6$ and $FcBF_4$ were obtained from Aldrich and recrystallized prior to use. ESI-MS were acquired using a Micromass Quattro QHQ quadrupole-hexapole-quadrupole instrument. ^1H and ^{31}P NMR was acquired on Varian UNITY INOVA 500NB and UNITY 500 NB instruments. Elemental analyses were performed by the School of Chemical Sciences Microanalysis Laboratory utilizing a model CE 440 CHN analyzer. UV irradiation wasa performed by a Spectroline model MB 100 which emits a UV intensity of 27,000 μW/cm² at 6-inch.

$Fe(P_2O_2)(CO)_2$. A solution of 991.3 mg (3.47 mmol) of $Fe(bda)(CO)_3$ and of 2.012 g (6.93 mmol) of $Ph_2PC_6H_4CHO$ in 30 mL of THF was heated to 60 ºC for 4 hours in a Schlenk flask fitted with reflux condenser. The reaction was

followed by solution IR spectroscopy. After 2 hours, the IR signals for the $Fe(bda)(CO)_3$ were no longer apparent. A large amount of bright yellow precipitate formed. The volume of the slurry was concentrated to 15 mL under reduced pressure and filtered to remove bda. The solid was washed with 5 mL of additional THF. The solid was washed with 3 X 10 mL of hexanes, and sample was left under reduced pressure overnight. ^1H NMR analysis confirmed the crystalline product contains ½ an equivalent of co-crystallized THF. The crystalline yellow solid was collected in a drybox as the ½ THF complex. Yield: 2.26 g (89.4%). The THF solvate can be removed by dissolving the solid in CH_2Cl_2 followed by removal of solvent under reduced pressure, leavinga yellow powder. Larger scale reactions consistently gave increased yields of product. ^1H NMR (500 MHz, CD_2Cl_2): δ (ppm) 4.49 (s, 2H, OC*H*), 7.10-7.64 (m, 24 H, Phenyl-H), 8.06 (s, 4H, Phenyl-H). ^{31}P NMR (202 MHz, CD_2Cl_2): δ (ppm) 21.2 (s). IR spectrum (CH_2Cl_2): ν_{CO} = 1965, 2025 cm^{-1}. Anal. Calcd: theoretical (found) for $C_{42}H_{30}FeO_2P_2$: C, (); H, (); N, ().%CHN.

$Fe(Ph_2P\text{-}C_6H_4CHO)(CO)_4$. A solution of 1g (3.44 mmol) of $Ph_2PC_6H_4CHO$ in 50 mL of THF was transferred via cannula onto 1.25 g (3.44 mmol) of solid $Fe_2(CO)_9$. The mixture was stirred at 23 ºC until all solids dissolved (40 min). The reaction solution was examined by ^{31}P NMR spectroscopy to assure all free phosphine had reacted. The solvent and most $Fe(CO)_5$ were removed under reduced pressure. The yellow residue was washed with 2 X 50 mL of hexanes. The solid was recrystallized from THF/hexanes, and residual solvent was removed under reduced pressure to give a yellow powder. Yield: 0.768 g (49%).

^{1}H NMR (500 MHz, CD_2Cl_2): δ 6.80-8.28 (m, 14 H, Phenyl-H), 10.14 (s, C*H*O). ^{31}P NMR (202 MHz, CD_2Cl_2): δ 68.2 (s). IR spectrum (CH_2Cl_2): ν_{CO} = 1943 (br), 1978 (br), 2052 (sh) cm^{-1}. CHN

Detection of Intermediates in Formation of $Fe(P_2O_2)(CO)_2$. A solution of 9.5 mg (0.02 mmol) of $Fe(Ph_2P\text{-}C_6H_4CHO)(CO)_4$ in 0.8 mL of toluene-d_8 was prepared in a J. Young NMR tube. The tube was sealed, and ^{1}H and ^{31}P NMR spectra were obtained. The tube was then irradiated, and ^{1}H, ^{31}P, and $^{31}P\{^{1}H\}$ NMR spectra were collected periodically over the course of 2 hours. After 2 h, a large quantity (see Figure 7.9) of the hydride product was detected with $Fe(P_2O_2)(CO)_2$ also formed, the sealed tube was placed in the dark at 23 ºC. After 24 hours, the hydride product was no longer detectable, and the quantity of $Fe(P_2O_2)(CO)_2$ had increased.

In situ detection of hydride intermediate: ^{1}H NMR (500 MHz, CD_2Cl_2): δ -7.7 (d, 47.5 Hz, 1 H, Fe-H). $^{31}P\{^{1}H\}$ NMR (202 MHz, CD_2Cl_2): δ 89.5 (s, P-Fe-H). ^{31}PNMR (202 MHz, CD_2Cl_2): δ 89.5 (d, 47.5 Hz, P-Fe-H).

In situ detection of κ^1, η^2-P,CO complex : ^{1}H NMR (500 MHz, CD_2Cl_2): δ 5.91 (s 1 H, Fe-(C*H*O)). ^{31}P NMR (202 MHz, CD_2Cl_2): δ 58.2 (s, P-Fe).

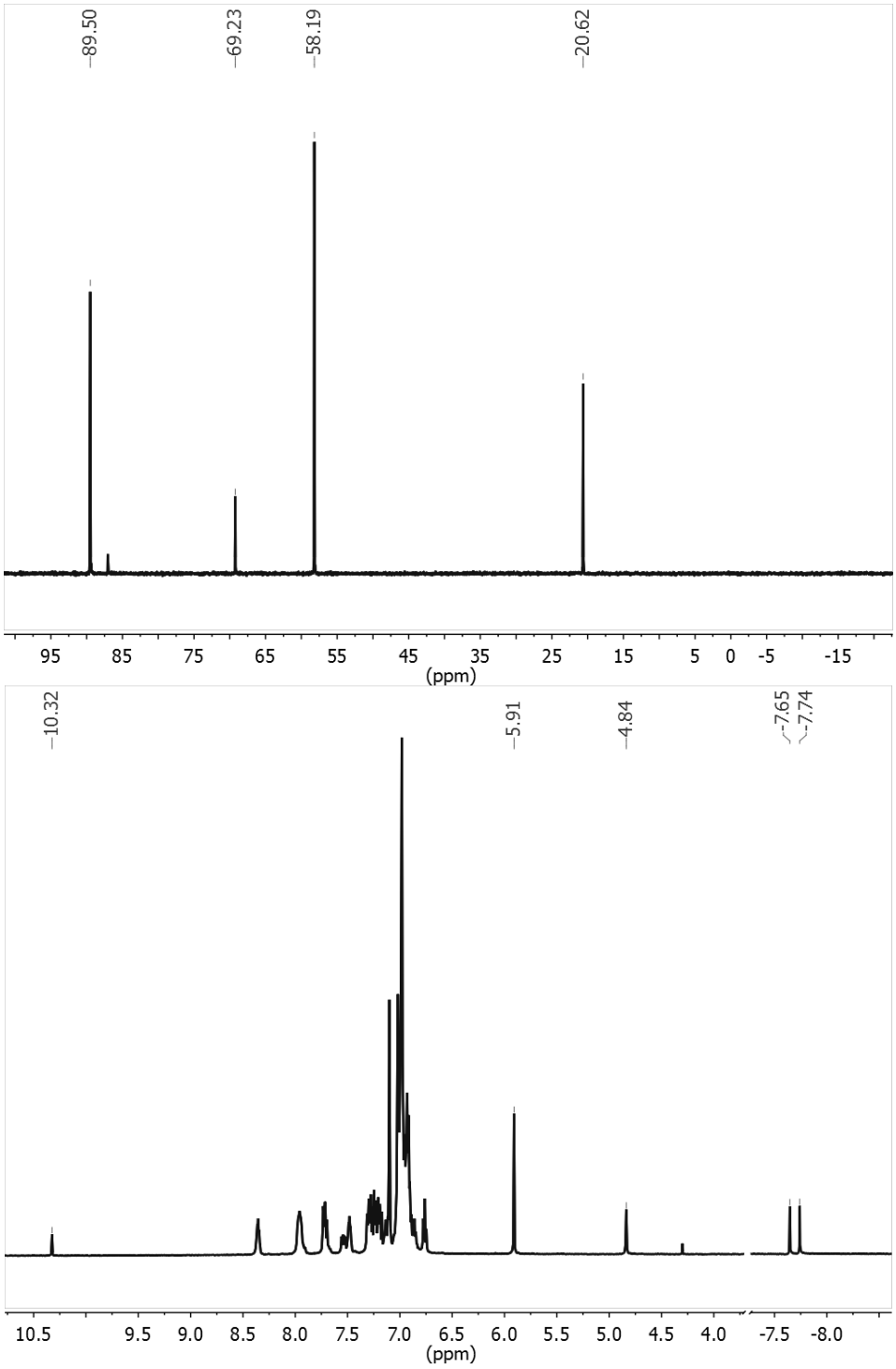

Figure 7.9. ^{31}P NMR spectrum (top) and ^{1}H NMR spectrum (bottom) of $Fe(Ph_2P\text{-}C_6H_4CHO)(CO)_4$ in toluene-d_8 after 2 hours of irradiation

Conversion of $Fe(P_2O_2)(CO)_2$ to $Ph_2P\text{-}C_6H_4CHO$. A slurry of 65 mg (0.094 mmol) of $Fe(P_2O_2)(CO)_2$ in 9 mL of MeCN was irradiated for 1 hour with formation of a gray solid and the IR spectrum of solution was collected. The mixture was irradiated a further 4 hours and the solution IR spectrum contained no CO bands. The mixture was filtered and the ^{31}P NMR spectrum of the filtrate was collected. The spectrum showed ~90 % conversion to free $Ph_2P\text{-}C_6H_4CHO$. The leftover gray solid was dissolved in CH_2Cl_2 and the solution IR spectrum contained no CO bands. The ^{31}P NMR spectrum contained no signals.

Attempted Oxidation of $Fe(P_2O_2)(CO)_2$. ($FcPF_6$). A yellow solution of 54 mg (0.078 mmol) of $Fe(P_2O_2)(CO)_2$ in 13 mL of CH_2Cl_2 under a N_2 atmosphere was first check by IR spectroscopy. Solid $FcPF_6$ (26 mg, 0.078 mmol) was added to the solution, giving an initially blue colored solution. An IR spectrum of this blue solution was collected after 10 minutes. The solution was stirred for an additional 20 minutes during which a gray precipitate appeared and solution became yellow. An IR spectrum of the yellow supernatant solution had not noticeably changed over the course of the hour. IR spectrum (CH_2Cl_2): ν_{CO} = 2052, 2002 cm^{-1}.

($FcBF_4$) A blue solution of $FcBF_4$ (261.1 mg, 0.957 mmol) in 15 mL of CH_2Cl_2 was stirred and ~90 % of solution was added to a yellow solution of 664 mg (0.911 mmol) of $Fe(P_2O_2)(CO)_2$ in 25 mL of CH_2Cl_2. An IR spectrum was collected immediately and after an hour. The remaining solution of $FcBF_4$ in CH_2Cl_2 was then added, and the mixture was stirred 20 minutes. The IR spectrum of this solution showed starting material was consumed. No precipitate

formed. The solvent was removed under reduced pressure, and the solid was washed with hexanes (3 X 20 mL). The addition of Et_2O to the solid gave a yellow solution that contained CO bands in the solution IR spectrum. The solid was washed with 100 mL of Et_2O and concentrated to give a yellow powder. IR spectrum (CH_2Cl_2): ν_{CO} = 2053, 2004 cm^{-1}. A concentrated Et_2O solution of this product was stored at -30 ºC to give crystals of $Fe[P_2O_2(BF_3)_2](CO)_2$ suitable for X-ray diffraction.

NMR Tube Reaction of $Fe(P_2O_2)(CO)_2$ with $FcBF_4$. A solution of 15.1 mg (0.0207 mmol) of $Fe(P_2O_2)(CO)_2$ and of 4.0 mg (0.024 mmol) of CH_2Ph_2 (integration standard) in 0.75 mL of CD_2Cl_2 was prepared in a J. Young tube. ^1H and ^{31}P NMR spectra were obtained. Solid $FcBF_4$ (5.8 mg, 0.0207 mmol) was added to the tube in a drybox. ^1H and ^{31}P NMR spectra were obtained several times over the next hour. After sitting for several days, a large crystal formed and was submitted for analysis by X-ray diffraction. The analysis confirmed that the crystal corresponded to $Fe[P_2O_2(BF_3)_2](CO)_2$. Subsequent studies showed that $Fe[P_2O_2(BF_3)_2](CO)_2$ crystallizes readily from concentrated CH2Cl2 solutions.

Lewis Acid Adducts of $Fe(P_2O_2)(CO)_2$. BF_3 Derivatives. A solution IR spectrum of 563 mg (0.813 mmol) of $Fe(P_2O_2)(CO)_2$ in 20 mL of CH_2Cl_2 was obtained. The solution was treated with 0.10 mL (0.813 mmol) of BF_3OEt_2 added dropwise by syringe. A solution IR spectrum was collected immediately followed by addition of a second 0.10 mL (0.813 mmol) aliquot of BF_3OEt_2. The IR spectrum was obtained immediately, showing a single product with 2 CO bands

(2048, 1995 cm^{-1}). The solvent was removed under reduced pressure, and the yellow powder was recrystallized from CH_2Cl_2/hexanes. Residual solvent was removed under reduced pressure overnight. The product was obtained as a microcrystalline yellow solid of $Fe(P_2O_2(BF_3)_2)(CO)_2$. Yield: 673 mg (95%). IR spectrum (CH_2Cl_2): ν_{CO} = $Fe(P_2O_2(BF_3))(CO)_2$: 2066, 2023 cm^{-1}. ^{19}F NMR (XX MHz, THF): δ -145 s. ^{31}P NMR (202 MHz, THF): δ 31.9 s.

$TiCl_4$ Adducts. A solution IR spectrum of 100 mg (0.137 mmol) of $Fe(P_2O_2)(CO)_2$ in 30 mL of CH_2Cl_2 was obtained. A 1M solution of $TiCl_4$ in CH_2Cl_2 (0.15 mL, 0.148 mmol) was added dropwise, giving a yellow precipitate. An IR spectrum of the yellow solution was obtained (ν_{CO} = immediate: 2068, 2025 cm^{-1}). Upon stirring 10 minutes, the solids dissolved to give a homogeneous solution (ν_{CO} = 2050, 2000 cm^{-1}). The solution IR was obtained. The solution was allowed to stir at 23 ºC over 24 h with no noticeable change in the solution IR spectrum.

***d,l*-$[Ph_2PC_6H_4CH(OH)]_2$.** A solution of 206.7 mg (0.25 mmol) of $Fe[P_2O_2(BF_3)_2](CO)_2$ in 20 mL of degassed wet (0.004% H_2O) THF was stirred for 24 hours giving a gray precipitate. The IR spectrum of the supernatant showed no CO bands. ^{31}P NMR spectrum of the solution contained a singlet at -16.3 ppm. The ^{19}F NMR spectrum had broad signals. The solids were removed by filtration, and the solvent was removed from the filtrate under reduced pressure. The residue was stirred with 50 mL of Et_2O for 1 h and filtered through a short plug of silica gel in a dry box. The solvent was removed under reduced pressure to give a light yellow powder. Yield: 40 mg (27.5 %). ^{31}P NMR (202

MHz, THF): δ (ppm) -16.3 s. ESI-MS m/z = + 583.3, (Ph_2P-$C_6H_4CH(OH)CH(OH)C_6H_4$-$PHPh_2$)]$^+$). Anal. Calcd: theoretical (found) for $C_{38}H_{32}O_2P_2$: C, 78.34 (77.84); H, 5.54 (5.19); N, 0.00 (0.37).

References:

[1] Royer, A. M.; Rauchfuss, T. B.; Gray, D. L. "Oxidative Addition of Thioesters to Iron(0): Active-Site Models for Hmd, Nature's Third Hydrogenase." *Organometallics*, **2009**, *28*, 3618-3620.

[2] Royer, A. M.; Rauchfuss, T. B.; Salomone-Stagni, M.; Meyer-Klaucke, W. "Iron Acyl Thiolato Carbonyls: Structural Models for the Active Site of the [Fe]-Hydrogenase (Hmd)" *J. Am. Chem. Soc.* (accepted)

[3] Garralda M.A. *"*o-(Diphenylphosphino)benzaldehyde: a versatile ligand and a useful hemilabile ligand precursor." *C. R. Chimie,* **2005**, *8*, 1413-1420.

[4] Ainscough, E. W.; Brodie, A. M.; Ingham, S. L.; Waters, J.M. "Functionalised phosphine complexes of Group 6 metal carbonyls: structure of pentacarbonyl(phenyl-2-carbaldehyde diphenylphosphine-κP)tungsten" *Inorg. Chim. Acta.* **1995**, *234*, 163-167.

[5] Rauchfuss, T. B. "Transition metal activation of aldehydes: platinum metal derivatives of o-diphenylphosphinobenzaldehyde." *J. Am. Chem. Soc.* **1979**, *101*, 1045-1047.

[6] Watkins, S. E.; Craig, D. C.; Colbran, S. B. "A palladium(II) complex of a new iminophosphine ligand derived from diethylenetriamine and 2-(diphenylphosphino)benzaldehyde." *Inorg. Chim. Acta*, **2000**, *307*, 134-138.

[7] Schumann, H.; Hemling, H.; Ravindar, V.; Badrieh, Y.; Blum, J. "Effects of changes in the ligands on the skeleton and the catalytic activity of some new rhodium complexes with pyrazolato moieties." *J. Organomet. Chem.,* **1994**, *469,* 213-219.

[8] El Mail, R.; Garralda, M. A.; Hernández, R.; Ibarlucea, L. "Reaction of $[RhCl(CO)_2]_2$ or $[RhCl(COD)]_2$ with *o*-(diphenylphosphino)benzaldehyde. Formation of hemiaminals in the subsequent reaction with dihydrazones." *J. Organomet. Chem.* **2002**, *648*, 149-154.

[9] Barbaro, P.; Bianchini, C.; Meali, C.; Masi, D. "Chloro[*o*-(diphenylphosphino)benzaldehyde]{*N*-[*o*-(diphenylphosphino)benzylidene]ethylamine}(tetrachloro-*o*-catecholato)iridium(III)." *Acta Crystallogr. Sect. C* **1994**, 1414-1417.

[10] Chen, X.; Femia, F. J.; Babich, J.W.; Zubieta, J. "Synthesis and structural characterization of rhenium(I) tricarbonyl complexes with the bidentate ligands *o*-(diphenylphosphino)benzaldehyde (P∩O) and *o*-[(diphenylphosphino)benzylidene]analine (P∩N)." *Inorg. Chim. Acta* **2001**, *315,* 147-152.

[11] Lenges, C. P.; Brookhart, M.; White, P. S. "Structure and reactivity of a cobalt(I) phthalaldehyde complex with both σ- and π-bonded aldehyde groups." *Angew. Chem., Int. Ed.* **1999**, *38*, 552-555.

[12] Yeh, W. Y.; Lin, C. S.; Peng, S. M.; Lee, G. H. "Syntheses and Structures of Tungsten *o*-(Diphenylphosphino)benzaldehyde Complexes Bearing π-Bonded Aldehyde Groups." *Organometallics* **2004**, *23*, 917-920.

[13] Bianchini, C.; Meli, A.; Peruzzini, M.; Ramirez, J. A.; Vacca, A.; Vizza, F.; Zanobini, F. "Oxidative addition/reductive elimination of aldehydes and ketones at rhodium" *Organometallics* **1989**, *8*, 337-345.

[14] El Mail, R.; Garralda, M. A.; Hernández, R.; Ibarlucea, L.; Pinilla, E.; Torres, M. R. "Hydroxyalkyl Complexes and Hemiaminal Formation in the Reaction of *o*-Diphenylphosphinobenzaldehyde with Rhodium(I) Dihydrazone Complexes" *Organometallics* **2000**, *19*, 5310-5317.

[15] Landvatter, E. F.; Rauchfuss, T. B. "Chelate-assisted oxidative addition of functionalized phosphines to iridium(I)" *Organometallics* **1982**, *1*, 506-513.

[16] Garralda, M. A.; Hernández, R.; Ibarlucea, L.; Pinilla, E.; Torres, M. R. "New acylhydridorhodium(III) complexes containing terdentate PNN ligands from the reaction of diolefinic rhodium(I) complexes with *o*-(diphenylphosphino)benzaldehyde in the presence of chelating amino ligands." *Organometallics* **2003**, *22*, 3600-3603.

[17] Koh, J. J.; Lee, W. H.; Williard, P. G.; Risen, W. M. "The $PtP(C_6H_{11})_3(C_2H_4)_2$ mediated activation of aldehyde C-H bonds via chelate-assisted oxidative addition reactions." *J. Organomet. Chem.* **1985**, *284*, 409-419.

[18] Ghilardi, C. A.; Midollini, S.; Moneti, S.; Orlandini, A. "Reactivity of *o*-diphenylphosphinobenzaldehyde toward $[Pt(C_2H_4)(PPh_3)_2]$. *X*-ray structure of

[Pt(OCC$_6$H$_4$PPh$_2$-*o*)H(PPh$_3$)]·C$_6$H$_6$." *J. Chem. Soc., Dalton Trans.* **1988**, 1833-1836.

[19] Klein, H. F.; Lemke, U.; Lemke, M.; Brand, A. "2-Diphenylphosphinobenzaldehyde as Chelating Ligand in Trimethylphosphine Complexes of Cobalt and Nickel." *Organometallics* **1998**, *17*, 4196-4201.

[20] Refosco, F.; Bandoli, G.; Mazzi, U.; Tisato, F.; Dolmella, A.; Nicolini, M. "Unusual synthesis and x-ray structure of cis-dichloro[1,2-bis(o-(diphenylphosphino)phenyl)ethane-1,2-diolato(2-)]technetium(IV) hemiethanol solvate." *Inorg. Chem.* **1990**, *29*, 2179-2180.

[21] Conder, H. L.; Darensbourg, M. Y. "The Synthesis of Group V Substituted Derivatives of Iron Pentacarbonyl in High Yield." *J. Organomet. Chem.*, **1974**, *67*, 93-97.

[22] Chatterjee, A.; Joshi, N. N. "Evolution of the Stereoselective Pinacol Coupling Reaction." *Tetrahedron*, **2006**, *62*, 12137-12158.

[23] Schlenk, A; Thal, A. "Metal Ketyls, a Large Class of Compounds with Trivalent Carbon. II." *Ber.*, **1913**, *46*, 2840-2854.

[24] McMurray, J. E.; Choy, W. "On the Mechanism of the Thermal Isomerization of 1,2-Diolates. Is the Pinacol Coupling Reaction Reversible?" *J. Org. Chem.*, **1978**, *43*, 1800-1803.

[25] Cardaci, G,; Bellachioma, G.; Reichenbach, G. "Preparation of the complexes Fe(CO)$_2$(PMe$_3$)$_2$CH$_3$X and insertion reaction of carbon monoxide." *XIII Congresso Nazionale di Chimica Inorganica*, **1980**, *13*, 78-80.

[26] Landau, S. E.; Morris, R. H.; Lough, A. J. "Acidic Dicationic Iron(II) Dihydrogen Complexes and Compounds Related by H_2 Substitution." *Inorg. Chem.*, **1999**, *38*, 6060-6068.

[27] Halfen, J. A.; Moore, H. L.; Fox, D. C. "Synthetic Models of the Reduced Active Site of Superoxide Reductase." *Inorg. Chem.*, **2002**, *41*, 3935-3943.

[28] Quesada, M.; de la Peña-O'Shea, V. A.; Aromí, G.; Geremia, S.; Massera, C.; Roubeau, O.; Gamez, P.; Reedijk, J. "A Molecule-Based Nanoporous Material Showing Tuneable Spin-Crossover Behavior near Room Temperature." Adv. Mater., 2007, 19, 1397-1402.

[29] Verbiest, J.; van Ooijen, J. A. C.; Reedijk, J. "Dimeric, fluoro-bridged, six-coordinate, transition-metal compounds derived from tetrafluoroborates and bis(3,5-dimethylpyrazolyl)methane." *J. Inorg. Nucl. Chem.*, **1980**, *42*, 971-975.

[30] Reger, D. L.; Watson, R. P.; Gardinier, J. R.; Smith, M. D.; Pellechia, P. J. "Metallacycles of Iron, Zinc, and Cadmium Assembled by Polytopic Bis(pyrazolyl)methane Ligands and Fluoride Abstraction from BF_4^-." *Inorg. Chem*. **2006**, *45*, 10088-10097.

[31] Tomat, E.; Cuesta, L.; Lynch, V. M.; Sessler, J. L. "Binuclear Fluoro-Bridged Zinc and Cadmium Complexes of a Schiff Base Expanded Porphyrin: Fluoride Abstraction from the Tetrafluoroborate Anion." *Inorg. Chem.*, **2007**, *46*, 6224-6226.

[32] Vela, J.; Smith, J. M.; Yu, Y.; Ketterer, N. A.; Flaschenriem, C. J.; Lachicotte, R. J.; Holland, P. L. "Synthesis and Reactivity of Low-Coordinate Iron(II) Fluoride Complexes and Their Use in the Catalytic Hydrodefluorination of Fluorocarbons." *J. Am. Chem. Soc.*, **2005**, *127*, 7857–7870

[33] de Beer, J. A.; Haines, R. J.; Greatrex, R.; van Wyk, J. A. "Reactions of Metal Carbonyl Derivatives. Part XV. Oxidation Studies of Some η-Cyclopentadienyl Bridging Sulphido- and Phosphino-derivatives of Iron." *J. Chem. Soc. Dalton Trans.* **1973**, 2341-2346.

[34] Hoots, J. E.; Rauchfuss, T. B.; Wrobleski, D. A. "39. Substituted Triaryl Phosphines." *Inorg. Synth.*, **1982**, *21*, 175-179.

[35] Alcock, N. W.; Richards, C. J.; Thomas, S. E. "Preparation of Tricarbonyl(η^4-vinylketene)iron(0) Complexes from Tricarbonyl(η^4-vinyl ketone)iron(O) Complexes and Their Subsequent Conversion to Tricarbonyl(η^4-vinylketenimine)iron(0) Complexes." *Organometallics*, **1991**, *10*, 231-238

Author's Biography

Aaron Mathew Royer was born in Crawfordsville, IN on November 24, 1982. After graduating Southmont High School in New Market, IN in 2001, he attended Indiana University Bloomington. In the fall of 2003, he began undergraduate research in the laboratory of Professor Jeffrey Zaleski examining the detection of silicates in water. He graduated from Indiana University Bloomington with a B.S. degree in chemistry with departmental honors in May 2005. Upon completion of his degree, he moved to the University of Illinois at Urbana/Champaign and conducted research in the laboratory of Professor Thomas B. Rauchfuss. He focused his research on catalytic H_2 activation and modeling hydrogenase enzymes. Following the completion of his Ph.D. in the fall of 2010, Aaron will begin working at SABIC Innovative Plastics in Mt. Vernon, IN.